Impact of land-use changes on the methanotrophic community structure

Loïc Nazaries

A thesis submitted to the Department of Life Sciences
in fulfilment of the requirements for the degree of Doctor of Philosophy

March 2011

University of Warwick
Coventry, UK

Table of contents

List of tables

List of figures

Abbreviations

%	percent
‰	permille
°C	degree Celsius
•OH	hydroxyl radical
^{13}C	isotopic carbon
αKGDH	alpha-ketoglutarate dehydrogenase
Ac-CoA	acetyl-coenzyme A
AcS/CODH	acetyl-CoA synthase and carbon monoxide dehydrogenase
AK	acetate kinase
AMMI	Additive Main effect and Multiplicative Interaction
AMO	ammonium monooxygenase
amo	gene coding for AMO
ANME	anaerobic methanotrophic *Archeae*
ANOVA	analysis of variance
AOM	anaerobic oxidation of methane
bp	base pair
BSA	bovine serum albumine
C	carbon atom
CBC	copper-binding compound
CFC	chloro-fluoro carbon
CH_4	methane
ca.	*circa* (around)
CO	carbon monoxide
CO_2	carbon dioxide
CoA	coenzyme A
CoB	coenzyme B
CoM	coenzyme M
Cu	copper atom
Cu-mb	copper-containing methanobactin
CytC	cytochrome C
DCA	detrended correspondence analysis
DEPC	diethylpyrocarbonate
dH_2O	distilled water
DNA	deoxyribonucleic acid
DNDC	denitrification and decomposition
dNTP	deoxynucleotide triphosphate

DTT	dithiothreitol
e.g.	*example gratia* (for example)
et al.	*et alii* (and others)
etc.	*et cetera* (and the rest)
ECH	energy-converting hydrogenase
EDTA	ethylene diamine tetraacetic acid
F_{420}	coenzyme F_{420}
FAD	flavin adenine dinucleotide
FAM	carboxyfluorescein
Fd	ferredoxin
FDH	formaldehyde dehydrogenase
FDH	formate dehydrogenase
Fe	iron atom
Fe^{3+}	ferric ion
FID	flame ionisation detector
g	gram
GAP	glyceraldehyde-3-phosphate
GC-MS	gas chromatography-mass spectroscopy
GC-C-IRMS	gas chromatography-combustion-isotope ratio mass spectrometry
GHG	greenhouse gas
GK	glycerate kinase
H_2	dihydrogen
H_2O	water
H_4MPT	tetrahydromethanopterin
H_4SPT	tetrahydrosarcinapterin
ha	hectare
HDR	heterodisulfide reductase
He	helium gas
*Hha*I	*Haemophilus haemolyticus* type I
HPR	hydroxypyruvate reductase
i.e.	*id est* (that is)
ICM	intracytoplasmic membrane
ID	inner diameter
IPC	interaction principal component
IPCA	interaction principal component analysis
IPCC	intergovernmental panel on climate change
KCl	potassium chloride
kDa	kilodalton
km	kilometre
K_m	Michaelis constant
KOH	potassium hydroxide
kPa	kilopascal
kt	kilotonne
L	litre

LBT	larger-the-better
m	metre
M	molar
MANOVA	multivariate analysis of variance
mb	methanobactin
*Mbo*I	*Moraxella bovis* type I
MCR	methyl-coenzyme M reductase
mcr	gene coding for MCR
MDH	methanol dehydrogenase
MFR	methanofuran
$MgCl_2$	magnesium chloride
min	minute
MMO	methane monooxygenase
mmo	operon coding for soluble MMO
mRNA	messenger RNA
MRT	methyl reductase two
mrt	gene coding for MRT
*Msp*I	*Moraxella* sp. type I
MTR	methyltransferase
N/A	non-applicable
N_2	nitrogen gas
N_2O	nitrous oxide
NaCl	sodium chloride
NAD	nicotinamide adenine dinucleotide
NH_3	ammonia
NH_4^+	ammonium ion
Ni	nickel atom
NO	nitric oxide
NO_2^-	nitrite ion
NO_3^-	nitrate ion
NO_x	nitrogen oxides
NZ	New Zealand
O_2	oxygen
O_3	ozone
OA	orthogonal array
OD	outer diameter
OTU	operational taxonomic unit
P	phosphorous atom
PC	principal component
PCA	principal component analysis
PCR	polymerase chain reaction
PLFA	phospholipid fatty acid
PLFAME	phospholipid fatty acid methyl ester
pMMO	particulate MMO

pmo	operon coding for pMMO
ppb	part per billion
ppm	part per million
RC	rice cluster
RDA	redundant analysis
rpm	revolution per minute
RNA	ribonucleic acid
rRNA	ribosomal RNA
RubisCO	ribulose bisphosphate carboxylase/oxygenase
RuMP	ribulose monophosphate
s	second
S	sulfur atom
SSC	sodium chloride sodium citrate
S.E.M.	standard error of the mean
SDS	sodium dodecyl sulfate
SGAT	serine-glyoxylate aminotransferase
SHTM	serine-hydroxytransmethylase
SIP	stable isotope probing
sMMO	soluble MMO
SN	signal-to-noise ratio
SO_4^{2-}	sulfur ion
sp.	species
spp.	species (plural)
SRB	sulfate-reducing *Bacteria*
TCA	tricarboxylic acid
TD	touchdown
Tg	teragram
T_m	melting temperature
T-REX	T-RFLP expedited
T-RF	terminal-restriction fragment
T-RFLP	terminal-restriction fragment polymorphism
U	unit of enzyme
USC	upland soil cluster
UV	ultra violet
vs.	*versus* (against, as opposed to))
w/v	weight-to-volume
WFPS	water-filled pore space
yr	year
$ZnCl_2$	zinc chloride

Acknowledgements

I am grateful to all my supervisors for the help and guidance they provided me with, in their own way, in particular when I was pushing them with short deadlines. Specifically, thanks a lot to Dr Brajesh Singh for his support and patience during all my whinging. I also really enjoyed you sending me across the globe to New Zealand for sampling soil samples. ☺ Thank you for all the extra financial support.

I need to recognise many people at the Macaulay Land Use Research Institute:

- I must thank Dr Singh's team: Nadine Thomas and Lucinda Robinson are great research assistants which help and kindness were invaluable to the completion of this project.
- I am grateful to Dr Barry Thornton for his help with the PLFA-SIP analysis and for kindly responding to all my enquiries related to the implementation of the methane measurements on the gas chromatography.
- I also want to thank Allan Sim for his help with the incubation chambers and Dr Allan Lilly for using the hanging-water columns and for useful discussions related to my data.
- Of course I must say a big thank you to everyone else in the microbiology lab, and more particularly to Dr Duncan White, our lab manager. Also, thank you Dr Roxane Andersen for your many advices on statistical analyses, as well as for reviewing my paper.
- Finally, collection of the soil samples would not have been possible without the great help provided by Richard Gwatkin, Lucinda Robinson and Luca Giaramida.

I cannot finish without acknowledging people at Landcare Research, Palmerston North, NZ. Thanks to Prof. Surinder Saggar for welcoming me and to Dr Jagrati Singh and the late Dr Des Ross for their help with field and laboratory work. Moreover, I am more than grateful to Dr Kevin Tate for answering all my questions as well as for his great input on the paper.

I acknowledge the financial support of the Macaulay Development Trust, as well as the moral support from Dr Stewart Rhind as PhD student coordinator.

A special thank you to Tero, Christine, Denis, Dino, the Heavenly guys and to the Aberdeen University Volleyball Club. Go AUVC!! Thanks to Christina for her patience.
I am grateful to my parents for the crucial financial support during the writing of this thesis.

This thesis is dedicated to Lucas, Selly and Charles Darwin.

Declaration

I declare that the work presented in this thesis was conducted by me under the direct supervision of Associate Professor Brajesh K. Singh, Professor J. Colin Murrell, Professor Peter Millard and Professor Elizabeth M. Baggs, with the exception of those instances where the contribution of others has been specifically acknowledged. None of the work presented has been previously submitted for any other degree. The data presented in Chapter 4 have been published as a short communication in the ISME Journal:

Nazaries L., Tate K.R., Ross D.J., Singh J., Dando J., Saggar S., Baggs E.M., Millard P., Murrell J.C. & Singh B.K. (2011). Response of methanotrophic communities to afforestation and reforestation in New Zealand. ISME Journal, In Press.

Loïc Nazaries

Abstract

Methane (CH_4) is one of the most potent greenhouse gases and its increasing concentration in the Earth's atmosphere is linked to today's global warming. The types of land and land-use have an impact on net CH_4 fluxes, *e.g.* wetlands are generally net CH_4 emitters while upland forest soils are a sink for CH_4. This project aimed to elucidate the effect of afforestation and reforestation on net CH_4 fluxes and to determine the control of the CH_4-oxidising bacteria (methanotrophs) on net CH_4 flux rate. This was investigated using a combination of molecular (T-RFLP, cloning/sequencing, microarray) and activity-specific (PLFA-SIP) approaches. Several sites were selected to analyse soil methanotrophs under shrubs regenerating after a fire compared to a native mature forest (in New Zealand), and under bog, grass, heath, pine and birch vegetation (in Scotland). Furthermore, a simple bottom-up approach was applied to seasonal measurements of local net CH_4 fluxes in Scotland. These were upscaled to annual values in order to estimate the contribution to the national CH_4 budget for each habitat investigated. The effect on CH_4 mitigation of the conversion of different types of non-forested habitat to forests was then estimated. Afforestation/reforestation was always found to induce net CH_4 oxidation at rates much faster than previously estimated. This preliminary analysis suggests that heathland conversion to birch forest was beneficial in term of CH_4 sinks but it also induced large and permanent losses of soil C. However, bog afforestation with pine trees can potentially neutralise the national CH_4 emissions from non-forested areas, while preserving soil C stocks. This project also revealed that changes in net CH_4 flux due to land-use changes were closely related to shifts in the structure of the methanotrophic community. The relative abundance of members of the USCα cluster (high-affinity methanotrophs) was a strong predictor of net CH_4 fluxes. Finally, the sole presence of trees suggested a niche-specific adaptation of the methanotrophs, which may have been correlated to some of the soil characteristics.

Chapter 1 Introduction

1. Methane in the context of global warming

The appearance of the greenhouse effect was a vital factor for the emergence of non-aquatic life. Several gases (carbon dioxide (CO_2) and water vapour (H_2O)) and other trace gases (methane (CH_4), nitrous oxide (N_2O)) are recognised as potent greenhouse gases (GHGs) (Lacis *et al.*, 1981). The increase in concentration of these gases in the atmosphere impacts on global warming (mainly CO_2, CH_4 and N_2O). Other contributions to the phenomenon involve destruction of the stratospheric ozone (O_3) layer (by halogenated compounds and N_2O) and increase in tropospheric (pollutant) O_3 (by NO_x, CO and hydrocarbons) (Conrad, 1996). Also, CH_4 reacts with hydroxyl free radicals (•OH) (see section 2.2), whose oxidative effect is essential to atmospheric cleansing (Le Mer & Roger, 2001). As a result, other pollutants, such as chloro-fluoro carbons (CFCs) are not eliminated, leading to an increased longevity of other GHGs (O_3, CO, CO_2).

For centuries, the atmospheric concentration of the three main anthropogenic GHGs (CO_2, CH_4 and N_2O) was stable, but major increases have occurred since the beginning of the industrial era as a consequence of human activities (**Figure 1.1**). CH_4 constitutes the second most significant greenhouse gas after CO_2, and it is thought to account for up to 20-30% of global warming (IPCC, 2007). It had a stable, relatively constant abundance of 700 ppb (parts per billion) until the 19^{th} century when a steady increase brought CH_4 mixing ratio to 1,745 ppb in 1998. During the late 1970s and early 1980s, the rate of increase in CH_4 concentration was as high as $1\%.yr^{-1}$ but a minor slowdown started in the mid-1980s. Atmospheric CH_4 has

since stabilised at a value of 1.77-1.78 ppm in 2005. Today, a slight imbalance towards an annual increase of about 0.1%.yr^{-1} of CH_4 emission has been calculated (IPCC, 2007).

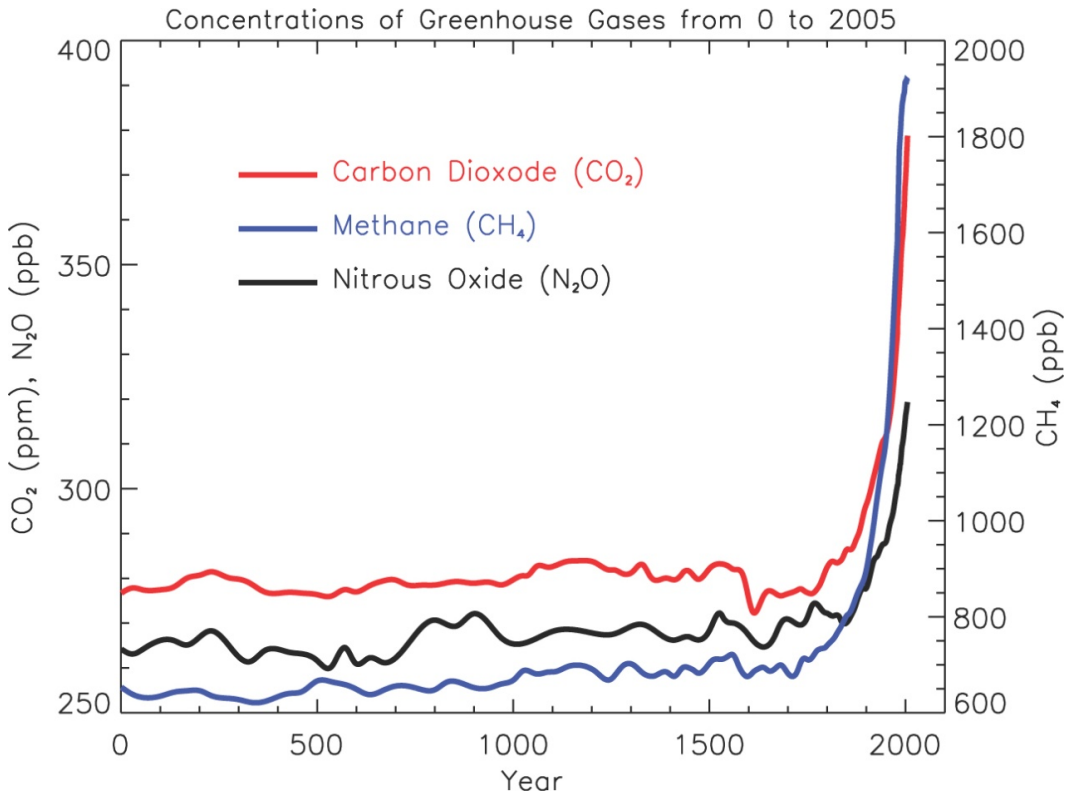

Figure 1.1: Atmospheric concentrations of important greenhouse gases over the last 2,000 years. Increases since about year 1750 are attributed to human activities in the industrial era. Concentration units are parts per million (ppm) or parts per billion (ppb). Source: IPCC (IPCC, 2007).

Despite a short lifetime of approximately 8 years in the atmosphere, CH_4 is 25 times more efficient than CO_2 as a greenhouse gas, over a 100-year horizon and on a mass basis (Shindell *et al.*, 2009). Yet, an increase of atmospheric CH_4 concentration to 2.55 ppm and a lifetime of 8.4 years are predicted by 2050 based on current rates of CH_4 emissions and subsequent decrease in •OH radical concentration (Lelieveld *et al.*, 1998). In addition, it was suggested that recently observed slowdown in global CH_4 emissions was only temporary and atmospheric CH_4 might rise again (Bousquet *et al.*, 2006). Consequently, it is essential to understand the processes responsible for the sources and sinks of CH_4 in order to efficiently mitigate the global warming effect of this gas.

2. The carbon and methane cycles

2.1. Definition

Atmospheric gases like CO_2 and CH_4 are each part of a cycle in which living organisms, such as plants and microbes, are either consumers or producers. In particular, trace gases can be substrates for microbial growth by acting as electron donors or acceptors (Conrad, 1996). Although the CH_4 sources are numerous and relatively well known, CH_4 is removed from the atmosphere by only a few processes (see section 2.2).

Microbial CH_4 production (methanogenesis) is performed by a specific group of *Archaea* called methanogens, and always occurs in anoxic environments as a consequence of fermentation, the anaerobic degradation of organic matter (see section 2.4). Archaeal methanogens only constitute the last step of fermentation and rely on the presence of a larger bacterial consortium including hydrolytic, fermenting, syntrophic and acetogenic bacteria (Cicerone & Oremland, 1988) (**Figure 1.2**). Recently, a controversy arose concerning the ability of plants to abiotically produce CH_4 (see section 2.2). However, it is well known that some plants, such as in rice paddies, can emit CH_4 produced in deeper soil layers after passive transport through the transpiration stream (aerenchyma) (Butterbach-Bahl *et al.*, 1997; Neue *et al.*, 1997), effectively bypassing the zone of CH_4 oxidation (see below).

In contrast, microbial CH_4 consumption (methanotrophy) is achieved by a unique group of *Proteobacteria* called methanotrophs (see section 3). The majority of methanotrophs are aerobic organisms. Thus, CH_4 oxidation usually takes place at anoxic/oxic boundaries such as sediments, where methanotrophs play an important role in attenuating CH_4 emissions to the atmosphere after production in the deeper anoxic environments (Conrad, 2009) (**Figure 1.2**).

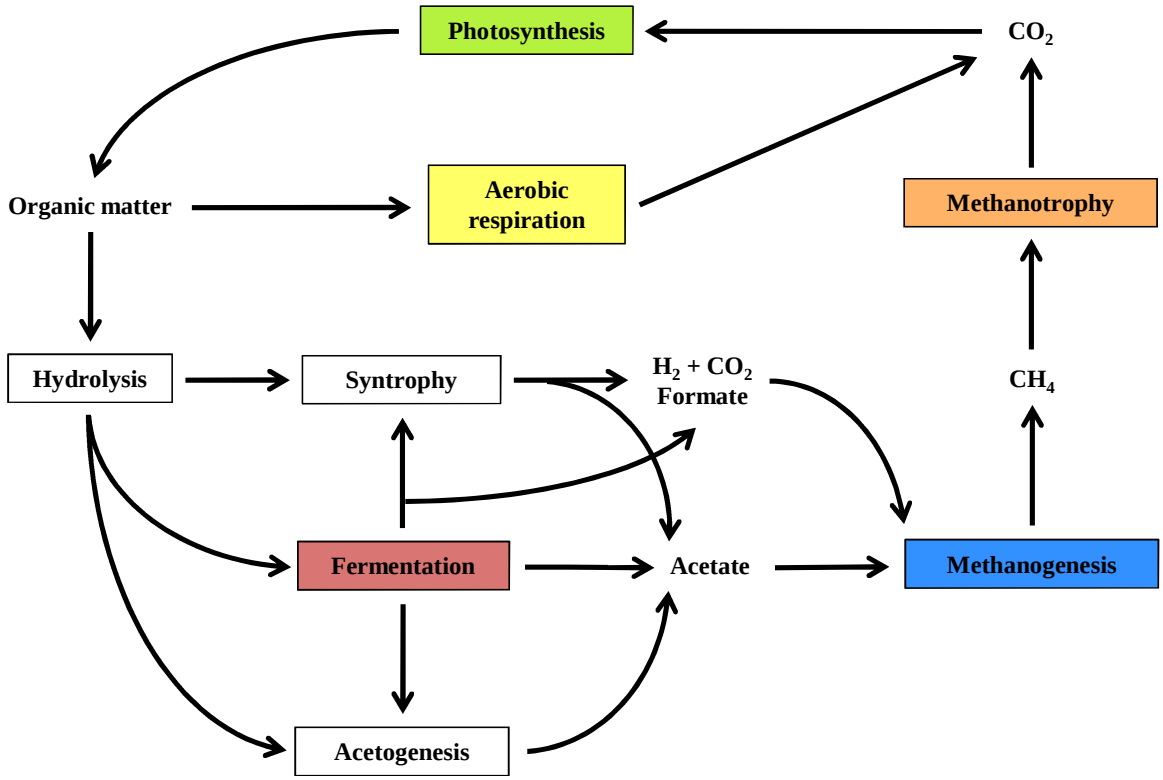

Figure 1.2: Global carbon cycle in nature.
The five main compartments of C processing are indicated by the coloured boxes. Arrows indicate either the substrates produced by a process or for which other process intermediates are produced. Adapted from Liu & Whitman (2008) and Ferry (2010).

2.2. Sources and sinks of CH_4 on Earth

An environment is a CH_4 source when the balance between production by methanogens and consumption by methanotrophs is positive, resulting in net CH_4 emission. When the balance is negative, the environment is a CH_4 sink (Le Mer & Roger, 2001). The global budget of CH_4 is about 600 Tg of CH_4 emitted per year (Conrad, 2009; Lelieveld *et al.*, 1998). Interestingly, this is matched by corresponding levels of CH_4 sink (Le Mer & Roger, 2001). Methane is naturally emitted from sources such as wetlands, oceans, plants, termites and geological sources (*e.g.* gas seepage, hydrates). Wetlands represent the largest source with 62% of the (natural) CH_4 budget (see Figure 1.3). Anthropogenic sources include rice agriculture, livestock, landfills and waste treatment, biomass burning, and fossil fuel

extraction, transport and consumption. As mentioned earlier, most of the natural CH_4 sources are of microbial origin (Conrad, 1996). Emissions from biogenic sources account for 69% of the global total. Unexpectedly, abiotic production of CH_4 through plant leaves *via* the possible aerobic degradation of pectin was revealed by Keppler *et al.* (2006). Unfortunately, these findings could not be reproduced (Beerling *et al.*, 2008; Dueck *et al.*, 2007). However, if true, CH_4 emission from plants could have a significant contribution to global CH_4 budget (Conrad, 2009). More details on emission of CH_4 from plants, as well as from upland forest soils, can be found elsewhere (Conrad, 2009; Megonigal & Guenther, 2008; Nisbet *et al.*, 2009).

During the pre-industrial era, natural sources represented over 90% of total emission. In contrast, man-made emissions dominate present-day CH_4 budgets, accounting for 63% of the total global budget (Conrad, 2009), and occur mostly in the Northern Hemisphere (Lelieveld, 2006). **Figure 1.3** shows the detailed global CH_4 sources, both natural and anthropogenic.

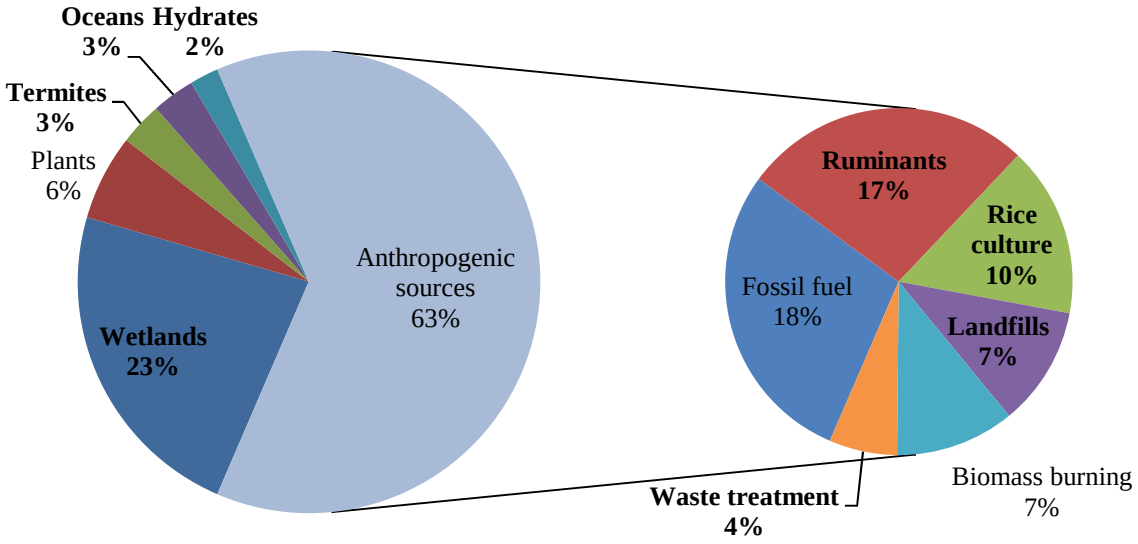

Figure 1.3: Global sources of atmospheric CH_4.
The left side of the left pie chart represents the natural CH_4 sources, whereas its right side gives an estimate of the anthropogenic sources as detailed in the right pie chart. In bold are the microbial-related productions. Source: adapted from IPCC (2001) and Conrad (2009).

In the troposphere, chemical removal of CH_4 from the atmosphere represents 88% of the total sink. It is performed through the photochemical oxidation of CH_4 initiated by the reaction with •OH radicals, according to the reaction: $CH_4 + \bullet OH \rightarrow CH_3\bullet + H_2O$ (Cicerone & Oremland, 1988). The loss of CH_4 in the stratosphere accounts for about 7% of the sink. Finally, CH_4 is also eliminated from the atmosphere by uptake in upland soils due to microbial oxidation (5%) (Conrad, 2009).

2.3. Importance of terrestrial CH_4 in relation to climate change

The management of global CH_4 sources and sinks is essential for efficient mitigation of global warning. It is possible to impact on the CH_4 budget by reducing anthropogenic emissions. This was the primary goal of the establishment of the Kyoto Protocol of 1997 (UNFCCC, 1998). This would include, for example, better management of landfills, livestock or rice cultivation. A more detailed discussion is found in Le Mer & Roger (2001) and Reay *et al.* (2010). However, the impact that we can have on CH_4 consumption is limited because the terrestrial sink contribution to the global budget is weak (only 5%), nonetheless important, and because ultimately, this process will determine whether an ecosystem is a source or sink for CH_4. This is in particular true since it is estimated that more than 50% of CH_4 produced below ground is oxidised before reaching the atmosphere (Kvenvolden & Rogers, 2005; Reeburgh, 2003). Besides, most of this sink occurs in upland soils, especially in temperate forests (Le Mer & Roger, 2001; Ojima *et al.*, 1993). Therefore, it is important to better understand the mechanisms involved in CH_4 emission from and sinks to soil. Progress could be made to enhance this terrestrial sink, for example by improving the land managements and uses through the implementation of appropriate policies (Chazelas *et al.*, 2006; Schulze *et al.*, 2009).

Soil CH_4 sink is performed by a particular group of methanotrophs, which have a high affinity for CH_4 (Bender & Conrad, 1992) but have not yet been isolated (Henckel *et al.*, 2000a; Holmes *et al.*, 1999; Knief *et al.*, 2003). These microorganisms can survive and thrive on the trace concentrations of atmospheric CH_4 fluxes between atmosphere and soils. They are affected by numerous environmental factors of the soils (see section 5.1). Thus, deciphering the mechanisms that can lead to an improvement of terrestrial CH_4 sinks may help with choosing more adapted approaches for the mitigation of climate change.

2.4. Methane-producing *Archaea* (methanogens)

2.4.1. Definition and taxonomy

Methanogens are CH_4-producing *Archaea*, or methanoarchaea, and earned their name from their ability to produce CH_4 as a result of energy production and growth. Methanogens are obligate CH_4 producers and strictly anaerobic microorganisms, which can feed on few substrates, depending on the type of CH_4-production pathway they use (see section 2.4.3). Methanogenesis, a form of anaerobic respiration, forms the terminal step of the anaerobic food chain by converting methanogenic substrates to CH_4 (Hedderich & Whitman, 2006).

Methanoarchaea constitute an ancient monophyletic lineage within the *Euryarcheota* phylum and are extremely diverse despite their limited substrate range (Boone *et al.*, 1993; Whitman *et al.*, 2001). They are classified into three classes, six orders, eleven families and 32 genera (**Table 1.1**).

Table 1.1: Taxonomy of major methanogens.

The extremophilic/tolerant methanogens are also colour-coded: blue: extreme thermophiles (growth >80°C); yellow: extreme halophiles (growth at 4.3 M NaCl).

Domain / Kingdom / Phylum	Class	Order	Family	Genus	Major CH_4 production pathway
Archaea / Archaebacteria / Euryarchaeota	*Methanobacteria*	*Methanobacteriales*	*Methanobacteriaceae*	*Methanobacterium* *Methanobrevibacter* *Methanosphaera* *Methanothermobacter*	H_2/CO_2, methylotrophic
			Methanothermaceae	*Methanothermus*	
	Methanococci	*Methanococcales*	*Methanococcaceae*	*Methanococcus* *Methanothermococcus*	H_2/CO_2
			Methanocaldococcaceae	*Methanocaldococcus* *Methanotorris*	
		Methanomicrobiales	*Methanomicrobiaceae*	*Methanomicrobium* *Methanoculleus* *Methanofollis* *Methanogenium* *Methanolacinia* *Methanoplanus*	H_2/CO_2
			Methanospirillaceae	*Methanospirillum*	
			Methanocorpusculaceae	*Methanocorpusculum* *Methanocalculus*	
		Methanocellales (RC-I)	*Methanocellacaea*	*Methanocella*	H_2/CO_2
		Methanosarcinales	*Methanosarcinaceae*	*Methanosarcina* *Methanococcoides*	Aceticlastic, methylotrophic
				Methanohalobium *Methanohalophilus* *Methanolobus* *Methanomethylovorans* *Methanimicrococcus* *Methanosalsum*	Methylotrophic
			Methanosaetaceae	*Methanosaeta*	Aceticlastic
	Methanopyri	*Methanopyrales*	*Methanopyraceae*	*Methanopyrus*	H_2/CO_2

A novel lineage of methanogens, rice cluster I (RC-I), was identified from rice roots by culture-independent approaches (Großkopf *et al.,* 1998; Lueders *et al.,* 2001). However, RC-I members are widely distributed in other habitats around the world (Conrad *et al.,* 2006). They form a distinct clade within the *Methanomicrobiales* and *Methanosarcinales* radiation based on the genetic analysis of 16S rRNA and *mcrA* (coding for the methyl-coenzyme M reductase) (Großkopf *et al.,* 1998; Lueders *et al.,* 2001). The RC-I methanogens have a selective advantage over the other methanoarchae that allows them to survive in the (oxic) rhizosphere of rice roots (Erkel *et al.,* 2006). This is because these organisms possess a unique set of antioxidants and O_2-sensitive enzymes. Recently, two novel members of RC-I were isolated in pure culture, *Methanocella paludicola* and *Methanocella arvoryzae,* and the new *Methanocellales* order was created (Sakai *et al.,* 2007; 2008; 2010) (see Table 1.1).

2.4.2. Ecology of methanogens

Most of the methanogens are mesophiles, however, several genera of methanogens (see Table 1.1) can be found in extreme environments such as marine geothermal sediments and hot springs, as well as in hypersaline sediments. Mesophilic methanogens are mostly found in marine and freshwater sediments, animal gastrointestinal tracts, rice paddies and anaerobic digestors (Liu & Whitman, 2008).

Because methanogens cannot use complex organic compounds, they need the presence of bacterial anaerobes in the environment to degrade these compounds into simple sugars and fatty acids. These are further fermented by syntrophic bacteria to form acetate, formate, hydrogen (H_2) and CO_2, which constitute the substrates for methanogenesis (also see Figure 1.2). Acetogens (acetate-producing bacteria) are part of this syntrophic consortium when methanogens consume H_2 and formate efficiently (Stams, 1994). Methanogens are found in anaerobic environments where CO_2 constitutes the main electron acceptor. However, because

CO_2 is less thermodynamically favourable, methanogens are outcompeted by sulfate-reducing bacteria, denitrifiers or iron-reducing bacteria if other electron acceptors such as SO_4^{2-}, NO_3^- or Fe^{3+}, respectively, are dominant. But since CO_2 is produced during fermentation, it never constitutes a limiting factor and anaerobic respiration by methanogens (*i.e.* methanogenesis) can become dominant in anaerobic environments (Liu & Whitman, 2008).

Most methanogens are H_2-consumers because they need H_2 as electron donor (see section 2.4.3). Therefore, they need to closely interact with H_2-producing microorganisms, and also as a way to dispose of reducing equivalents. This important interaction is called interspecies hydrogen transfer (Hedderich & Whitman, 2006; Stams & Plugge, 2009).

2.4.3. CH_4-production pathways

The complexity and uniqueness of methanogenesis as a form of anaerobic respiration resides in the requirement of six unusual coenzymes (ferredoxin (Fd), methanofuran (MFR), tetrahydromethanopterin (H_4MPT), coenzyme F_{420} (F_{420}), coenzyme M (CoM) and coenzyme B (CoB)); a long, multistep pathway and several unique membrane-bound enzyme complexes coupled to the generation of a proton gradient driving ATP synthesis (Ferry, 2010). The three main methanogenic substrates are CO_2, acetate and methyl-group containing compounds (such as methanol, methylated amines and methylated sulfides). Therefore, three distinct pathways for CH_4 production exist (Deppenmeier, 2002; Ferry, 1999) (see **Figure 1.4**). The hydrogenotrophic methanogenesis represents the production of CH_4 from reduction of CO_2 with H_2, while the conversion of acetate to CO_2 and CH_4 is called aceticlastic methanogenesis. They represent the two major pathways for CH_4 production by methanogens, whereas methylotrophic methanogenesis (utilisation of methyl groups) only has a minor contribution (Ferry, 2010).

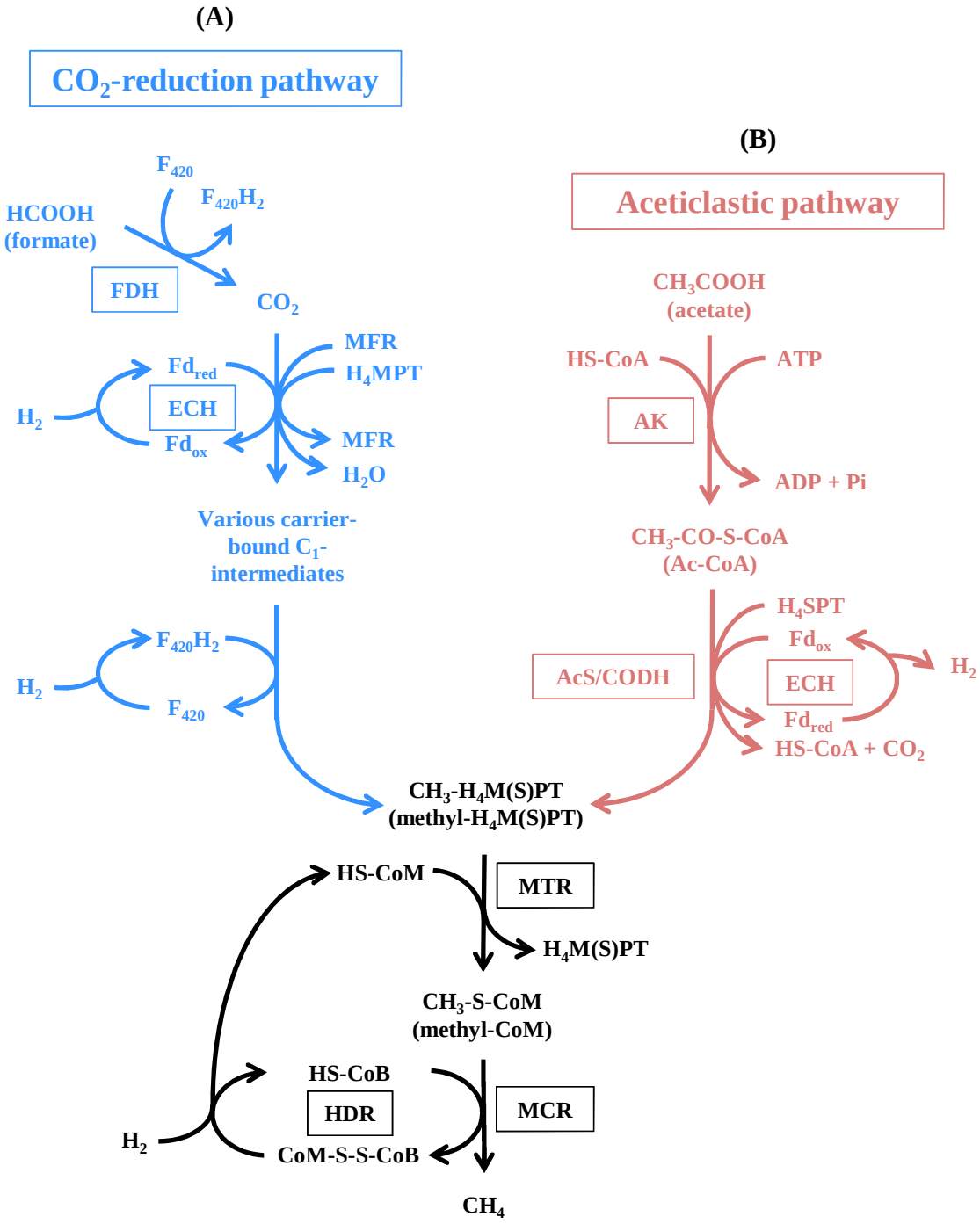

Figure 1.4: Major pathways of CH_4 production in methanogens: (A) CO_2-reduction pathway; (B) aceticlastic pathway.

Abbreviations: Ac-CoA = acetyl-coenzyme A; AcS/CODH = acetyl-CoA synthase and carbon monoxide dehydrogenase; AK = acetate kinase; CoB = coenzyme B; CoM = coenzyme M; ECH = enrgy-converting hydrogenase; F_{420} = coenzyme F_{420}; Fd = ferredoxin; FDH = formate dehydrogenase; H_4MPT = tetrahydromethanopterin; H_4SPT = tetrahydrosarcinapterin; HDR = heterodisulfide reductase; MCR = methyl-coenzyme M reductase; MFR = methanofuran; MTR = methyltransferase.

Similarities between the three types of methanogenesis

Although the intermediates and enzymatic reactions of the three pathways are different, they share common features in the final steps of CH_4 production (**Figure 1.4**). The hydrogenotrophic and aceticlastic pathways both result in the production of a carrier-bound methyl-intermediate. The carrier protein is H_4MPT in the hydrogenotrophic pathway and tetrahydrosarcinapterin (H_4SPT), a derivative of H_4MPT, in the aceticlastic pathway. The transfer of the methyl-group to CoM by a specific, membrane-bound methyltransferase (MTR), and the subsequent reduction of methyl-CoM to CH_4 by the key enzyme methyl-coenzyme M reductase (MCR) (see section 2.4.4), is common is all three pathways. During this last step, CoB is the electron donor and the heterodisulfide CoM-S-S-CoB is then formed. Finally, the heterodisulfide reductase (HDR), another membrane-bound enzyme, regenerates the thiols (**Figure 1.4**). Another important membrane-bound enzyme is the energy-converting hydrogenase (ECH), which is involved in the reduction/oxidation of Fd.

*CO_2-reduction pathway (**Figure 1.4A**)*

Most methanogens, including members of the novel RC-I clade, can oxidise CO_2, using H_2 as primary electron donor. Many hydrogenotrophs can also use formate as electron donor from the activity of the formate dehydrogenase (FDH) (Liu & Whitman, 2008). Hydrogenotrophic methanogenesis is the most complex pathway and requires all six of the unusual coenzymes. Basically, H_2/CO_2 methanogenesis consists in a series of enzymatic reactions involving one-carbon (C_1) intermediates bound to the carrier molecules MFR, H_4MPT and CoM (DiMarco *et al.*, 1990; Gorris & van der Drift, 1994).

*Aceticlastic pathway (**Figure 1.4B**)*

Only the species of *Methanosarcina* and *Methanosaeta* are aceticlastic methanogens but they are responsible for two-thirds of CH_4 biologically generated (Liu & Whitman, 2008). The cleavage of acetate forms CO_2 from the oxidation of the carboxyl-group, and CH_4 from the reduction of the methyl-group (Ferry, 1997). In this pathway, the unusual coenzymes Fd, H_4SPT, CoM and CoB are involved. Coenzyme A (CoA) is also used. Here, the acetate is activated to acetyl-CoA (Ac-CoA) by acetate kinase (AK), before the C-C bond is cleaved by the multienzyme complex of acetyl-CoA synthase and carbon monoxide dehydrogenase (AcS/CODH).

Methylotrophic pathway

Only members of the *Methanosarcinales* order, except the *Methanosaeta* genus, can use methylated compounds to produce CH_4 (Table 1.1). They are called methylotrophic methanogens but their pathway is not a major contributor of methanogenesis. More details are found elsewhere (Liu & Whitman, 2008).

2.4.4. MCR, the key enzyme in methanogenesis

This specific enzyme catalyses the transfer of CoM to the other thioenzyme CoB to form the heterodisulfide CoM-S-S-CoB and CH_4 (Thauer, 1998). MCR consists of a dimer of three subunits, α (McrA), β (McrB) and γ (McrG), and contains a unique porphinoid nickel (Ni)-containing active site called coenzyme F_{430} (Gunsalus & Wolfe, 1980). The enzyme's apparent molecular mass is about 300 kDa. Two distinct isoenzymes of methyl-CoM reductase were identified (Steigerwald *et al.*, 1993). The second enzyme, designated MRT for methyl reductase two, has a different substrate affinity (Bonacker *et al.*, 1993).

MCR activity is encoded by the *mcrBDCGA* operon, while the *mrtBDGA* operon codes for the MRT (Thauer, 1998). The equivalent of the gene *mcrC* is missing in the *mrt* operon (Pihl *et al.*, 1994). The products of the genes *mcrC* (McrC), *mcrD* (McrD) and *mrtD* (MrtD) are below 20 kDa. Their function is still unknown, but they might be involved in the post-translational modification of the α-subunit (Reeve *et al.*, 1997). *mcrA* constitutes a good functional marker for the analysis of the phylogeny of methanogens and gave congruent results compared to 16S rRNA-based studies (Conrad *et al.*, 2006).

Regulation of gene expression in methanogens is not well understood. Primary sensors and signal transduction cascades have not been elucidated (Hedderich & Whitman, 2006). However, evidence was found for regulation by trace elements and their availability. This is because many catabolic enzymes of methanogenesis contain trace metals (molybdenum, tungsten, selenium, nickel) in their active site. The coenzyme F_{390} has a hypothetical important role in cell. For example, a mutant of *Methanothermobacter thermoautotrophicus* was unable to form F_{390} under H_2-deprived conditions. As a consequence, this mutant was also lacking the ability to synthesise MCR (Pennings *et al.*, 1998). Availability of the substrate H_2 was found to regulate the formation of some key enzymes of methanogenesis, such as MRC. In *Methanothermobacter* species, the expression of the two isoenzymes of MCR is differently regulated by H_2 availability, with isoenzyme I (MCR) predominantly expressed in H_2-limiting conditions (Bonacker *et al.*, 1992; Morgan *et al.*, 1997).

3. Methane-oxidising *Bacteria* (methanotrophs)

3.1. Definitions

Aerobic methanotrophs

Methanotrophs are Gram-negative aerobic bacteria and earned their name from their ability to oxidise CH_4 in order to use it as a source of carbon (C) and energy. Methanotrophs are related to the methylotrophs because they can grow on one-carbon (C_1) substrates. But methylotrophs are not able to oxidise CH_4. Methanotrophs are often found at the anoxic/oxic interface of various habitats such as geothermal reservoirs, landfills, soils, peat bogs, wetlands or aquatic environments and sediments, where they consume the CH_4 diffusing from the underground methanogenic sources and are thus able to reduce or completely eliminate these CH_4 emissions (Conrad, 1996; Conrad & Rothfuss, 1991; Whalen *et al.*, 1990). Methanotrophs can also live in symbiosis with plants (*Sphagnum* spp. for which they produce CO_2 (Raghoebarsing *et al.*, 2005; van Winden *et al.*, 2010)) and with marine invertebrates from hydrothermal vents and cold seeps in the deep sea by providing nutrients to them in exchange of electron donors (Petersen & Dubilier, 2009). These methanotrophs are capable of oxidising high concentrations of CH_4 (>10,000 ppm) and can be isolated and cultivated. However, other methanotrophs have the ability to oxidise CH_4 only at atmospheric levels (~1.8 ppm) but they cannot be cultured, although they have been identified in upland soils (Henckel *et al.*, 2000a; Holmes *et al.*, 1999; Knief *et al.*, 2003).

The majority of aerobic methanotrophs use CH_4 as their sole source of C and energy (obligate methanotrophs). Yet, facultative methanotrophs exist and proved to be able to feed on multicarbon substrates (see section 3.4.2). The large majority of aerobic methanotrophs are neutrophiles (growth at a neutral pH of 6.5-7.5) and mesophiles (growth at temperatures

between 20 and 40°C) (Whittenbury *et al.*, 1970). Nevertheless, several species of extremotolerant methanotrophs have been isolated from extreme ecosystems displaying high and low values of temperature, pH or salinity (Trotsenko & Khmelenina, 2002). These extremophiles are shown in **Table 1.2**.

Anaerobic methanotrophs

Anaerobic oxidation of methane (AOM) can be achieved by particular methanotrophs, called anaerobic methanotrophic *Archeae* (ANME) and related to methanogens, by coupling with sulfate-reducing bacteria (SRB) (Boetius *et al.*, 2000; Hinrichs *et al.*, 1999). AOM involves the use of sulfate as electron acceptor to oxidise CH_4 *via* a process of reversed methanogenesis (Thauer & Shima, 2008). More recently, AOM coupled to denitrification was described by Raghoebarsing *et al.* (2006) from enriched cultures. In particular, the bacterium *Methylomirabilis oxyfera* was found to be able to reduce nitrite to form its own supply of O_2 *via* a new intra-aerobic pathway (Ettwig *et al.*, 2010). Genomic analysis revealed that this organism does not use reversed methanogenesis to oxidise CH_4 but rather the typical aerobic methanotrophic mechanism (Wu *et al.*, 2011). Apart from using sulfate and nitrate/nitrite as electron acceptors, AOM was also found to be dependant of the metals manganese and iron in marine environments (Beal *et al.*, 2009).

Table 1.2: Taxonomy of aerobic methanotrophs.

The extremophilic/tolerant methanotrophs are also colour-coded: orange: psychrophiles (growth at 5-10°C but not above 20°C); purple: haloalkaliphiles (growth at 12% NaCl and at pH of 9-11); yellow: halophiles (growth at 15% NaCl); blue: thermophiles (growth >45°C); green: acidophiles (growth at pH of 4.5-5.5); grey: thermoacidophiles (growth at 60°C and at pH of 2).

Domain: *Bacteria* / Kingdom: *Eubacteria* / Phylum: *Proteobacteria*				Phylum: *Verrucomicrobia*
Class: *Gammaproteobacteria* Order: *Methylococcales*			Class: *Alphaproteobacteria* Order: *Rhizobiales*	Class: *Verrucomicrobiae* Order: *Methylacidiphilales*
Family: *Methylococcaceae*			Family: *Methylocystaceae*	Family: *Methylacidiphilaceae*
Methylobacter	***Methylomonas***	***Methylocaldum***	***Methylocystis***	***Methylacidiphilum***
Methylobacter bovis	*Methylomonas aurantiaca*	*Methylocaldum gracile* [5]	*Methylocystis echinoides*	*Methylacidiphilum infernorum* [11]
Methylobacter chroococcum	*Methylomonas fodinarum*	*Methylocaldum szegediense* [5]	*Methylocystis heyeri* [10]	*Methylacidiphilum fumarolicum* [12]
Methylobacter luteus	*Methylomonas methanica*	*Methylocaldum tepidum* [5]	*Methylocystis hirsute*	*Methylacidiphilum kamchatkensis* [13]
Methylobacter marinus	*Methylomonas rubra*	***Methylococcus***	*Methylocystis methanolicus*	
Methylobacter psychrophilus [1]	*Methylomonas scandinavica* [1]	*Methylococcus capsulatus* [15]	*Methylocystis minimus*	
Methylobacter tundripaludum	***Methylosarcina***	*Methylococcus thermophilus* [1]	*Methylocystis parvus*	
Methylobacter vinelandii	*Methylosarcina fibrata*	***Methylogaea***	*Methylocystis pyriformis*	
Methylomicrobium	*Methylosarcina lacus*	*Methylogaea oryzae* [21]	*Methylocystis rosea*	
Methylomicrobium agile	*Methylosarcina quisquiliarum*		***Methylosinus***	
Methylomicrobium album	***Methylosphaera***		*Methylosinus sporium*	
Methylomicrobium buryatense [1]	*Methylosphaera hansonii* [2]		*Methylosinus trichosporium*	
Methylomicrobium pelagicum [1]	***Methylothermus***		Family: *Beijerinckiaceae*	
Methylohalobius	*Methylothermus thermalis* [4]		***Methylocapsa***	
Methylohalobius crimeensis [3]	*Methylothermus subterraneus* [14]		*Methylocapsa acidiphila* [6]	
Methylosoma	***Methylovulum***		*Methylocapsa aurea* [16]	
Methylosoma difficile	*Methylovulum miyakonense* [18]		***Methylocella***	
			Methylocella palustris [7]	
Clonothrix	***Crenothrix***		*Methylocella silvestris* [8]	
Clonothrix fusca [19]	*Crenothrix polyspora* [20]		*Methylocella tundrae* [9]	
			Methyloferula	
			Methyloferula stellata [17]	
Type I		Type X	Type II	

References: [1] Trotsenko & Khmelenina (2002); [2] Bowman *et al.* (1997); [3] Heyer *et al.* (2005); [4] Tsubota *et al.* (2005); [5] Bodrossy *et al.* (1997); [6] Dedysh *et al.* (2002); [7] Dedysh *et al.* (2000); [8] Dunfield *et al.* (2003); [9] Dedysh *et al.* (2004); [10] Dedysh *et al.* (2007); [11] Dunfield *et al.* (2007); [12] Pol *et al.* (2007); [13] Islam *et al.* (2008); [14] Hirayama *et al.* (2010); [15] Bowman *et al.* (1993); [16] Dunfield *et al.* (2010); [17] Vorobev *et al.* (2010); [18] Iguchi *et al.* (2011); [19] Stoecker *et al.* (2006); [20] Vigliotta *et al.* (2007); [21] Geymonat *et al.*(2010).

Oxidation of CH_4

It is performed in methanotrophs by a unique enzyme called methane monooxygenase (MMO). MMO exists in two forms: a soluble form (sMMO) and a membrane-bound, or particulate, form (pMMO) (Hakemian & Rosenzweig, 2007; Lipscomb, 1994; Prior & Dalton, 1985b). Although these two enzymes catalyse the same reaction, their mechanism and origin are very different (Holmes *et al.*, 1995) (see section 3.3.3). The oxidation of CH_4 into methanol is followed by the formation of formaldehyde by the enzyme methanol dehydrogenase (MDH). Formaldehyde constitutes the central point of methanotroph metabolism as two pathways were identified for its assimilation and these were used to separate methanotrophs into two groups (type I and type II) (**Figure 1.5**). The type I methanotrophs use the ribulose monophosphate (RuMP) pathway whereas the type II methanotrophs assimilate formaldehyde through the serine pathway (Lawrence & Quayle, 1970; Trotsenko & Murrell, 2008). This distinction was correlated by the presence of intracytoplasmic membranes (ICM) typical to each pathway. However, some exceptions were recently observed in the genera *Methylocella* and *Methylacidiphilum* (Table 1.3).

Only a portion (~50%) of the formaldehyde is assimilated into cellular biomass, *i.e.* for the production of energy (Prior & Dalton, 1985b). The remaining is converted into formate and ultimately into CO_2 (**Figure 1.5**). For this reason, methanotrophs are seen as playing a key role in climate mitigation (Conrad, 1996).

3.2. Taxonomy of aerobic methanotrophs

For a long time, the taxonomy of aerobic methanotrophs was fairly straightforward (Bowman *et al.*, 1993; Whittenbury *et al.*, 1970) but recent progress shed more light on their complex organisation due to the existence of several organisms that did not “follow the rules”. To

date, aerobic methanotrophs have representatives in two phyla, three orders and four families. A total of 20 genera and 52 species have been identified (**Table 1.2**).

Based on morphological, physiological and genetic differences (see section 3.3), CH_4-oxidising bacteria were divided into the two groups type I and type II. Type X was also created to accommodate methanotrophs of the genus *Methylococcus* and later, of the genera *Methylocaldum* and *Methylogaea* (**Table 1.2**). Type X methanotrophs share characteristics of both type I and type II (see section 3.4.1). However, type X microorganisms should be considered a sub-set of type I methanotrophs (Bowman *et al.*, 1993; Semrau *et al.*, 2010). Type I (and type X) methanotrophs belong to the *Methylococcaceae* family of the class of the *Gammaproteobacteria* of the *Proteobacteria* phylum, whereas type II methanotrophs are *Alphaproteobacteria* divided into two families: the *Methylocystaceae* and the *Beijerinckiaceae* (Bowman *et al.*, 1993; Op den Camp *et al.*, 2009). Among the *Methylococcaceae*, two unique genera are present: *Clonothrix* and *Crenothrix* (Stoecker *et al.*, 2006; Vigliotta *et al.*, 2007). The two species that represent them are filamentous, sheathed microorganisms with a unique and complex life complex and were isolated from groundwater environments. Although 16S rRNA-based studies relate them to type I methanotrophs, *Crenothrix* shows a very divergent encoding sequence for pMMO (Stoecker *et al.*, 2006) (see section 3.5.2).

Recently, CH_4-oxidising bacteria of the *Verrucomicrobia* phylum were identified and the three species that were isolated from geothermal habitats in Italy, New Zealand and Russia (Dunfield *et al.*, 2007; Islam *et al.*, 2008; Pol *et al.*, 2007) were classified under the *Methylacidiphilum* family and *Methylacidiphilales* order (Op den Camp *et al.*, 2009) (**Table 1.2**). These methanotrophic *Verrucomicrobia* represent a unique group of methanotrophs although they share many characteristics of methanotrophic *Proteobacteria*, especially of *Alphaproteobacteria* (type II methanotrophs). However, it should be clear that aerobic

methanotrophs are now of two types: proteobacterial methanotrophs (type I and type II) and verrucomicrobial methanotrophs (see section 3.4.3).

3.3. Differences between aerobic methanotrophs

These differences are summarised in **Table 1.3**.

3.3.1. Intracytoplasmic membrane (ICM) formation

The ICM is an important characteristic since all type I methanotrophs contain ICM organised as bundles of vesicular disks distributed throughout the cell and perpendicular to the cell periphery (Trotsenko & Murrell, 2008). The RuMP pathway associated to this type I ICM and to the assimilation of formaldehyde used to be unique to type I methanotrophs. However, a novel type II methanotroph, *Methyloferula stellata*, was recently found to use the RuMP pathway (Vorobev *et al.*, 2010), where all the other type II methanotrophs use the serine pathway to assimilate formaldehyde. The ICM formation in type II methanotrophs is different. For the members of the *Methylocystaceae*, ICM are stacks packed in parallel to the periphery of the cell (Trotsenko & Murrell, 2008). However, the methanotrophs of the *Beijerinckiaceae* have a different ICM formation: in *Methylocapsa* sp. ICM are membrane vesicles packed parallel to only one side of the cell membrane (described as type III by Dedysh *et al.* (2002)), whereas *Methylocella* spp. contain vesicular membranes connected to the ICM (Dedysh *et al.*, 2000) (Table 1.3). Verrucomicrobial methanotrophs do not possess an ICM system that is found in proteobacterial methanotrophs (see section 3.4.3).

3.3.2. Formaldehyde assimilation pathways

After oxidation of CH_4 into formaldehyde, two metabolic pathways are available (the RuMP and serine pathway) resulting in the synthesis of (phospho)trioses. These pathways were reviewed in great length by Trotsenko and Murrell (2008) and will be discussed briefly here.

Table 1.3: Some characteristics of known aerobic methanotrophs.

When not mentioned, data were compiled from Semrau *et al.* (2010) and Op den Camp *et al.* (2009).

Gram-negative, aerobic	Type I	Type X	Type II		
Phylum/class	*Gammaproteobacteria*		*Alphaproteobacteria*		*Verrucomicrobia*
Genera	*Methylobacter, Methylomicrobium, Methylomonas, Methylosarcina, Methylosphaera, Methylohalobius, Methylothermus, Methylosoma, Methylovulum, Clonothrix, Crenothrix*	*Methylocaldum, Methylococcus, Methylogaea*	*Methylocystis, Methylosinus*	*Methylocapsa, Methylocella, Methyloferula*	*Methylacidiphilum*
Methanotrophy	Obligate		Obligate	Obligate Facultative [*]	Obligate
ICM formation	Bundles of vesicular disks distributed throughout the cell and perpendicular to cell periphery		*Methylocystaceae* – membrane stacks packed in parallel to cell periphery *Methylocapsa* – membrane vesicles packed parallel to only one side of cell membrane *Methylocella* – vesicular membranes connected to ICM		No but carboxysome-like structures or vesicular membranes
Formaldehyde assimilation	RuMP pathway	RuMP pathway; Low levels of enzymes of the serine pathway	Serine pathway	Serine pathway RuMP pathway [**]	A variant of the serine pathway
MMO activity	pMMO; sMMO [€]		pMMO; sMMO	pMMO [‡]; sMMO [‡‡]	pMMO
pmoA genotype affiliation associated with oxidation of atmospheric CH_4 [§]	USCγ; cluster 1, cluster 3 *Methylococcaceae*		*Methylocystaceae*	USCα; cluster 5 *Beijerinckiaceae*	*Methylacidiphilaceae*
Major PLFA biomarkers	14:0; 16:0; 16:1ω7c 18:1ω7 [#]	16:0; 16:1ω7c	18:1ω8c 18:2 ω6c,12c; 18:2 ω7c,12c [##]	18:1ω7c	i14:0; a15:0; 18:0
Nitrogen fixation	*Methylosphaera, Methylosoma, Methylogaea* and *Methylococcus* only [†]		yes		yes
RubisCO activity	no	yes	*Methyloferula* only [¥]		yes
G+C (mol%)	43-63	57-65	62-67	56-63	41-46

[*] Only in *Methylocella* (Dedysh *et al.*, 2005) and *Methylocapsa aurea* (Dunfield *et al.*, 2010). ** Only in *Methyloferula* (Vorobev *et al.*, 2010). [€] Only in *Methylomonas* (Koh *et al.*, 1993; Shigematsu *et al.*, 1999), *Methylomicrobium* (Fuse *et al.*, 1998), *Methylovulum* (Iguchi *et al.*, 2010a; 2010b) and *Methylococcus* (Bowman *et al.*, 1993). [‡] Not in *Methylocella* (Dedysh *et al.*, 2005) or *Methyloferula* (Vorobev *et al.*, 2010). [‡‡] Not in *Methylocapsa* (Dedysh *et al.*, 2002; Dunfield *et al.*, 2010). [§] Kolb (2009). [#] Only in *Methylohalobius* (Heyer *et al.*, 2005). [##] Bodelier *et al.* (2009). [†] From, respectively, Bowman *et al.* (1997), Rahalkar *et al.* (2007), Geymonat *et al.* (2010), Bowman *et al.* (1993). [¥] Vorobev *et al.* (2010).

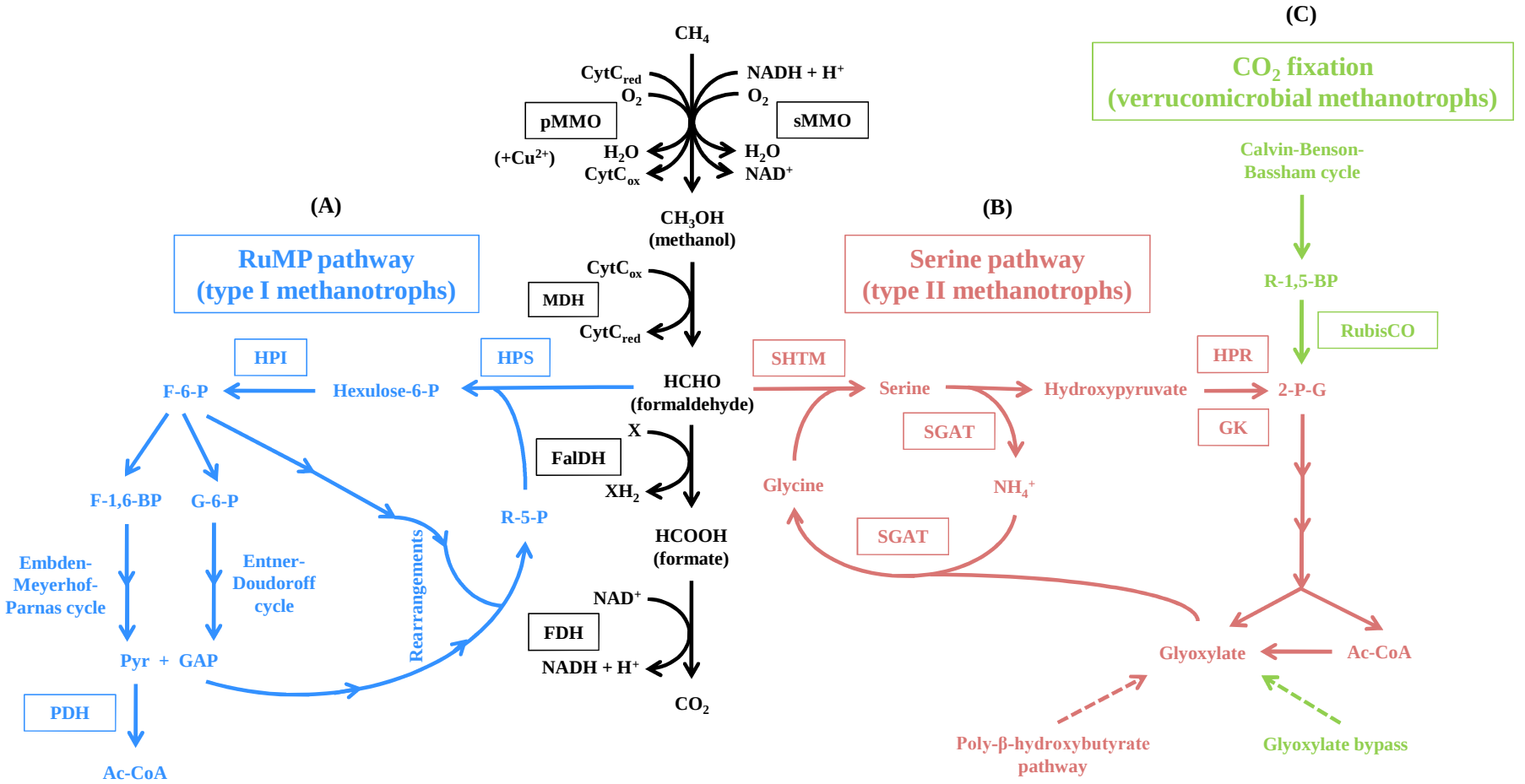

Figure 1.5: Oxidation of CH_4 and simplified pathways of carbon assimilation in methanotrophs: (A) RuMP pathway of type I methanotrophs; (B) Serine pathway of type II methanotrophs; (C) CO_2 fixation *via* Calvin-Benson-Bassham cycle.

Multiple arrows represent consecutives enzymatic reactions which are not detailed here. Abbreviations: Ac-CoA = acetyl-coenzyme A; CytC = cytochrome C; FalDH = formaldehyde dehydrogenase; FDH = formate dehydrogenase; F-1,6-BP = fructose-1,6-bisphosphate; G-6-P = glucose-6-phosphate; GAP = glyceraldehydes-3-P; GK = glycerate kinase; HPI = hexulose-6-P isomerase; HPS = hexulose-6-P synthase; MDH = methanol dehydrogenase; Pyr = pyruvate; PDH = pyruvate dehydrogenase; R-5-P = ribulose-5-P; R-1,5-BP = ribulose-1,5-bisphosphate; SGAT = serine-glyoxylate aminotransferase; SHTM = serine-hydroxytransmethylase; 2-P-G = 2-phospho-glycerate.

*The RuMP cycle (**Figure 1.5A**).*

In a first step, formaldehyde is combined to a ribulose-5-phosphate (R-5-P) molecule *via* the activity of a key enzyme, the hexulose-6-phosphate synthase (HPS). The resulting product is quickly isomerised to fructose-6-P (F-6-P) by the unique hexulose phosphate isomerase (HPI). In the second step, the phosphohexose is cleaved into pyruvate (Pyr) and glyceraldehyde-3-P (GAP) *via* variants of the Embden-Meyerhof-Parnas (*i.e.* glycolysis) and Entner-Doudoroff cycles. Pyruvate can then be oxidise by the pyruvate dehydrogenase (PDH) to acetyl-coenzyme A (Ac-CoA), which constitutes the start of tricarboxylic acid (TCA) cycle (also known as citric acid cycle or Krebs cycle) involved in the production of energy and of precursors of some amino acids. However, in type I and type X methanotrophs, this cycle is incomplete due to the absence of the enzymatic activity of the alpha-ketoglutarate dehydrogenase (αKGDH) (Wood *et al.*, 2004). Nonetheless, the genes encoding this enzyme were present in the genome of *Methylococcus capsulatus* (Bath) (Ward *et al.*, 2004). The last step of the RuMP pathway is the regeneration of the R-5-P from GAP and F-6-P through a series of reactions (rearrangements).

*The serine pathway (**Figure 1.5B**).*

In a first step, formaldehyde reacts with glycine to form serine *via* the activity of a key enzyme, the serine-hydroxytransmethylase (SHTM). Next, the specific enzyme serine-glyoxylate aminotransferase (SGAT) transfers the amino group of serine to glyoxylate (transamination) resulting in the formation of glycine and hydroxypyruvate. Then, the unique enzymes hydroxypyruvate reductase (HPR) and glycerate kinase (GK) form 2-phospho-glycerate (2-P-G). Other enzymes specific to the serine pathway subsequently form glyoxylate and Ac-CoA. From this point, Ac-CoA can enter a complete TCA cycle due to the presence an active αKGDH in type II methanotrophs. The last step of the serine pathway is

the regeneration of glycine from the first step but also by oxidation of Ac-CoA into glyoxylate. Alternatively, glyoxylate can be regenerated from the biosynthesis pathway of poly-β-hydroxybutyrate (Korotkova *et al.*, 2002), which is known as a storage compound in methanotrophs (Kolb, 2009; Murrell & Jetten, 2009). In most methanotrophs, and in particular in type II (except in *Methylacidiphilum* – see section 3.4.3), glyoxylate cannot be formed through the glyoxylate bypass, due to the absence of the enzymes isocitrate lyase and malate synthase (Trotsenko & Murrell, 2008). Yet, Chen *et al.* (2010) identified the genes encoding the enzymes of the glyoxylate shunt in *Methylocella silvestris*.

3.3.3. MMO activity

The first step in the oxidation of CH_4 by methanotrophs is achieved by the specific enzyme CH_4 monooxygenase (MMO) (Hakemian & Rosenzweig, 2007; Lieberman & Rosenzweig, 2004; Semrau *et al.*, 2010). Both enzymatic forms require O_2 to perform the reaction but they use a different electron donor/acceptor system: NADH + H^+/NAD^+ in the case of sMMO and cytochrome C with pMMO (**Figure 1.5**). pMMO is present in all methanotrophs, except in *Methylocella* and *Methyloferula* spp. (Dedysh *et al.*, 2000; 2004; 2003; Vorobev *et al.*, 2010). Yet, many methanotrophs (*Methylomonas*, *Methylomicrobium*, *Methylovulum*, *Methylococcus*, *Methylocystis* and *Methylosinus*) contain both enzymes (**Table 1.3**).

Detection of MMO activity

The MMO enzymatic activity is unique to methanotrophs and its putative active site is encoded by the *pmoA* (pMMO) or *mmoX* (sMMO) genes (see section 3.5.1). Thus, these two functional genes represent ideal molecular markers for the study of methanotroph communities. In fact, phylogenetic studies based on 16S rRNA, *mmoX* and *pmoA* sequences gave congruent results and allowed to observe a distinct separation between type I and type II methanotrophs (Holmes *et al.*, 1999; Horz *et al.*, 2001; McDonald *et al.*, 2008).

3.3.4. Phospholipids fatty acid (PLFA) signature

Another difference between type I, type X and type II methanotrophs, which makes them distinguishable, is the range of PLFAs present in their cell membrane (see section 4.1) (**Table 1.3**). The PLFAs 14:0, 16:0 and 16:1ω7 are most abundantly found in type I methanotrophs while type II methanotrophs contain mainly the PLFAs 18:1ω7c (*Beijerinckiaceae*) and 18:1ω8c (*Methylocystaceae*) (Bodelier *et al.*, 2009; Bowman *et al.*, 1993). Recently, the PLFAs 18:2ω6c,12c and 18:2ω7c,12c were found to be characteristically found in members of the *Methylocystaceae* family (Bodelier *et al.*, 2009).

However, one exception exists with *Methylohalobius crimeensis*, a type I methanotroph that contains 18:1ω7 as a major PLFA (Heyer *et al.*, 2005). Other PLFAs, such as 16:1ω8c or 18:1ω9c are present in both types of methanotrophs but they are less abundant (Dedysh *et al.*, 2007). The novel methanotrophs of the *Methylacidiphilum* genus contain a unique PLFA signature composed of i14:0, a15:0 and 18:0 (Op den Camp *et al.*, 2009).

3.3.5. N_2 fixation

Another difference that used to be considered important between type I and type II methanotrophs was the ability of type II (and type X) methanotrophs to assimilate atmospheric nitrogen (N_2) whereas it was believed type I could not (Hanson & Hanson, 1996; Murrell & Dalton, 1983). However, recent findings revealed that members of the genera *Methylosphaera*, *Methylosoma* and *Methylogaea* can fix N_2 and possess the *nifH* gene (Bowman *et al.*, 1997; Geymonat *et al.*, 2010; Rahalkar *et al.*, 2007). Similarly, members of the *Methylacidiphilum* genus were identified as being able to assimilate N_2 (Khadem *et al.*, 2010; Op den Camp *et al.*, 2009).

3.4. Particularities to the type I/type II separation

3.4.1. The case of type X methanotrophs

As mentioned earlier, type X methanotrophs display characteristics of both type I and type II cells (**Table 1.3**). Type X methanotrophs assimilate formaldehyde using the RuMP pathway but they also show low levels of the enzymes of the serine pathway. Furthermore, they have the genes encoding the sMMO enzyme, which is mostly found in type II methanotrophs. The PLFA signature of type X methanotrophs is similar to type I representatives. Finally, the G+C content in type X methanotrophs is more characteristic of type II representatives because type I methanotrophs tend to have a lower G+C content (Table 1.3).

Until recently, type X methanotrophs used to be the only ones to possess the ribulose bisphosphate carboxylase/oxygenase (RubisCO) activity (fixation of CO_2) (Baxter *et al.*, 2002; Stanley & Dalton, 1982). However, the novel type II methanotroph *Methyloferula stellata* (as well as members of *Methylacidiphilum* – see section 3.4.3) also display this activity (Vorobev *et al.*, 2010).

3.4.2. The case of facultative methanotrophs

Methylocella species are unique to the other methanotrophs because they proved to be able to grow on several substrates containing C-C bonds, *i.e.* they are facultative methanotrophs. The multicarbon metabolites include acetate, pyruvate, succinate, malate and ethanol (Dedysh *et al.*, 2005). This ability was explained by the fact that *Methylocella* only relies on the sMMO enzyme to oxidise CH_4 because of the lack of the pMMO enzyme (Dedysh *et al.*, 2000; Dedysh *et al.*, 2004; Dunfield *et al.*, 2003). Remarkably, it is now well known that sMMO is a very versatile enzyme capable of oxidising a wide range of alkanes, aliphatics and aromatic

compounds (Colby *et al.*, 1977), which could explain the facultative methanotrophy of *Methylocella*. However, the evolutionary reasons behind obligate methanotrophy are still unknown (Dedysh *et al.*, 2005; Theisen & Murrell, 2005). In most type II methanotrophs, the glyoxylate bypass is not active (see above). This cycle is essential for growth on two-carbon compounds (Chung *et al.*, 1988) but seems to be functioning in *Methylocella silvestris* (Chen *et al.*, 2010).

Recently, another facultative type II methanotroph was isolated, *Methylocapsa aurea* (Dunfield *et al.*, 2010). Like *Methylocella*, it is found in acidic soils. Yet, it is quite different since the pMMO enzyme was detected but the sMMO was not. And like *Methylocapsa acidiphila*, the typical ICM formation was present (Table 1.3). In contrast, the recently identified type I methanotroph *Crenothrix polyspora* also proved to be facultatively methanotrophic in the absence of CH_4 (Stoecker *et al.*, 2006).

3.4.3. The case of *Methylacidiphilum*

Until recently, methanotrophic bacteria were only represented by *Proteobacteria* (α- and γ-classes). Yet, the novel *Methylacidiphilum* genus does not fit in the type I/type II classification of methanotrophs, except that its members are obligate and aerobic cells. Based on 16S rRNA gene analyses, *Methylacidiphilum* belongs to the *Verrucomicrobia* phylum. In contrast, based on *pmoA* phylogeny, *Methylacidiphilum* appears to be evolutionary related to proteobacterial methanotrophs (Hou *et al.*, 2008; Op den Camp *et al.*, 2009).

Verrucomicrobial methanotrophs possess a different membrane system than the ICM system found in proteobacterial methanotrophs but like most type II methanotrophs, *Methylacidiphilum* uses the pMMO enzyme to oxidise CH_4 (Table 1.3). Genomic analysis postulated the presence of a possible serine pathway to assimilate formaldehyde in verrucomicrobial methanotrophs. However, it is unclear whether formaldehyde is a precursor

for C fixation. Indeed, the enzyme glycerate kinase, essential to the serine pathway, was not detected in the genome. Instead, it is believed that *Methylacidiphilum* could primarily fix carbon autotrophically *via* a complete Calvin-Benson-Bassham cycle (Op den Camp *et al.*, 2009) (**Figure 1.5C**). In fact, it was observed that the growth of *Methylacidiphilum infernorum* was strongly dependant on CO_2 (Dunfield *et al.*, 2010). Nevertheless, Op den Camp *et al.* (2009) suggested that *Methylacidiphilum* members are true methanotrophs rather than ammonia oxidisers since all three isolated strains were not able to grow on NH_4^+-containing medium in the absence of CH_4 (see below). Verrucomicrobial methanotrophs also possess a complete TCA cycle but unlike type II methanotrophs, they are able to replenish their stocks of glyoxylate through an operational set of enzymes (isocitrate lyase and malate synthase) of the glyoxylate bypass (Hou *et al.*, 2008).

3.5. sMMO *vs*. pMMO

3.5.1. Structure of sMMO and pMMO

Soluble methane monooxygenase (sMMO)

sMMO is a well-characterised enzyme. It consists of three components: a hydroxylase, a reductase (MmoC) and a regulatory protein, or protein B (MmoB) (Stirling & Dalton, 1979). The hydroxylase component of the enzymatic complex consists of a dimer of three subunits (α, β and γ) of 61, 45 and 20 kDa, respectively. The α-subunit acts as the active site of CH_4 catalysis and is characterised by the presence of a non-heme, binuclear Fe-centre, that is to say two iron (Fe) atoms bridged by an oxygen atom (Green & Dalton, 1985). MmoC (39 kDa) contains a Fe_2S_2 and FAD centre and uses NADH + H^+ for the reduction reaction (Fox *et al.*, 1989). MmoB (16 kDa) acts as a coupling protein of the oxidation of NADH and CH_4, and its activity might be controlled by proteolysis of its terminal amino acid (Lloyd *et al.*, 1997). A model of the structure of sMMO was proposed by Murrell *et al.* (2000a).

sMMO is coded by the *mmoXYBZDC* gene cluster (Stainthorpe *et al.*, 1990) (**Figure 1.6**).

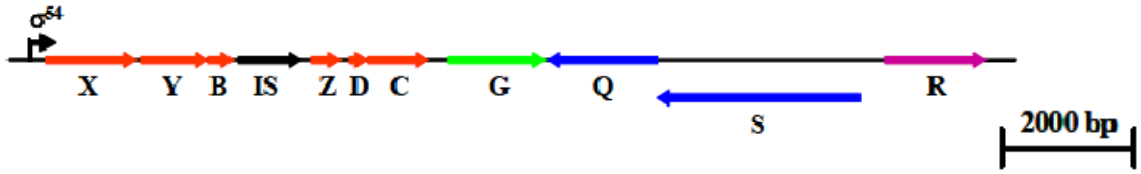

Figure 1.6: Physical map of the sMMO operon from *Methylococcus capsulatus* (Bath).
The genes encoding for the sMMO enzyme (*mmoXYBZDC*) are highlighted in red. The regulatory genes, *mmoG* and *mmoR* are highlighted in green and purple, respectively. The genes encoding for a two-component senor-regulatory system are highlighted in blue. The location and direction of transcription from the σ^{54} promoter is indicated with a black arrow. The gene boundaries are shown to scale and are indicated by the scale bar.

Among this (*mmo*) operon of six genes, *mmoX*, *mmoY* and *mmoZ* code for, respectively, the α-, β- and γ-subunits of the hydroxylase component, while *mmoB* and *mmoC* encode MmoB and MmoC, respectively. *mmoD* (also know as *orfY*) codes for the protein MmoD (12 kDa), the exact role of which is unknown except that it is probably involved in the assembly of the di-iron centre of the hydroxylase component (Merkx & Lippard, 2002). The genes *mmoR* and *mmoG* are also found in the vicinity of the *mmo* operon, although their exact location will vary among methanotrophs (Scanlan *et al.*, 2009). These genes were found to code for proteins involved in the regulation of sMMO expression (Csáki *et al.*, 2003; Scanlan *et al.*, 2009; Stafford *et al.*, 2003). *mmoR* codes for MmoR, a σ^{54}-dependant transcriptional activator/regulator for the transcription of *mmoXYBZDC*. *mmG* encodes MmoG, a putative GroEL-like chaperone, that could be involved in the folding and/or assembly of sMMO (Scanlan *et al.*, 2009; Stafford *et al.*, 2003). In *Methylococcus capsulatus* (Bath), *mmoS* and *mmoQ* were found to code for a putative two-component signal transduction system (MmoS/MmoQ) (Csáki *et al.*, 2003). MmoS would act as copper-sensing element, which phosphorylation would signal MmoQ to interact with MmoR for the activation of sMMO production. A summary diagram of the model for the transcriptional regulation of the *mmoXYBZDC* operon can be found elsewhere (Csáki *et al.*, 2003; Hakemian & Rosenzweig, 2007). sMMO has a broad range of substrate and hence is seen as a useful tool for pollutant bioremediation (Hanson & Hanson, 1996; Semrau *et al.*, 2010; Shigematsu *et al.*, 1999).

Particulate methane monooxygenase (pMMO)

pMMO, in contrast to sMMO, is a less well understood enzyme. It consists of a trimer of three subunits (α, β and γ) of 45, 27 and 23 kDa, respectively (Zahn & Dispirito, 1996). The 45- and 27-kDa subunits are thought to constitute the active site of pMMO, as they can be inhibited by the suicide substrate acetylene (DiSpirito *et al.*, 1991; Prior & Dalton, 1985a). pMMO is an iron- and copper-containing enzyme but much debate exists as to the exact number and type of metal centres, as well as on the nature of the electron donor (Lieberman & Rosenzweig, 2004; Semrau *et al.*, 2010).

pMMO is coded by the *pmoCAB* gene cluster (Gilbert *et al.*, 2000; Semrau *et al.*, 1995; Stolyar *et al.*, 1999) (**Figure 1.7**). Among this (*pmo*) operon of three genes, *pmoC*, *pmoA* and *pmoB* code for the α-, β- and γ-subunits, respectively, of pMMO.

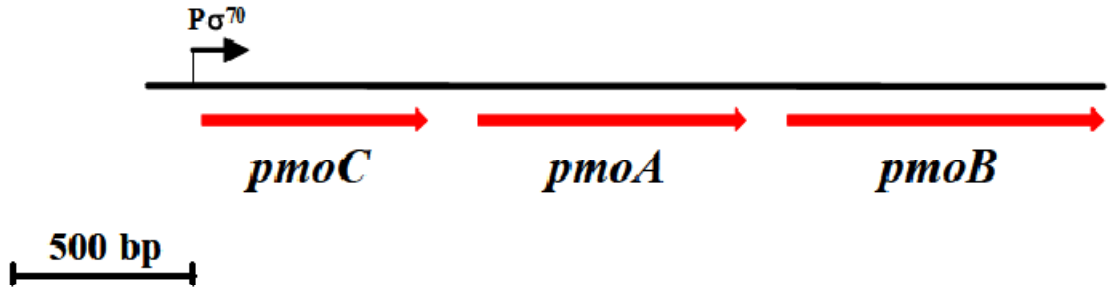

Figure 1.7: Structural gene organisation of the pMMO operon in methanotrophs.
The *pmoCAB* operon encodes for the α-, β- and γ-subunits of pMMO, respectively. The location and direction of transcription from the σ^{70} promoter is indicated with the black arrow. The gene boundaries are shown to scale and are indicated by the scale bar.

The *pmoA* gene was described as highly conserved while *pmoCAB* was shown to be evolutionary linked to the *amoCAB* gene cluster, coding for the ammonia monooxygenase (AMO), found in nitrifying bacteria of the *Betaproteobacteria* and *Gammaproteobacteria* phyla (Holmes *et al.*, 1995). Despite a very different physiological function, pMMO and AMO share a very similar polypeptide structure and can both oxidise methane and ammonia,

although their affinity for these substrates are different, and they are activated by different concentrations of copper (Hanson & Hanson, 1996). A second *pmoCAB* operon (*pmoCAB2*) was identified in *Methylocystis* sp. strain SC2 (see below) and was reported to code for a functional equivalent to the conventional pMMO (Ricke *et al.*, 2004). Furthermore, the *pmoCAB2* gene cluster showed a degree of conservation similar to the *pmoCAB* and *amoCAB* operons, confirming an evolutionary relationship rather than a recent horizontal transfer. However, the authors suggested that the novel pMMO-like enzyme may have a different functional role in *Methylocystis* strain SC2. This was confirmed later by the evidence that the products of *pmoCAB1* and *pmoCAB2* (PmoCAB1 and PmoCAB2, respectively) were two isoenzymes with different CH_4 oxidation kinetics (Baani & Liesack, 2008). Indeed, the authors showed that pMMO1 was activated when CH_4 concentrations were >600 ppm, whereas pMMO2 was expressed constitutively and could oxidise CH_4 with an apparent K_m that would correspond to atmospheric CH_4 mixing ratios (Bender & Conrad, 1992), which was recently confirmed by Kravchenko *et al.* (2010). Thus, this would provide these organisms with a mechanism for survival in dry upland soil for extended time by using atmospheric CH_4 (Baani & Liesack, 2008). This would be in agreement with the frequent detection of *Methylocystaceae* in forest soils (Kolb, 2009), and the ability of *Methylocystis* spp. to use reserve material such as poly-β-hydroxybutyrate (Knief & Dunfield, 2005).

3.5.2. Gene copy number and variations

It is now well known that most methanotrophs that possess the pMMO activity have two nearly identical copies of the *pmoCAB* operon (Gilbert *et al.*, 2000; Semrau *et al.*, 1995; Stolyar *et al.*, 1999; Ward *et al.*, 2004). A third copy of *pmoC* (*pmoC3*), coding for a functional PmoC that may be essential to cell growth, was also found in *Methylococcus capsulatus* (Bath) (Semrau *et al.*, 1995; Stolyar *et al.*, 1999). The physiological explanation

for the presence of multiple copies of the *pmoCAB* operon is not clear. However, Stolyar *et al.* (1999; 2001) showed that the relative expression of the two operons was dependent on the copper levels.

Remarkably, a novel *pmoA*-like gene, named *pmoA2*, was discovered in *Methylocystis* sp. strain SC2 and *Methylosinus trichosporium* strain KS21 (Dunfield *et al.*, 2002). *pmoA2* is actually widely found in many *Methylocystaceae* type II microorganisms but not in type I methanotrophs (Tchawa Yimga *et al.*, 2003). All proteobacterial *pmoA2* sequences form a consistent cluster distinctly separated from the conventional *pmoA* (*pmoA1*).

Crenothrix polyspora has a divergent/unusual *pmoA* gene (u-*pmoA*), which places this type I methanotroph apart in the *pmoA* phylogeny (Stoecker *et al.*, 2006; Vigliotta *et al.*, 2007). Three copies of *pmoA* were identified in *Methylacidiphilum*, with the verrucomicrobial *pmoA* being phylogenetically separated from the conventional proteobacterial *pmoA* (Op den Camp *et al.*, 2009; Semrau *et al.*, 2010). A fourth copy of *pmoA* was found in *Methylacidiphilum kamchatkense* and it formed a monophyletic cluster with the verrucomicrobial *pmoA1* and *pmoA2*, while *pmoA3* was separated from them (Op den Camp *et al.*, 2009).

A duplicate copy of *mmoX* was identified in *Methylosinus sporium* 5 but the authors concluded that only one copy was functional (Ali *et al.*, 2006).

3.5.3. Regulation by copper and copper-uptake system

Copper (Cu) plays a major role in the regulation of the MMO activity. In an early study by Green *et al.* (1985), it was observed that sMMO activity can be inhibited by copper. In contrast, pMMO needs Cu to be active since its active form contains 15 Cu atoms per enzyme molecule (Zahn & Dispirito, 1996). In methanotrophs that contain both forms of MMO, the expression of the genes encoding both sMMO and pMMO is dependent on the Cu levels in the environment (Stanley *et al.*, 1983). More specifically, a switch between the expression of

the two enzymes occurs when the copper-to-biomass ratio changes (Murrell *et al.*, 2000b; Nielsen *et al.*, 1997). When Cu availability is high, pMMO is expressed while sMMO is not. In contrast, the *mmo* operon expression is activated (positive control) in copper-deficient conditions, while the *pmo* operon is repressed (negative control). This positive regulation of the *mmo* operon may be seen as a survival mechanism in methanotrophs that are able to synthesise both MMO forms (Hanson & Hanson, 1996; Knapp *et al.*, 2007). The model for the dual regulation of the genes encoding pMMO and sMMO proposed by Murrell *et al.* (2000a) was since updated and reviewed elsewhere (Hakemian & Rosenzweig, 2007; Trotsenko & Murrell, 2008).

Methanobactin (mb) is a novel siderophore-like peptide (1.2 kDa). Since it has high affinity for binding Cu, it is therefore called a chalkophore. It was identified as a Cu transporter, which methanotrophs release to sequester extracellular copper (Kim *et al.*, 2004; 2005). It was observed that a Cu-binding compound (CBC), *i.e.* methanobactin, was associated with pMMO (Zahn & Dispirito, 1996) and that the addition of Cu-containing mb (Cu-mb) increased pMMO activity when the Cu-to-mb ratio was >0.6 Cu atom per mb (Choi *et al.*, 2005). Further to the evidence that Cu-mb regulates CH_4 oxidation by the pMMO, constitutive sMMO ($sMMO^c$) mutants of *Methylosinus trichosporium* OB3b could not express pMMO or form the corresponding ICM and were defective in Cu uptake (Fitch *et al.*, 1993; Phelps *et al.*, 1992). The correlation between Cu regulation and MMO expression, *i.e.* the "switchover" model proposed by Murrell *et al.* (2000a), is not only dependent on the Cu-to-biomass ratio but also the Cu-to-mb ratio as well as the Cu geochemistry, *i.e.* the mineral form of Cu available (Choi *et al.*, 2005; Knapp *et al.*, 2007). Knapp *et al.* (2007) also suggested that the ability of mb to mediate Cu release from a mineral phase could be an important factor for shaping methanotroph community structure and influencing CH_4

oxidation rates in natural systems. This finding was supported by Choi *et al.* (2010) who observed that the mb secreted by alphaproteobacterial (type II) methanotrophs was competing with the mb produced by gammaproteobacterial (type I) methanotrophs.

To summarise, the chalkophore mb has three identified functions due to its Cu-chelating properties: 1) Cu shuttle; 2) regulation of MMO activity; and 3) reduction of Cu toxicity (Choi *et al.*, 2005; Fitch *et al.*, 1993; Kim *et al.*, 2005). Methanobactin can be produced by many *Methylococcaceae* and *Methylocystaceae* but it is not known yet if *Beijerinckiaceae* and *Methylacidiphilaceae* can secrete mb (Semrau *et al.*, 2010; Yoon *et al.*, 2010).

4. Techniques used for identifying methanotrophs

Like the majority of soil microorganisms, many methanotrophs cannot be cultured. This applies in particular to the high-affinity methanotrophs responsible for the oxidation of atmospheric CH_4 (Bender & Conrad, 1992). Thus, studies often use culture-independent methods to investigate methanotrophic diversity and composition in the environment. Several physiological, biochemical and molecular techniques are also available to help link environmental processes to specific microbial taxa (Gutierrez-Zamora & Manefield, 2010; McDonald *et al.*, 2008; Singh & Thomas, 2006; Torsvik & Ovreas, 2002). These include the use of stable or radioactive isotope probing methods, fluorescent probe-based approaches, or detection of biomarkers or fingerprinting of genetic markers extracted directly from environmental samples. Only a few of them will be reviewed here although there were discussed in detail in the above references.

4.1. Biochemical techniques

Phospholipid fatty acids (PLFAs) are present in the cell membrane of bacteria and are assumed to be degraded relatively rapidly after cell death. Hence, they are considered to be good biomarkers of living microorganisms (Bowman *et al.*, 1993; Frostegård *et al.*, 2010) as well as for observation of shifts in community structures and microbial biomass (Frostegård *et al.*, 1993a; Frostegård *et al.*, 1993b). PLFA extraction and identification methods are well established (Bligh & Dyer, 1959; Frostegård *et al.*, 1991). In brief, after extraction and fractionation of the total lipids, polar lipids are trans-esterified using a mild alkaline methanolysis, producing PLFA methyl esters (PLFAMEs), and derivatisation is performed using dimethyl disulfide. Samples can then be analysed by gas chromatography-mass spectrometry (GC-MS). The resulting separation of fatty acids produces unique PLFA patterns specific to the microorganisms from which they originated.

Although PLFA profiles give an indication of the microbial taxa present in the soil at the time of the sampling, its resolution level is low (Singh *et al.*, 2006a) and it does not provide information of the particular active species responsible for the process under study, *e.g.* methanotrophy, unless coupled to stable isotope probing (Boschker & Middelburg, 2002) (see section 4.2.3). Furthermore, it is now known that some PLFAs that were originally thought to be unique to a taxum are actually not, as discussed elsewhere (Frostegård *et al.*, 2010; Ruess & Chamberlain, 2010). Similarly, Sundh *et al.* (2000) concluded that PLFA analysis on its own should not be used for the study of the methanotrophic community structure in upland forest soils, *i.e.* where CH_4 is present at trace levels. Other misuses of PLFA measurements in soils were discussed recently by Frostegård *et al.* (2010).

4.2. Biomolecular techniques

4.2.1. Terminal-restriction fragment length polymorphism (T-RFLP)

T-RFLP is an automated, sensitive and semi-quantitative technique widely used for the comparison of microbial communities and change in their structure (Osborn *et al.*, 2000; Singh *et al.*, 2006a). Based on the PCR amplification of genes using fluorescently-labelled primers (Bruce, 1997; Liu *et al.*, 1997), amplicons are subjected to enzymatic digestion, separation by size by electrophoresis and detection by excitation of the fluorescent dye. Several fluorescently-labelled terminal restriction fragments (T-RFs) are produced based on the degree of conservation between species present in the environmental samples. Thus, it gives a unique description of the structure and composition of the microbial community through production of characteristic fragmentation patterns (Blackwood *et al.*, 2003; Kitts, 2001; Tiedje *et al.*, 1999). Because several dyes can be detected at once, genes specific to different phylogenetic groups (*e.g. Bacteria*, *Archaea*, and Fungi) can be studied simultaneously by using multiplex T-RFLP (Singh *et al.*, 2006b; Singh & Thomas, 2006).

The resolution power of T-RFLP can be reasonably high and allow detecting variations between different species at ±1 base pair (bp), in theory. However, care should be used as the accuracy of the detection will vary depending on factors such as true T-RF length, purine content or performance of the genetic analyser and associated capillary column (Kaplan & Kitts, 2003; Schütte *et al.*, 2008). These can induce discrepancies, or T-RF drifts (difference between observed T-RF length and true T-RF length), which cannot be corrected. Kaplan & Kitts (2003) suggested a window of ±2 bp as an appropriate approach for "binning" T-RFs of similar sizes. Other advances made in T-RFLP analysis, including choosing the appropriate primers, restriction enzymes or statistical approaches for analysis of results, as well as the *in silico* methods available online, are found elsewhere (Culman *et al.*, 2009; Schütte *et al.*, 2008; Singh *et al.*, 2006a; Szubert *et al.*, 2007; Thies, 2007)

4.2.2. Cloning and sequencing

Cloning uses PCR products generated the same way as from the T-RFLP procedure but with non-labelled primers. The resulting clones are screened for the gene inserts of interest. The subsequent PCR amplicons can be purified and sequenced in order to identify the microorganisms present. As a result, a phylogenetic tree may be constructed to visualise the position of the clones compared to extant methanotrophs. Also, because the sequence of clones, or known organisms, is then accessible, it can be virtually digested (*in silico* analysis) and the true T-RF length can be compared with the observed T-RF length of a T-RFLP analysis (Kitts, 2001). Thus, cloning/sequencing is also a useful tool to assign the detected T-RFs to specific operational taxonomic units (OTUs) (Horz *et al.*, 2001; Horz *et al.*, 2005; Moeseneder *et al.*, 2001; Singh *et al.*, 2009).

4.2.3. Stable isotope probing (SIP)

The natural abundance of ^{13}C is about 1%. Therefore, the incubation of an environmental sample with a ^{13}C-labelled (>99%) substrate as unique C source will result in ^{13}C-incorporation into the different constituents (PLFA, DNA, RNA, protein) of the dividing cell (Dumont & Murrell, 2005; McDonald *et al.*, 2008). On this principal, it is possible to unravel the identity of a microorganism responsible for a particular environmental process (or biological function) under condition approaching those *in situ*. This "function-identity" method was successfully used for the detection of methanotrophs, using ^{13}C-CH_4 as substrate, from different habitats, as reviewed in Gutierrez-Zamora & Manefield (2010).

SIP of methanotrophs was applied to the labelling of lipids (Boschker *et al.*, 1998; Maxfield *et al.*, 2006) and nucleic acids – DNA (Radajewski *et al.*, 2000), rRNA (Noll *et al.*, 2008) and mRNA (Dumont *et al.*, 2011). Detailed methodology can be found elsewhere (Huang *et al.*, 2009; Neufeld *et al.*, 2007b; Whiteley *et al.*, 2007). The enrichment of proteins with ^{13}C-labelled substrate was recently achieved by Jehmlich *et al.* (2008; 2010). Recent advances on SIP and related technologies were reviewed by Murrell & Whiteley (2011).

Each of the above SIP techniques has its advantages and inconveniences. Although the resolution power of PLFA-based SIP (PLFA-SIP) is low due to the little variety of PLFAs in known methanotrophs, it has the highest sensitivity because it requires short incubation times (hours/days) (Neufeld *et al.*, 2007a). It also constitutes an inexpensive alternative to gather information on the groups of active methanotrophs and is ideal for detecting active methanotrophs at atmospheric CH_4 levels, *i.e.* between 2 and 10 ppm (Bull *et al.*, 2000; Crossman *et al.*, 2005; Maxfield *et al.*, 2006; Singh & Tate, 2007). On the other hand, DNA-SIP has the highest resolution power but is labour-intensive and requires careful attention to detail during the each experimental step (Neufeld *et al.*, 2007a). It also involves high substrate consumption (>10,000 ppm) and long incubation times (weeks), which can

potentially enhance cross-feeding of the labelled substrate (Neufeld *et al.*, 2007a). Finally, rRNA-SIP has a higher sensitivity because it does not involve cell division, like DNA-SIP, and requires less time (days/weeks) to reach sufficient levels of ^{13}C-incorporation (Lueders *et al.*, 2004; Manefield *et al.*, 2002). Nevertheless, it is only specific to a particular gene unlike DNA-SIP, which can target entire functional operons when coupled to metagenomic approach (Dumont *et al.*, 2006). *pmoA* mRNA-SIP is more sensitive than DNA-SIP and minimises the potential problems of cross-feeding (Dumont *et al.*, 2011).

4.2.4. Diagnostic microarrays

A DNA-based microarray relies on the hybridisation of oligonucleotide or gene probes to specific DNA sequences. It was originally developed for genome-wide expression analysis (Schena *et al.*, 1995). The microarray was first adapted as a diagnostic tool for the detection of microbial communities using probes targeting functional genes of known microorganisms at the strain, species or genus level (Wu *et al.*, 2001). It was quickly optimised for the community analysis of methanotrophs (Bodrossy *et al.*, 2003; Stralis-Pavese *et al.*, 2004).

The most recent *pmoA* diagnostic array contains 199 probes, which allow detection of most known genera of methanotrophs, mostly at the species level, as well as some ammonia oxidisers (Stralis-Pavese *et al.*, 2011). However, it does not resolve the most recently discovered methanotrophs, *i.e.* members of *Crenothrix*, *Clonothrix*, and *Methylacidiphilum*. Despite its high throughput and resolution, the *pmoA* diagnostic microarray is unable to identify new microbes. As a result, it should be used along genomics (McDonald *et al.*, 2008) or other fingerprinting techniques such as T-RFLP.

5. Regulation of aerobic methanotrophy

The composition of the soil methanotrophic community is dynamic. Changes in the methanotrophic population dynamic of a soil will affect its potential to act as source or sink for CH_4. As a result, changes in the particular use or management of a land, such as upland soils (*e.g.* grassland, pasture, forest), will influence CH_4 sinks (Ojima *et al.*, 1993). Methanotrophs and CH_4 oxidation rates are influenced by many abiotic and biotic factors, which will be briefly discussed below.

5.1. Effects of environmental factors on methanotrophs and CH_4 oxidation rates

As mentioned earlier, numerous environmental factors of the soil such as gas diffusion and moisture content, temperature, pH, substrate availability, *etc*. can influence methanotrophic activity (Bender & Conrad, 1995; Topp & Pattey, 1997).

Soil moisture

This was identified as a strong controller of CH_4 consumption (Castro *et al.*, 1995; Lessard *et al.*, 1994). Methanotrophic activity was found to be reduced when soil moisture increased above field capacity due to a decrease in O_2 availability (Czepiel *et al.*, 1995; Sitaula *et al.*, 1995). In temperate forest and poorly drained soils, when moisture ranged 60-100% water-filled pore space (WFPS), CH_4 oxidation rates decreased. This was attributed to limited O_2 availability and soil gas diffusivity (Bender & Conrad, 1995; Whalen & Reeburgh, 1990), in particular because CH_4 transport in water is 10,000 times slower than in air (Castro *et al.*, 1995; Whalen & Reeburgh, 1992). In contrast, when moisture is very low (<12%), CH_4 consumption is also inhibited as observed in desert and landfill cover soils (Striegl *et al.*, 1992; Whalen *et al.*, 1990). It was suggested that it was caused by increased osmotic stress and desiccation (Conrad, 1996; Jäckel *et al.*, 2001).

Temperature

The effect of temperature is inconsistent, indicating that soil methanotrophs adapt to different temperatures (Hanson & Hanson, 1996). This may be because methanotrophs are found to thrive in a large range of temperature due to the existence of mesophilic, psychrophilic and thermophilic members (Table 1.2). Although temperature changes were found to have little effect on overall CH_4 consumption, temperatures <10°C and >40°C seem to decrease significantly methanotrophic activity in forest and landfill cover soils, possibly due to the inhibition of mesophilic methanotroph activity (Castro *et al.*, 1995; Semrau *et al.*, 2010). Interestingly, methanogens are highly sensitive to temperature (and pH) variations, as discussed by Le Mer & Roger (2001). Thus, they may influence more the net CH_4 flux.

pH

Soil pH does not seem to be a strong controller of CH_4 oxidation since similar values were measured between pH 3.5 to 8 (Born *et al.*, 1990). Again, as with temperature, this could be explained by the range of pH values to which methanotrophs are adapted, because neutrophilic, alkaliphilic and acidophilic methanotrophs exist (Table 1.2). However, soil alkalisation and acidification were found to decrease net CH_4 fluxes in grassland and forest (Amaral *et al.*, 1998; Hütsch *et al.*, 1994; Reay *et al.*, 2001). In more recent years, pH was found to influence the community structure in forest soils. After reviewing several studies from conifer and deciduous forests, Kolb (2009) observed that type I-related methanotrophs and members of the upland soil cluster γ (USCγ) were predominantly found in neutral soils, while type II-related methanotrophs and members of the USCα thrived in acidic soils. Also, the recent finding of the verrucomicrobial members of the *Methylacidiphilum* genus proved that CH_4 consumption at very acidic pH (<1) is possible (Op den Camp *et al.*, 2009).

Copper and nitrogen

Copper has an important effect on methanotrophic activity due to its involvement in the regulation of sMMO and pMMO and the role of the Cu shuttle methanobactin, which were both discussed earlier (see section 3.5.3). Nitrogen, mainly supplemented as inorganic fertiliser or *via* atmospheric deposition, also plays a significant role in methanotrophy but this will be discussed below (section 5.2) with the use of fertilisers. However, based on culture experiments, type II methanotrophs were found to outcompete type I methanotrophs under copper- and nitrogen-limited conditions (Graham *et al.*, 1993).

Concentration of CH_4

The concentration of CH_4 was shown to affect the CH_4 oxidation rates (Bender & Conrad, 1995). It was proved that when a very high concentration of CH_4 was present (10,000 ppm), with low O_2 concentrations, type II methanotrophs outcompeted type I methanotrophs, while growth of type I methanotrophs was favoured at lower CH_4 (1,000 ppm) and high O_2 concentrations (Amaral & Knowles, 1995; Henckel *et al.*, 2000b). However, this would only apply to methanotrophs that have a low affinity to CH_4, which is when CH_4 input is high, *e.g.* due to intense methanogenesis. Then, the trend is reversed and type II methanotrophs become more oligotrophic (Knief & Dunfield, 2005). High-affinity methanotrophs are able to oxidise trace concentrations of CH_4 (Bender & Conrad, 1992), such as found in upland soils. These microbes are mainly grouped into two clades, USCα and USCγ, and are distantly related to, respectively, type II and type I methanotrophs (Bull *et al.*, 2000; Holmes *et al.*, 1999; Knief *et al.*, 2003; Knief *et al.*, 2006; Singh & Tate, 2007). Only soil pH seems to be a strong controller of the presence of either clade (see above).

Soil structure

As well as the soil moisture (see above), the nature of the soil can influence net CH_4 fluxes. Specifically, soil texture and mineralogy are believed to be another strong controller of CH_4 consumption (Castro *et al.*, 1995; Le Mer & Roger, 2001). Soils containing some types of clay protect organic matter from mineralization (Oades, 1988) and soils with a high clay content are known to retain CH_4 by preventing diffusion (Sass *et al.*, 1994). At low soil moisture, soil texture plays a role in CH_4 transport, in particular gas diffusivity. Soil characteristics such as porosity, WFPS and bulk density are closely linked to soil water content and therefore influence O_2 availability and CH_4 diffusion in soils (Ball *et al.*, 1997; Smith *et al.*, 2003).

In summary, soil moisture, WFPS and porosity are recognised as important drivers of CH_4 oxidation rates. Although temperature is not a major controller of methanotrophy, elevated temperature and levels of CO_2 may have an indirect effect on CH_4 production and global warming, as discussed by Singh *et al.* (2010).

5.2. Effects of change in land management and land use

Influence of land management

Fertilisation is an important practice for land management. Conflicting reports on the precise effect of inorganic nitrogenous fertilisers (ammonia- or nitrate-based) on CH_4 consumption exist, showing either no effect, inhibition or stimulation (Bodelier & Laanbroek, 2004; Mohanty *et al.*, 2006). However, several studies showed that inorganic fertilisers inhibit methanotrophs in many land uses such as rice paddies, grassland and forests (Conrad & Rothfuss, 1991; Hanson & Hanson, 1996; Hütsch *et al.*, 1994). This was attributed to the possible competition of NH_4^+ for binding to the MMO, or through the toxicity of NO_3^-. Long-

term application of ammonium-N fertiliser decreased soil sink strength whereas nitrate-N did not (Willison *et al.*, 1995). On the other hand, organic fertilisers (compost but not manure) had no effect on methanotrophy in comparison to inorganic fertilisers (Seghers *et al.*, 2005). Thus, the choice of the form of fertiliser (organic *vs*. inorganic) as well as the form of N (NH_4^+-N *vs.* NO_3^--N) are important.

The effects of biocides (insecticides, pesticides and herbicides) on CH_4 uptake were also investigated. Some lowered CH_4 oxidation rates (Boeckx *et al.*, 1998; Mosier *et al.*, 1991; Priemé & Ekelund, 2001; Topp, 1993) whereas others did not have an effect (Hütsch, 1996; Seghers *et al.*, 2003b; 2005). Few studies evaluated the impact of fertiliser and herbicides on methanotrophic abundance and community structure. Seghers *et al.* (2003a; 2003b; 2005) concluded that application of organic fertiliser improved CH_4 oxidation rates and the abundance of methanotrophs, in particular type II, whereas the combined application of herbicides had no effect. Maxfield *et al.* (2008) identified a decrease in the biomass of uncultured high-affinity methanotrophs and CH_4 oxidation rates due to fertiliser application.

Agricultural practices such as tillage and ploughing were found to reduce CH_4 consumption, although tillage seemed to be less damaging while direct seeding improved CH_4 oxidation (Hütsch, 1998). Also, site preparation for afforestation indicated that drainage had reduced CH_4 emissions compared to mounding (Mojeremane *et al.*, 2010).

Influence of land use

The way a land is used, and changes in its use, such as afforestation, can influence the CH_4 sink strength. From several studies, the following trend was observed (in decreasing order of sink strength): woodland > non-cultivated upland > grassland > cultivated soils (Dobbie & Smith, 1996; Hütsch *et al.*, 1994; Le Mer & Roger, 2001; Willison *et al.*, 1995). More specifically, an effect of land-use change on CH_4 oxidation rates was associated to tree species (Borken & Beese, 2006; Menyailo *et al.*, 2010; Menyailo & Hungate, 2003; Reay *et al.*, 2001; Reay *et al.*, 2005; Saggar *et al.*, 2007). Different tree species had varied effects on CH_4 consumption but a common trend was that soils under hardwood species (aspen, beech, birch, oak) consumed more CH_4 than soils under coniferous species (larch, pine, spruce). Interestingly, Reay *et al.* (2001; 2005) observed that soils under alder were not able to oxidise significant amounts of CH_4. This was correlated with high nitrification rates and it was suggested that the high concentrations of nitrate measured were the result of N_2 fixation by the symbiotic *Frankia* sp. in the root nodules and subsequent conversion of ammonia to nitrate by ammonia-oxidising bacteria.

Compared to cultivated soils, uncultivated set-aside soils showed little or no difference in CH_4 oxidation rates, indicating that recovery from agricultural use was not immediate (Dobbie & Smith, 1996; Hütsch, 1998). Similarly, Priemé *et al.* (1997) found that, in Denmark and Scotland, over 100 years were necessary to reach pre-cultivation levels of CH_4 oxidation rates after land-use change from arable culture to woodland. This was later confirmed to be true for many other Northern European soils (Smith *et al.*, 2000).

Afforested soils were found to have increased oxidation rates of ambient concentrations of CH_4 due to a change in the methanotrophic community structure from type I to type II methanotrophs when shifting from pasture to pine forest (Singh *et al.*, 2007; Singh *et al.*, 2009). In contrast, forest clear-felling and deforestation were shown to change the soil from

being a sink for CH_4 into a net source (Keller *et al.*, 1990; Keller & Reiners, 1994; Zerva & Mencuccini, 2005). Dörr *et al.* (2010) associated this change with a shift from type II methanotrophs of the *Beijerinckiaceae* towards type I methanotrophs of the *Methylococcaceae* occurring after conversion of forest to farmland.

In summary, changes in methanotrophic activity and atmospheric CH_4 consumption are due to environmental and ecological factors. Increased CH_4 uptake rates were mostly correlated with low water content and lack of chemical fertilisation in soils and sediments. In addition, competition between type I and type II methanotrophs occurs through copper availability, N, CH_4 and O_2 concentrations.

5.3. Importance of afforestation/reforestation in relation to climate change

Because upland soils and forests represent the major terrestrial and biological sinks for CH_4, it is essential to police their management in order to reduce GHG emissions (Schulze *et al.*, 2009). Moorland burning, peat extraction and peatland disturbance through drainage are common practises in Scotland which are known to increase C losses. Similarly, land-use changes can alter soil C content and net CH_4 flux. While conversion of natural vegetation to cultivated land is known to induce increased CH_4 emissions (see above) and induce large losses of C (Post & Kwon, 2000), reversion to woodland is thought to improve CH_4 sinks (see above) and C sequestration after a lag phase during which the soil C must recover from soil disturbance (Hargreaves *et al.*, 2003; Trotter *et al.*, 2005). The main reasons for C loss are reduced inputs of organic matter, decreased physical protection to decomposition (*e.g.* due to tillage) and increased decomposability (Post & Kwon, 2000), whereas changes in net CH_4 fluxes are caused by modification of the methanotrophic and methanogenic activities.

Under the Kyoto Protocol (UNFCCC, 1998), world-wide projects were implemented for the improvement of forested areas, either through tree planting or natural regeneration of forests (Article 3.3), in order to increase C sequestration (Article 3.4). Afforestation and reforestation also have an impact on the global CH_4 budget by mitigating CH_4 emissions and improving CH_4 sinks. As a result, the "Kyoto forests" may constitute an advantage in response to global warming and represent a component of the carbon market (Article 17 of the Kyoto Protocol) (Trotter *et al.*, 2005; UNFCCC, 1998). For these reasons, and because of the importance of terrestrial CH_4 sinks, the biological mechanisms involved should be determined since forestation impacts on CH_4 oxidation rates *via* modification of soil abiotic and biotic properties.

6. Aims of the study

Several studies have monitored how net CH_4 fluxes are affected by differing land-use changes and land managements (Saggar *et al.*, 2007; Singh *et al.*, 2007; Tate *et al.*, 2007), but the specific mechanisms involved remain controversial. This study aims to examine how changes in land use, such as afforestation/reforestation, can influence the sink for atmospheric CH_4 in soils and especially how change in net CH_4 flux is linked with methanotrophic diversity and activity. In this thesis, the following hypotheses were tested:

a. A change in the use of a land, such as by afforestation/reforestation, can affect CH_4 oxidation rates.

This was tested by measuring net CH_4 fluxes from field sites with differing land uses.

b. The changes in the CH_4 oxidation rates are related to changes in the methanotrophic diversity and activity.

In Scotland, the effect of land-use change on the methanotrophic community structure was investigated using T-RFLP and a diagnostic microarray, while the active methanotrophs were identified using PLFA-SIP. Also, re-establishment of a stable and active methanotroph community structure after fire was examined and compared to a native forest in New Zealand using similar approaches as in Scotland, except that the identity of the methanotrophs present was investigated by cloning and sequencing instead of microarray analysis.

c. Afforestation can help offsetting of the national CH_4 emissions in Scotland.

A bottom-up approach was adopted to upscale the local flux data generated to the Scottish national level by applying a model based on one used in New Zealand (Tate *et al.*, 2005). The upscaling helped to assess the potential of afforestation in the mitigation of CH_4 in Scotland.

Chapter 2 Materials and methods

1. Field site description

For this work, several field sites were chosen in New Zealand (two) and in Scotland (four).

1.1. In New Zealand

Two sites were explored: the Puruki indigenous forest and the Turangi site (**Figure 2.1**). These two sites were chosen because they were on (Puruki) and nearby (Turangi) sites that had been used by previous studies, data from which were included in this work for comparative purposes.

Figure 2.1: Location of the Puruki and Turangi sites in the North Island of New Zealand.

The Puruki indigenous forest (Puruki-Native) was described by Beets & Brownlie (1987). It is located in the Purukohukohu experimental basin in central North Island, about 30 km south of Rotorua, New Zealand (38°26' S and 176°13' E) and was initially used as part of a long-term hydrological study (Beets and Brownlie, 1987). The site was situated at an elevation of *ca*. 550 m. Meteorological data collected between 1976 and 1985 showed that precipitation averaged 1500 mm yr^{-1} (range, 1150-2010 mm) and that average annual temperature ranged between 9 and 11^{o}C. Soils in the Experimental Basin were described by Rijkse and Bell (1974). They are Oruanui sandy loams and are classified as ashy over pumiceous Typic Udivitrands. Litter depth in the forest was very variable but averaged 80 mm for FH material; roots were often abundant in this FH layer. A typical soil profile contained an Ah horizon at 0-100 mm depth and a Bs horizon at *ca*. 100-200 mm depth.

The indigenous forest has a three-tiered structure and is rich in plant species: rimu (*Dacrydium cupressinum*) emerged over a canopy dominated by kamahi (*Weinmania racemosa*), hinau (*Elaeocarpus dentatus*), rewarewa (*Knightia excelsa*), mangeao (*Litsea calicaris*) and tawa (*Beilschmiedia tawa*). The sparse understorey comprises hardwood trees, shrubs and ferns.

The Turangi site was previously described in detail by Scott *et al.* (2000). It is located in Tongariro National Park in central North Island, New Zealand (39°05' S, 175°45' E). Until the late 1940s, when active fire suppression began, the original indigenous primary forest had been subjected to intermittent fires (Rogers, 1994). Mean annual temperature is about 9.3^{o} C and annual rainfall about 1520 mm (Whitehead *et al.*, 2004). The soils were developed from a series of rhyolytic and andesitic volcanic eruptions, and are classified as Podzolic Orthic Pumice soils of the Rangipo series (Hewitt, 1993); they are roughly similar to Vitrands (Soil

Survey Staff 1990). The most recent additions of volcanic ash were from eruptions from Mt Ruapehu in 1995 and 1996, with <2 mm of a medium-fine-grade layer of andesitic material being deposited (Cronin *et al.*, 2003).

At the time of sampling, in 2008, the area was covered by a variety of shrubs of varying age, comprised mainly of manuka (*Leptospermum scoparium*) and kanuka (*Kunzea ericoides* var. *ericoides*), with some broadleaf canopy species and an understorey of mosses. Two stands were selected with actual stand ages since burning being about 47 and 67 years (here referred to as Turangi-47 and Turangi-67, respectively). The edge of the 35-year-old stand was about 100 m west of the 55-year-old stand.

Table 2.1 shows some meteorological data that characterised the field sites in the month during sampling.

Table 2.1: Some meteorological data from the field sites in New Zealand.
Within brackets is indicated the weather station closest to the field site.

	Turangi – Feb. 08 (Taupo)[1]			**Puruki – Jan. 08 (Rotorua)[2]**		
	Temperature (°C)	**Humidity (%)**	**Precipitation (mm)**	**Temperature (°C)**	**Humidity (%)**	**Precipitation (mm)**
High	26.0	N/A	25.9	34.1	98.0	51.3
Low	6.0	N/A	-	8.5	24.0	-
Av.	17.0	N/A	-	19.4	69.8	-

[1,2] data from **http://www.wunderground.com/weatherstation/**

1.2. In Scotland

Four sites were explored between 2008 and 2009: the Tulchan Estate, the Craggan forest, Bad à Cheo and the Glensaugh Research Station (**Figure 2.2**).

Figure 2.2: Location of the four sampling sites in Scotland.
Position of the sites on the map is not accurate.

The Glensaugh Research Station is part of the Macaulay Land Use Research Institute and is located in Laurencekirk, Aberdeenshire, Scotland, UK (national grid reference NO671782). The study site is an agroforestry plot that was used to study experimental planting and grazing management between 1988 and 2001 (Glensaugh Agroforestry Demonstration, http://www.macaulay.ac.uk/aboutus/researchstations/agroforestry.html). The site is a pasture occupied by ewes and lambs, with regular fertiliser applications during each grazing season. In 1988, a subplot was planted with Scots pine (*Pinus sylvestris*). Therefore, the pine forest was about 20-years old at the time of this study. No fertilizer was applied since.

Bad à Cheo is situated near Thurso, in Northern Scotland, along the A9 (national grid reference ND169503) and is part of the Rumster forest. It had been the subject of detailed hydrochemical studies (Miller *et al.*, 1996). The study site is composed of an open bog of deep blanket peat dominated by a mixture of peat moss (*Sphagnum* spp.), deergrass (*Trichophorum cespitosum*) and cotton-grass (*Eriophorum* spp.). Adjacent to the bog, experimental forestry plots were drained, ploughed and planted in 1968 and 1988 with a mixture of Sitka spruce (*Picea sitchensis*) and lodgepole pine (*Pinus contorta*) (Anderson *et al.*, 1992). Therefore, at the time of this study, the young and old pine forests were about 20- and 40-years old, respectively. Because of the age difference, the younger pine forest lay on much wetter ground compared to the older pine forest. Also, at the time of sampling, natural colonisation of the bog by conifers was observed.

The Craggan forest is also described elsewhere (Miles & Young, 1980; Mitchell *et al.*, 2007). It is located in Moray, near the Spey River, Scotland, UK (national grid reference NJ190322) and was originally used in 1978 in a study testing the durability of changes caused by *Betula* spp. on moorland (Miles & Young, 1980). Open *Calluna*-dominated moorland is adjacent to

a natural chronosequence of birch trees (*Betula* spp.) aged about 53, 62 and 88 years. During the colonisation phase, heather (*Calluna vulgaris*) was replaced by wavy hairgrass (*Deschampsia flexuosa*) and bilberry (*Vaccinium myrtillus*) before long-term establishment of birch woodland (Hester *et al.*, 1991; Miles, 1981). For our study, soil samples were taken from the 62-year-old stand (young birch forest) and the 88-year-old stands (old birch forest) only. It is worth noting that the moorland was cleared of trees in 1974 but has since been progressively naturally colonised by birch. Also, due to the old age of the 88-year-old stands, few trees were left standing and alive, with mainly colonial bentgrass (*Agrostis capillaris*) present as understorey vegetation. The Craggan site was situated on the slope of a hill.

The Tulchan Estate is described in more detail elsewhere (Hester *et al.*, 1991; Miles & Young, 1980). Briefly, the study site is located on the Tulchan Estate, Speyside, Scotland, UK (national grid reference NJ154373). The site contains a natural heather moorland-birch woodland chronosequence. The open *Calluna*-dominated moorland is adjacent to two stands of birch trees (*Betula pubescens*) following natural invasion of the heathland in *ca.* 1953 (young birch forests, 55-year-old) and *ca.* 1943 (old birch forests, 65-year-old) (Keith *et al.*, 2006). Like in Tulchan, similar changes in vegetation occurred (Hester *et al.*, 1991).

To summarise, four sites were investigated in Scotland. There were three habitats per site (non-forested, young forest and old forest; except for Glensaugh: no old forest) but only five different habitats in total (grassland, bog, moorland, conifer forest and birch woodland). As a result, three types of land-use change were examined: conversion of grassland to pine forest, afforestation of bog with pine trees, and natural colonisation of moorland by birch stands.
Table 2.2 shows some meteorological data that characterised the field sites in the month prior to, as well as during sampling.

Table 2.2: Some meteorological data from the field sites in Scotland for each season.

Within brackets is indicated the weather station closest to the field site. The month prior to and of sampling are displayed. The year averages are also shown.

		Glensaugh (Laurencekirk) [1]			Bad à Cheo (Thurso) [2]			Craggan/Tulchan (Spey) [3]		
		Temperature (°C)	Humidity (%)	Precipitation (mm)	Temp. (°C)	Hum. (%)	Precip. (mm)	Temp. (°C)	Hum. (%)	Precip. (mm)
Oct. 08	**High**	18.8	98.0	33.8	16.4	96.0	125.2	17.0	N/A	95.8
	Low	0.7	38.0	-	-0.2	59.0	-	-4.2	N/A	-
Autumn	**Av.**	8.3	75.6	-	7.6	86.3	-	6.3	N/A	-
	High	13.8	98.0	37.1	12.8	96.0	72.4	13.1	N/A	53.0
Nov. 08	**Low**	-6.1	37.0	-	-4.9	60.0	-	-9.6	N/A	-
	Av.	5.5	79.0	-	5.7	88.9	-	3.7	N/A	-
Jan. 09	**High**	37.8	94.0	94.0	12.2	95.0	31.0	11.9	N/A	26.0
	Low	-3.3	46.0	-	-4.1	75.0	-	-12.6	N/A	-
Winter	**Av.**	8.3	81.3	-	3.3	89.2	-	1.7	N/A	-
	High	28.0	98.0	43.4	12.1	96.0	45.2	11.6	N/A	72.2
Feb. 09	**Low**	-6.0	49.0	-	-7.5	63.0	-	-19.5	N/A	-
	Av.	4.8	80.3	-	4.1	88.4	-	1.7	N/A	-
Mar. 09	**High**	17.4	98.0	29.2	17.5	95.0	93.5	18.7	N/A	71.4
	Low	-3.7	38.0	-	-4.1	62.0	-	-7.9	N/A	-
Spring	**Av.**	6.2	77.2	-	5.4	87.6	-	4.6	N/A	-
	High	17.2	98.0	30.7	17.9	95.0	38.6	19.1	N/A	27.0
Apr. 09	**Low**	0.7	42.0	-	-0.5	44.0	-	-2.6	N/A	-
	Av.	8.4	82.0	-	8.3	83.3	-	7.9	N/A	-
Jun. 09	**High**	22.5	98	51.3	27.4	95.0	41.4	27.4	N/A	53.6
	Low	4.2	40.0	-	3.0	52.0	-	-0.7	N/A	-
Summer	**Av.**	12.4	81.8	-	11.8	82.4	-	12.4	N/A	-
	High	25.6	98.0	100.3	30.1	93.0	0.0	28.7	N/A	122.5
Jul. 09	**Low**	9.0	41.0	-	13.6	56.0	-	4.0	N/A	-
	Av.	15.4	80.1	-	17.6	85.0	-	14.3	N/A	-
	High	26.5	98.0	778.3	26.9	97.0	785.4	17.6	N/A	809.8
Av. 08	**Low**	-6.1	29.0	-	-6.8	35.0	-	-4.8	N/A	-
	Av.	8.9	78.3	-	8.1	86.0	-	7.1	N/A	-
	High	37.8	98.0	887.5	30.1	96.0	847.6	18.9	N/A	883.5
Av. 09	**Low**	-6.0	29.0	-	-7.5	43.0	-	-5.6	N/A	-
	Av.	9.4	82.1	-	7.9	86.5	-	7.4	N/A	-

[1,2] data from http://www.wunderground.com/weatherstation/

[3] data from http://www.strathspeyweather.co.uk/

2. Soil sampling

2.1. In New Zealand

Puruki forest

Samples were taken on 29th January 2008 from three different areas of about 40-50 m^2. One area was located towards the bottom of the slope, the second *ca.* 30-40 m upslope, and the third a further 10-20 m upslope and close to the original sampling area used by Ross *et al.* (1999). In each area, six intact soil cores (10 cm diameter, 0-10 cm depth) were collected in stainless steel rings, after removal of L (litter) and FH (fermentation-humus) material. The (eighteen) cores were taken at random within the sampling area, except for locations with large roots that prevented the core being inserted to its full depth. Each core was retained in the metal liner and sealed with cling film to minimise moisture loss, and to protect the soil surface. The cling film was, however, pierced with several holes to allow airflow into the core. In addition, after removal of L and FH material, four small cores (2.5 cm diameter, 0-10 cm depth) were taken equidistantly apart within *ca.* 5 cm of a "large" core, and pooled for subsequent analyses. These pooled samples were sieved (5.6 mm) and stored at 4°C within 24 hours of collection.

Turangi site

The 47- and 67-year old stands were sampled on 20th February 2008. After removal of the L and FH materials, a hand-held stainless steel soil corer (2.5 cm diameter) was used to extract soil cores (0-10 cm depth) in duplicate and at random along a transect composed of six adjacent plots. In each plot, three cores were sampled about 30 to 50 cm apart, and then pooled to give one soil sample for each of the six plots, for both 47- and 67-year old stands (each n=6). Soils were sieved (5.6 mm) and kept at 4ºC within 24 h of collection.

2.2. In Scotland

Each site was visited four times over the period of a year (2008-2009), as a sampling campaign occurred once during each season: autumn (October/November 2008), winter (February 2009), spring (April 2009) and summer (July 2009).

The sampling procedure was the same for each site and similar to the method used at the Puruki forest in New Zealand (see above). In brief, stainless steel rings (10 cm diameter, 0-10 cm depth) were used to extract soil cores after removal of the L and FH layers. For each site, twelve replicates per habitat were sampled at random, and were randomly grouped in four sets of three cores for measurement of net CH_4 fluxes (see section 4.). Therefore, n=4 for each habitat, for each site, for each season (n=176 in total). Within a few hours of sampling, the soil cores were taken to the laboratory and left overnight in an environment-controlled chamber (minimum 70% humidity). For each seasonal experiment, the temperature of the chamber was set using a value close to the site's air temperature at the time of sampling: 5°C in winter, 10°C in spring, 15°C in summer and 20°C in autumn. The temperature of the latter was a bit too high due to an error in the protocol. The following day, measurements of net CH_4 fluxes were performed and the soil cores were then stored at 4ºC.

Also, during summer, smaller intact cores (5 cm diameter, 0-5 cm depth) were taken in triplicate from each habitat from each site for bulk density, porosity and water retention analysis (n=33).

3. Soil analyses

3.1. New Zealand soils

Several chemical properties (pH, total C and N, mineral N (NH_4^+-N and NO_3^--N) and moisture) were measured on the composite samples (2.5 cm diameter, 0-10 cm depth) collected at Turangi-47, Turangi-67 (each n=6) and Puruki-Native (n=9). The analytical procedures were described by Singh *et al.* (2009). Briefly, soil pH was determined in a 1:2.5 water suspension (Blakemore *et al.*, 1987). Total C and N were measured by combustion in a Leco FP-2000 CNS analyser (LECO Corporation, USA). Mineral N (NH_4^+-N and NO_3^--N) was extracted from field-moist soil (5.0 g oven-dry equivalent) by shaking with 50 mL of 2 M KCl for one hour and determined with a Lachat QuickChem FIA 800 (Zellweger Analytics, USA). Moisture in the sieved-soil samples was determined by drying overnight at 105°C to constant weight (Blakemore *et al.*, 1987).

At Turangi-47 and Turangi-67, a second set of composite samples (each n=6) was used for CH_4 uptake measurements as well as for soil incubation with enriched CH_4 (^{13}C-CH_4) and microbial analyses. At Puruki-Native, the 18 intact soil cores collected in stainless steel rings (10 cm diameter, 0-10 cm depth) were paired for measurement of net CH_4 fluxes and soil physical properties, as well as for soil incubation and microbial analyses (n=9).

3.2. Scottish soils

Following gas measurements (see section 4.), the soils were processed for physico-chemical analysis, as well as for biochemistry and molecular work. I processed the soils myself but most of the chemical analyses were performed by the analytical group at the Macaulay Land Use Research Institute. References of the methods used are available from Dr Jason Owen or Dr Andy Midwood. However, pH and physical properties were measured by me.

3.2.1. Processing of soils

Fresh soil cores were wet-sieved through a 5.6 mm-mesh sieve to separate the vegetation from the soil. A fresh sub-sample was kept at 4ºC for subsequent NH_4^+/NO_3^- analysis (KCl extraction) and moisture measurement; but also for soil enrichment (PLFA-SIP) and DNA extraction for PCR/T-RFLP analysis. During wet-sieving, the triplicate soil cores from each set of four chambers were sieved together to obtain a homogenous sample (total n=176). The remaining soil was dried at 30ºC and then dry-sieved through a 2 mm-mesh sieve for pH and particle size analysis. A sub-sample was milled (Retsch mill, 5 minutes at 60 strokes per second) for subsequent use for total C and N analysis.

The smaller soil cores from the summer campaign were dried using hanging water columns for measurement of soil bulk density, porosity and water-filled pore space (WFPS).

3.2.2. Chemical analyses

Field-moist 5.6-mm sieved soils were extracted with 1 M KCl for 1 hour and extracts were analysed colorimetrically for mineral N (NH_4^+-N and NO_3^--N).

Moisture content was measured after drying the fresh soil samples in an oven at 105ºC overnight. Data are expressed per gram of soil on an oven-dry basis.

Dried soils were used to determine soil pH in water after mixing thoroughly the soil water slurry (1:2.5 suspension) for 30 minutes. Particle size distribution analysis was performed on the dried soils using laser diffraction on a Malvern Mastersizer 2000 particle size analyser fitted with a Malvern Hydro 2000G sample dispersion tank (Malvern, UK). Briefly, the soil sample was mixed with a dispersant agent and the liquid suspension was circulated through a cell, through which a laser was passed. The laser was diffracted by the suspended particles and a series of detectors registered the degree of diffraction. The angle of diffraction was

directly proportional to the angle of incidence encountered by the laser, *i.e.* the smaller the particle the higher the angle of incidence and the greater the diffraction. A mathematical model resolved the required particle size distribution to account for the observed diffraction of the laser.

Milled soils were used to measure soil total C and N by combustion in a Thermo-Finnigan Elemental Analyser (FlashEA 1112 Series). The combustion products were carried by a constant flow of helium through an oxidation catalyst, copper oxide and platinised Alumina. CO_2, N_2, NO_x and H_2O then flowed into a reduction reactor containing copper wires held at 680ºC, where excess oxygen was removed and any nitrogen oxides were converted into nitrogen gas. Water was then absorbed by magnesium perchlorate.

3.2.3. Physical analyses

Soil bulk density, porosity and water-filled pore space (WFPS) were measured by saturating the small field-moist cores with water. The volume of pores was estimated by measuring the gravimetric soil water content, after equilibrating the cores at 10, 50, 100 and 150 kPa suction pressures, using hanging water columns. The pore volume was computed from the volume of water extracted between successive intervals of applied suction (Nielsen *et al.*, 2008).

WFPS was estimated for each core as the ratio of the volumetric soil moisture content to the total pore space, or porosity (Linn & Doran, 1984). Porosity was estimated to be equivalent to the volumetric water content at water saturation. Volumetric water content was calculated as the ratio of the gravimetric water content to the bulk density. Bulk density corresponded to the oven-dry soil weight (105°C overnight) divided by the volume of the core.

4. Gas flux measurements

4.1. Gas sampling

New Zealand soils

Turangi-47 and -67 samples: Air samples were collected from six field-based static chambers as described in Saggar *et al.* (2007). Briefly, the PVC chambers were fitted with a gas sampling tube and a 3-way tap through which 25 mL of air were sampled using a plastic syringe fitted with Luer lock (Fisher Scientific, UK). The gas sample was then quickly injected into a pre-evacuated 12-mL glass Exetainer (Labco Ltd, UK) in order to create a positive pressure in the Exetainer. Headspace sampling was performed at three time points: immediately after locking the lid (T_0), and after 30 and 60 minutes (T_{30} and T_{60}).

Puruki-Native samples: Headspace gas samples were taken using nine laboratory-based closed PVC chambers, similar to the field-based static chambers. The replicate intact cores from each habitat were grouped in pairs inside each chamber. Before starting any measurements, the cling film was removed from the soil cores and the latter were left in the open chamber for 2-3 hours (see **Figure 2.3**). The gas sampling procedure was similar to the Turangi-47 and Turangi-67 soils. All measurements were performed in a constant temperature room at 20ºC. These two approaches (field and lab based chamber measurements) have been evaluated before and reported to produce identical results (Tate *et al.*, 2007).

Figure 2.3: Closed-chamber set-up for the measurement of net CH_4 fluxes.
With the NZ samples (Puruki-Native only), two soil cores per (PVC) chambers were used, whereas, with Scottish soils, each chamber contained three cores (as displayed here, left). A sampling tube was attached to the lid of a chamber and was fitted with a three-way tap through which air was sampled using a plastic syringe (see above, right).

Scottish soils

Headspace gas samples were taken using closed PVC chambers (~9 L) fitted with a gas sampling tube and a 3-way tap. Out of the twelve replicates from each habitat, three soil cores per chamber were used, so for each habitat n=4. Before starting any measurements, the soil cores were unwrapped and left in the open chamber for 2-3 hours.

Immediately after locking the lid of the chambers (T_0), 12 mL of air were sampled from the chamber's headspace using a plastic syringe fitted with Luer lock (Fisher Scientific, UK) and 3-way tap, and quickly injected into a pre-evacuated 12-mL glass Exetainer (Labco Ltd, UK) using a Luer syringe needle 24 mm, 25G (Fisher Scientific, UK). Headspace sampling was repeated after 30, 60 and 90 minutes (T_{30}, T_{60} and T_{90}, respectively).

4.2. Gas analysis

GC measurements of the New Zealand samples were performed by Dr Jagrati Singh. I was only observing. However, I implemented the GC system at the Macaulay Land Use Institute and analysed all the Scottish samples myself.

New Zealand samples

Exetainers containing the gas samples were loaded onto an automated gas analysis system (Shimadzu-2010 gas chromatograph, Japan) described in Hedley *et al.* (2006). Briefly, the air samples were injected into a 1-mL sample loop and directed through a 0.91 m pre-column [OD = 3 mm] and 3.66 m analytical column [OD = 3 mm]. The columns were both filled with Porapak QS 80/100, and heated at 60°C. Concentrations of CH_4 in the atmosphere were detected with a flame ionisation detector (FID) running at 250°C. Concentrations were estimated using the Shimadzu GC Solution (version 2.21 SU1) software, based on an in-house calibration curve. A series of standards ranging 0.01% to 1% CH_4 was prepared daily before a run. A 0.1% standard was run every 30 samples to check for accuracy. Precision was 0.87% with a method-detection limit of 0.04 ppm. Detailed description of the headspace set-up and gas measurements are presented elsewhere (Saggar *et al.*, 2004; Tate *et al.*, 2007). Change in headspace CH_4 was calculated based on the equation presented below:

Equation 2.1: Headspace gas flux measurement function from Saggar *et al.* (2007).

$$F = \rho \frac{V}{A} \times \frac{\Delta c}{\Delta t} \times \frac{273}{T + 273}$$

where F is the net CH_4 flux ($mg.m^{-2}.h^{-1}$); ρ the density of CH_4 ($kg.m^{-3}$) at the corresponding experimental temperature; V the headspace volume in the jar/chamber which accounts for the volume occupied by the glass containers/cores (m^3); A the surface area of the glass containers/cores in the jar/chamber (m^2); $\Delta c/\Delta t$ the average rate of change of concentration with time ($ppm.h^{-1}$); T the temperature (ºC) in the chamber.

Scottish samples

Atmospheric CH_4 concentrations inside the chamber headspace were measured on a gas chromatograph (TRACE™ GC, Thermo-Finnigan, Italy) using an analytical capillary column PLOT Al_2O_3/KCl FS [L = 50 m x ID = 0.53 mm x OD = 0.70 mm, 10 µm-film thickness] (Varian, UK) and a flame ionisation detector (FID) for the detection of CH_4. The carrier gas was helium (He). The analytical parameters of the GC were the following:

- FID with split injection mode and constant flow of carrier gas (variable pressure)
    - Oven temperature = 80ºC
    - Column flow = 9 mL.min^{-1}
    - Split ratio = 20
    - Inlet temperature = 200ºC
- Detection method (FID):
    - Fuel gas = H_2 (35 mL/min) + air (350 mL.min^{-1})
    - Make-up gas = N_2 (30 mL.min^{-1})
    - Base temperature = 250ºC
- Run time = 120 s

Using a gas-tight precision injection glass syringe, 1 mL of sample was taken from the Exetainer and injected into the column. A 20 ppm CH_4 standard (CryoService Limited, UK) was analysed after every 20 samples to check for accuracy. Precision was 3.31% with a method-detection limit of 0.19 ppm.

The atmospheric CH_4 concentrations (at T_0, T_{30}, T_{60} and T_{90}) of the unknown samples were calculated by comparing the peak area from the chromatogram to the peak area of the CH_4 standard. The results were then used to estimate the atmospheric CH_4 concentration variation inside the chamber headspace using **Equation 2.1** from Saggar *et al.* (2007).

5. Methanotroph characterisation of using molecular methods

5.1. DNA extraction

Because fewer soil samples were from the New Zealand sites, DNA from soil (500 mg) was extracted using a tube-based procedure provided by the PowerSoil™ DNA isolation kit (MoBio, USA). Since a lot more soil samples from Scotland were involved, a 96-well plate-based extraction procedure was available with the PowerSoil-htp™ 96-well soil DNA isolation kit (Mobio, USA) to extract DNA from soil (250 mg). Both kits used similar reagents and manufacturer's instructions were followed except that DNA was eluted in 50 µL instead of the recommended 100 µL, in order to increase the final concentration. Measurement of DNA concentrations was performed using a spectrophotometer (Nano-Drop® ND-1000, NanoDrop Technologies, USA) and calculations were completed by the associated software (version 3.5.2).

5.2. PCR conditions for T-RFLP analysis

Two genes were amplified: the gene coding for the 16S rRNA for both type I and type II methanotrophs; also the functional gene *pmoA* coding for the putative active site of the particulate methane monooxygenase (pMMO) enzyme (McDonald *et al.*, 2008), which is found in all methanotrophs except *Methylocella* and *Methyloferula* spp. (Dedysh *et al.*, 2000; Dunfield *et al.*, 2003; Vorobev *et al.*, 2010). **Table 2.3** provides a list of the different primers (and target genes) used in this study.

Table 2.3: PCR conditions for the amplification of the 16S rDNA genes of the type I and type II methanotrophs and of *pmoA* genes.

Primer sets	Fluorescent label [a]	Sequence (5' to 3') [b,c]	Target gene (predicted amplicon size)	Specificity	Reference
Type IF	6-FAM™	ATGCTTAACACATGCAAGTCGAACG (44-68)	16S rRNA (681 bp)	Type I methanotrophs	Chen *et al.* (2007)
Type IR	NED™	CCACTGGTGTTCCTTCMGAT (706-725)			
Type IIF	none	GGGAMGATAATGACGGTACCWGGA (445-493)	16S rRNA (550 bp)	Type II methanotrophs	Chen *et al.* (2007)
Type IIR	VIC®	GTCAARAGCTGGTAAGGTTC (975-995)			
pmo189F	VIC	GGNGACTGGGACTTCTGG	*pmoA* (500 bp)	All methanotrophs [d]	Bourne *et al.* (2001)
pmo650R	none	ACGTCCTTACCGAAGGT			

[a] 6-FAM™: 6-carboxyfluorescein; NED™ and VIC®: registered trademarks of Life Technologies Corporation.
[b] Numbers in brackets corresponding to position of *Escherichia coli* 16S rRNA gene sequence aligned in the ARB database.
[c] R represents A or G; M represents A or C; W represents A or T; N can be any base.
[d] Except *Methylocella* and *Methyloferula* spp.

5.2.1. Target preparation

The amplification of the two genes used the following optimised master mix (see Chapter 3) (final concentrations given): 1x NH_4^+ reaction buffer, 6 mM $MgCl_2$, 50 µM of each deoxynucleotide, 0.02 $U.\mu L^{-1}$ BioTaq™ DNA polymerase (all reagents from Bioline, UK), 0.3 $\mu g.\mu L^{-1}$ bovine serum albumin (Roche diagnostic, UK), 0.3 µM of each primer and 3 $ng.\mu L^{-1}$ DNA template (only 1µL of DNA template for the analysis of 16S rRNA genes).

For the *pmoA* gene, an optimised touchdown PCR programme was used (see Chapter 3): initial denaturation at 95ºC for 7 min, denaturation at 94ºC for 1 min, annealing at 65ºC for 1.5 min, extension at 72ºC for 1 min for 15 cycles with a decrement of 0.8ºC/cycle, and then denaturation at 94ºC for 1 min, annealing at 53ºC for 1 min, extension at 72ºC for 1 min for 20 cycles, and a final extension at 72ºC for 10 min.

Both type I and type II 16S rRNA genes were amplified using a classic PCR program: initial denaturation at 95ºC for 5 min, denaturation at 94ºC for 1 min, annealing at 60ºC for 1 min, extension at 72ºC for 1 min for 30 cycles and a final extension at 72ºC for 10 min. PCRs were performed on a DYAD™ DNA Engine® Peltier thermal cycler (MJ Research, USA). Purity and size of the PCR amplicons were checked by loading 5 µL of each reaction mix on a 1% (w/v) agarose gel stained with ethidium bromide and observed under UV light.

5.2.2. Target purification

PCR products were purified using the UltraClean-htp™ 96-well PCR Clean-up™ kit (MoBio, USA) according to the manufacturer's instructions, except that DNA was eluted in 35 µL instead of the recommended 100 µl, to increase the final concentration. Concentrations of the purified PCR products were then measured on the Nano-Drop ND-1000.

5.3. Terminal-restriction fragment length polymorphism (T-RFLP) analyses

A known concentration of purified PCR amplicon (10 ng.μL^{-1}) from each target gene was digested with three restriction enzymes: *Msp*I (*pmoA* gene and 16S rRNA gene of type I and type II methanotrophs), *Hha*I (*pmoA* gene and 16S rRNA gene of type I methanotrophs) and *Mbo*I (16S rRNA gene of type II methanotrophs). **Table 2.4** provides a summary of the different reactions.

Table 2.4: Individual enzymatic reactions performed on the target genes under investigation.

Gene	Restriction enzyme		
	***Msp*I**	***Hha*I**	***Mbo*I**
16S rRNA type I [a]	X	X	
16S rRNA type II	X		X
pmoA [a]	X	X	

[a] Although the PCR products of the 16S rRNA genes from type I methanotrophs and *pmoA* genes were digested separately, the two were mixed together before analysis on the sequencer.

In a 10-μL reaction mix, the final concentrations of the different components were as follows: 10 ng.μL^{-1} of DNA template, 1x of enzyme solution, 1x of enzyme buffer and 0.1 μg.μL^{-1} of bovine serum albumine (all reagents from Promega, UK). Samples were then digested for 3 hours at 37ºC on a DYAD™ thermal cycler, and the enzyme reaction was stopped by incubation at 95ºC for 15 min.

1-μL aliquots of digested PCR products were transferred onto a MicroAmp® optical 96-well plate (Applied Biosystems, UK) and mixed with 12 μL of Hi-Di™ formamide (Applied Biosystems, UK). 0.3 μL of LIZ-labelled GeneScan™-500 internal size standard (Applied Biosystems, UK) was added and the reaction was denatured at 95°C for 5 min. T-RFLP analysis was carried out on an automated sequencer, an ABI Prism® 3130*xl* genetic analyzer (Applied Biosystems, UK). Terminal restriction fragments (T-RFs) generated by the

sequencer were analyzed using the size-calling software GeneMapper™ 4.0 (Applied Biosystems, UK) and quantified by advanced mode using second order algorithm. T-RFs in a T-RFLP profile were selected by the software if their minimum peak height was above the noise observed with the negative control (usually above 25 relative fluorescence units). Only peaks 30-550 bp were considered in order to avoid T-RFs caused by primer-dimers and to obtain fragments within the linear range of the internal size standard (Singh *et al.*, 2007).

5.4. Cloning and sequencing analysis

This was performed on the New Zealand samples only.

5.4.1. Target preparation

The PCR products for cloning and sequencing of the *pmoA* gene were generated in the same way as detailed earlier for T-RFLP (see section 5.2.), except that no fluorescently-labelled primer was used. Purification of PCR products was performed as described previously (see section 5.2.2). In order to minimise PCR bias and sample variation, replicates from each site (Turangi and Puruki) were pooled prior to cloning: for the Turangi library (Turangi-47 and Turangi-67 were combined), 12 replicates were pooled; and 18 replicates for the Puruki (Puruki-Native) library.

5.4.2. Cloning reaction

In total, two separate clone libraries were obtained, one for each individual sampling area (Puruki-Native and Turangi shrublands). Details of the cloning and sequencing methods have been described before (Singh *et al.*, 2007; 2009). In brief, the *pmoA* gene amplicons obtained were cloned in *Escherichia coli* using a TOPO TA Cloning® kit (Invitrogen, UK). 16 clones were selected from each library and were amplified with the vector-specific T3 / T7 primers.

The reacted products were purified using the Wizard® SV Gel and PCR Clean-Up System (Promega, USA) following the manufacturer's instructions. Samples were submitted for sequencing to Macrogen Europe (The Netherlands). Sequencing was conducted under BigDye™ terminator cycling conditions on an ABI Automatic Sequencer 3730XL (Macrogen Europe, The Netherlands).

5.4.3. Alignment and identification of clone sequences

The analysed sequences were used to find matches with prokaryotic genes using the NCBI database (http://www.ncbi.nlm.nih.gov). All sequences were manually checked for chimeras, and the sequences with a split in alignment were removed from further analysis. Clone sequences were aligned on the forward and reverse primers using Kodon software (Applied Maths, Belgium). Kodon was also used to translate the nucleotide sequences of the *pmoA* gene in order to confirm that inserts coded for functional proteins (absence of stop codon).

Finally, the derived *pmoA* amino acid sequences were used to construct a phylogenetic tree using the MEGA 5 (Molecular Evolutionary Genetics Analysis) software (Kumar *et al.*, 2008) by performing neighbour-joining tree analysis with 1,000 bootstrap replicates using the Poisson algorithm. To match individual clones with a specific T-RF, sequences were run with REMA software (http://macaulay.ac.uk/rema) to predict the (virtual) size of the T-RF for individual clones (Szubert *et al.*, 2007).

Following selection of 16 colonies from each of the two cloning reactions, 15 clone colonies produced a PCR product with the *pmoA* gene for each library. In total, 15 clean *pmoA* sequences were obtained from Turangi shrublands (Turang-47 and Turangi-67) and 13 clean *pmoA* sequences from Puruki-Native. These clones were merged with clones obtained from the previous studies on these sites. Translated amino acid sequences were used for constructing a phylogenetic tree.

5.4.4. Nucleotide sequence accession numbers

The *pmoA* sequence data of the New Zealand samples were submitted with annotated features to the EMBL (European Molecular Biology Laboratory) nucleotide sequence database (http://www.ebi.ac.uk/embl/) under the accession numbers FR715958 to FR715985.

5.5. Diagnostic *pmoA* microarray analysis

This was performed on the Scottish samples only, using n=4 for each habitat of each site (total n=44). Microarray analysis was carried out using a modified method of Stralis-Pavese *et al.* (2004; 2011). The different steps involved are briefly described below:

5.5.1. Target preparation

The PCR products for the *pmoA* gene for the microarray assay were generated in the same way as detailed earlier for T-RFLP (see section 5.2), except that no fluorescently-labelled primer was used. Also the reverse primer for the amplification of the *pmoA* gene (pmo650R) contained the T7 promoter site (5'-TAATACGACTCACTATAG-3') at its 5' end, which enabled T7 RNA polymerase-mediated *in vitro* transcription, using the PCR products as template, to generate fluorescently-labelled RNA for hybridisation on the microarray slides. Purification of PCR products was performed as described previously (see section 5.2.2).

5.5.2. *In vitro* transcription

In vitro transcription was carried out under RNAase-free conditions. The procedure was as follows (20 µl final volume): 8 µL purified PCR product (50 $ng.\mu L^{-1}$), 4 µL 5x T7 RNA polymerase buffer, 2 µL DTT (100 mM), 0.5 µL RNAsin (40 $U.\mu L^{-1}$) (Promega), 1 µL of

each ATP, CTP, GTP (10 mM), 0.5 µL UTP (10 mM), 1 µL T7 RNA polymerase (40 $U.\mu L^{-1}$) (Invitrogen) and 1 µL Cy3-UTP (5 mM) were added into a 1.5 mL Eppendorf tube and incubated at 37°C for 4 hours. RNA was purified immediately based on the RNeasy Mini Kit (Qiagen): 80 µL of DEPC-treated water were added to IVT mixture, followed by adding 350 µL of RLT and 250 µL of ethanol, and then mixed thoroughly. Samples were transferred to an Rneasy mini tube and 500 µL of RPE were added. Tubes were centrifuged at 10,000 rpm for 15 sec. Another 500 µL of RPE were added, and then centrifugation at 10,000 rpm for 2 min. Purified RNA was eluted into 50 µL of dH_2O. RNA yields and dye incorporation rates were measured by spectrophotometry. Purified RNA was fragmented by incubating with 9.5 mM $ZnCl_2$ and 24 mM TrisCl (pH7.4) at 60°C for 30 min. Fragmentation was stopped by the addition of 12 mM EDTA (pH 8.0) to the reaction and putting it on ice. 1 µL of RNAsin (40 $U.\mu L^{-1}$) was added to the fragmented target.

5.5.3. Hybridisation

Hybridisation was carried out (in triplicate) in an aluminium block on a Belly Dancer (Stovall Life Sciences, USA), which was preheated to 55°C for at least 1 hour. For each hybridisation, the following was added to a 1.5 mL Eppendorf tube (100 µl final volume) and incubated at 65°C for 1 min: 62 µL of DEPC-treated water, 1 µL of 10% SDS, 30 µl of 20x SSC (3 M sodium chloride, 0.3 M sodium citrate, pH 7.0), 2 µl of 50x Denhardt's reagent (Sigma) and 5 µl of target RNA (corresponding to about 200 ng of RNA). Preheated hybridisation mixtures were applied onto the preheated slides containing the arrays. The assembled microarray slides were incubated overnight in the HybriWell hybridisation chambers (Grace BioLabs) at 55°C at maximum bending and lowest rotation. Following hybridisation, the slides were washed by shaking at room temperature for 5 min in 2x SSC, 0.1% (w/v) SDS; twice for 5 min in 0.2x SSC and finally for 5 min in 0.1x SSC. Slides were dried using an airgun.

5.5.4. Scanning and data analysis

Hybridised slides were scanned at 10 µm resolution with a GenePix 4000 laser scanner (Axon, USA) at a wavelength of 532 nm. Fluorescent images were analyzed with the GenePix software (Axon, USA). Micosoft Excel was used for statistical analysis and presentation of results.

Results were normalised to a positive control. The hybridisation signal for each probe was expressed as a percentage of the signal (median of signal minus background) of the positive control probe mtrof173 on the same array (Bodrossy *et al.*, 2003). As each slide contained triplicate arrays, normalised signal intensities of the triplicate spots on a slide were used to determine average results and standard deviations. Hybridisation between a probe and a target was considered positive if the signal was at least 5% of the strongest signal obtained for that probe with the validation set of reference strains/clones. For probes where no perfect match reference target was available or the strongest signal was less than 60 (% of the signal obtained for mtrof173), this reference value was arbitrarily set to 60. This was found to minimize false positive calls while not creating any false negative calls (Stralis-Pavese *et al.*, 2004).

The current version of the *pmoA* array contains 199 oligonucleotide probes targeting *pmoA* of methanotrophs, *amoA* (encoding a subunit of ammonia monooxygenase) of ammonia oxidisers and other functionally-related bacteria (Stralis-Pavese *et al.*, 2011). A selection of the probes used can be found in **Appendix Table 0.1**.

6. Microcosm experiments and stable isotope probing of phospholipid fatty acids (PLFA-SIP)

6.1. PLFA-SIP

New Zealand samples

10 g of field-moist 5.6-mm sieved soils (n=18 for Puruki-Native; n=6 for each Turangi-47 and Turangi-67) were transferred into 125-mL Wheaton glass serum bottles (Sigma-Aldrich, UK), and left overnight in the dark at 20ºC. The following day, bottles were sealed and injected through the rubber septum with 1.25 mL of ^{13}C-CH_4 (>99 atom%, CK Gas, UK) from a ~5,000 ppm in order to have a starting headspace concentration of ~50 ppm. Soils were incubated in the dark at 20ºC for 14 days (Tate *et al.*, 2007). ^{13}C-CH_4 concentration in the headspace was measured at the start and end of the experiment to monitor the level of incorporation. After incubation was complete, ^{13}C-enriched soils were kept frozen at -20ºC.

Scottish samples

10 g of field-moist 5.6-mm sieved soils were transferred into 125-mL Wheaton glass serum bottles (Sigma-Aldrich, UK), and left overnight in the dark at 20ºC. The following day, bottles were sealed and injected through the rubber septum with 2.5 mL of ^{13}C-CH_4 (>99 atom%, CK Gas, UK) from a ~5,000 ppm in order to have a starting headspace concentration of ~100 ppm. Soils were incubated in the dark at 20ºC.

PLFA-SIP was performed on the autumn and summer soils only, and on all chamber replicate soils (n=4) from each habitat from each site (total n=88). The autumn samples were all incubated for 14 days whereas the summer samples were incubated until >90% of ^{13}C-CH_4 had been incorporated (between 4 and 32 days depending on the activity of the soils).

After incubation was complete, ^{13}C-enriched soils were kept frozen at -20ºC.

6.2. PLFA extraction

A sub-sample (between 0.25 and 1 g) of the ^{13}C-enriched soils was freeze-dried, milled and used for extracting PLFAs following the method described by Singh *et al.* (2007) and Tate *et al.* (2007). Briefly, the extraction of total lipids was achieved by subjecting the soil preparation to the solvents chloroform and methanol and a citrate buffer (1:2:0.8). After fractionation of the total lipids by acid chromatography, the polar lipids were trans-esterified using a mild alkaline methanolysis (0.2 M KOH), producing PLFA methyl esters (PLFAMEs), and derivatisation was performed using dimethyl disulfide. During the process, a pure C19:0 methyl ester internal standard was added for quality control and calculation purposes (Frostegård *et al.*, 1991; 1993b).

6.3. Compound-specific isotope analysis via gas chromatography-combustion-isotope ratio mass spectrometry (GC-C-IRMS)

The isotopic composition of individual PLFAs was determined using a Trace Ultra GC with combustion column attached *via* a GC Combustion III to a Delta V Advantage isotope ratio mass spectrometer (all Thermo Finnigan, Germany). Samples (2 µL) were injected in splitless mode onto a J&W Scientific HP-5 column [L = 50 m x ID = 0.2 mm, 0.33 µm-film thickness] (Agilent Technologies Inc, USA). The oven temperature was programmed, following an isothermal hold at 100°C for 1 min, to 190°C at a rate of 20°C.min^{-1}, then to 235°C at 1.5°C.min^{-1}, then to 295°C at 20°C.min^{-1}, followed by an isothermal hold for 10 min. Other running conditions were as described by Paterson *et al.* (2007). The C isotope ratios were calculated with respect to a CO_2 reference gas injected with every sample and traceable to International Atomic Energy Agency reference material NBS 19 TS-Limestone.

Repeated analysis, over a two-month period, of the $\delta^{13}C$ value of a C19:0 FAME internal standard gave a standard deviation of 1.11‰ (n=18).

Standard nomenclature was used for PLFAs (Frostegård *et al.*, 1993b). The number before the colon is the number of C atoms in the molecule, the number after the colon gives the number of double bonds and their location (ω) from the methyl end of the molecule. Prefixes Me, cy, i and a indicate methyl-, cyclopropyl-groups, and iso-, anteiso-branching, respectively.

Quantification of PLFA contents was based on the normalised peak area of each PLFA, which were compared to the peak area of the C19:0 PLFA internal standard, accounting for the weight of soil used for the PLFA extraction (personal communication from Dr Barrie Thornton).

7. Data analysis

7.1. New Zealand experiment

We compared the data from this experiment (Turangi-47, Turangi-67 and Puruki-Native) with data from three previous studies (Singh *et al.*, 2007; Singh *et al.*, 2009; Tate *et al.*, 2007) using the same (Puruki) or nearby (Turangi) sites but different land-use types (**Table 2.5**). Although the sampling campaigns from the different sites and land uses occurred during different years, this always happened in the warmer months of the year (from October to February, as shown below).

Table 2.5: Description of the different sites and land uses of the comparative analysis.

Site [a]	Land use	Name used in this study [b]	Description	Date of sampling	Reference
Turangi	Pasture	Pasture (5) (n=4)	Pasture adjacent to a 5-year-old pine forest	January 2007	Singh *et al.* (2009)
		Pasture (10) (n=4)	Pasture adjacent to a 10-year-old pine forest		
	Pine forest (*Pinus radiata*)	Pine (5) (n=4)	5-year-old pine forest		
		Pine (10) (n=4)	10-year-old pine forest		
	Shrubland	Turangi-47 (n=6)	47-year-old shrubland	February 2008	This study
		Turangi-67 (n=6)	67-year-old shrubland		
Puruki	Pasture	Pasture (7) (n=3)	Pasture adjacent to a 7-year-old pine forest	October 2004	Singh *et al.* (2007) Tate *et al.* (2007)
	Pine forest (*Pinus radiata*)	Pine (7) (n=3)	7-year-old pine forest		
	Native forest	Puruki-Native (n=9)	Mature native forest	January 2008	This study

[a] Soil physical data from Puruki-Native were compared to data from Pasture (7) and Pine (7). The soil chemical properties, net CH_4 fluxes, PLFA composition, T-RF abundance and clone sequences were also compared between the different land uses for both Turangi and Puruki sites.
[b] The age of the pasture and pine stands (y) is shown in brackets. The pastures correspond to the adjacent pasture of each pine stand. The number of samples used for each habitat is also shown.

7.2. T-RFLP data processing

Raw data from GeneMapper™ were exported to be used with *T-REX* (**T**-**R**FLP analysis **EX**pedited), online software for the processing and analysis of T-RFLP data (http://trex.biohpc.org/) developed by Culman *et al.* (2009). The software allows for simultaneous processing of large number of sample files and to clean raw data from fragment analysis. The T-RFLP data were subjected to several quality control procedures: for the New Zealand samples, noise filtering (peak area, standard deviation multiplier = 1), T-RF alignment (clustering threshold = 2 bp) and T-RFs omitted if they occur in less than 2% of samples; whereas for the Scottish samples, no noise filtering was used.

T-REX software also permits the use of several functions such as definition of replicates in order to observe variability in T-RFs; construction of two-way data matrices based on T-RF presence, (relativised) peak height or (relativised) peak area; and analysis of a data matrix using the additive main effect and multiplicative interaction (AMMI) model based on analysis of variance (ANOVA) as discussed by Culman *et al.* (2008). In brief, the AMMI model, also called doubly-centered principal component analysis (PCA), is interfaced with MATMODEL 3.0 (Gauch, 2007) and uses a two-way ANOVA. First, it will partition the variation into 'main effects' and 'interactions', and then applies PCA to the interactions (IPCAs) in order to analyse the 'interaction effects' (Gauch, 1992). Only the first four dimensions of the IPCA are used to capture the interaction signal variation. Therefore, AMMI focuses on the differential responses of the T-RFs to the environment (or treatment) instead of examining the overall variability of the data (Culman *et al.*, 2008). Conceptually, if the percentage of main effects is high, this means that the environments being investigated (*e.g.* land-uses, seasonal changes) display similar bacterial communities. Inversely, very dissimilar microbial communities will be characterised by a high interaction effect component. This is displayed by *T-REX* software in a summary table including the percentage

of variation of the main and interaction effects, the latter showing variations due to pattern and noise when using replicated data. Also given are the percentages of variation of the predicted interaction signal captured by the four axes of the IPCA.

Raw peak heights only (no binary data used in this study) were relativised to account for uncontrolled differences in the quantity of DNA between samples (Culman *et al.*, 2008). The relative abundance of a detected T-RF within a given T-RFLP profile was calculated as the respective signal height of each peak divided by the total peak height of all the peaks of the T-RFLP profile. Only the T-RFs that were considered "true" by the *T-REX* analysis were used for subsequent analysis.

7.3. Statistical tests

The significance of differences in soil characteristics, net CH_4 fluxes and relative abundance of the dominant T-RFs was determined by nested ANOVA in order to test the effect of habitat (land-use change) as well as seasonal changes within each habitat. Regression analysis was used to explore the linear relationship between the methanotroph community (IPC scores) in each habitat and the corresponding net CH_4 fluxes. The effect of land-use change on the methanotroph population was assessed by changes in the hybridisation intensity of the microarray probes, which were investigated by one-way ANOVA using habitat as factor. PCA was also applied on the positive microarray probes to observe shifts associated with land-use changes. ANOVA and MANOVA were then used on the PC scores to confirm the significance of these shifts. Similarly, nested ANOVA and MANOVA were utilised on the IPC scores from the *T-REX* analysis. Before ANOVA/MANOVA, environmental data were checked for normality. When a Gaussian distribution was not observed, the relevant sets of data were log- or square root-transformed. All ANOVAs were followed by Tukey's test for multiple pairwise comparisons between the different treatments.

Finally, following the square root transformation of the PLFA data (% of total enriched PLFA content), cluster analysis, based on a Bray-Curtis similarity matrix, was performed using the group average linking method in order to affiliate the active methanotroph population present in the soils with published methanotrophs. The above statistical analyses were carried out using GenStat® 11th edition software (VSN International Limited, UK).

However, the following statistical analyses were performed using CANOCO for Windows version 4.53 (Biometris, The Netherlands). Detrended correspondence analysis (DCA) was first applied on the 15 most abundant (*pmoA*) T-RFs in order to estimate the gradient length of the T-RF diversity. Redundancy analysis (RDA) was then applied on the T-RFs to investigate the effect of some environmental variables on the individual T-RFs. This resulted in a triplot showing the scores of the samples, T-RF species and environmental variables.

Results of soil properties and biochemical and molecular analyses are presented as means, together with standard errors of the means (S.E.M.) for Turangi (n=6), Puruki (n=9) and the Scottish samples (n=4); unless otherwise stated.

Chapter 3 Experimental results (1)

PCR optimisation for the detection of a functional gene (*pmoA*) using the Taguchi methods

1. Brief introduction

Originally, the Taguchi methods were formulated for the optimisation of industrial processes, where several factors (3 to 50) of complex multifactorial experiments were tested at different levels (Taguchi, 1986). The Taguchi methods use orthogonal arrays to organise the 'control' parameters/factors affecting a process and the levels at which they should vary in order to predict the optimum conditions of a process, whilst accounting for performance variations due to 'noise' factors beyond the control of the design (Taguchi, 1986). Also, in a normal factorial strategy, every parameter should be individually tested at several levels, thus becoming extremely time-consuming, labour-intensive and expensive. By using an orthogonal array and a particular algorithm (quadratic loss function), only a few combinations are tested, therefore dramatically decreasing the total number of experiments and simultaneously identifying the optimum condition of several factors. For example, if four parameters were to be tested at three different levels, a factorial design would require performing 81 experiments (3^4), whereas with Taguchi methods, only nine would be needed. Nowadays, the Taguchi methods are widely employed in different areas of biotechnology as reviewed by Rao *et al.* (2008).

Because some functional genes are present only in small fractions of microbial communities, and only few copies can be present in each genome, their detection by classical PCR methods can be challenging. Optimisation of the experimental conditions of a PCR requires the same approach as an industrial process because several factors can be controlled simultaneously. They include the different components of the reaction mix (concentrations of salt, primers, enzyme, DNA template, *etc*.) as well as the cycling features (time and temperature of the denaturation, annealing and extension steps, number of cycles, *etc*.). Therefore, the optimum experimental conditions of a PCR should be investigated every time a new gene is under investigation. To date, the Taguchi methodology has seldom been applied to the optimisation of PCR (Ballantyne *et al.*, 2008; Ballantyne *et al.*, 2010; Caetano-Anollés, 1998; Cobb & Clarkson, 1994). However, this approach has never been applied to the optimisation of the detection by PCR of functional genes of non-cultivable microorganisms present in environmental samples. Furthermore, although only one previous study (Caetano-Anollés, 1998) optimised both the concentrations of the master mix components and the cycling parameters, none attempted to optimise a touchdown PCR.

The aim of this chapter was to test the different parameters involved in a (touchdown) PCR and estimate the optimum settings for the detection of the functional gene *pmoA*. It is the gene coding for the putative active site of the particulate methane monooxygenase, involved in the oxidation of methane by the methanotrophs (Hanson & Hanson, 1996).

2. The Taguchi methodology: the theoretical background and experimental approaches

The optimisation of a process using the Taguchi methods involves several steps:

- Determining the appropriate experimental matrix
- Performing the necessary experiments
- Analysing the optimisation data
- Validating the optimised conditions

2.1. Defining the experimental matrix

The Taguchi approach uses a number of progressive trials/experiments in which only a few permutations are explored, instead of testing every possibility. These are organised into an orthogonal array (OA). First, the 'control' factors – that is the parameters that have a direct impact on the process – have to be chosen along with the number of levels to explore – hence, the range at which these factors vary must be known. Therefore, the number of experiments that are needed will vary. Thus, the type of OA to use will change. **Appendix Table 0.2** shows how to select an array according to the factors and levels to be tested.

2.2. Conducting the designed experiments

Once the OA has been selected, the experiments should be performed according to the specifications of the chosen OA. **Table 3.1** describes the organisation of a L_9 OA. Each experiment should be performed in duplicate or triplicates to account for noise interferences, thus reducing experimental error and also to observe the variance of each parameter. The output value of each experiment (and their replicates) should then be recorded and organised for data analysis.

Table 3.1: Taguchi orthogonal array L_9 * for 4 factors at 3 levels (A, B and C) each.

	Factor			
Experiment	**[1]**	**[2]**	**[3]**	**[4]**
1	A	A	A	A
2	A	B	B	B
3	A	C	C	C
4	B	A	B	C
5	B	B	C	A
6	B	C	A	B
7	C	A	C	B
8	C	B	A	C
9	C	C	B	A

* The subscript number next to the letter L corresponds to the number of experiments required (see **Appendix Table 0.2**).

2.3. Analysing the experimental data

The literature offers two approaches to the calculation of the effect of a factor: the classical Taguchi method and a modified one.

2.3.1. Classical Taguchi approach

The Taguchi approach uses several types of quadratic loss functions to calculate the effect of a factor on the process under investigation. It is called a signal-to-noise (SN) ratio. If the aim of the Taguchi approach is to maximise the performance characteristic, which in the case of a PCR is equivalent to the PCR product yield, then the objective is to maximise the PCR product yield and the type of SN ratio to use is thus "larger-the-better" (LBT). The classical Taguchi approach was not used here but more information can be found in Rao *et al.* (2008).

2.3.2. Modified Taguchi approach

A modified Taguchi approach was developed by Cobb & Clarkson (1994). It differs from the classical Taguchi approach in the method for calculating the SN ratios. Instead of calculating the SN ratio from the averaged replicates of an experiment, factor effects are estimated by analysis of the replicate means (not the individual replicates). In other words, the SN ratio is calculated from the averaged means of each experiment level, as an alternative to averaging the SN ratio of each experiment level. **Equation 3.1** shows the algorithm to use for estimating the optimum conditions of a process.

Equation 3.1: The modified Taguchi loss function for LBT signal-to-noise ratio calculation of a given factor level.

$$\mathrm{SN}_{\mathrm{v,w}} = -10 \log\left[\frac{1}{\mathrm{n}}\sum_{\mathrm{w}=1}^{\mathrm{n}}\left(\frac{1}{\mathrm{Y}_{\mathrm{w}}^{2}}\right)\right]$$

where *SN* is the signal-to-noise ratio of the factor level; *v* the factor number; *w* the level number; *n* the number of levels; and *Y* the mean value of the performance characteristic (or PCR product yield in the case of a PCR) at the level w.

First, the average value of the performance characteristic of the replicates is calculated (**Table 3.2**). Then, the means of the performance characteristic of the experiments sharing the same levels (see Table 3.1 and Table 3.2) are pooled (**Table 3.3**). For example, the SN ratio for the level A of the factor [1] ($SN_{[1],A}$) is calculated by averaging the SN ratio of the experiments 1, 2 and 3 (SN_1, SN_2 and SN_3, respectively). Similarly, the SN ratio for level C of the factor [4] ($SN_{[4],C}$) is the average of SN_3, SN_4 and SN_8.

Table 3.2: Means of the performance characteristic (Y) for each experiment of a L_9 OA.
y is the output value of the performance characteristic for each individual replicate.

	Replicate			Mean
Experiment	**a**	**b**	**c**	
1	$y_{a,1}$	$y_{b,1}$	$y_{c,1}$	Y_1
2	$y_{a,2}$	$y_{b,2}$	$y_{c,2}$	Y_2
3	$y_{a,3}$	$y_{b,3}$	$y_{c,3}$	Y_3
4	$y_{a,4}$	$y_{b,4}$	$y_{c,4}$	Y_4
5	$y_{a,5}$	$y_{b,5}$	$y_{c,5}$	Y_5
6	$y_{a,6}$	$y_{b,6}$	$y_{c,6}$	Y_6
7	$y_{a,7}$	$y_{b,7}$	$y_{c,7}$	Y_7
8	$y_{a,8}$	$y_{b,8}$	$y_{c,8}$	Y_8
9	$y_{a,9}$	$y_{b,9}$	$y_{c,9}$	Y_9

Table 3.3: Pool of the performance characteristic means for each factor and level.

	Factor			
Level	**[1]**	**[2]**	**[3]**	**[4]**
A	Y_1 Y_2 Y_3	Y_1 Y_4 Y_7	Y_1 Y_6 Y_8	Y_1 Y_5 Y_9
B	Y_4 Y_5 Y_6	Y_2 Y_5 Y_8	Y_2 Y_4 Y_9	Y_2 Y_6 Y_7
C	Y_7 Y_8 Y_9	Y_3 Y_6 Y_9	Y_3 Y_5 Y_7	Y_3 Y_4 Y_8

A tabulated version of the averaged SN ratio is built (**Table 3.4**), and the range (Δ) of the SN ratios for each factor is calculated from the difference between the highest and lowest SN ratios. Therefore, each factor can be ranked according to the importance of its effect on the output of the process. If looking at larger-the-better effect, the factor with the largest range

will be the one having the biggest effect on the process. Also, the level with the highest SN ratio will constitute the optimum condition of each factor (**$SN_{opt,v}$**).

Table 3.4: SN ratios ($SN_{v,w}$) for each factor and level, and calculated from the pooled means.

	Factor			
Level	**[1]**	**[2]**	**[3]**	**[4]**
A	$SN_{[1],A}$	$SN_{[2],A}$	$SN_{[3],A}$	$SN_{[4],A}$
B	$SN_{[1],B}$	$SN_{[2],B}$	$SN_{[3],B}$	$SN_{[4],B}$
C	$SN_{[1],C}$	$SN_{[2],C}$	$SN_{[3],C}$	$SN_{[4],C}$
Δ	$\Delta_{[1]}$	$\Delta_{[2]}$	$\Delta_{[3]}$	$\Delta_{[4]}$
Rank				

2.3.3. Analysis of variance and regression analysis

As well as calculating the SN ratios, an ANOVA test can be performed to quantify more accurately the contribution of each factor to the overall effect (Caetano-Anollés, 1998). The results from Table 3.4 only give an indication of which level of a factor gives the best effect by choosing the $SN_{opt,v}$. If a polynomial regression is performed for each factor using the SN ratios of the different levels, the shape of the trendline can be used to maximise the SN ratio for each factor (**$SN_{max,v}$**); and thus estimate the optimum level value even if not tested (Cobb & Clarkson, 1994).

2.4. Validation experiment and verification test

In the Taguchi methods, an additive model is used to predict the influence of the 'control' factors on the response. The model refers to the sum of the individual factor effects. One major purpose of the **validation experiment** is to provide evidence demonstrating that the

additive equation applies and that interactions are low. If the result (calculated SN) of an experiment – using the optimised factor values – is similar to the predicted result, that experiment is considered successful. If the result of a verification test differs widely from the prediction, it is obvious that interactions are significant. The interaction must be discovered and eliminated, and the experimental procedure must be planned again (Taguchi, 1986).

Practically, the **verification test** involves using what is called a predictive equation (Caetano-Anollés, 1998). First, the overall experimental average SN ratio (**SN_{exp}**) is calculated accounting for all $SN_{v,w}$ (**Equation 3.2**).

$$SN_{exp} = \frac{\sum_{v}^{w} SN_{v,w}}{n_{v,w}} \qquad \textbf{Equation 3.2}$$

where $n_{v,w}$ is the total number of factors (n_v) and levels (n_w). Therefore, $n_{v,w} = n_v \times n_w$.

Then, the difference between SN_{exp} and the optimum SN ratio of each factor (**$SN_{opt.v}$**) is calculated. If polynomial regressions are used, the maximum SN ratio predicted (**$SN_{max,v}$**) can also be used instead of $SN_{opt.v}$. As a result, that difference represents the predicted improvement in SN ratio for each factor (**$SN_{pred,v}$**, **Equation 3.3**).

$$SN_{pred,v} = SN_{max,v} - SN_{exp} \qquad \textbf{Equation 3.3}$$

Since the Taguchi methodology uses an additive model, the predictive equation defines the overall improvement of the SN ratio (**SN_{pred}**, **Equation 3.4**) as the sum of the SN_{exp} (Equation 3.2) and the $SN_{pred,v}$ (Equation 3.3) of each factor.

$$SN_{pred} = SN_{exp} + \sum_{v=1}^{n} SN_{pred,v} \qquad \textbf{Equation 3.4}$$

where *n* is the number of factors and *v* the factor level.

Finally, $\mathbf{SN_{test}}$ represents the SN ratio calculated after the validation experiment is run using the optimum conditions. The above terms and the verification test of the validation experiment are shown in **Table 3.5**.

Table 3.5: Verification test after validation experiment.

	Factor				
Level	**[1]**	**[2]**	**[3]**	**[4]**	
A	$SN_{[1],A}$	$SN_{[2],A}$	$SN_{[3],A}$	$SN_{[4],A}$	
B	$SN_{[1],B}$	$SN_{[2],B}$	$SN_{[3],B}$	$SN_{[4],B}$	**Overall average**
C	$SN_{[1],C}$	$SN_{[2],C}$	$SN_{[3],C}$	$SN_{[4],C}$	**SN_{exp}**
$SN_{opt,v}$ or $SN_{max,v}$	$SN_{opt,[1]}$ or $SN_{max,[1]}$	$SN_{opt,[2]}$ or $SN_{max,[2]}$	$SN_{opt,[3]}$ or $SN_{max,[3]}$	$SN_{opt,[4]}$ or $SN_{max,[4]}$	
$SN_{pred,v}$	$SN_{pred,[1]}$	$SN_{pred,[2]}$	$SN_{pred,[3]}$	$SN_{pred,[4]}$	**SN_{pred}**
					SN_{test}

2.5. Summary of the Taguchi methodology

The general procedure for the optimisation of the *pmoA* genes using the Taguchi methodology was as follows:

1. Defined the appropriate experimental OA for the variables to be investigated.
2. Conducted subsequent experiments after choosing the appropriate range of each level.
3. Analysed the experimental data using the **modified Taguchi approach**
4. Performed a polynomial regression on each variable investigated to estimate the maximum SN ratios and optimum settings (no ANOVA was used).
5. Carried out a validation experiment followed by a verification test (based on the SN_{max} instead of SN_{opt}).

3. Optimisation of the detection of *pmoA* genes

3.1. Primer sets

Three sets of primers were tested. The forward primer was always pmo189F (Holmes *et al.*, 1995), whereas the reverse primers were pmo682R (Holmes *et al.*, 1995), pmo661R (Costello & Lidstrom, 1999) or pmo650R (Bourne *et al.*, 2001). All three reverse primers are valid and have been widely used, except that some differences were observed related to the methanotrophs they are able to detect. The primer pmo682R, along with primer pmo189F, also allows the detection of some nitrifying bacteria due to a strong conserved sequence between the *pmoA* and *amoA* genes (Holmes *et al.*, 1995). The pmo189F-pmo661R and pmo189F-pmo650R primer sets on the other hand only target the *pmoA* genes. However, the pmo189F-pmo661R primer set fails to detect high-affinity methanotrophs related to the "upland soil cluster alpha" (Bourne *et al.*, 2001). The characteristics of the three primer sets are presented in **Appendix Table 0.3**. The pmo189F-pmo650R primer set was used in the optimisation process presented here.

3.2. Pre-optimisation work

Several approaches were tested and a summary of the different stages is presented below:

- The three above primer sets were tested using similar PCR conditions as the ones described in the original publications. Only the use of the primer set pmo189F-pmo682R allowed the observation of faint bands, including some smearing, on an agarose gel.
- The use of a touchdown (TD) approach improved the results a little for the primer set pmo189F-pmo682R, though smearing was stronger. Unfortunately, no PCR products were obtained with the primer sets pmo189F-pmo661R and pmo189F-pmo650R.

- A nested PCR was tested. The primer set pmo189F-pmo682R was used in the first round of PCR with TD conditions. The PCR products were then used as template for the second round of PCR. Amplification was performed with the primer sets pmo189F-pmo661R or pmo189F-pmo650R. Contaminations in the negative controls were observed and could not be avoided due to the nature of the experiment. Indeed, on one hand, methanotrophs were detected in the negative control of the second round of PCR using the negative control of the first round as template (which was not contaminated). On the other hand, no contamination was present in the negative control of the second round of PCR (similar as a first round PCR negative control). This proves that there was no problem due to contaminated PCR reagents.

Because of all the above failed attempts, a whole different approach was decided, using the Taguchi methodology. The method employed was actually the modified Taguchi approach (see section 2.3.2).

3.3. Quantification of PCR product yields

Firstly, 5µL of PCR amplicon were mixed with 5µL of 2x loading buffer (sucrose-based solution) and then loaded on a 1% (w/v) agarose gel stained with ethidium bromide. After capture by a UV camera, the picture was analysed with the ImageJ software (version 1.42q, National Institute of Health, USA). A box was formed around each band representing the *pmoA* gene, and ImageJ calculated their maximum brightness. The background intensity was also measured and its value was used as blank. Finally, the resulting values were used to represent the relative PCR product yields.

3.4. Optimisation of the master mix components for the amplification of the *pmoA* genes using the primer set pmo189F-pmo650R

3.4.1. Protocol

Six components (or factors) of the PCR master mix, out of seven, were tested at three different concentrations (or levels) as shown in **Table 3.6**. The component that was not tested was the concentration of the NH_4^+ buffer. The main reason behind this choice was based on personal experience that variation in the buffer concentration would negatively impact on the performance of the PCR. Thus, the final concentration of the NH_4^+ buffer was always 1x.

Table 3.6: Concentration levels for the components of the master mix for the amplification of *pmoA*.

	Factor					
Level	**BSA ($\mu g.\mu L^{-1}$) ***	**$MgCl_2$ (mM)**	**dNTPs (µM)**	**Enzyme ($U.\mu l^{-1}$)**	**Primer (µM)**	**DNA template ($ng.\mu L^{-1}$)**
A	0.2	1	50	0.005	0.1	1
B	0.4	4	100	0.013	0.2	2.5
C	-	8	300	0.025	0.4	5

* Only two concentrations of BSA were tested as required from the Taguchi array (**Appendix Table 0.4**)

In order to test six factors each at three levels, a L_{18} orthogonal array was needed (see Appendix Table 0.2). The 18 experiments were prepared in 18 individual reaction tubes with the appropriate concentration of each component as shown in **Appendix Table 0.4**. Yet, the 18 reactions were run simultaneously on the same thermocycler using an optimised TD PCR program. Prior to the optimisation of the master mix, the cycling parameters of the TD PCR were also optimised using the Taguchi approach, but the results are not shown. However, the optimised values of the cycling conditions are presented in **Appendix Table 0.5**. Additionally to duplicated environmental samples, the reactions were performed on positive and negative controls for quality assurance purposes.

3.4.2. Results and discussion

The PCR product yields of the replicates and their mean are presented in **Table 3.7**. Already, it shows that the concentrations used for the components in experiment #5 produced the highest yield with 0.2 µg.µL^{-1} of BSA, 4 mM of $MgCl_2$, 100 µM of dNTPs, 0.013 U.µL^{-1} of *Taq* enzyme, 0.4 µM of each primer and 5 ng.µL^{-1} of DNA template.

Table 3.7: PCR product yields after experimental optimisation of the TD PCR master mix using a L_{18} OA.

	Replicate		Mean PCR product yield	Correction *
Experiment	**a**	**b**		
1	0	0	0	1
2	14	4	9	9
3	0	0	0	1
4	116	100	108	108
5	148	142	145	145
6	26	68	47	47
7	74		74	74
8	28	76	52	52
9	110	84	97	97
10	46	42	44	44
11	0	0	0	1
12	0	0	0	1
13	46	126	86	86
14	58	80	69	69
15	86	68	77	77
16	66	2	34	34
17	12	18	15	15
18	10	10	10	10

* The SN ratio analysis requires a minimum product yield of 1. Consequently, a yield of 0 was arbitrarily changed to 1.

Table 3.8 shows the pool of the performance characteristic of the experiments sharing the same levels, as explained in Table 3.3, which was used to calculate the SN ratios of each component of the master mix (**Table 3.10**). The concentration of BSA had no effect on the PCR product yields (Δ=0). Thus, an intermediate concentration of 0.3 $\mu g.\mu L^{-1}$ was chosen for the optimised master mix. The concentration of $MgCl_2$ and DNA template had the strongest effect on the PCR product yield.

Table 3.8: Pool of the TD PCR product yields for each optimised component of the master mix.

	Factor					
Level	**BSA** *	**$MgCl_2$**	**dNTPs**	**Enzyme**	**Primer**	**DNA template**
A	1	1	1	1	1	1
	9	9	108	108	47	47
	1	1	74	97	74	52
	108	44	44	1	1	1
	145	1	86	77	69	86
	47	1	34	15	10	15
B	74	108	9	9	9	9
	52	145	145	145	108	108
	97	47	52	74	52	97
	44	86	1	1	1	44
	1	69	69	86	77	69
	1	77	15	10	34	10
C	86	74	1	1	1	1
	69	52	47	47	145	145
	77	97	97	52	97	74
	34	34	1	44	44	1
	15	15	77	69	86	77
	10	10	10	34	15	34

* Only two concentrations of BSA were tested, as previously mentioned.

In order to visualise and estimate which concentration of each component was the optimum value that gave the highest yield, polynomial regressions were plotted (**Figure 3.1**). Since we were interested in the highest yield possible, the optimum concentration of a component was the highest point of the curve, *i.e.* the concentration that corresponded to the highest SN ratio

on the trendline (SN_{max}). **Table 3.9** provides the estimated optima for the master mix components.

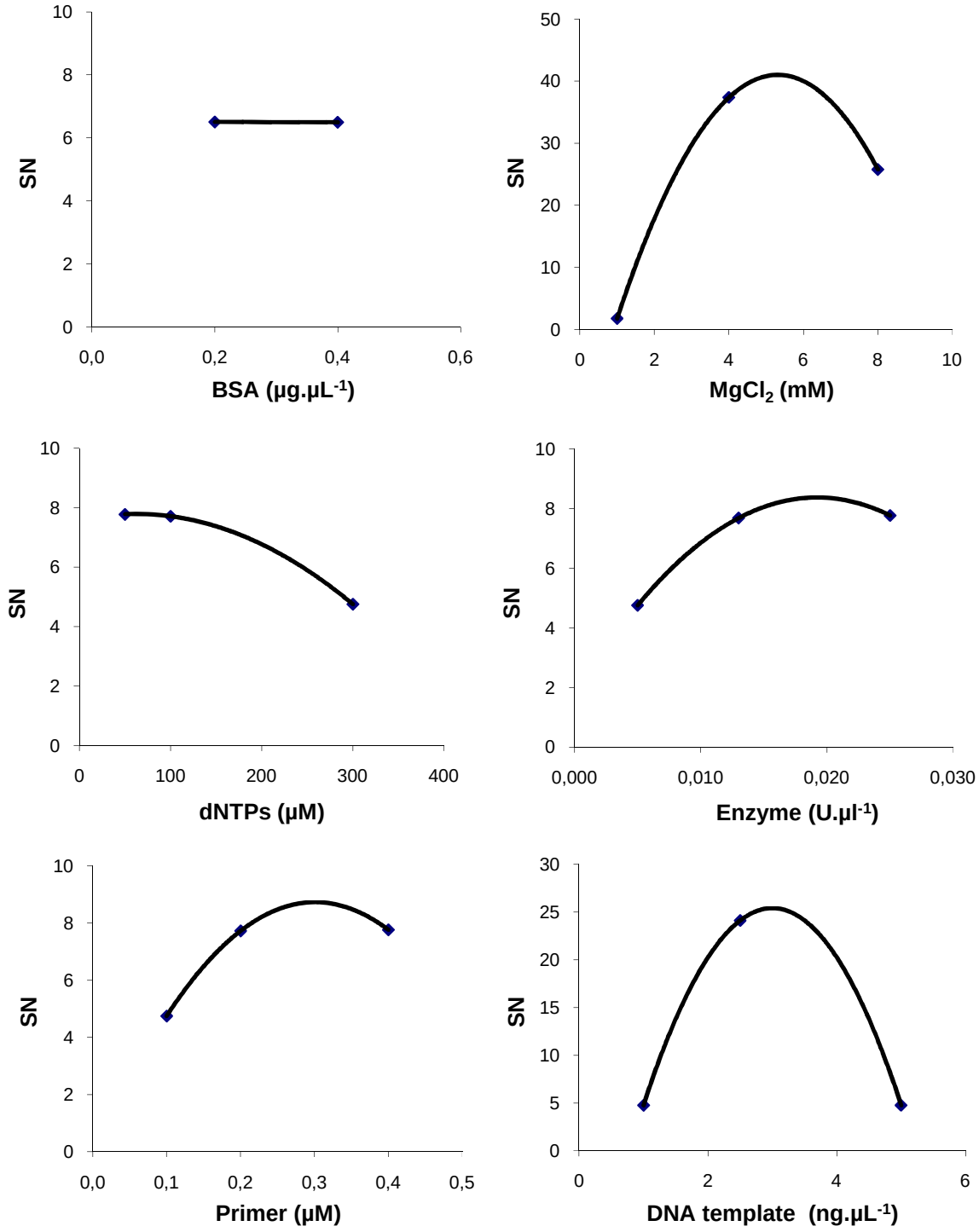

Figure 3.1: Effects of the components of the master mix on the SN ratios for the amplification of the *pmoA* genes with a TD PCR.

Table 3.9: Original and optimum conditions for the master mix used for the amplification of *pmoA*.

Components of master mix	Original concentration	Optimum concentration	SN_{max} **
$NH4^+$ buffer	1x	1x	-
BSA ($\mu g.\mu L^{-1}$)	0.4	0.3	6.50
$MgCl_2$ (mM)	2	6	41.00
dNTPs (µM)	200	50	7.77
Enzyme ($U.\mu L^{-1}$)	0.025	0.020	8.10
Primer (µM)	0.4	0.3	8.50
DNA template ($ng.\mu L^{-1}$)	(1 µL) *	3	25.50

* Originally, 1µL of DNA template was added to the PCR reaction (50 µL total volume); with no respect of the concentration of DNA in the sample.
** Maximum SN obtained from the polynomial regressions in **Figure 3.1**.

The validation experiment involved observing the yield of PCR products after running a PCR using the master mix with the optimised concentration of the components compared to the original conditions (**Figure 3.2**). With the original conditions of the PCR (**Figure 3.2**, top gel), the environmental samples had less smearing and no primer-dimer formation when using the optimised master mix. However, the signal was weaker with the optimised master mix. For the positive control, a non-specific product >1,000 bp was observed with the original master mix but was absent when using the optimised master mix. This was surprising and was the reason for using the TD approach.

With the optimised TD PCR (**Figure 3.2**, bottom gel), the original master mix produced bands that were shorter than expected, as well as some smearing. However, the use of the optimised master mix removed some of the smearing and also produced thinner bands. Furthermore, the optimised master mix did not allow for the amplification of the non-specific product (>1,000 bp) in the positive control. Overall, the use of the optimised master mix, in conjunction to the TD PCR, had a positive effect on the detection of the *pmoA* genes. This was confirmed by the verification test (see below).

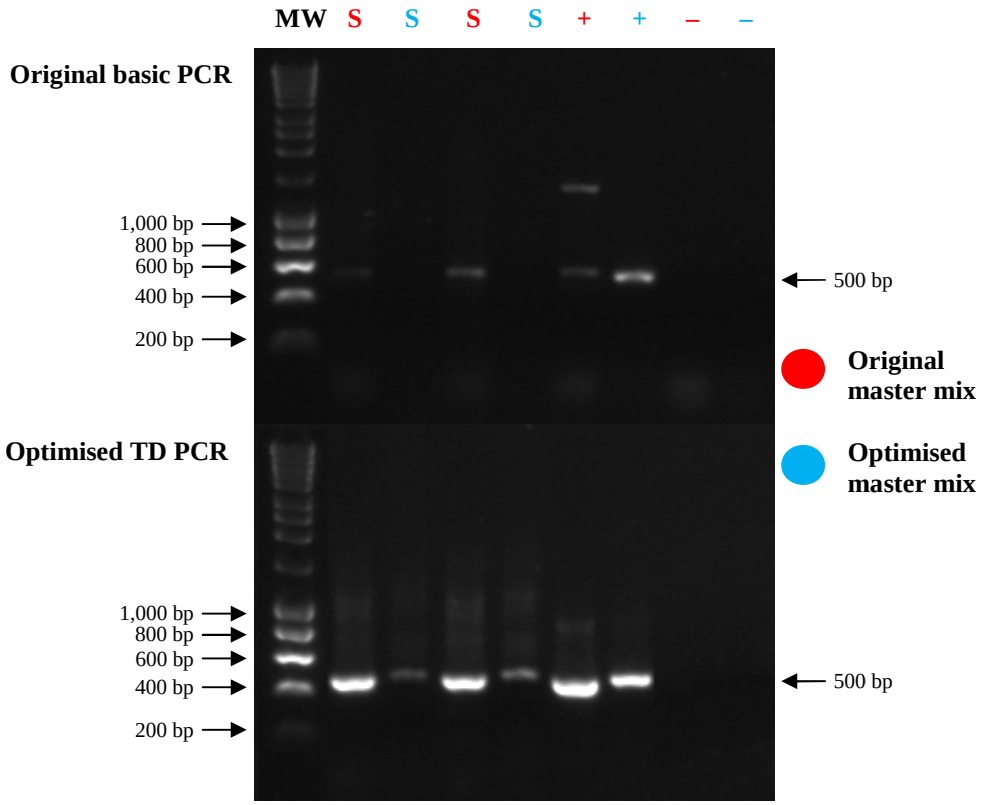

Figure 3.2: Differences in PCR product yield between the original and optimised settings for the amplification of the *pmoA* genes.

The top gel represents the PCR yields of the environmental samples when using the original cycling parameters of the basic PCR. The bottom gel represents the same samples but run with the optimised cycling conditions of the TD PCR. The effect of using the optimised master mix is also shown.
MW = molecular weight markers

The PCR product yields for the optimised reaction were used for the verification test to calculate the SN_{test} of this validation experiment. The SN_{test} was ~43 which was a similar value to the predicted SN (SN_{pred}~47) (**Table 3.10**). The verification test therefore confirmed that the optimised master mix improved the PCR product yield.

Table 3.10: Verification test for the optimisation of the master mix for the TD PCR used for the amplification of the *pmoA* genes.

	Factor						
Level	**BSA**	**$MgCl_2$**	**dNTPs**	**Enzyme**	**Primer**	**DNA**	
A	6.50	1.75	**7.77**	4.76	4.75	4.76	
B	**6.50**	**37.37**	7.71	7.68	7.72	**24.11**	**SN_{exp}**
C	-	25.75	4.75	**7.77**	**7.76**	4.77	**10.13**
Δ	0.01	35.62	3.03	3.01	3.01	19.36	
Rank	**5**	**1**	**3**	**4**	**4**	**2**	
$SN_{max,v}$ *	6.50	41.00	7.77	8.10	8.50	25.50	**SN_{pred}**
$SN_{pred,v}$	-3.63	30.87	-2.36	-2.03	-1.63	15.37	**46.73**
						SN_{test}	**43.05**

* SN estimated from the polynomial regressions (**Figure 3.1**) and displayed in **Table 3.9**.

3.5. Conclusion

The Taguchi optimisation was useful to adjust the concentration of the different components of the master mix, in particular $MgCl_2$, dNTPs and DNA template. It was also used to effectively optimise the cycling parameters of the TD PCR program (data not shown).

The experimental settings for the amplification of the *pmoA* genes were optimised, increasing by several folds the yields of amplicons after a single round of PCR where a nested PCR approach was previously required (Singh *et al.*, 2007; 2009). However, a touchdown method had to be used to improve the specificity of the detection. It was observed that the use of the calculated optimum SN ratios (SN_{opt}) would give enough information but the maximum SN ratios (SN_{max}) estimated from the polynomial regressions added more accuracy and flexibility for refining PCR conditions. The Taguchi methodology for the optimisation of the PCR conditions was very useful, and its application saved a lot of time and money after several months of unsuccessful attempts. The optimised PCR conditions presented in **Appendix Table 0.5** (cycling parameters) and **Table 3.9** (master mix components) were applied to the samples from New Zealand (Chapter 4) and Scotland (Chapter 5 and Chapter 6) for the detection of the *pmoA* genes.

Chapter 4 Experimental results (2)

Response of methanotrophic communities to afforestation and reforestation in New Zealand [1]

1. Brief introduction

A previous study showed that New Zealand forest soils, especially from a pristine temperate forest, displayed strong atmospheric CH_4 sinks compared to most Northern Hemisphere forest soils (Price *et al.*, 2003). This was attributed to New Zealand's isolation, the low rate of atmospheric nitrogen deposition, as well as limited anthropogenic soil disturbance. Indeed, changes in land use and management are known to alter the composition of the methanotroph community and, therefore, limit CH_4 oxidation (MacDonald *et al.*, 1997; Ojima *et al.*, 1993). Smith *et al.* (2000) calculated that the global soil CH_4 sink had declined by 71% due to the conversion of natural soils for agricultural use. They also estimated that it could take >100 years for the soil CH_4 sink strength of an afforested soil in Northern Europe to recover from disturbance by land-use change (Smith *et al.*, 2000).

In this study, two sites were selected: a regenerating native forest (shrubland) after burning (Turangi) and an indigenous forest adjacent to pasture and exotic pine trees (*Pinus radiata*) (Puruki). Pastures and pine forests near the Turangi site, and at Puruki, were studied previously (Singh *et al.*, 2007; Singh *et al.*, 2009; Tate *et al.*, 2007). Refer to Table 2.3 in the

[1] This chapter has been published as a short communication in the ISME Journal, and can be found in the Appendix Section. Reference: **Nazaries L., Tate K.R., Ross D.J., Singh J., Dando J., Saggar S., Baggs E.M., Millard P., Murrell J.C. & Singh B.K.** (2011). Response of methanotrophic communities to afforestation and reforestation in New Zealand. ISME Journal, In Press.

Materials and Methods section (**Chapter 2**) for a summary of the different land uses in the two sites, as well as the names used in this study. Although the sampling campaigns from the different sites and land uses occurred during different years, this always happened in the warmer months of the year (October to February).

After sampling of the soils, net CH_4 flux measurements were performed at 20°C in a constant temperature room using closed PVC chambers. Sieved soils (sampled in autumn and summer) were then incubated with ^{13}C-CH_4 (~50 ppm) to isolate active populations, from which PLFA extraction and analysis of levels of enrichment by GC-C-IRMS were performed. Molecular biological work (T-RFLP analysis) allowed identification of the methanotroph community structure under each habitat. Cloning/sequencing analysis of the *pmoA* gene was also performed to identify the methanotrophs present and to investigate the effect of land-use change. Refer to Chapter 2 (sections 1.1, 2.1, 3.1, 4, 5.1 to 5.4, and 6) for more details.

The objectives were to:

1) Determine the time required after reforestation for soils to achieve high CH_4 oxidation rates comparable to a mature native forest soil.

2) Determine if the change in CH_4 oxidation rates related to a shift in methanotrophic communities at the ecosystem level.

2. Soil physical and chemical properties

Soils at the Puruki-Native site were better aerated (lower bulk density and WFPS, and greater porosity) than the adjacent soils under pine and pasture (P<0.001, **Table 4.1**). In fact there was a trend toward better aeration in forest soils compared to pasture soils at both sites (data not shown).

Table 4.1: Selected physical properties of the soils from the Puruki site.
Data are means (S.E.M. in brackets) of the averages from soils in each chamber. Before ANOVA, the appropriate transformations were performed on data sets that did not have a normal distribution. Results followed by different letters (a, b, c) within a column are statistically different according to the multiple pairwise comparison test (P<0.05).

Vegetation	Bulk density (g.cm^{-3})	Porosity (%)	WFPS (%)
Pasture [1]	0.53 (0.01) [a]	75.5 (0.3) [a]	65.3 (2.0) [a]
Pine (7) [1]	0.46 (0.01) [b]	79.2 (0.6) [b]	53.6 (1.4) [b]
Puruki-Native	0.33 (0.03) [c]	84.4 (1.1) [c]	30.3 (2.1) [c]

[1] data taken from Tate *et al.* (2007). The ages of the pine stand (y) is shown in brackets.

Selected chemical properties for soils from both Turangi and Puruki sites are summarised in **Table 4.2**. Similar observations could be made from both sites: land-use change, and more specifically forests, significantly decreased soil moisture content (P=0.011 at Turangi, P=0.017 at Puruki) and concentrations of NO_3^--N (P<0.001 at Turangi, P=0.003 at Puruki) as well as total N (P<0.001 at Turangi, P=0.024 at Puruki). Also, C:N ratio increased with afforestation (P<0.001 at both sites) whereas total C and NH_4^+-N concentrations and pH were not influenced by it.

Table 4.2: Selected chemical properties of the soils at the Turangi and Puruki sites.

The data are means (S.E.M. in brackets) of the averages from soils in each jar/chamber. Before ANOVA, the appropriate transformations were performed on data sets that did not have a normal distribution. For each site, results followed by different letters (a, b, c) within a column are statistically different according to the multiple pairwise comparison test ($P<0.05$).

Site	Land use	pH	Total C ($g.kg^{-1}$)	Total N ($g.kg^{-1}$)	C:N	NH_4^+-N ($mg.kg^{-1}$)	NO_3^--N ($mg.kg^{-1}$)	Moisture ($g.kg^{-1}$)
Turangi	Pasture (5) [1]	5.5 (0.06) [a]	77 (2) [ab]	5.8 (0.2) [ab]	13 (0.2) [a]	43 (26) [a]	1.0 (0.5) [ab]	510 (23) [ab]
	Pine (5) [1]	5.6 (0.07) [a]	66 (2) [b]	5.1 (0.2) [a]	13 (0.1) [a]	5.2 (1.0) [b]	2.2 (0.6) [b]	503 (12) [ab]
	Pasture (10) [1]	5.5 (0.05) [a]	86 (5) [a]	6.2 (0.3) [b]	14 (0.3) [a]	8.1 (2.9) [ab]	2.1 (0.4) [b]	575 (21) [a]
	Pine (10) [1]	5.4 (0.07) [a]	74 (6) [ab]	5.0 (0.3) [a]	15 (0.3) [a]	6.8 (1.0) [ab]	2.1 (0.4) [b]	600 (41) [a]
	Turangi-47	5.5 (0.08) [a]	71 (1) [ab]	3.4 (0.1) [c]	21 (0.6) [b]	6.7 (0.9) [ab]	0.2 (0.09) [ac]	490 (49) [ab]
	Turangi-67	5.4 (0.04) [a]	63 (1) [b]	3.1 (0.07) [c]	20 (0.7) [b]	4.7 (1.6) [ab]	0.04 (0.03) [c]	439 (23) [b]
Puruki	Pasture (7) [2]	5.4 (0.04) [a]	133 (4) [a]	11 (0.5) [a]	12 (0.1) [a]	21 (3) [a]	26 (4) [a]	1186 (28) [a]
	Pine (7) [2]	5.2 (0.1) [a]	116 (8) [a]	5.6 (0.2) [b]	21 (0.9) [b]	13 (2) [a]	8.4 (2.8) [ab]	1091 (42) [b]
	Puruki-Native	5.0 (0.3) [a]	174 (35) [a]	9.8 (1.5) [b]	17 (0.9) [c]	21 (4) [a]	7.1 (2.7) [b]	825 (109) [b]

[1, 2] data respectively taken from Singh *et al.* (2009) and Tate *et al.* (2007). The age of the pasture and pine stands (y) is shown in brackets. The pastures correspond to the adjacent pasture of each pine stand.

3. Methane fluxes

Soil atmospheric CH_4 oxidation rates were significantly influenced by afforestation/ reforestation at both Turangi and Puruki sites ($P<0.001$) (**Figure 4.1**). At Turangi, the soil CH_4 oxidation in Pine (5) and Pine (10) were not significantly different from rates in the adjacent pastures (**Figure 4.1A**). In contrast, atmospheric CH_4 oxidation rates were much higher at Turangi-47 and Turangi-67 than in all other land uses (**Figure 4.1A**). At Puruki, CH_4 oxidation rates in Puruki-Native were significantly higher than those in the adjacent Pasture (7) and Pine (7) (**Figure 4.1B**). The atmospheric CH_4 oxidation rates were significantly lower at Turangi-47 and Turangi-67 compared to Puruki-Native ($P<0.001$).

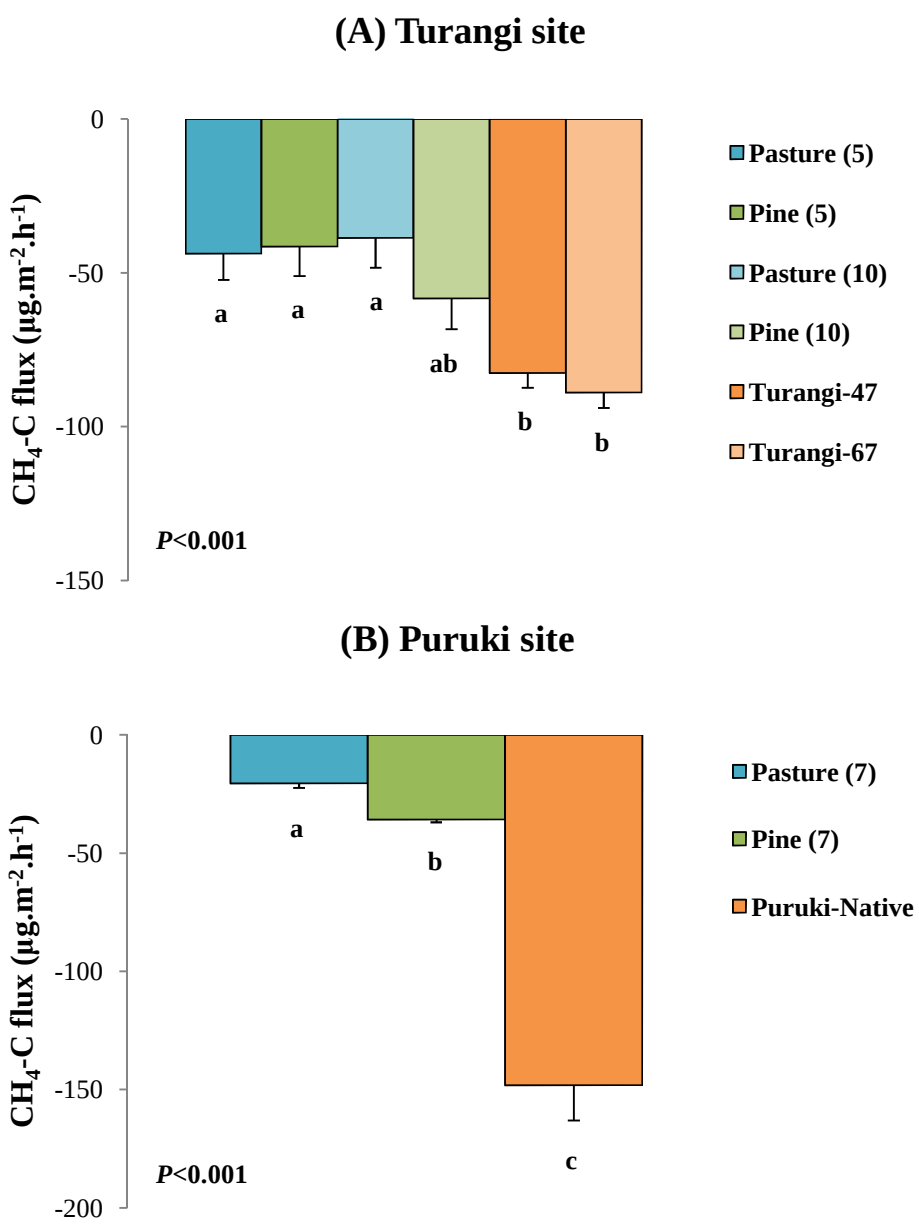

Figure 4.1: Mean net CH_4 fluxes from the different land uses at Turangi (A) and Puruki (B).

Data of the pastures and pines at Turangi were taken from Singh *et al.* (2009), whereas net CH_4 fluxes of pasture and pine at Puruki were from Tate *et al.* (2007). For this study, means of the CH_4 oxidation rates come from the field-based chambers (Turangi-47 and Turangi-67) or from the paired intact cores in the closed chambers (Puruki-Native). The errors bars represent the S.E.M. For each figure, land uses followed by different letters within a dataset (series) are statistically different according to the multiple pairwise comparison test ($P<0.05$).

4. Methanotroph community structure in soils

4.1. T-RFLP data

pmoA genes from the different soils were detected by PCR. Digestion of the PCR products of the *pmoA* genes produced two dominant T-RFs of 26 and 77 bp with the restriction enzyme *Msp*I, and three main T-RFs (T-RF 33, T-RF 129 and T-RF 245) with *Hha*I (**Table 4.3**).

Table 4.3: Most abundant T-RFs (>80%) produced after digestion of the *pmoA* genes with the restriction enzymes *Msp*I and *Hha*I for the Turangi and Puruki sites.

The differences between similar T-RFs were due to analytical drifts and were all within a range of expected discrepancies of ±2 bp.

Site		**Turangi**				**Puruki**		
Land use		Pasture (5 and 10) [1]	Pine (5 and 10) [1]	Turangi-47	Turangi-67	Pasture (7) [2]	Pine (7) [2]	Puruki-Native
Restriction enzyme	***Msp*I**	N/A	N/A	T-RF 26 T-RF 77	T-RF 26 T-RF 77	N/A	N/A	T-RF 26 T-RF 77
	***Hha*I**	T-RF 35 T-RF 128 T-RF 245	T-RF 35 T-RF 128 T-RF 245	T-RF 33 T-RF 129	T-RF 33 T-RF 129	T-RF 127 T-RF 244	T-RF 127 T-RF 244	T-RF 33 T-RF 129

[2, 1] data taken from Singh *et al.* (2007; 2009), respectively. N/A means that no data were available due to differences in experimental design.

In previous studies (Singh *et al.*, 2007; 2009) and also in the present study, the T-RFs 33 and 129 (digestion with *Hha*I) were found to be related to *Methylocapsa* spp. (see section 4.2). The relative abundance of these two T-RFs was combined in order to show the general trend of the dominant population related to type II methanotrophs. Likewise, the T-RF 245 was used to describe the general trend of type I-related methanotrophs as identified for *Methylococcus capsulatus*-like *pmoA* sequences (Singh *et al.*, 2007; 2009). Based on the relative abundance of the three dominant T-RFs, the relative dominance of type II-related methanotrophs (T-RFs 33 and 129) increased with the age of the forest at the expense of type I-related methanotrophs (T-RF 245) (**Figure 4.2**, $P<0.001$).

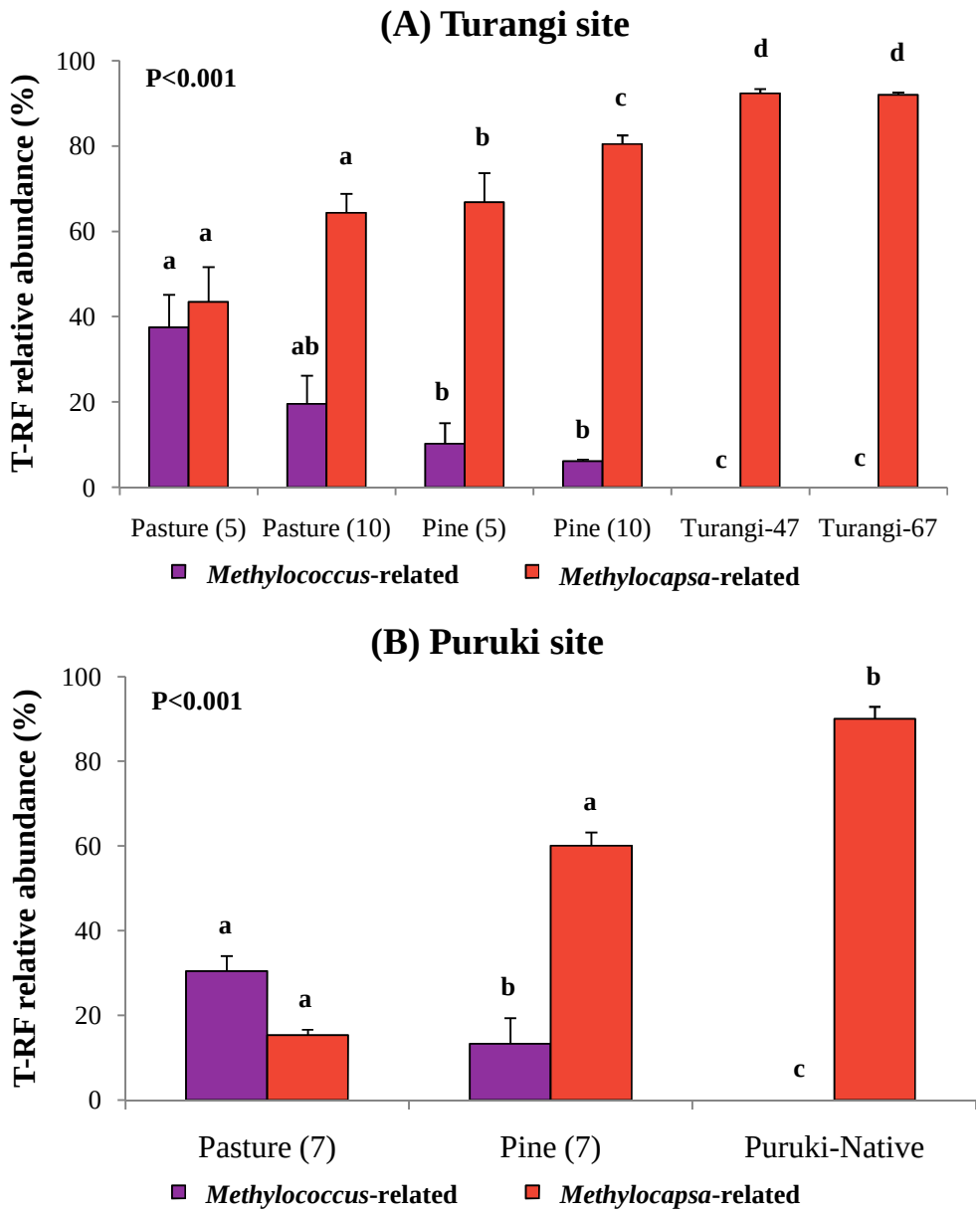

Figure 4.2: Means (S.E.M.) of the relative abundance of the dominant T-RFs in soils under the different land uses at (A) Turangi (n=6) and (B) Puruki (n=9).

Type I methanotrophs were related to *Methylococcus capsulatus* (T-RF 245) and type II methanotrophs to *Methylocapsa acidiphila* (T-RF 33 and T-RF 129). Values for each land use did not add up to 100% because the graph only displays the contribution of the T-RFs 33, 129 and 245. In particular, soils under pasture at Puruki (Pasture-7) contained a high proportion (~30%) of the T-RF 81, which was identified as an OTU related to *Methylocystis* and *Methylosinus* spp. (Singh *et al.*, 2009). Data for the pastures and pines at Turangi were taken from Singh *et al.* (2009), whereas CH_4 fluxes of pasture and pine at Puruki were from Tate *et al.* (2007). Data for Turangi-47, Turangi-67 and Puruki-Native are from this study. For each figure, land uses followed by different letters within a dataset (series) are statistically different according to the multiple pairwise comparison test ($P<0.05$).

Regression analysis suggested that there was a strong relationship between the relative dominance of type II-related methanotrophs and the rate of atmospheric CH_4 oxidation (P=0.004 at Turangi and P=0.003 at Puruki) (**Figure 4.3**).

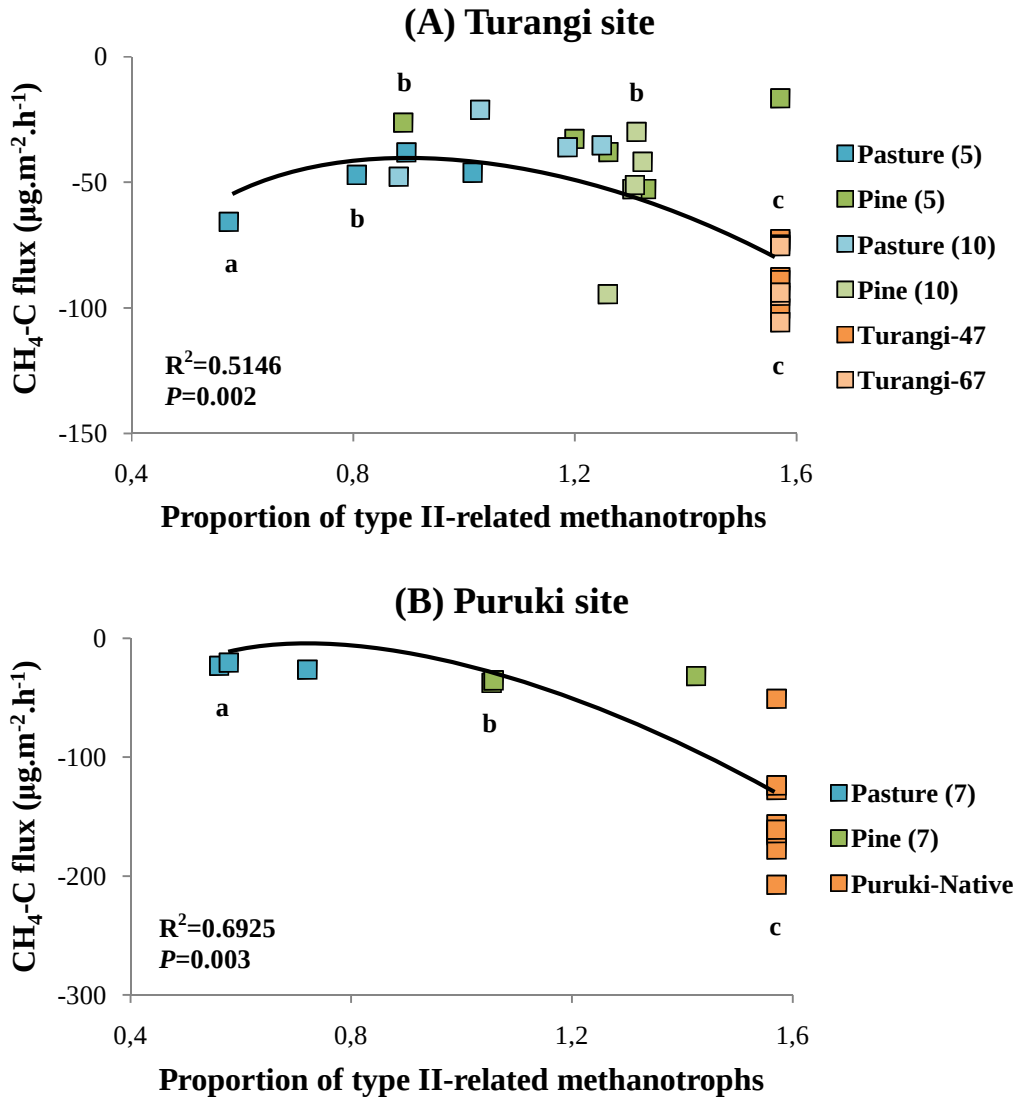

Figure 4.3: Relationship between net CH_4 flux and methanotroph community structure at (A) Turangi (n=28); and (B) Puruki (n=15).

The polynomial regression is based on the angular transformation (arcsine of the square root) of the proportion of the relative abundance of the dominant type II-related T-RFs (T-RF 33 + T-RF 129) over the total relative abundance of the three dominant T-RFs (T-RFs 33, 129 and 245). Relative abundance was calculated as a percentage of the total number of T-RFs from each profile produced after digestion of the PCR products for *pmoA* genes with the enzyme *Hha*I. Atmospheric CH_4 oxidation rates are those of the different land uses, as displayed in Figure 4.1. Data for the pastures and pines at Turangi were taken from Singh *et al.* (2009), whereas CH_4 fluxes of pasture and pine at Puruki were from Tate *et al.* (2007). Data for Turangi-47, Turangi-67 and Puruki-Native are from this study. For each figure, land uses followed by different letters within a dataset are statistically different according to the multiple pairwise comparison test (P<0.05).

The T-RFLP profiles of *pmoA* were analysed with *T-REX* online software using the AMMI model. Guidelines for the interpretation of the AMMI model results are as such: a low interaction effect between the T-RFs means that the environments being investigated (the land uses in this study, *i.e.* Turangi-47, Turangi-67 and Puruki-Native) display similar bacterial communities, and inversely, very dissimilar bacterial communities will be characterised by a low percentage of the main effect component of the ANOVA output (Culman *et al.*, 2008). To summarise for this study, no significant differences were found in the T-RF composition between the different sites (Turangi-47, Turangi-67 and Puruki-Native), based on the T-RF presence/absence and T-RF relative abundance (**Table 4.4**).

Table 4.4: Similarity analysis of T-RFLP profiles of soils under shrubland (47- and 67-year old stands) and native forest.

Results presented are the ANOVA output after analysis using the AMMI model of *T-REX* online software (**http://trex.biohpc.org/**). The data used were the T-RFLP profiles obtained from the digestion of the *pmoA* genes with the restriction enzyme *Hha*I.

Main effects	Binary	Height
T-RFs	81.36%	91.32%
Environments	0.97%	0.03%
Interaction effects		
Pattern	4.70%	1.34%
Noise	12.97%	7.31%

4.2. Cloning and sequencing

The *pmoA* clone sequences from the pasture soils were related to *pmoA* from type I methanotrophs, more specifically close relatives (99% similarity) of *pmoA* genotypes from *Methylococcus capsulatus*, whereas clone sequences from soils under the pine forests (5, 7 and 10 years), shrublands and native forest were all distantly related (98% similarity) to *pmoA* genotypes from *Methylocapsa acidiphila*, a type II methanotroph (**Figure 4.4**).

Methylocapsa-related microorganisms are part of the RA14/USCα clade as described by Holmes *et al.* (1999) and Knief *et al.* (2003). The *in silico* digestion of the *pmoA* sequences with *Hha*I predicted two T-RFs of 38 and 130 bp, present in most of the sequences in the forested soils except for one clone from Puruki-Native (c9Pur) for which an *in silico* T-RF of 248 bp was predicted. Although the theoretical T-RFs 38, 130 and 248 were slightly different in size from the experimental T-RFs (T-RFs 33, 129 and 245; **Table 4.3**), this was considered to be a normal drift due to capillary migration during electrophoresis and the lack of precision of the GeneMapper™ software to estimate accurately T-RF sizes below 50 bp. Nonetheless, the *in silico* digests confirmed the identity of the T-RF 33 and T-RF 129 as being two distinct operational taxonomic units (OTUs) distantly related to *Methylocapsa* sp., one belonging to the USCα clade (T-RF 38) and the other one being related to it (T-RF 130) and often called Cluster 5 (Dörr *et al.*, 2010; Knief *et al.*, 2005), as shown in Figure 4.4. This is also supported by the *in silico* digestion of the same *pmoA* gene sequences with *Msp*I, which predicted two T-RFs of 33 and 79 bp in all clone sequences but one. The exception was c9Pur (Puruki-Native), which predicted a T-RF of 114 bp. Again, these predicted T-RFs are similar in size to the experimental T-RFs (T-RFs 26 and 77) of the digestion of the *pmoA* genes with *Msp*I (**Table 4.3**). Furthermore, the clone sequences predicting the T-RF 38 with *Hha*I also predicted the T-RF 33 with *Msp*I. Similarly, the clone sequences predicting the T-RF 130 with *Hha*I also predicted the T-RF 79 with *Msp*I. The Puruki-Native clone (c9Pur) that predicted a T-RF 247 with *Hha*I also predicted a T-RF 114 with *Msp*I. This was identified on the phylogenetic tree as being distantly related to *pmoA* from type I methanotrophs (**Figure 4.4**). Further analysis of the clone sequences using REMA software suggests that, following *in silico* digestion with *Hha*I, sequences from pastures produce T-RF 248 while clones from the forests (pine, shrub and native) produce T-RFs 38 and 130. Only dominant T-RFs were identified by this approach as only a small number of clones (16 per site) was sequenced.

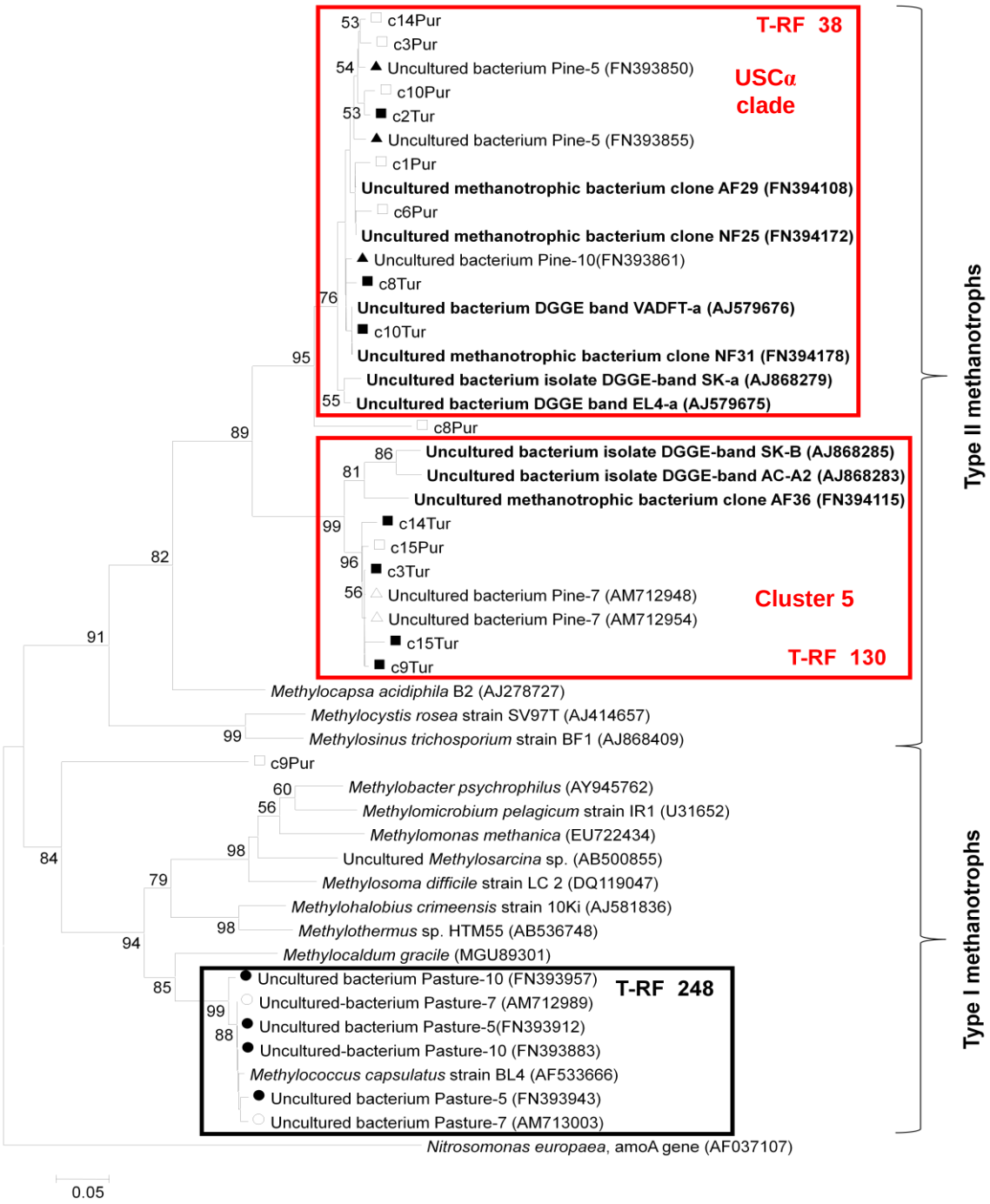

Figure 4.4: Phylogenetic relationships of selected amino acid sequences of PmoA derived from partial *pmoA* sequences retrieved from different soils to PmoA sequences from the public domain.

Clone sequences from pasture and pine forest soils were retrieved from Singh *et al.* (2007; 2009). The amino acid sequence of each clone was aligned to selected sequences from the GenBank database using MEGA 5 software. The phylogenetic tree was constructed with MEGA 5 using the neighbour-joining method with 1,000 bootstrap replicates. The evolutionary distances were computed using the Poisson correction method and are in the units of the number of amino acid substitutions per site. The analysis involved 48 amino acid sequences. The scale bar represents 5% dissimilarity between amino acid positions. The tree was rooted to the *amoA* (ammonia monooxygenase) gene of *Nitrosomonas europaea*.

Clone sequences in the tree can be identified as such: full shapes represent clones from Turangi, whereas empty shapes represent clones from Puruki. Clone sequences from the different types of land uses are identified by squares (Turangi-47, Turangi-67 and Puruki-Native), triangles (Pine-5, Pine-7 and Pine-10) and circles (Pasture-5, Pasture-7 and Pasture-10). Clone sequences in **bold** were retrieved from soils under natural forests and afforested sites in Germany, Thailand and Brazil (Dörr *et al.*, 2010; Knief *et al.*, 2003; Knief *et al.*, 2005).

4.3. PLFA-SIP data

The percentages of ^{13}C-labelled PLFAs indicated that the most enriched fatty acid was 18:1ω7 (a signature of type II methanotrophs) at all sites (**Figure 4.5**). A high enrichment of the PLFA ai17:0 in the pastures and pine forests was observed previously (Singh *et al.*, 2007; Singh *et al.*, 2009; Tate *et al.*, 2007) and reported to be characteristic of uncultivable methanotrophic bacteria. This particular fatty acid was not dominant in Turangi-47, Turangi-67 and Puruki-Native, although it showed a good incorporation (17-29% enrichment) of ^{13}C from applied ^{13}C-CH_4 (**Appendix Figure 0.1**).

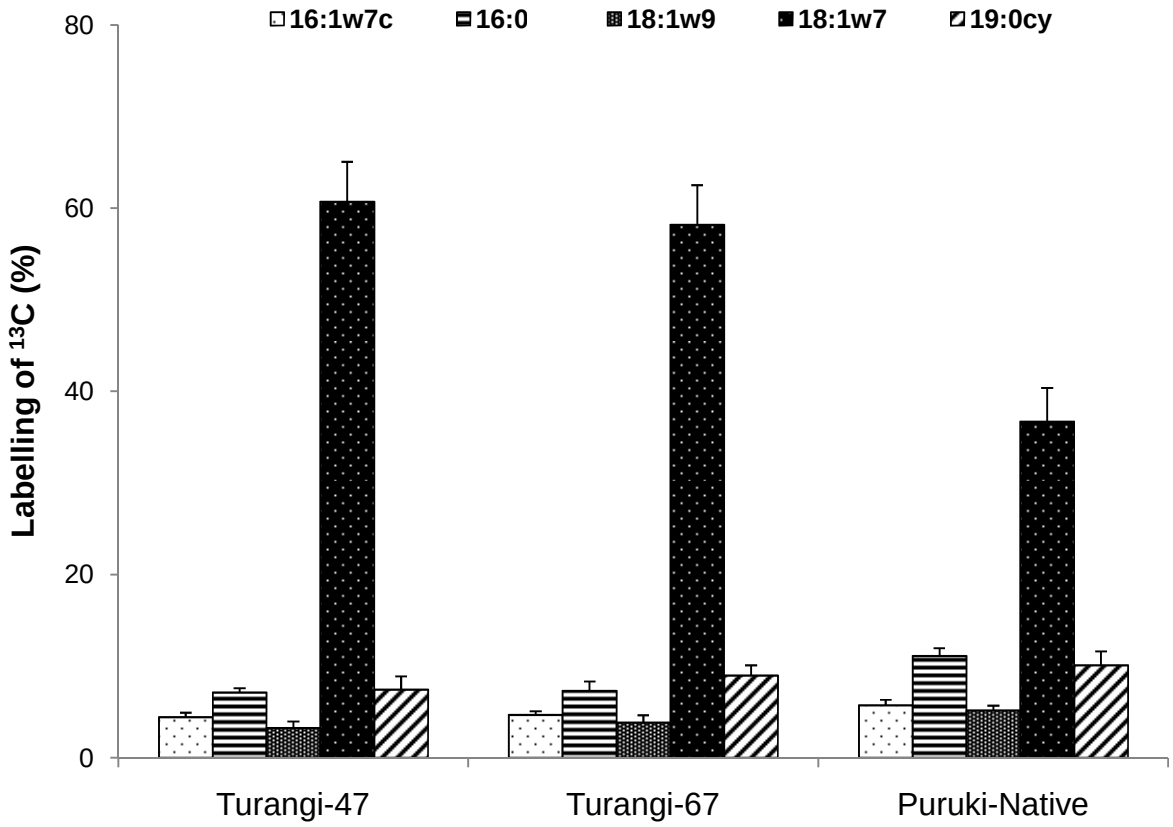

Figure 4.5: Percentage labelling of ^{13}C into each of the most dominant PLFAs extracted from soil following incubation with ~50 ppm of ^{13}C-CH_4.

Each bar represents the amount of ^{13}C in each PLFA fraction as a percentage of the total ^{13}C in all fractions. Error bars are S.E.M.

5. Discussion

5.1. Reforestation/afforestation of pasture and net CH_4 fluxes

Both afforestation and reforestation are still common land-use changes in New Zealand (Trotter *et al.*, 2005). Changes in the aeration status of soils undergoing these land-use changes can be assessed by measuring soil physical properties. Singh *et al.* (2009) found that afforestation of pasture with *Pinus radiata* at Turangi did not show an improvement of soil aeration in Pine (5), whereas the difference became significant in Pine (10) with lower bulk density and higher porosity. Similarly, at Puruki, soils from Pine (7) showed minor change in soil aeration status, due in part to the lack of major physical disturbance during harvesting the previous tree crop (Tate *et al.*, 2007). In the current study, soils in Puruki-Native were better aerated (lower bulk density and WFPS, and higher porosity), indicating that afforestation of pastures and reforestation may have improved soil aeration (Tate *et al.*, 2007). The relationship between improvement of soil aeration and increased atmospheric CH_4 oxidation rate was previously reported (Ball *et al.*, 1997; MacDonald *et al.*, 1996). While my results are consistent with these previous studies, they also reflect the fact that the naturally open structure of volcanic soils strongly favour high atmospheric CH_4 oxidation rates (Tate *et al.*, 2007). Although Singh *et al.* (2009) observed a small (non-significant) increase in CH_4 oxidation rates at Pine (10), the results indicate higher atmospheric CH_4 oxidation rates in the soils at Turangi-47 and Turangi-67 (Figure 4.1A) despite being lower than those in the Puruki-Native soils (Figure 4.1B). Nonetheless, our data suggest that CH_4 oxidation rates stabilised in Turangi shrubland after 47 years of reforestation as there was no apparent subsequent change over 20 years. Shrublands dominated by manuka and kanuka at previously disturbed sites are often seral communities, and in the absence of fire are succeeded over 150-500 years by a permanent cover of tall forest (Ross *et al.*, 2009). However, it is likely that

local climo-edaphic factors including very high annual rainfall (*ca*. 2500 mm) that periodically limits soil aeration, and very low N availability (Ross *et al.*, 2009), may be limiting further changes at the Turangi site. At the Puruki site (*ca*. 1500 mm of rainfall), CH_4 oxidation rates measured using large field chambers following clear-cutting of the nearby 24-year-old pine (Tate *et al.*, 2006) were comparable with rates in the Puruki-Native soil. This suggests that with minimal soil disturbance and high aeration status, soil CH_4 oxidation rates under second rotation pine (Pine (7), see Table 2.5) can reach those of a mature forest in as little as 31 years (first rotation to clear-cut, 24 years plus second rotation, 7 years). The high CH_4 oxidation rate from the Puruki-Native soil was also comparable to that of another pristine forest soil at Craigieburn in New Zealand South Island (Price *et al.*, 2003).

5.2. Shifts in the methanotroph community structure

Comparison with the previous studies (Table 4.3) confirmed the dominance of type II-related methanotrophs (represented here by T-RF 33 and T-RF 129) in forest and shrubland soils. These are distantly related to *Methylocapsa* spp. and belong to the RA14/USCα clade. The results also showed the absence of type I methanotrophs (T-RF 245) related to *Methylococcus capsulatus*, in Turangi-47, Turangi-67 and Puruki-Native suggesting that *Methylococcus*-related type I methanotrophs are progressively replaced in soils by *Methylocapsa*-related type II methanotrophs due to afforestation and reforestation (Figure 4.2). This observation was associated with a progressive increase in soil net atmospheric CH_4 oxidation (Figure 4.3). Conversely, a recent study showed a shift from type II methanotrophs of the *Beijerinckiaceae* towards type I methanotrophs of the *Methylococcaceae* occurring during deforestation (conversion of forest to farmland) (Dörr *et al.*, 2010).

The AMMI analysis, based on T-RF comparison, confirmed that the shrubland and native forest soil methanotroph communities were similar, which was further supported by cloning and sequencing data. Furthermore, the community structure in Turangi-47 and Turangi-67 was similar to each other and to Puruki-Native. The data of this study provide evidence that the increase in atmospheric CH_4 oxidation rates in afforested and reforested sites are linked to a shift in population of methanotrophic bacteria towards a dominance of type II-related methanotrophs (Figure 4.3), as previously suggested (Dörr *et al.*, 2010; Singh *et al.*, 2009).

The data may also suggest that the soil methanotrophic community recovered first after land-use changes followed by the CH_4 oxidation rates. Indeed, the relative abundance of the type II-related methanotrophs in the 10-year-old pine forest was already close to that found in the older forests (Figure 4.2), while CH_4 oxidation rate appeared to be at an intermediate stage (Figure 4.1).

Also, it seems that there was a triggering effect in the increase of CH_4 oxidation rates. Indeed, although the soils under pine were already dominated by the presence of type II-related methanotrophs similar to the ones observed in the old-growth shrubs and native forest (Figure 4.4), the oxidation rates were not as high as in Turangi-47, Turangi-67 and Puruki-Native (Figure 4.1). The trigger for higher oxidation rates could be a significant change in the soil physical and chemical properties, or, more likely, a threshold in the proportion of type II-related methanotrophs (or the complete disappearance of type I-related methanotrophs). Figure 4.2 shows that soils under Pine (10) contained about 80% of *Methylocapsa* sp. (and less than 10% of *Methylococcus capsulatus*) suggesting that this could be a threshold for inducing high CH_4 sink activity as displayed in Figure 4.3. The shift towards a dominance of type II-related methanotrophs in afforested soils appears consistent throughout New Zealand (Singh *et al.*, 2007; Singh *et al.*, 2009; Singh & Tate, 2007; Tate *et al.*, 2007). This combined set of data also suggests that *Methylococcus capsulatus* and two distant relatives of

Methylocapsa sp. may be three of the most dominant phenotypes across New Zealand soils; however, to prove this conclusively, in-depth sampling across the country will be needed.

The *pmoA*-based cloning and sequencing data confirmed the identity of the two OTUs producing the T-RF observed with the T-RFLP data, *i.e.* dominance of two distinct types of bacteria, both distantly related to *Methylocapsa acidiphila* (98% amino acid similarity), in the forest soils (Figure 4.4). The use of the *pmoA* gene did not allow for the detection of bacteria belonging to the genera *Methylocella* and *Methyloferula* – the only known methanotrophs that do not possess the pMMO enzyme (Dedysh *et al.*, 2000; Vorobev *et al.*, 2010) – but the phylogenetic analysis of the 16S rRNA gene sequences of type II methanotrophs showed that only two clones (12.5%) were closely related to *Methylocella* sp. (99% gene identity, see Appendix Table 0.6). Yet, this could be a strong evidence for the long-term survival and establishment of active *Methylocapsa*-related cells in soils undergoing reforestation and afforestation.

A limitation of these findings was that the soils used were sampled at different times. Based on a previous study (Price *et al.*, 2003), changes in soil moisture rather than temperature were responsible for most of the observed seasonal changes in soil CH_4 oxidation. In these volcanic soils, a combination of good aeration and moisture storage characteristics generally ensures these seasonal changes are quite small (Tate *et al.*, 2006). Consequently to minimise any seasonality effects, all soils in this study were sampled in summer (October to February).

The phylogenetic analysis of amino acid sequences of *pmoA* (Figure 4.4) suggested that the microorganisms responsible for the oxidation of atmospheric CH_4 in New Zealand soils were a genotype related to an uncultivable *Methylocapsa acidiphila*. Such *pmoA* sequences were also found in forest soils from both temperate (Germany) and tropical (Thailand, Brazil)

regions (Dörr *et al.*, 2010; Knief *et al.*, 2003; Knief *et al.*, 2005). The presence of this *pmoA* genotype was reported from soils under various natural forests and sites afforested with different tree species. Yet, interestingly, when compared to the New Zealand clone sequences, all *pmoA* sequences appeared to be closely related, and they all clustered into the two OTUs producing the virtual T-RFs 38 and 130 after *in silico* digestion of the *pmoA* genes with the restriction enzyme *Hha*I (Figure 4.4). This finding suggests that the two genotypes (T-RFs 38 and 130) are dominant in these forest soils irrespective of the tree species.

5.3. Identifying active methanotrophs by PLFA-SIP

Most of the ^{13}C was incorporated in the PLFA 18:1ω7 (Figure 4.5), which is the main PLFA signature in forest soils for the type II methanotrophs of the genera *Methylocapsa* and *Methylocella* (Crossman *et al.*, 2005; Singh & Tate, 2007). This result was confirmed by the observation of a similar PLFA signature in the Turangi and Puruki sites afforested with pines in previous studies (Singh *et al.*, 2009; Tate *et al.*, 2007). Overall, it confirms previous finding that most soil microbial oxidation of atmospheric CH_4 is by type II-related methanotrophs (Knief *et al.*, 2006; Kolb, 2009; Singh & Tate, 2007). Also, this result shows that most of the atmospheric CH_4 oxidation activity observed in Figure 4.1 was performed by *Methylocapsa*-related methanotrophs, as validated by the phylogenetic analysis (Figure 4.4).

6. Conclusions

In this study, the effect of land-use change, and more particularly, reforestation and afforestation of pastures were analysed. Enhancement of the soil CH_4 sink was favoured by improved soil aeration and accompanied by a shift in the community structure of the soil methanotrophic bacteria. Type I methanotrophs related to *Methylococcus capsulatus* were progressively replaced by type II methanotrophs related to the *Methylocapsa* genus, which were involved in the oxidation of atmospheric CH_4 (Knief *et al.*, 2006; Singh *et al.*, 2009). This study shows that this process was observed since afforestation occurred and was stronger in the older forests. It also potentially demonstrated that, in these soils, less than 47 years upon afforestation were needed for soils to become as active as under a native forest and this was linked to a shift in the methanotrophic community.

Together, changes in net CH_4 fluxes, soil characteristics and microbial community diversity, as well as PLFA signature of methanotrophs, were identical in the shrubland and native forest soils. This suggests that New Zealand soils and their associated methanotroph community are highly resilient and that although land-use change to pasture lowered the capacity of soils to oxidise CH_4, subsequent afforestation or reforestation (after forest burning) appeared to allow native type II-related methanotroph populations to become dominant and active again.

However, local climo-edaphic factors appear to be limiting methanotroph activity. The data further suggest a niche-specific adaptation, and microbial control of the observed changes in soil CH_4 oxidation. The mechanism associated would require the prior establishment of a type II-related methanotrophic community before significant increase in CH_4 oxidation rates could occur. These significant findings need to be taken into consideration in future prediction of changes in CH_4 emissions due to afforestation and reforestation.

Chapter 5 Experimental results (3)

Effect of afforestation of a peatland and grassland into pine forest on the mitigation of CH_4 and the shift in methanotrophic diversity

1. Brief introduction

Scotland's contribution to GHG emissions in the UK is 8.6%, while CH_4 emissions in Scotland represent 12.9% of total GHG and have fallen by 43.1% since 1990 mainly due to significant reductions in CH_4 emissions from waste disposal and coal mining (Sneddon *et al.*, 2010). It is also possible to increase atmospheric CH_4 sinks by changing land use. Although grasslands can be net CH_4 sinks, their afforestation with pine trees can enhance CH_4 oxidation rates (Singh *et al.*, 2007; Singh *et al.*, 2009). In contrast, wetlands such as peat bogs are responsible for the emission of large amounts of CH_4 (Conrad, 1996; Glatzel & Bareth, 2006). Grassland pasture (or improved grassland) and bogs represent respectively 13% and 25% of the broad habitat area in Scotland (McGowan *et al.*, 2002), whereas coniferous woodlands cover only 12% of Scotland. Therefore, improving the pine woodland cover from the conversion of grassland and bog could help to further improve atmospheric CH_4 sinks.

For this study, two sites were selected in Scotland: a peatland bog and grassland (pasture), which are predicted to be net emitters of CH_4. The bog (Bad à Cheo) was dominated with peat moss (*Sphagnum* spp.), and had two adjacent forests, afforested with lodgepole pine (*Pinus contorta*) about 20 and 40 years ago (called young pine and old pine forest hereafter). The grassland (Glensaugh) was a grazing field, and had only one adjacent afforested area of

Scots pine (*Pinus sylvestris*), aged ~20 years (called young pine forest). Refer to Chapter 2 (sections 1.2, 2.2, 3.2, 4, 5.1 to 5.3, 5.5 and 6) for more details.

The objectives were to:

1) Examine changes in atmospheric CH_4 oxidation rates due to afforestation of peatland and grassland with pine trees.
2) Link soil methanotrophic composition with the observed changes in atmospheric CH_4 oxidation rates.

The hypothesis was that afforestation with pine should have a positive effect on the net CH_4 oxidation, which would be correlated with a shift in the structure of the methanotrophic community. Such changes in process and community structure should also be independent of the sites and the original land-use type.

2. Environmental variables

2.1. Chemical properties

The effects of afforestation as well as seasonal variations on some chemical properties of the soils from the different habitats of the two sites are presented in **Table 5.1** and **Table 5.2**. Although the data were not always statically significant and consistent between habitats and sites, trends could be identified. Afforestation consistently decreased soil pH ($P<0.001$). Total C and N concentrations were significantly lower in summer compared to autumn in the bog and grassland ($P<0.001$, except for total N in the bog). A similar but non-significant trend was observed in the forested areas, apart from the total N in the young pine forest at Bad à Cheo ($P<0.001$). Total C and N concentrations also significantly decreased with afforestation at both sites, except for total C concentration at Bad à Cheo, which remained unchanged. C:N ratio was weakly affected by afforestation, with a little (but significant) increase at Glensaugh ($P=0.007$), although the trend was not significant ($P=0.063$) at Bad à Cheo. This increase in C:N ratio was due to a decrease in the concentration of NH_4^+-N observed at both sites ($P<0.001$). However, NH_4^+-N concentration was higher in summer compared to winter (with intermediate values in autumn and spring) in the bog ($P=0.01$) and grassland ($P<0.001$). In contrast, afforestation had no effect on the NO_3^--N concentration at both sites. A similar pattern was observed with the moisture level, except that it was statistically lower in the old pine forest at Bad à Cheo ($P<0.001$).

Table 5.1: Selected chemical soil properties from the Bad à Cheo site.

The data are means ± S.E.M. of each season for each habitat. Within each column, statistical differences between seasons within each habitat are indicated by different Roman letters (a, b, c), while Greek letters (α, β, γ) indicate statistical differences between habitats, according to multiple pairwise comparison (P<0.05). N/A means that no data were available.

Habitat	Season	pH †		Total C † (g.kg^{-1})		Total N † (g.kg^{-1})		C:N ratio †		NH_4^+-N (mg.kg^{-1})		NO_3^--N (mg.kg^{-1})		Moisture (%)	
Bog	Autumn	3.5±0.00	**a**	99±3	**a**	3.4±0.13		30±2		141±29	**a**	178±23	**a**	87±1	**a**
	Spring	N/A		N/A		N/A		N/A		165±27	**a**	160±19	**a**	87±1	**a**
	Summer	3.7±0.04	**b**	88±1	**b**	2.9±0.15	**a**	30±2	**a**	203±33	**a**	122±35	**a**	89±1	**a**
	Winter	N/A		N/A		N/A		N/A		106±16	**b**	209±42	**b**	85±2	**b**
			α		**α**		**α**		**α**		**α**		**α**		**α**
Young Pine	Autumn	3.5±0.02		93±2		3.3±0.18	**a**	28±1		84±7		140±8	**a**	87±0	
	Spring	N/A		N/A		N/A		N/A		69±9		112±4	**a**	88±1	
	Summer	3.6±0.07	**a**	88±2	**a**	2.6±0.12	**b**	34±2	**a**	92±14	**a**	125±34	**a**	89±0	**a**
	Winter	N/A		N/A		N/A		N/A		110±20		190±19	**b**	87±1	
			β		**α**		**αβ**		**α**		**β**		**α**		**α**
Old Pine	Autumn	3.4±0.03	**a**	94±1		2.8±0.10		33±1		90±8		157±13	**a**	75±1	**a**
	Spring	N/A		N/A		N/A		N/A		41±3	**a**	86±5	**b**	79±1	**ab**
	Summer	3.0±0.02	**b**	90±1	**a**	2.6±0.06	**a**	34±1	**a**	84±5		71±14	**c**	82±0	**b**
	Winter	N/A		N/A		N/A		N/A		109±7	**a**	215±15	**a**	79±1	**ab**
			γ		**α**		**β**		**α**		**β**		**α**		**β**

† Analysis performed on autumn and summer samples only.

Table 5.2: Selected chemical soil properties from the Glensaugh site.

The data are means ± S.E.M. of each season for each habitat. Within each column, statistical differences between seasons within each habitat are indicated by different Roman letters (a, b, c), while Greek letters (α, β) indicate statistical differences between habitats, according to multiple pairwise comparison ($P<0.05$). N/A means that no data were available.

Habitat	Season	pH †		Total C † (g.kg^{-1})		Total N † (g.kg^{-1})		C:N ratio †		NH_4^+-N (mg.kg^{-1})		NO_3^--N (mg.kg^{-1})		Moisture (%)	
Grassland	Autumn	4.1± 0.03		8.0± 1.04	**a**	0.76± 0.08	**a**	10±0		45±8	**a**	125 ±55		34±2	**ab**
	Spring	N/A		N/A		N/A		N/A		16±1	**b**	168 ±34		31±1	**ab**
	Summer	4.2± 0.09	**a** **α**	3.8± 0.21	**b** **α**	0.40± 0.02	**b** **α**	9.7± 0.3	**a** **α**	38±4	**a** **α**	120 ±50	**a** **α**	28±1	**c** **α**
	Winter	N/A		N/A		N/A		N/A		20±1	**b**	109 ±27		35±1	**a**
Young Pine	Autumn	3.9± 0.07		4.6± 0.27		0.43± 0.02		11±0		20±1		217 ±26	**a**	31±1	
	Spring	N/A		N/A		N/A		N/A		14±1		105 ±20	**ab**	28±2	
	Summer	3.9± 0.05	**a** **β**	3.4± 0.09	**a** **β**	0.29± 0.01	**a** **β**	11±0	**a** **β**	18±1	**a** **β**	210 ±10	**a** **α**	30±2	**a** **α**
	Winter	N/A		N/A		N/A		N/A		15±2		60 ±4	**b**	32±1	

† Analysis performed on autumn and summer samples only.

2.2. Physical properties

Afforestation of the bog and the grassland had little effect on soil physical properties (**Table 5.3**). Indeed, afforestation did not improve the soil aeration because the porosity, WFPS or bulk density were not affected at either site. However there was a non-significant trend towards a reduced WFPS at both sites. There was a significant effect of afforestation on soil particle size at both sites, with bigger particles found in the pine forest soils at Bad à Cheo (P=0.011). However, the age of the pine forest had no influence. At Glensaugh, the trend was different, with afforestation decreasing the abundance of large-sized particles (P=0.023).

Table 5.3: Selected physical soil properties from Bad à Cheo and Glensaugh.
The data are means ± S.E.M (n=3) of each habitat during the summer only. Within each column, results followed by different Greek letters (α, β) are statistically different for each habitat, according to multiple pairwise comparison (P<0.05).

Site	Habitat	Particle size (% of total)						Bulk density		Porosity		WFPS at field capacity (at 50 kPa)	
		0.02-2.00 µm		2-20 µm		20-2000 µm		($g.cm^{-3}$)		(%)		(%)	
Bad à Cheo	Bog	1.5± 0.32	α	21 ±3	α	77 ±3	α	0.18± 0.03	α	98 ±4	α	76±6	α
	Young Pine	0.38± 0.14	β	10 ±2	β	90 ±2	β	0.12± 0.02	α	98 ±2	α	71±8	α
	Old Pine	0.40± 0.17	β	10 ±2	β	90 ±2	β	0.16± 0.001	α	99 ±3	α	66±6	α
Glensaugh	Grassland	3.8± 0.38	α	34 ±1	α	63 ±2	α	0.65± 0.03	α	68 ±7	α	72±6	α
	Young Pine	4.6± 0.31	α	39 ±1	β	56 ±2	β	0.73± 0.06	α	71 ±3	α	59±3	α

3. Methane fluxes

The effect of afforestation and seasonal variations on the net CH_4 flux of the soils from the different habitats and sites were investigated (**Figure 5.1**). Afforestation of the bog and grassland significantly improved the CH_4 sink in soils (P<0.001), although the age of the pine forest did not make a difference at Bad à Cheo. Also, seasonal variations did not influence net CH_4 flux at either site.

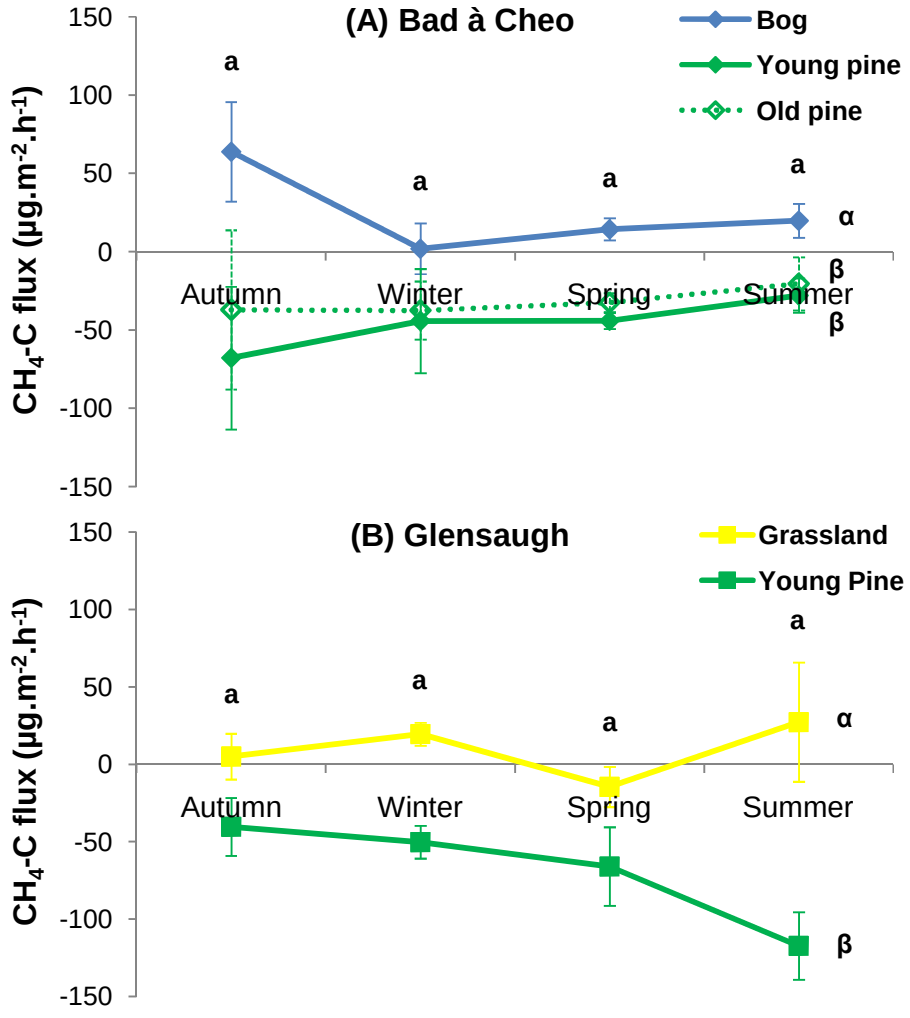

Figure 5.1: Net CH_4-C fluxes from soils from Bad à Cheo (A) and Glensaugh (B).
A positive value means that a production of CH_4 occurs, whereas a negative flux denotes a sink of CH_4. The data are means (error bars are S.E.M.) of each season for each habitat from the closed-chamber experiment. For each site, statistical differences between seasons within each habitat are indicated by different Roman letters (a, b), while Greek letters (α, β) indicate statistical differences between habitats, according to multiple pairwise comparison (P<0.05).

4. Methanotrophic community structure in soils

4.1. Characterisation by molecular methods

The detection of methanotrophs in soils under different habitats was performed by T-RFLP using two genes: *pmoA* (specific to all methanotrophs except *Methylocella* and *Methyloferula* spp.), and 16S rRNA of both type I and type II methanotrophs. All T-RFLP profiles were analysed with *T-REX* software using the raw data exported from GeneMapper software. However, it should be noted that, for *pmoA* analysis, the overall fluorescence detected for the samples from the old pine forest at Bad à Cheo was very low due to the quality of the soil and the difficulty to extract the DNA. Thus, results from the old pine forest at Bad à Cheo were not presented. The *pmoA* microarray was used to confirm the results from the *pmoA*-based T-RFLP analysis, and to identify the methanotroph species present in the soils.

4.1.1. T-RFLP analysis of the *pmoA* genes

The T-RFLP profiles obtained following digestion of the *pmoA* genes with the restriction enzymes *Hha*I and *Msp*I were processed through the *T-REX* software. T-RFs which relative abundance was less than 3% were removed from the analysis. At Bad à Cheo, six *Hha*I and five *Msp*I unique T-RFs were identified, representing most of the total T-RF relative abundance (>87% and >91%, respectively). At Glensaugh, seven *Hha*I and four *Msp*I unique T-RFs were identified, representing, respectively, >82% and >95% of the total T-RF relative abundance. Nested ANOVA was applied in order to investigate the effect of seasonal variations, within each habitat, on individual T-RFs (**Appendix Table 0.7** to **Appendix Table 0.10**). Seasons only had an effect on some T-RFs but no consistent seasonal pattern could be demonstrated at either sites (**Appendix Figure 0.2** and **Appendix Figure 0.3**), as confirmed later by the AMMI analyses (see below). Therefore, the annual average of the T-RFLP profiles of methanotrophs was also presented (**Figure 5.2**).

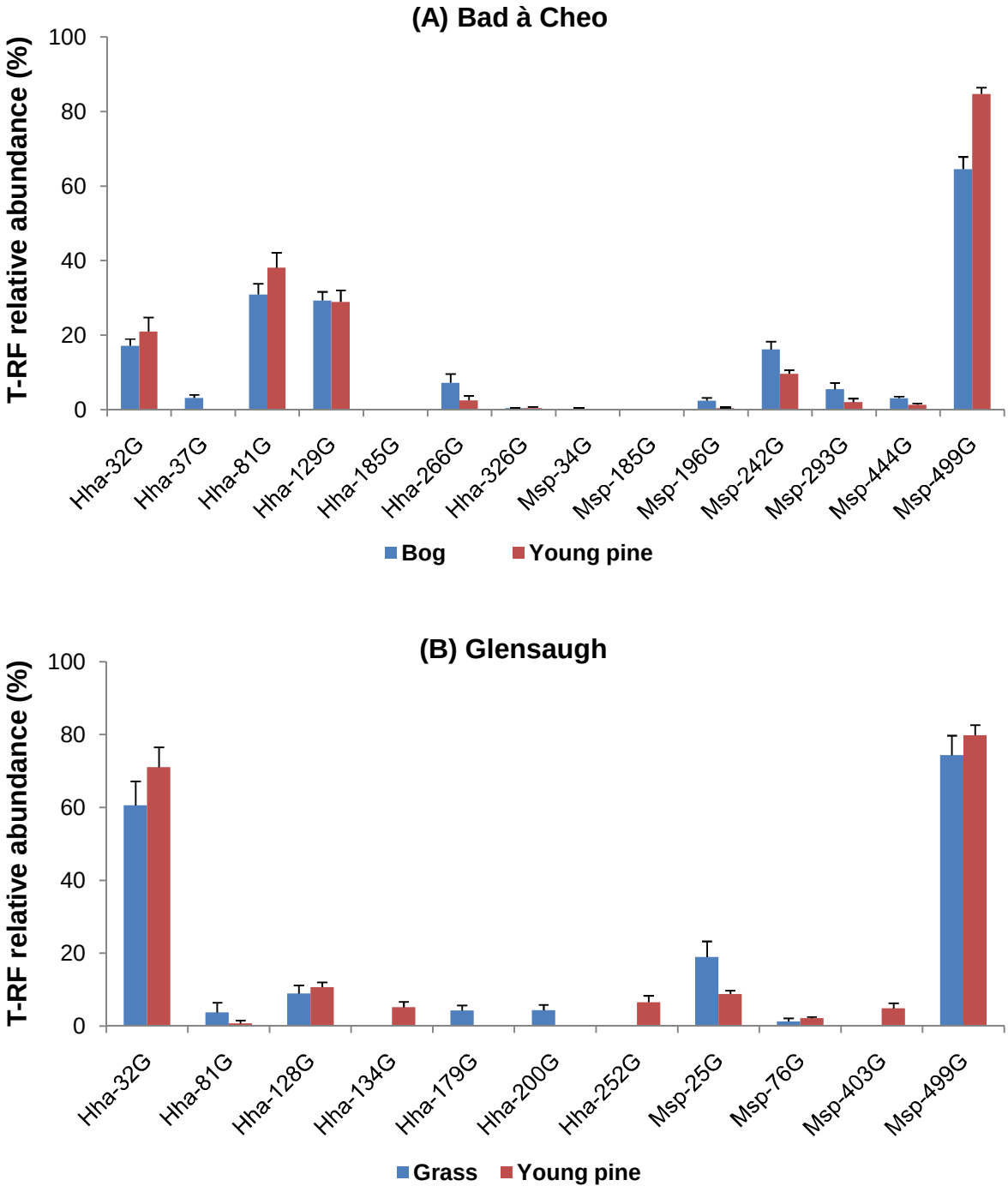

Figure 5.2: T-RFLP profiles of methanotrophs (*pmoA*) at Bad à Cheo (A) and Glensaugh (B).

The total relative abundance (annual average ± S.E.M.) of the T-RFs (n=16) generated by *Hha*I or *Msp*I is accounted for separately. The letter G (green) represents the colour of the dye.

At Bad à Cheo (**Figure 5.2A**), soils from the bog were characterised by the presence of the T-RFs 37 and 266 (digestion with *Hha*I) and the T-RFs 196, 293 and 444 (digestion with *Msp*I) ($P<0.05$), although their relative abundance was very low, ranging ~3-7%. T-RFs *Hha*-32, *Hha*-81 and *Hha*-129 (related to type II methanotrophs, see below) were equally present in the soils under the bog and young pine forest, although there was a trend towards an increase of their relative abundance in the young forest. Also, soils under the young pine forest were characterised by the presence of a lower abundance of the T-RF *Msp*-242 ($P=0.002$) and a higher abundance of the T-RF *Msp*-499 ($P<0.001$).

At Glensaugh (**Figure 5.2B**), only soils under grassland contained the T-RFs *Hha*-179 and *Hha*-200 ($P=0.005$ and $P=0.004$, respectively) whereas the T-RFs *Hha*-134, *Hha*-252 and *Msp*-403 were only found in the young pine forest soils ($P=0.003$) although their relative abundance was low, ranging ~5-8%. Also, T-RF *Msp*-25 was significantly more abundant in soils under grassland than under the young pine forest ($P=0.008$). The soils under grassland and young pine forest had similar abundance of the type II methanotroph T-RFs *Hha*-32, *Hha*-81, *Hha*-128 and *Msp*-76, as well as the T-RF *Msp*-499, although, like at Bad à Cheo, there was a trend towards an increased abundance in the young forest.

T-RFs related to type II methanotroph were present in high abundance in soils from Bad à Cheo and Glensaugh (**Table 5.4**). Microorganisms distantly related to *Methylocystis* sp. constituted ~35% (T-RF *Hha*-81) or ~15% (T-RF *Msp*-242) of all methanotrophs present at Bad à Cheo, whereas bacteria related to *Methylocapsa* sp. (T-RFs *Hha*-32 and *Hha*-129) were dominant (>70%) at Glensaugh.

Table 5.4: Phylogenetic affiliation of the most abundant T-RFs (digestion of *pmoA* with *Hha*I and *Msp*I) found in soils from Bad à Cheo and Glensaugh.

Site	T-RF ID (*enzyme*-bp)	T-RF relative abundance (%)	Associated organism	Reference
Bad à Cheo	*Hha*-32 *Hha*-129	~20 ~30	Distant relative of *Methylocapsa acidiphila*	Singh *et al.* (2009)
	Hha-81	~35	Distant relative of *Methylocystis* sp. and *Methylosinus* sp.	Singh *et al.* (2009)
	Msp-242	~15	*Methylocystis* sp.	Horz *et al.* (2001)
	Msp-499	65-85	Unknown	N/A
Glensaugh	*Hha*-32 *Hha*-128	~65 ~10	Distant relative of *Methylocapsa acidiphila*	Singh *et al.* (2009)
	Hha-81	<5	Distant relative of *Methylocystis* sp. and *Methylosinus* sp.	Singh *et al.* (2009)
	Msp-25 *Msp*-76	<20 ~2	Distant relative of *Methylocapsa acidiphila*	Chapter 4, section 4.2
	Msp-499	~80	Unknown	N/A

Data were further analysed to understand the influence of different environmental variables on individual T-RFs. First, DCA gave a gradient length of 0.975 (Bad à Cheo) and 1.241 (Glensaugh) on the first axis, which suggested that RDA was suitable for the analysis of relationships of T-RFs with environmental variables. No environmental variables were found to significantly influence the T-RFs. However, C:N ratio and porosity showed a weak influence at, respectively, Bad à Cheo (P=0.066) and Glensaugh (P=0.060), on the T-RFs related to *Methylocapsa* sp. (T-RFs *Hha*-32, *Hha*-129 and *Msp*-25).

The AMMI analysis of the T-RFs generated from the digestion with the restriction enzymes *Hha*I and *Msp*I, using habitats and seasons as environments, found a small difference in the methanotrophic community structure. Indeed, the interaction effect was ~11% (at Bad à Cheo) and ~15% (at Glensaugh) of the total variation, which is indicative of an interaction

between the pattern of the T-RFs and their respective environments (or treatment, *i.e.* habitat and/or season). This was confirmed by the MANOVA on the four IPC scores of the AMMI analysis which gave an overall significant effect ($P<0.001$) of land-use change at both sites (**Table 5.5**).

Table 5.5: Effects of afforestation and seasonal changes on the methanotrophic community at Bad à Cheo and Glensaugh (digestion of *pmoA* with *Hha*I and *Msp*I).

The data are *P* values corresponding to the first four IPC scores of the AMMI analyses, and were obtained by nested ANOVA and MANOVA. Within each column, statistical differences between seasons within each habitat are indicated by different Roman letters (a, b), while Greek letters (α, β) indicate statistical differences between habitats, according to multiple pairwise comparison ($P<0.05$).

		IPC 1	**IPC 2**	**IPC 3**	**IPC 4**	**MANOVA**
Bad à Cheo	% variation	42.0	26.5	14.2	9.3	
	Habitat	**0.008**	0.374	0.088	**0.007**	**<0.001**
	Habitat/Season	0.755	0.295	0.239	0.386	0.390
Bog	Autumn Spring Summer Winter	**a α**	**a α**	**a α**	**a α**	
Young Pine	Autumn Spring Summer Winter	**a β**	**a α**	**a α**	**a β**	
		IPC 1	**IPC 2**	**IPC 3**	**IPC 4**	**MANOVA**
Glensaugh	% variation	55.8	23.2	8.0	5.1	
	Habitat	0.840	**0.044**	**0.003**	**0.027**	**<0.001**
	Habitat/Season	0.476	**0.011**	0.208	0.507	**0.014**
Grassland	Autumn Spring Summer Winter	**a α**	**a** **a** **b** **a** **α**	**a α**	**a α**	
Young Pine	Autumn Spring Summer Winter	**a α**	**a β**	**a β**	**a β**	

The differences in community structure can be seen on the graphical representation of the IPC scores (**Figure 5.3**). Afforestation – but not seasonal variations – had a significant effect on the community structure when considering the IPCs 1 and 4 at Bad à Cheo (**Table 5.5** and **Figure 5.3A**). In contrast, a seasonal effect was found on the second dimension only (P=0.011) at Glensaugh (**Table 5.5**) where the grassland had a statistically different methanotrophic structure in summer. This result was not correlated to a significant change in net CH_4 flux (see Figure 5.1). Community structure was affected by afforestation on the last three IPCs at Glensaugh (cumulated effect <37% of the total variation detected) (**Table 5.5** and **Figure 5.3B**).

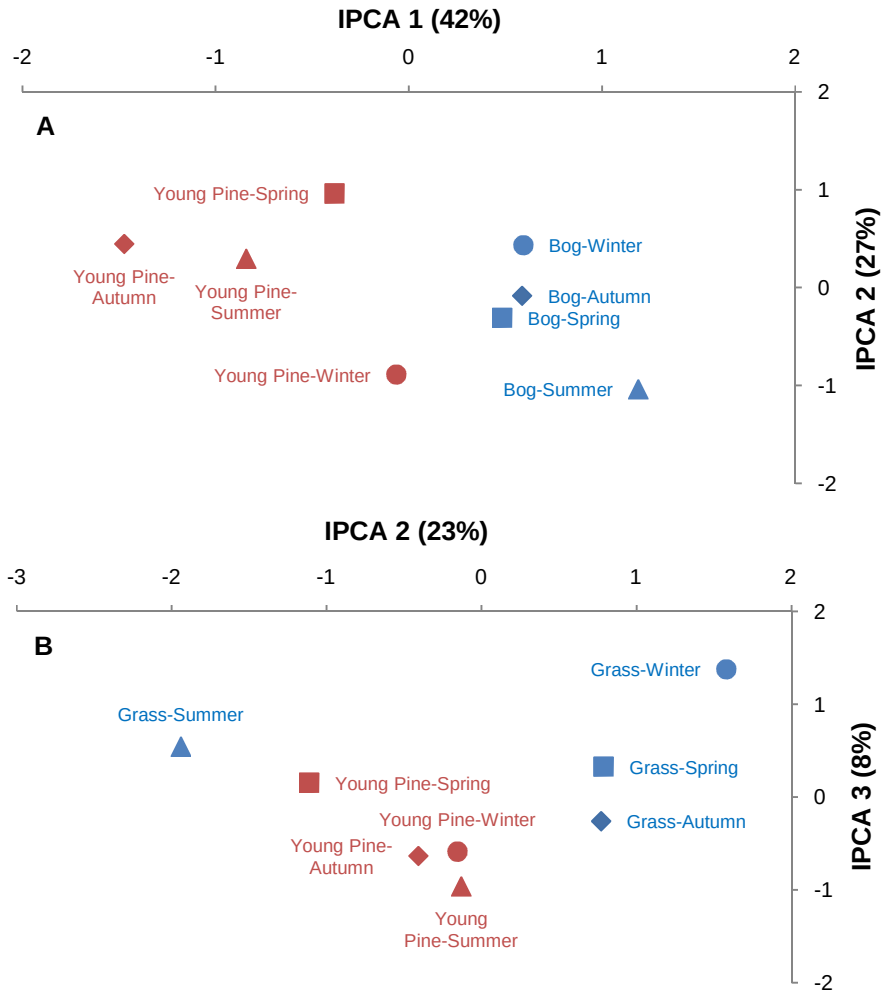

Figure 5.3: Methanotrophic community structure at Bad à Cheo (A) and Glensaugh (B) after analysis of the T-RFLP profiles (digestion of *pmoA* with *Hha*I and *Msp*I) with the AMMI model.
The data points within each habitat represent the averages over replicates (n=4) of the IPC scores of each season.

4.1.2. Analysis of the 16S rRNA genes of type II and type I methanotrophs

The AMMI analysis, using habitats and seasons as environments (replicates were averaged), found a difference in the community structure of type II and type I methanotrophs. The interaction effects were ~26% and ~17% at Bad à Cheo for type II and type I, respectively. They were ~22% and ~12% at Glensaugh (type II and type I, respectively). This means there was some interaction of the T-RFs with their environment (or treatment). This was confirmed by the MANOVAs on the four IPC scores of the AMMI analyses which showed that the effect of afforestation and season on type II and type I methanotrophs was significant at both sites (P<0.001), except for the type I methanotrophs at Glensaugh (P=0.063) (**Table 5.6**). These differences were observed on the graphical representation of the IPC scores of the AMMI models (**Figure 5.4**).

At Bad à Cheo, afforestation and the age of the forest had a significant effect on the structure of both type II and type I methanotrophic communities on, at least, the first two dimensions (**Table 5.6**, P<0.001; and **Figure 5.4A1** and **B1**). There was also a seasonal effect with type II and type I microbial communities being most dissimilar in winter and summer, with transitional state in spring and autumn (**Appendix Table 0.11** and **Appendix Table 0.12**). At Glensaugh, afforestation did not have such a strong effect on the structure of type II (IPC 1, P<0.001; IPC 2 P=0.168) and type I (IPC 1, P<0.001; IPC 2, P=0.035) methanotrophic communities (**Figure 5.4A2** and **B2**). However, seasonal differences were observed in type II methanotrophs under grassland in autumn and under young pine forest in spring-summer (IPCs 1 and 2, P<0.001), whereas a difference in type I methanotrophs was only detected on the fourth IPCA, which represent ~8% of the total variation (**Appendix Table 0.11** and **Appendix Table 0.12**).

Table 5.6: Effects of afforestation and seasonal changes on the methanotrophic community at Bad à Cheo and Glensaugh (16S rRNA of type II methanotrophs – digestion with *Mbo*I and *Msp*I; 16S rRNA of type I methanotrophs – digestion with *Hha*I and *Msp*I).

The data are *P* values corresponding to the first four IPC scores of the AMMI analyses. A more detailed version of this table, including multiple pairwise comparisons, can be found in **Appendix Table 0.11** and **Appendix Table 0.12**.

Type II		**IPC 1**	**IPC 2**	**IPC 3**	**IPC 4**	**MANOVA**
Bad à Cheo	% variation	73.2	19.4	5.0	1.0	
	Habitat	**<0.001**	**<0.001**	0.067	0.751	**<0.001**
	Habitat/Season	0.682	**0.002**	**0.034**	0.273	**0.014**
Glensaugh	% variation	55.1	22.8	13.4	4.2	
	Habitat	**<0.001**	0.168	0.374	0.568	**<0.001**
	Habitat/Season	**<0.001**	**<0.001**	**0.031**	**0.009**	**<0.001**

Type I		**IPC 1**	**IPC 2**	**IPC 3**	**IPC 4**	**MANOVA**
Bad à Cheo	% variation	71.0	9.1	5.8	4.4	
	Habitat	**<0.001**	**<0.001**	**0.004**	0.720	**<0.001**
	Habitat/Season	0.063	**0.006**	**0.012**	**0.007**	**<0.001**
Glensaugh	% variation	41.2	17.6	15.2	8.1	
	Habitat	**<0.001**	**0.035**	**0.013**	0.249	**<0.001**
	Habitat/Season	0.860	0.550	0.321	**0.002**	0.063

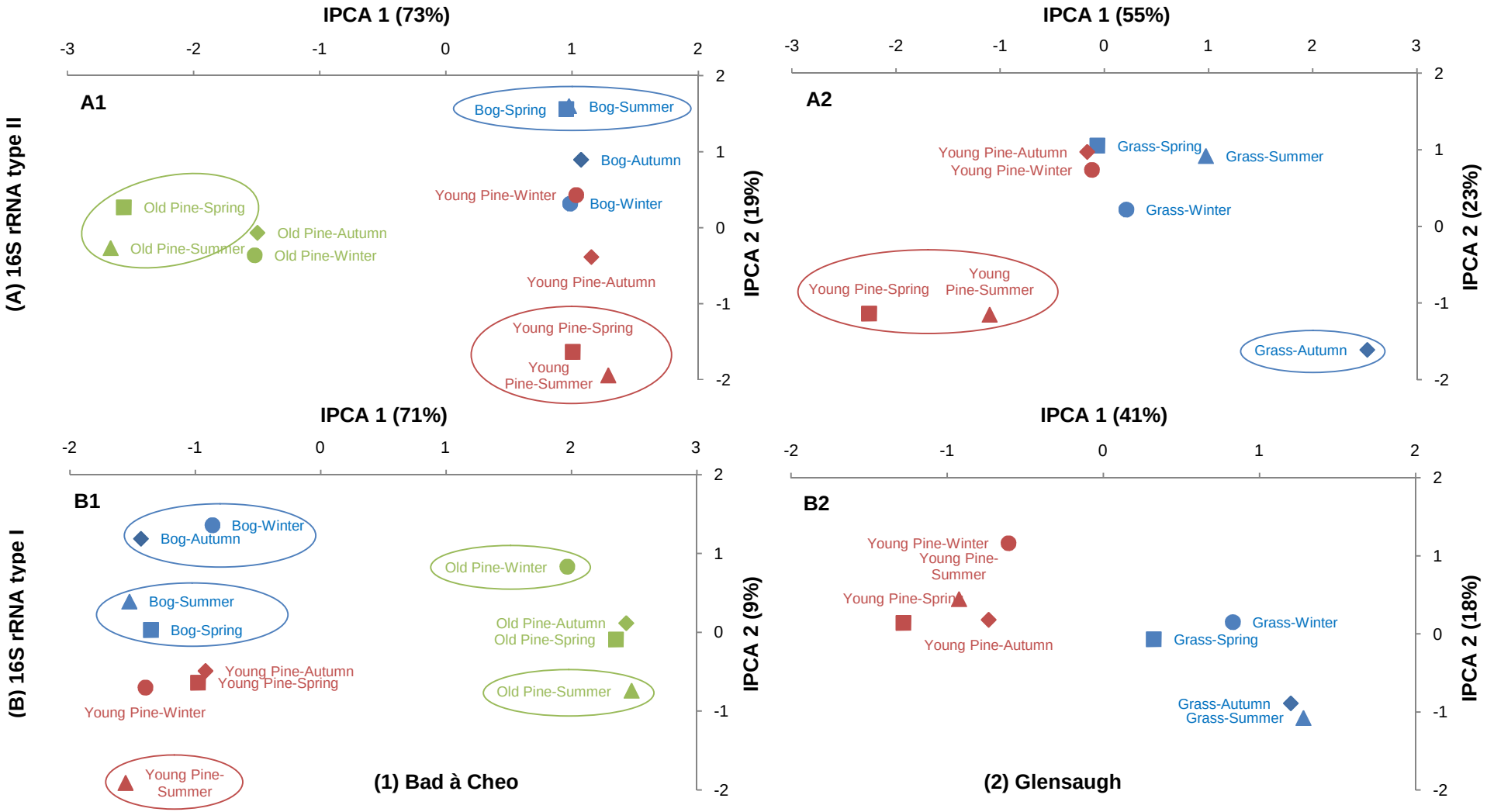

Figure 5.4: Type II (A) and type I (B) methanotroph community structure at Bad à Cheo (1) and Glensaugh (2) after analysis of the T-RFLP profiles (16S rRNA of type II methanotrophs – digestion with *Mbo*I and *Msp*I; 16S rRNA of type I methanotrophs – digestion with *Hha*I and *Msp*I) with the AMMI model.

The data points within each habitat represent the averages over replicates (n=4) of the IPC scores of each season. The circles show seasons that were statistically different within each habitat.

4.1.3. Diagnostic *pmoA* microarray

Type I methanotrophs were not detected at either sites (**Figure 5.5**), which confirms the *pmoA*-based T-RFLP findings (see Table 5.4). However, one soil sample from the old pine forest at Bad à Cheo contained type Ib methanotrophs related to *Methylococcus* sp. (probe Mc396) and *Methylohalobius* sp. (probe Mh-500) – type Ib methanotrophs are only thermophilic and halophilic (Stralis-Pavese *et al.*, 2004). Neither nitrifiers nor any *Methylocapsa* sp. were detected at either sites (**Figure 5.6**). Also, no novel *pmoA* genes of type II methanotrophs were present except in one soil sample from the old pine forest, which contained a novel *pmoA* gene related to *Methylocystis*/*Methylosinus* (probe LP21-232).

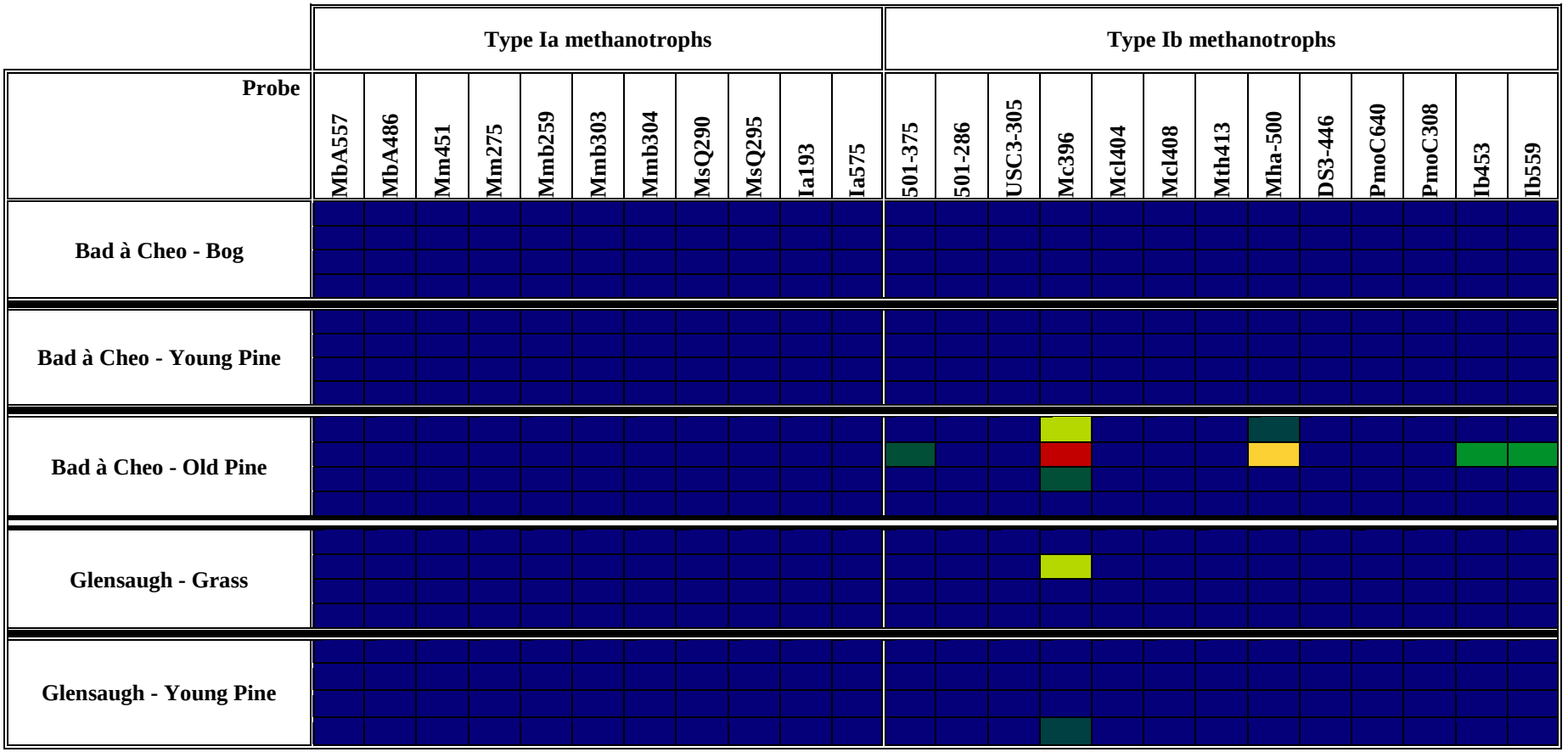

Figure 5.5: Type I methanotrophic community analysis at Bad à Cheo and Glensaugh using the *pmoA* microarray (n=4 for each habitat).

Within each habitat, each row represents a replicate. The results were first normalised to positive control probe mtrof173, then to the reference values determined individually for each probe (Bodrossy *et al.*, 2003). Colour coding is as such: red colour indicates maximum achievable signal for an individual probe, while blue colour indicates that no detectable PCR product hybridised to that probe. The colour gradient between blue and red reflects the proportion of hybridisation.

No hybridisation 100% hybridisation

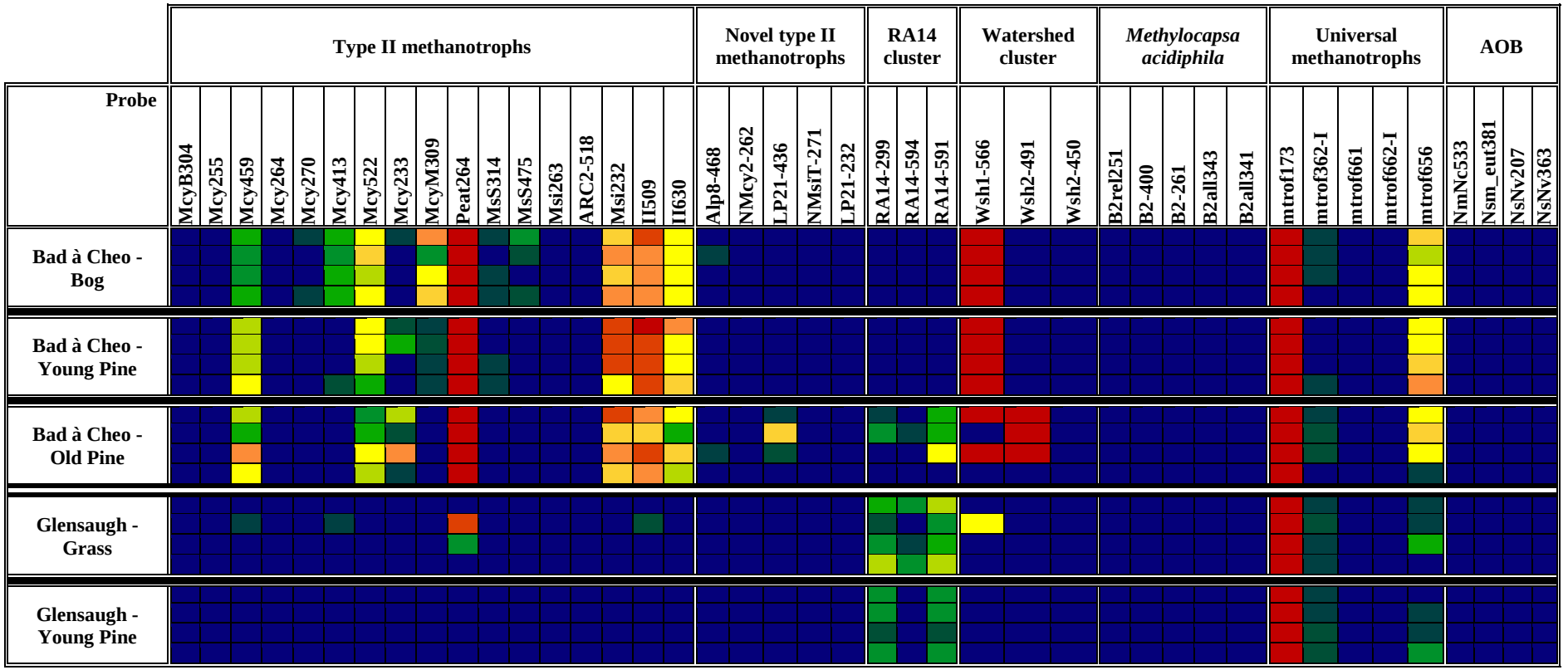

Figure 5.6: Type II methanotrophs and related organisms community analysis at Bad à Cheo and Glensaugh using the *pmoA* microarray (n=4).

Within each habitat, each row represents a replicate. The results were first normalised to positive control probe mtrof173, then to the reference values determined individually for each probe (Bodrossy *et al.*, 2003). Colour coding is as such: red colour indicates maximum achievable signal for an individual probe, while blue colour indicates that no detectable PCR product hybridised to that probe. The colour gradient between blue and red reflects the proportion of hybridisation.

Type II methanotrophs related to the RA14 cluster (probes RA14-299, RA14-594 and RA14-591) were detected in Glensaugh (**Figure 5.6**) but afforestation had no significant influence on their abundance. Overall, the soil methanotrophic community in Glensaugh was similar between the grassland and the young pine forest (**Table 5.7**). This is in contradiction with the community shift observed with the *pmoA*-based T-RFLP analysis (see Figure 5.3B). One soil sample from the grassland contained a peat-related uncultivated type II methanotroph (probe Peat264) and one related to the Watershed 1 clade (probe Wsh1-566).

At Bad à Cheo, the type II methanotrophic community consisted of *Methylocystis*/ *Methylosinus* (probes Mcy459, Mcy522 and Msi232), peat-related type II methanotrophs (probe Peat264) and watershed-clade (probe Wsh1-566) organisms (**Figure 5.6**). *Methylocystis*-related bacteria (probes Mcy413 and McyM309) were only present in the soil under the bog ($P<0.001$ and $P=0.012$, respectively), whereas methanotrophs of the RA14 (probe RA14-591) and Wsh2 (probe Wsh2-491) clades were only detected in the soil under the old pine forest ($P=0.038$ and $P=0.007$, respectively) (**Table 5.7**). Overall, PCA and subsequent MANOVA indicated that afforestation and the age of the forest changed the soil methanotrophic community at Bad à Cheo ($P=0.003$), but not at Glensaugh ($P=0.299$) (**Table 5.8**).

Table 5.7: Effects of afforestation on the methanotrophic community at Bad à Cheo and Glensaugh (*pmoA* microarray).

The data presented are some of the *pmoA* probes that showed higher levels of hybridisation, and their statistical difference (Greek letters [α, β, γ]) between each habitat, according to multiple pairwise comparison ($P<0.05$).

Site	Habitat	Probe								
		Mc396	**Mha500**	**Mcy413**	**McyM309**	**Peat264**	**Msi232**	**RA14-591**	**Wsh1-566**	**Wsh2-491**
Bad à Cheo	Bog	α	α	**α**	**α**	α	α	**α**	**α**	**α**
	Young pine	α	α	**β**	**β**	α	α	**α**	**β**	**α**
	Old pine	α	α	**β**	**β**	α	α	**β**	**γ**	**β**
		Probe								
		Mc396		**Peat264**	**RA14-299**	**RA14-594**	**RA14-591**		**Wsh1-566**	**Wsh2-491**
Glensaugh	Grassland	α		α	α	α	α		α	α
	Young pine	α		α	α	α	α		α	α

Table 5.8: Effects of afforestation on the methanotrophic community at Bad à Cheo and Glensaugh (PCA from the *pmoA* microarray).

The data are *P* values corresponding to the first five PC scores of the probe hybridisation intensities, and were obtained by MANOVA. Within each column, results followed by different Greek letters (α, β, γ) are statistically different for each habitat, according to multiple pairwise comparison ($P<0.05$).

		PC 1	PC 2	PC 3	PC 4	PC 5	MANOVA
Site/Habitat	**% variation**	74.23	15.93	6.07	2.22	0.66	
	P	**<0.001**	0.215	0.469	0.640	0.695	**0.003**
Bad à Cheo	Bog	**α**	α	α	α	α	
	Young pine	**β**	α	α	α	α	
	Old pine	**γ**	α	α	α	α	
Site/Habitat	**% variation**	63.88	34.65	1.170	0.230	0.050	
	P	0.934	**0.003**	0.821	0.811	0.598	0.299
Glensaugh	Grass	α	**α**	α	α	α	
	Young pine	α	**β**	α	α	α	

4.2. Linking community structure with function

This was first investigated by simple linear regression analysis (**Figure 5.7**) between the *pmoA* IPCA scores of each habitat from **section 4.1.1** and the corresponding net CH_4 flux values from **section 3**. At both sites, afforestation and change in net CH_4 flux were significantly related to a shift in the community structure ($P=0.022$ at Bad à Cheo; $P=0.027$ at Glensaugh). However, the relationship was stronger at Bad à Cheo ($R^2=0.6478$) when considering the first dimension, which accounted for 42% of the variation (**Figure 5.7A**). At Glensaugh, the correlation between CH_4 and community structure was significant only on the third dimension ($R^2=0.5473$), which accounted for only 8% of the variation (**Figure 5.7B**). When working with the second dimension (23%), linear regression analysis was still significant ($P=0.032$) but with a R^2 of 0.0289 (**Appendix Figure 0.4**).

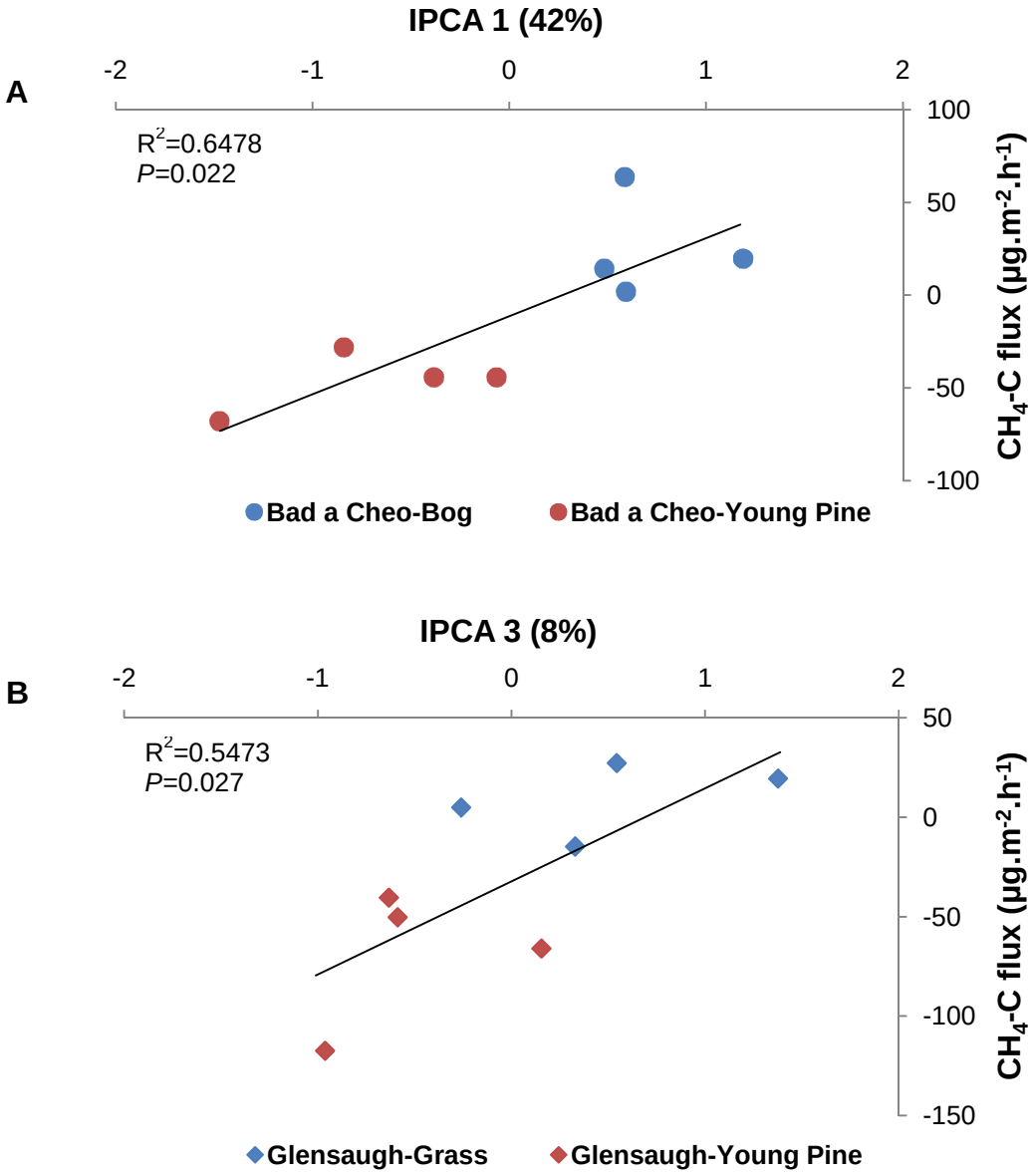

Figure 5.7: Relationship between net CH_4 flux and methanotrophic community structure at Bad à Cheo (A) and Glensaugh (B).
The data points represent the IPCA scores displayed in **Figure 5.3** and the net CH_4 fluxes from **Figure 5.1**.

PLFA-SIP analysis was used to link methanotrophic communities with their activity. Seasonal averages of the enriched PLFA content (% of ^{13}C-incorporation, **Figure 5.8**) were used for cluster analysis in order to identify the affiliation of the active methanotrophic community, in other words, the methanotrophs involved in the oxidation of atmospheric CH_4. **Figure 5.9** shows that the active methanotrophs in the soils under the bog and young pine forest (Bad à Cheo) were distant relatives (<90% similarity) of *Methylosinus sporium* and the

Beijerinckiaceae family (containing *Methylocella*/*Methylocapsa* spp.). The methanotrophs involved in the atmospheric oxidation of CH_4 in the soils under the old pine forest (Bad à Cheo), the grassland and young pine forest (Glensaugh) were more distantly related (<75% similarity) to the above methanotrophs. Afforestation of the bog and the grassland did not impact on the active methanotrophic community capable of oxidising atmospheric CH_4. The most enriched PLFA was always 18:1ω7 (**Figure 5.8**).

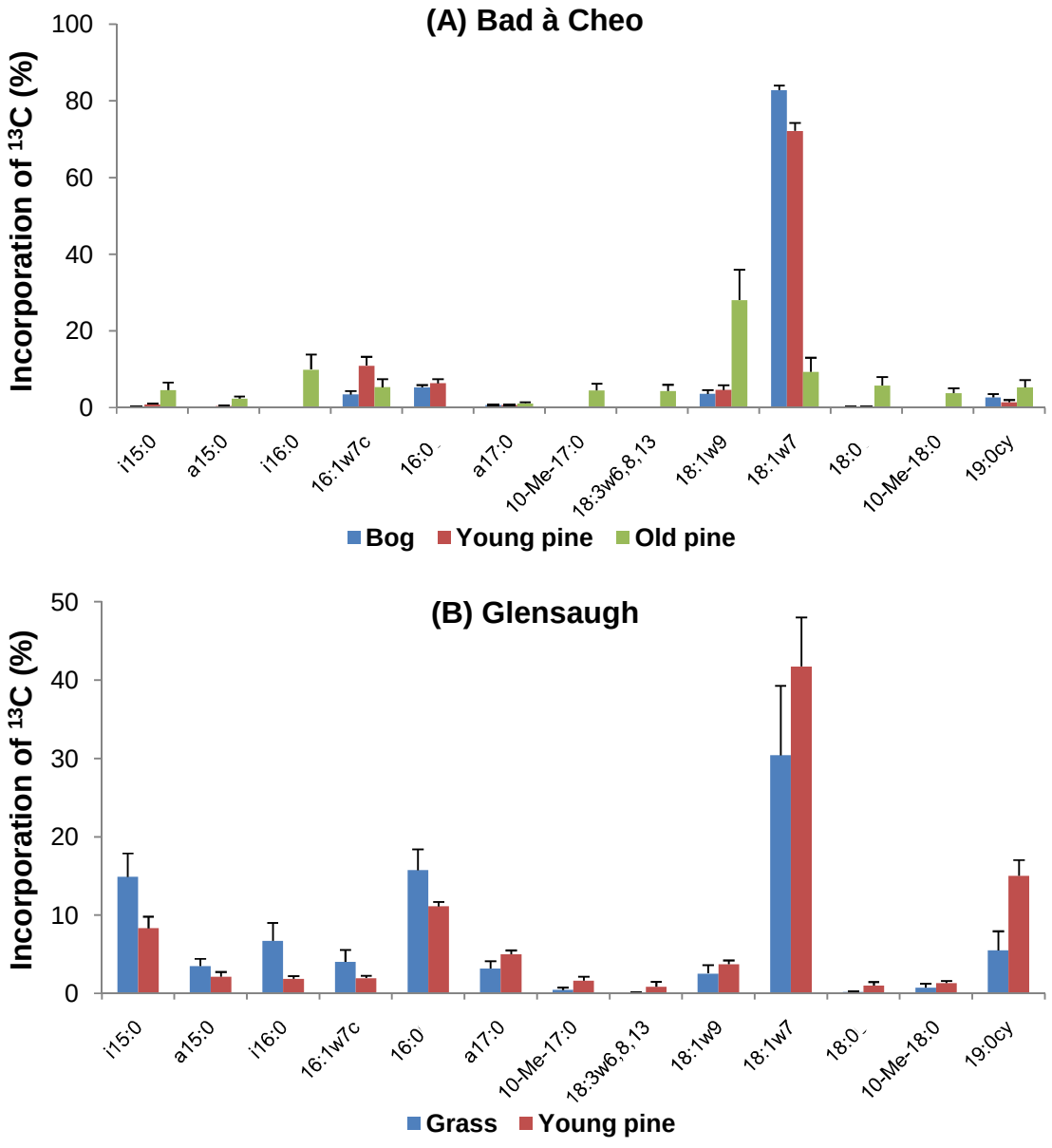

Figure 5.8: Percentage of incorporation of ^{13}C within the PLFAs after incubation with ~100 ppm of ^{13}C-CH_4 at Bad à Cheo (A) and Glensaugh (B).

The data are seasonal average ± S.E.M. (n=8) of the enriched PLFA content.

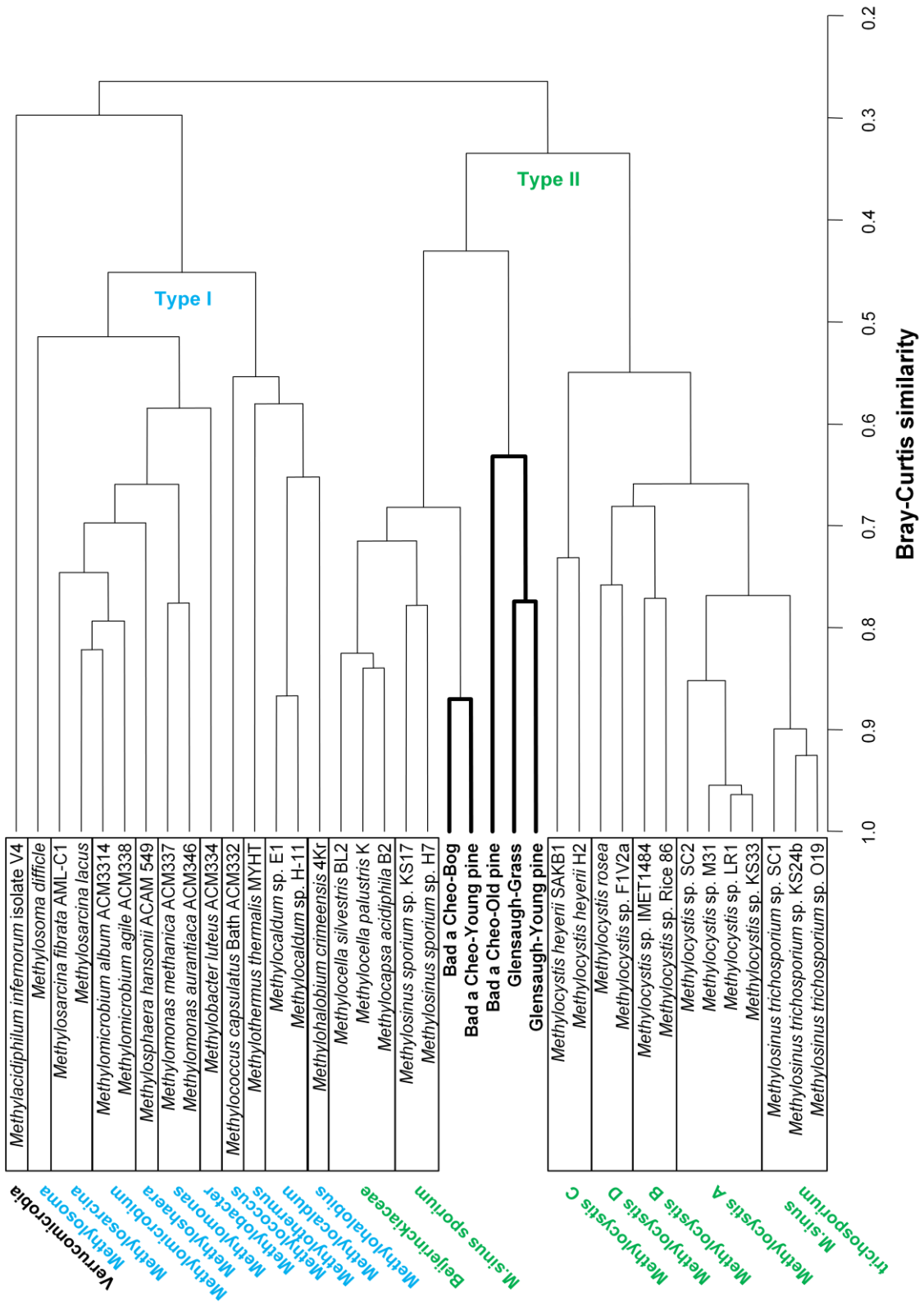

Figure 5.9: Cluster analysis of the PLFA profiles (based of % of ^{13}C-incorporation) of methanotrophs in the enriched soils (~100 ppm ^{13}C-CH_4) from Bad à Cheo and Glensaugh (n=4).

The dendrogram was built using data from this study, combined with data from the literature (Bodelier *et al.*, 2009). A Bray-Curtis similarity matrix was used, from the square root-transformation of the PLFA data (see **Figure 5.8**), to perform a group average linking cluster analysis with GenStat® software.

5. Discussion

5.1. Effect of seasonal changes and afforestation on abiotic properties

The chemical properties of the soils were not always statistically consistent with the season and land use (Table 5.1 and Table 5.2). The moisture data were in contradiction between the two sites, with moisture levels in winter being the lowest at Bad à Cheo but the highest in Glensaugh, compared to the other seasons. Although no heavy rains occurred while sampling, it is not possible to say if it rained (and for how long) in the days prior to sampling. This could have affected the results and it may be an explanation for the lack of consistency or pattern between the seasons. Therefore, one could assume that the seasonal variations observed could be due to experimental variations. However, total C and N concentrations were lower in summer compared to autumn in the non-forested areas maybe as a result of a higher growth of microbial communities and plants in summer due to a higher demand of N. Also, forest total C may have been degraded at a slower rate in summer in comparison to grassland and peatland.

The effect of afforestation on the chemical properties was not always the same at each site. Nevertheless, afforestation had some impact on the C and N cycles and soil pH. Firstly, pH decreased with afforestation as well as with the age of the forest. This was expected since tree planting results in soil acidification due to increased organic acid inputs, soil respiration or cation redistribution (Jobbágy & Jackson, 2003). Secondly, a decrease in soil moisture was expected due to water uptake by trees. However, the results did not support this, except in the old pine forest on the peatland site. Similarly, only a non-significant trend towards an increased porosity and reduced WFPS was observed (Table 5.3). This may suggest that, these types of soils (peatland, grassland) in Scotland may take >20 years to achieve significant

changes in these soil properties. This observation is in contrast to findings in New Zealand where only <10 years after afforestation resulted in significant changes in soil properties (Tate *et al.*, 2007). Finally, afforestation had little effect on the C:N ratio. This was because total C and N concentrations both decreased simultaneously with afforestation. The decrease of total N was concomitant with a decrease in the concentration of NH_4^+-N, and NO_3^--N (although non-significant). That is not surprising since available N may have been removed from soil due to increased activity of above ground vegetation. The total C content in the peatland site (Bad à Cheo) was about 15 times higher than could be measured in the grassland site (Glensaugh). That is not surprising since peat contains a lot of stored C (Harrison *et al.*, 1995). If we consider the soil C loss that can occur when a land-use change occurs (Post & Kwon, 2000), the small change in these soil properties would suggest that afforestation did not have a major impact on C losses, even with the peatland. Another explanation could be that the forest soils recovered from disturbance within 20 years. Paul *et al.* (2002) concluded that, depending on original land use, site preparation and tree species present, forest soils could take over 30 years to recover from a change from pastoral or agricultural use. Several studies on the effect of land management (fertilisation, drainage, thinning, tree species selection, forest rotation length) and land use (land conversion, afforestation, reforestation) on soil C were reviewed (Harrison *et al.*, 1995; Jandl *et al.*, 2007; Johnson, 1992; Paul *et al.*, 2002) and forests were always found to recover from C losses and improve C sequestration, although short forest rotations (30 years) should be avoided. Therefore, the present data show a potential for the mitigation of atmospheric CH_4 of through afforestation of bogs (see below) while preserving the long-term sequestration of C.

5.2. Effect of seasonal changes and afforestation on the net CH_4 fluxes

Seasons did not affect the measured net CH_4 fluxes from the soils at either site (**Figure 5.1**), which is in contradiction with several other studies reporting a seasonal variation of net CH_4 fluxes mostly associated with a change in soil temperature and/or moisture (Castro *et al.*, 1995; Saggar *et al.*, 2007). Yet, some reports exist that do not place temperature as a strong controller of CH_4 oxidation (Smith *et al.*, 2003). The present study suggests that CH_4 oxidation rates were influenced by soil moisture and WFPS rather than by air temperature since no effect of seasons was observed.

Afforestation played a major role in inverting the net CH_4 fluxes. However, the initial site preparation at Glensaugh (*i.e.* drainage of bog before tree planting) may have played a role in facilitating the establishment of aerobic conditions. At both sites, young pine forest soils were oxidising CH_4 at very high rates compared to bog and grassland. A study on a similar afforested blanket peat at a site near Bad à Cheo measured a CH_4 sink only when the soil moisture was significantly lower than in the bog (MacDonald *et al.*, 1996), which is the trend observed at Bad à Cheo. Many studies confirmed the positive impact of grassland afforestation on CH_4 sink (Hütsch *et al.*, 1994; MacDonald *et al.*, 1996; Saggar *et al.*, 2008; Tate *et al.*, 2007). Soil physical factors such as bulk density and gas diffusivity (related to WFPS and therefore porosity) were proposed as a strong controller of CH_4 oxidation rates (Ball *et al.*, 1997; Castro *et al.*, 1995; Saggar *et al.*, 2008; Smith *et al.*, 2003). In particular, CH_4 uptake was increased with better soil aeration (increased porosity, decreased WFPS). Although no statistically significant changes of these parameters occurred at either site, a trend was obvious, which could correlate the flux data.

Because there was no difference between the 20- and 40-year-old-pine forests at Bad à Cheo, it may indicate that 20 years were sufficient for turning previously non-forested areas

producing CH_4, into efficient CH_4 sinks; and for reaching stable oxidation rates. Fluxes in the pine forests ranged from -32 to -69 $\mu g.m^{-2}.h^{-1}$, which is within range of CH_4 oxidation rates measured in several countries of Northern Europe, including Scotland (Smith *et al.*, 2000).

5.3. Effect of seasonal changes on the methanotrophic community structure

It was difficult to find a pattern in *pmoA* T-RF abundance. When concentrating on the most abundant T-RFs, no major seasonal effect was observed in any of the habitats. Again, more extensive seasonal sampling might help observing seasonal pattern of particular species.

The structure of the methanotrophic community in the soils was affected by seasonal variations to some extent. The *pmoA*-based T-RFLP analysis failed to detect a community shift, while analysis of the 16S rRNA genes did not. In general, the methanotrophic community structure was different in winter compared to summer (Figure 5.4). This was probably as a consequence of a change in soil moisture and O_2 availability for methanotrophic activity rather than an effect of season (Reay *et al.*, 2005; Smith *et al.*, 2003).

5.4. Effect of afforestation on the methanotrophic community structure

The different analytical techniques used gave reasonably consistent results. Firstly, no type I methanotrophs were detected in the soils either by *pmoA*-based T-RFLP analysis or the *pmoA* diagnostic microarray. Yet, the T-RFLP analysis of 16S rRNA genes detected the presence of type I methanotrophs and that afforestation changed their structure (Figure 5.4B1 and B2). The primers used for the amplification of the 16S rRNA genes of type I methanotrophs were specifically designed to use with landfill soils which contain high quantities of low-affinity methanotrophs (Chen *et al.*, 2007). Since forest soils are not expected to contain high numbers of methanotrophs, non-specific amplification might have occurred. Cloning would help confirming the identity of the organisms identified.

Secondly, bacteria related to type II methanotrophs were found to be dominant with both *pmoA*-based T-RFLP and microarray analyses (Table 5.4 and Figure 5.6). The most abundant T-RFs were all related to *Methylocapsa* sp. and to members of *Methylocystaceae*, while the highest hybridisations were with probes related to *Methylocystis/Methylosinus* and peat-characteristic type II methanotrophs that were identified as being related to *Methylosinus* sp. (Chen *et al.*, 2008); as well as members of the RA14 group (USCα) and Watershed cluster – related to RA14 (Chen *et al.*, 2008) – which are thus all capable of oxidising atmospheric CH_4 (Holmes *et al.*, 1999; Ricke *et al.*, 2005).

The PLFA-SIP profiles of the soil methanotrophs under the different habitats were related to the *Beijerinckiaceae* family and *Methylosinus sporium* (Figure 5.9), which matches the molecular findings. However, methanotrophs under the old pine forest at Bad à Cheo, as well as under the grassland and young pine forest at Glensaugh, were very distantly related to *Methylocapsa* sp. and *Methylosinus* sp. This can be explained by the complete lack of ^{13}C-CH_4 incorporation (~20% at Bad à Cheo and ~50% at Glensaugh, data not shown) during the enrichment experiment. This could explain the lower levels of the labelled PLFA C18:1ω7 observed in these soils (Figure 5.8) and thus why they were distantly related to *Methylocapsa acidiphila*. Nonetheless, this confirms that the active oxidation of atmospheric CH_4 was performed by organisms related to high-affinity methanotrophs commonly found in upland soils (see Chapter 4, section 5.3).

Interestingly, the effect of afforestation on community structure was evident at Bad à Cheo with both T-RFLP and microarray analyses while it was not at Glensaugh because T-RFLP analysis of the two genes (16S rRNA and *pmoA*) found a significant difference ($P<0.001$) but the *pmoA* microarray did not ($P=0.299$). The lack of consistency at Glensaugh is not that

surprising since the effect of grassland afforestation on community structure detected by the AMMI analysis of the *pmoA* genes was only weak (Figure 5.3). It was unexpected though that a more pronounced effect was not observed since other similar studies detected a clear shift of type I methanotrophs towards type II methanotrophs when pastoral grasslands were afforested with pine trees (Knief *et al.*, 2005; Singh *et al.*, 2007; 2009). But since no type I methanotrophs were detected at Glensaugh such evident change could not occur. Instead, the soils under grass and pine at Glensaugh were dominated with members of the RA14 cluster. At Bad à Cheo, *Methylocystaceae* members were present in the soil under bog only while *Methylocapsa*-related cells were characteristic of the forest soils. This predominance of type II-related methanotrophs, in particular members of the USCα, in upland forest soils seems to be a world-wide trend, independent of the tree species, as discussed in Chapter 4, section 5.4.

5.5. Effect of community structure on net methane flux

Figure 5.7 explicitly shows that the change in net CH_4 flux associated with land-use change was related to a shift in the methanotrophic community structure. Although other studies investigated the relationship between land-use change and CH_4 oxidation rates (Smith *et al.*, 2000), or between land-use change and methanotrophic communities involved (Singh *et al.*, 2007), this is the first time that such relationship is characterised. Yet, the correlation was rather weak at Glensaugh because the third dimension of the AMMI analysis was used, representing 8% of the total interaction.

No transitional state was observed in the young pine forest, in terms of CH_4 sink capacity while the age of the forest showed an influence on the methanotrophs, as detected with the microarray. Thus, this would suggest that net CH_4 flux rates recovered from soil disturbance faster than the methanotrophs did, which is in contradiction with the findings of Chapter 4 (section 5.2).

6. Conclusions

Afforestation/reforestation has become a common practice in several countries for increasing financial return *via* the wood industry but also "carbon farming", which helps increasing national C sinks under the Kyoto Protocol guidelines (Trotter *et al.*, 2005; UNFCCC, 1998). The present study indicated a trend suggesting that afforestation of peatland and pasture with pine trees not only had the potential to improve the atmospheric CH_4 sinks, but also that soil C stocks seemed unchanged <20 years after disturbance following land-use change.

Associated to the change in CH_4 oxidation rates was a shift of the soil methanotrophic community structure. This shift was more pronounced after 20 years when considering afforestation of a bog (Bad à Cheo) compared to afforestation of grassland (Glensaugh). The improvement of the CH_4 sinks was within range of many temperate forests of the Northern Hemisphere (Smith *et al.*, 2000). Contrary to other international studies where afforestation led to a shift of type I methanotrophs towards type II methanotrophs, the data presented here indicate that at these sites in Scotland, afforestation induced a community change within type II methanotrophs only, more specifically *Methylocystaceae* cells were replaced by USCα microbes. The community structure change was correlated to the soil structure, in particular porosity and WFPS. Finally, the site (or original land use before afforestation) played a part in the type of methanotrophs present but not on the efficiency of sinking atmospheric CH_4. This suggests the community of methanotrophs established itself in soils under pine slower than the CH_4 sinks because high-affinity methanotrophs were found before CH_4 sinks occurred. This may be due to a slower improvement of forest soil moisture and aeration.

This study identified the strong relationship between land-use change (afforestation), enhancement of CH_4 sinks and methanotrophic community shift. This could have a consequence on the policies regarding land-use change as it shows the primordial role of the soil methanotrophs and how they can be affected by a land use and their effect on the net CH_4

flux. Moreover, this indicates that functional ecology and the understanding of the microbial processes involved in the life cycle of GHGs, such as CH_4, should not be overlooked by the models studying the effects of climate change.

Chapter 6 Experimental results (4)

Effect of invasion of heathland with birch trees on the mitigation of CH_4 and the shift in the methanotrophic diversity

1. Brief introduction

Although important decreases in CH_4 emissions in the United Kingdom were achieved in recent years (Sneddon *et al.*, 2010), it is also possible to increase atmospheric CH_4 sinks by changing land uses. Soils under hardwood trees such as birch are estimated to oxidise higher levels of atmospheric CH_4 compared to soils under coniferous species (Borken *et al.*, 2003; Menyailo *et al.*, 2010; Menyailo & Hungate, 2003). Heathland represents 12% of the broad habitat area in Scotland (McGowan *et al.*, 2002), whereas birch woodlands cover only 4% of Scotland. Therefore, improving the birch woodland cover from the conversion of heathland could help to further improve atmospheric CH_4 sinks.

Two sites were selected (Craggan and Tulchan) and constituted the same vegetation: a heathland (*Calluna*-dominated moorland), and its two adjacent woodlands, colonised with birch trees (*Betula pubescens*). The chronosequence in the forests was as such: 62- and 88-year-old stands at Craggan; and 55- and 65-year-old stands at Tulchan. For each site, the respective tree stands were referred to as “young birch” and “old birch” forests. The main difference resided in the heathland at Craggan being on a slope, whereas the moorland at Tulchan was on a flat terrain with a constant boggy state. The sampling procedure was

identical as in the Bad à Cheo and Glensaugh sites (see Chapter 5). Experimental work was similar to the analyses described in Chapter 5.

The objectives were to:

1) Examine changes in atmospheric CH_4 oxidation rates with changes in land use from heathland to birch trees.
2) Link soil methanotrophic composition with the observed changes in atmospheric CH_4 oxidation rates.

The hypothesis was that birch invasion should have a positive effect on the net CH_4 oxidation, which would be correlated with a shift in the structure of the methanotrophic community. Such changes in process and community structure should also be independent of the sites. Furthermore, there should be a transition state in the so-called “young birch” forests with net CH_4 fluxes and methanotrophic structure intermediate to the ones observed in the heathland and “old birch” forests.

2. Environmental variables

2.1. Chemical properties

The effects of tree invasion as well as seasonal variations on some chemical properties of the soils from the different habitats of the two sites are presented in **Table 6.1** and **Table 6.2**. The seasonal data were not significantly different for most soil properties and not consistent either between habitats or sites. At Craggan, total C and N and NH_4^+-N concentrations were significantly higher in summer in the young and old birch forests ($P<0.001$ for total C and NH_4^+-N; $P=0.012$ for total N). Tree invasion had a consistent effect on all the variables at both sites. There was a trend towards a small increase of soil pH in the birch forest soils ($P=0.013$ at Tulchan; only a small non-significant increase at Craggan). All the other soil properties (total C and N concentrations, C:N ratio, NH_4^+-N and NO_3^--N concentrations and moisture) significantly decreased with afforestation, without any effect of the age of the forest.

Table 6.1: Selected chemical soil properties from the Craggan site.

The data are means ± S.E.M. of each season for each habitat. Within each column, statistical differences between seasons within each habitat are indicated by different Roman letters (a, b, c), while Greek letters (α, β) indicate statistical differences between habitats, according to multiple pairwise comparison ($P<0.05$). N/A means that no data were available.

Craggan	Season	pH †		Total C † (g.kg^{-1})		Total N † (g.kg^{-1})		C:N ratio †		NH_4^+-N (mg.kg^{-1})		NO_3^--N (mg.kg^{-1})		Moisture (%)	
Moorland	Autumn	3.4± 0.05		73±6		2.9± 0.20		25±0		50±8		16±3	**a**	75±2	
	Spring	N/A		N/A		N/A		N/A		94±26		63±9	**b**	80±2	
	Summer	3.4 0.05	**a** **α**	78±8	**a** **α**	2.8± 0.26	**a** **α**	28±2	**a** **α**	109 ±26	**a** **α**	95±6	**c** **α**	79±1	**a** **α**
	Winter	N/A		N/A		N/A		N/A		79±2		110 ±8	**c**	82±0	
Young Birch	Autumn	3.3 0.04		35±6	**a**	1.6± 0.23	**a**	22±1		64±9	**a**	18±3		63±4	
	Spring	N/A		N/A		N/A		N/A		90±7	**ab**	29±2		62±4	
	Summer	3.5 0.04	**a** **α**	54±11	**b** **β**	2.5± 0.42	**b** **β**	23±1	**a** **β**	159 ±35	**b** **αβ**	41±9	**a** **β**	68±5	**a** **β**
	Winter	N/A		N/A		N/A		N/A		108 ±10	**ab**	50±10		73±2	
Old Birch	Autumn	3.5 0.01		52±3	**a**	2.4± 0.12	**a**	21±1		83±2	**a**	13±4		69±1	
	Spring	N/A		N/A		N/A		N/A		110 ±12	**a**	47±8		67±3	
	Summer	3.4 0.02	**a** **α**	75±1	**b** **α**	3.6± 0.36	**b** **α**	22±2	**a** **β**	191 ±26	**b** **β**	55±18	**a** **β**	70±2	**a** **β**
	Winter	N/A		N/A		N/A		N/A		81±12	**a**	34±8		72±2	

† Analysis performed on autumn and summer samples only.

Table 6.2: Selected chemical soil properties from the Tulchan site.

The data are means ± S.E.M. of each season for each habitat. Within each column, statistical differences between seasons within each habitat are indicated by different Roman letters (a, b, c, d), while Greek letters (α, β, γ) indicate statistical differences between habitats, according to multiple pairwise comparison (P<0.05). N/A means that no data were available.

Tulchan	Season	pH †		Total C † (g.kg^{-1})		Total N † (g.kg^{-1})		C:N ratio †		NH_4^+-N (mg.kg^{-1})		NO_3^--N (mg.kg^{-1})		Moisture (%)	
Moorland	Autumn	3.5± 0.05	**a α**	72±7	**a α**	2.9± 0.43	**a α**	25±1	**a α**	74±24	**a α**	41±11	**a**	79±3	**a α**
	Spring	N/A		N/A		N/A		N/A		43±7		109 ±11	**bc**	86±1	
	Summer	3.6± 0.02		87±1		3.4± 0.17		25±1		112 ±41		136 ±8	**c**	88±1	
	Winter	N/A		N/A		N/A		N/A		107 ±9		235 ±22	**d**	89±0	
Young Birch	Autumn	3.6± 0.06	**a β**	7.9± 1.12	**a β**	0.44± 0.06	**a β**	18±0	**a β**	36±11	**a β**	24±2	**a β**	39±2	**a β**
	Spring	N/A		N/A		N/A		N/A		30±6		26±8		36±2	
	Summer	3.7± 0.06		5.3± 0.85		0.27± 0.04		20±2		24±7		12±2		30±3	
	Winter	N/A		N/A		N/A		N/A		31±5		32±4		43±5	
Old Birch	Autumn	3.6± 0.03	**a αβ**	6.7± 1.23	**a β**	0.40± 0.04	**a β**	17±2	**a β**	41±10	**a β**	56±25	**a β**	37±2	**a β**
	Spring	N/A		N/A		N/A		N/A		23±3		24±4		51±5	
	Summer	3.6± 0.06		15±8		0.63± 0.30		22±2		52±11		23±9		43±8	
	Winter	N/A		N/A		N/A		N/A		38±13		27±5		37±6	

† Analysis performed on autumn and summer samples only.

2.2. Physical properties

Heathland colonisation by birch appeared to have had some effects on soil physical properties (**Table 6.3**). The soil aeration was significantly changed by afforestation due to increased bulk density (P=0.001 at Tulchan but a non-significant trend at Craggan), decreased porosity (P=0.037 at Craggan and P=0.012 at Tulchan) and increased WFPS (at Craggan only; P=0.014) in the soils under birch forest. The soil compaction was also modified at Tulchan, with birch invasion favouring the presence of small- and medium sized particles while decreasing the abundance of large-sized particles (P<0.001). A similar (non-significant) trend was observed at Craggan. Overall, the age of the forest had no effect, except for a transitional state in the young birch forest when considering the WFPS at Craggan and the porosity at both sites.

Table 6.3: Selected physical soil properties from Craggan and Tulchan.
The data are means ± S.E.M (n=3) of each habitat during the summer only. Within each column, results followed by different Greek letters (α, β) are statistically different for each habitat, according to multiple pairwise comparison (P<0.05).

Site	Habitat	Particle size (% of total)						Bulk density		Porosity		WFPS at field capacity (at 50 kPa)	
		0.02-2.00 µm		2-20 µm		20-2000 µm		($g.cm^{-3}$)		(%)		(%)	
Craggan	Moorland	1.8± 0.27	**α**	20 ±3	**α**	78 ±4	**α**	0.17± 0.03	**α**	102 ±1	**α**	60±3	**α**
	Young Birch	3.5± 0.42	**α**	36 ±3	**α**	60 ±3	**α**	0.18± 0.00	**α**	95 ±2	**αβ**	69±2	**αβ**
	Old Birch	2.9 0.69	**α**	33 ±8	**α**	64 ±8	**α**	0.23± 0.02	**α**	94±2	**β**	72±1	**β**
Tulchan	Moorland	0.55± 0.17	**α**	11 ±2	**α**	88 ±2	**α**	0.12± 0.01	**α**	96 ±3	**α**	64±3	**α**
	Young Birch	3.9± 0.05	**β**	28 ±3	**β**	68 ±3	**β**	0.46± 0.04	**β**	87 ±2	**αβ**	62±5	**α**
	Old Birch	3.1± 0.45	**β**	24 ±2	**β**	73 ±2	**β**	0.69± 0.10	**β**	75 ±5	**β**	62±9	**α**

3. Methane fluxes

The effect of tree invasion and seasonal variations on the net CH_4 flux of the soils from the different habitats and sites was investigated (**Figure 6.1**). Birch invasion of the heathland significantly increased the CH_4 sink in soils (P<0.001), with no influence of the age of the birch forest. Seasonal variations did not influence net CH_4 flux at Craggan (P=0.092). However, at Tulchan, significantly higher net CH_4 fluxes were observed in the moorland and higher CH_4 sinks in the young birch forest (P<0.001) during summer.

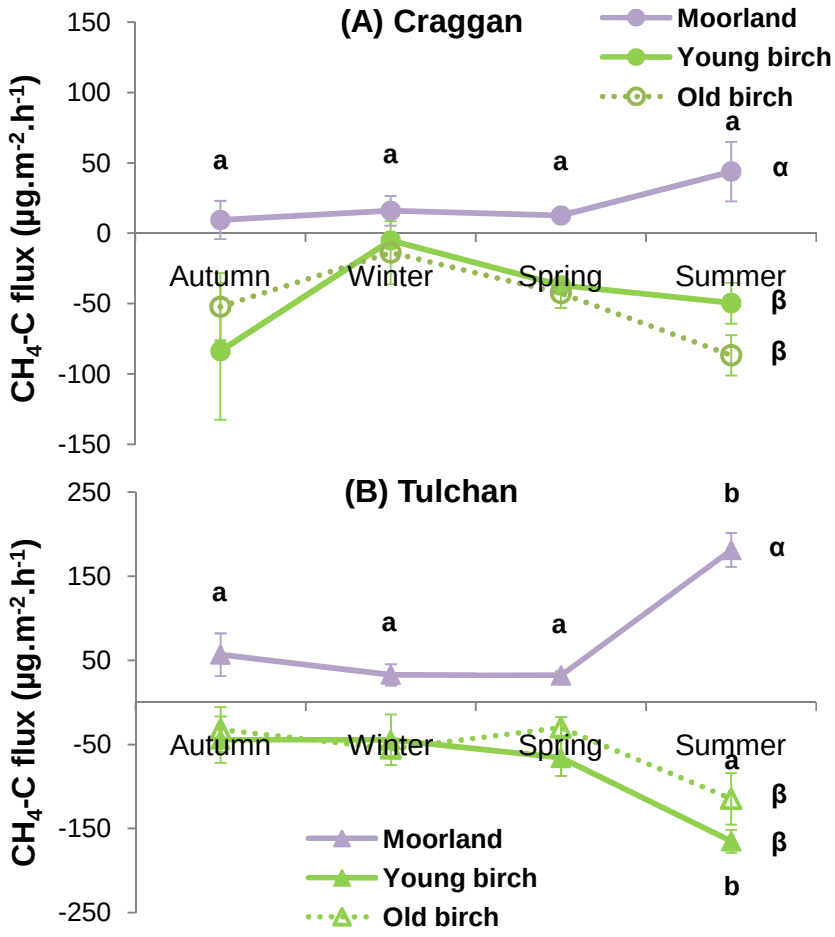

Figure 6.1: Net CH_4-C fluxes from soils from Craggan (A) and Tulchan (B).
A positive value means that a production of CH_4 occurs, whereas a negative flux denotes a sink of CH_4. The data are means (error bars are S.E.M.) of each season for each habitat from the closed-chamber experiment. For each site, statistical differences between seasons within each habitat are indicated by different Roman letters (a, b), while Greek letters (α, β) indicate statistical differences between habitats, according to multiple pairwise comparison (P<0.05).

4. Methanotrophic community structure in soils

4.1. Characterisation by molecular methods

The detection of the methanotrophs in soils was described in Chapter 5, section 4.

4.1.1. T-RFLP analysis of the *pmoA* genes

The T-RFLP profiles obtained following digestion of the *pmoA* genes with the restriction enzymes *Hha*I and *Msp*I were processed through the *T-REX* software. T-RFs which relative abundance was less than 3% were removed from the analysis. At Craggan, six *Hha*I and five *Msp*I unique T-RFs were identified, representing most of the total T-RF relative abundance (>86% and >84%, respectively). At Tulchan, six *Hha*I and six *Msp*I unique T-RFs were identified, representing >88% of the total T-RF relative abundance. Nested ANOVA was applied in order to investigate the effect of seasonal variations, within each habitat, on individual T-RFs (**Appendix Table 0.13** to **Appendix Table 0.16**). Seasons had no effect on the T-RFs at either sites (**Appendix Figure 0.5** and **Appendix Figure 0.6**), as confirmed later by the AMMI analyses (see below). However, it should be noted that the T-RFs *Hha*-81 and *Msp*-242 were significantly more abundant in the old birch forest at Tulchan during spring. But this was based on the analysis of only one sample. Therefore, the annual average of the T-RFLP profiles of methanotrophs was also presented (**Figure 6.2**).

A dominant and significant trend was observed at both sites (**Figure 6.2**). The establishment of forests increased the relative abundance of the T-RFs *Hha*-32 and *Msp*-25 ($P<0.001$), while it decreased for the T-RFs *Hha*-81 ($P=0.006$ at Craggan and $P<0.001$ at Tulchan), *Msp*-242 (non-significant trend at Craggan but $P<0.001$ at Tulchan), *Hha*-128 ($P=0.038$ at Craggan and $P=0.001$ at Tulchan), and *Msp*-451 ($P=0.001$ at Craggan and a non-significant trend at Tulchan), as well as *Hha*-50 ($P=0.007$, present at Craggan only). Also, the relative abundance of T-RF *Msp*-499 was always the lowest in the soils under moorland and other T-

RFs were characteristics of the heathland: *Hha*-191, *Msp*-314, *Hha*-73 (only at Craggan) and *Msp*-444 (only at Tulchan). However, these averaged 3-8% of the total T-RF abundance. Similarly, the T-RFs *Hha*-247 and *Hha*-359 were only found in the soils under old birch forest at Tulchan.

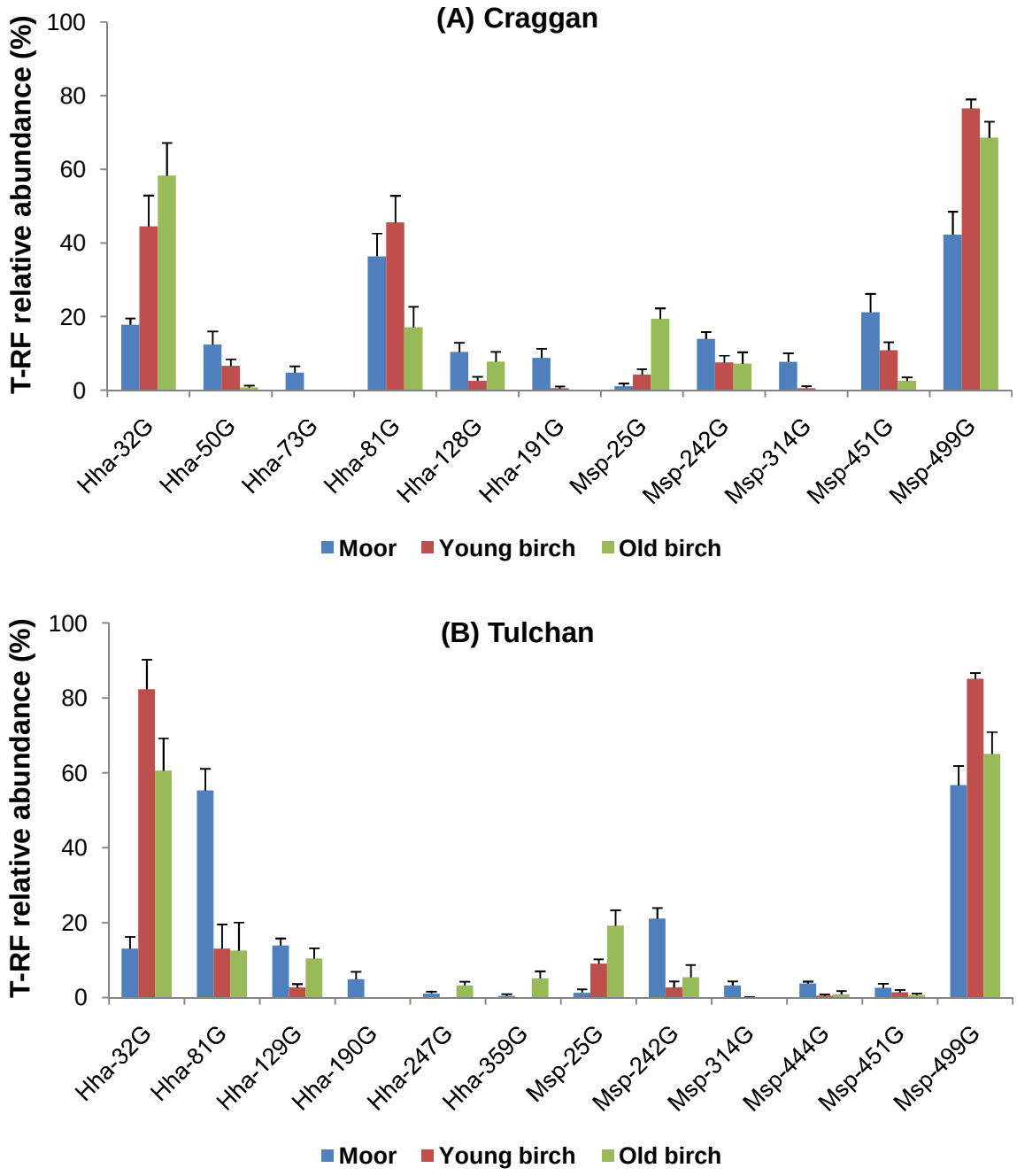

Figure 6.2: T-RFLP profiles of methanotrophs (*pmoA*) at Craggan (A) and Tulchan (B).
The total relative abundance (annual average ± S.E.M.) of the T-RFs (n=16) generated by *Hha*I or *Msp*I is accounted for separately. The letter G (green) represents the colour of the dye.

T-RFs related to type II methanotrophs were present in high abundance in soils from Craggan and Tulchan. They were the same as the methanotrophs detected at Bad a Cheo and Glensaugh (see Chapter 5, Table 5.5). Although the relative abundance of the T-RFs produced after digestion of the PCR products with *Hha*I did not match those of their *Msp*I-digested counterparts, birch invasion had a strong effect on specific OTUs. Indeed, at both sites, microorganisms distantly related to *Methylocystis* sp. and *Methylosinus* sp. (T-RFs *Hha*-81 and *Msp*-242) were dominant in soils under moorland whereas bacteria related to *Methylocapsa* sp./USCα clones (T-RFs *Hha*-32 and *Msp*-25) were dominant in soils under birch forest (**Figure 6.2**). This was also confirmed by the microarray data (see section 4.1.3).

Data were further analysed to understand the influence of different environmental variables on individual T-RFs. First, DCA gave a gradient length of 1.663 (Craggan) and 1.633 (Tulchan) on the first axis, which suggested that RDA was suitable for the analysis of relationships of T-RFs with environmental variables (data not shown). At Craggan, only soil porosity was found to significantly influence the T-RFs (P=0.020) by having a positive impact on the T-RFs related to *Methylocystaceae* (T-RFs *Hha*-81and *Msp*-242) and T-RF *Msp*-451; and a negative impact on the T-RFs related to *Methylocapsa* sp. (T-RFs *Hha*-32 and *Msp*-25). At Tulchan, soil moisture and the age of the birch forest significantly influenced the T-RFs (P=0.010). Soil moisture had a positive impact on the T-RFs related to *Methylocystis* /*Methylosinus* spp. (*Hha*-81 and *Msp*-242) as well as on T-RFs *Msp*-444 and *Msp*-451; while it had a negative impact on the T-RFs related to *Methylocapsa* sp. (*Hha*-32 and *Msp*-25).

The AMMI analysis of the T-RFs generated from the digestion with the restriction enzymes *Hha*I and *Msp*I, using habitats and seasons as environments, found a difference in the methanotrophic community structure. Indeed, the interaction effect was ~37% (at Craggan) and ~32% (at Tulchan) of the total variation, which is indicative of an interaction between the pattern of the T-RFs and their respective environments (or treatment, *i.e.* habitat and/or season). This was confirmed by MANOVA on the four IPC scores of the AMMI model which gave an overall significant effect ($P<0.001$) of land-use change at both sites (**Table 6.4**).

The differences can be seen on the graphical representation of the IPC scores of the AMMI model (**Figure 6.3**). Tree invasion and the age of the birch forest appeared to have had a significant effect on the community structure, and resulted in the detection of a different methanotrophic community structure in each habitat. Furthermore, there was no seasonal effect on the methanotrophic structure, except in spring in the heathland at Craggan (IPC 4, $P=0.007$) although it represented only 7% of the total variation detected. It can be noted that, in Figure 6.3B, the score for the old birch forest in spring was very different due to the fact that only one sample was available.

Table 6.4: Effects of birch invasion and seasonal changes on the methanotrophic community at Craggan and Tulchan (digestion of *pmoA* with *Hha*I and *Msp*I).

The data are *P* values corresponding to the first four IPC scores of the AMMI analyses, and were obtained by nested ANOVA and MANOVA. Within each column, statistical differences between seasons within each habitat are indicated by different Roman letters (a, b), while Greek letters (α, β) indicate statistical differences between habitats, according to multiple pairwise comparison ($P<0.05$).

		IPC 1	IPC 2	IPC 3	IPC 4	MANOVA
Craggan	% variation	47.9	24.5	10.8	7.2	
	Habitat	**<0.001**	**0.001**	0.063	0.089	**<0.001**
	Habitat/Season	0.116	0.334	0.852	**0.007**	**0.019**
Moor	Autumn				**a**	
	Spring	**a α**	**a α**	**a α**	**b α**	
	Summer				**ab**	
	Winter				**a**	
Young Birch	Autumn					
	Spring	**a α**	**a β**	**a α**	**a α**	
	Summer					
	Winter					
Old Birch	Autumn					
	Spring	**a β**	**a β**	**a α**	**a α**	
	Summer					
	Winter					
		IPC 1	**IPC 2**	**IPC 3**	**IPC 4**	**MANOVA**
Tulchan	% variation	75.7	11.4	6.8	2.2	
	Habitat	**<0.001**	0.060	**0.037**	**0.026**	**<0.001**
	Habitat/Season	0.053	0.341	0.411	0.389	0.233
Moor	Autumn					
	Spring	**a α**	**a α**	**a αβ**	**a αβ**	
	Summer					
	Winter					
Young Birch	Autumn					
	Spring	**a β**	**a α**	**a α**	**a α**	
	Summer					
	Winter					
Old Birch	Autumn					
	Spring	**a β**	**a α**	**a β**	**a β**	
	Summer					
	Winter					

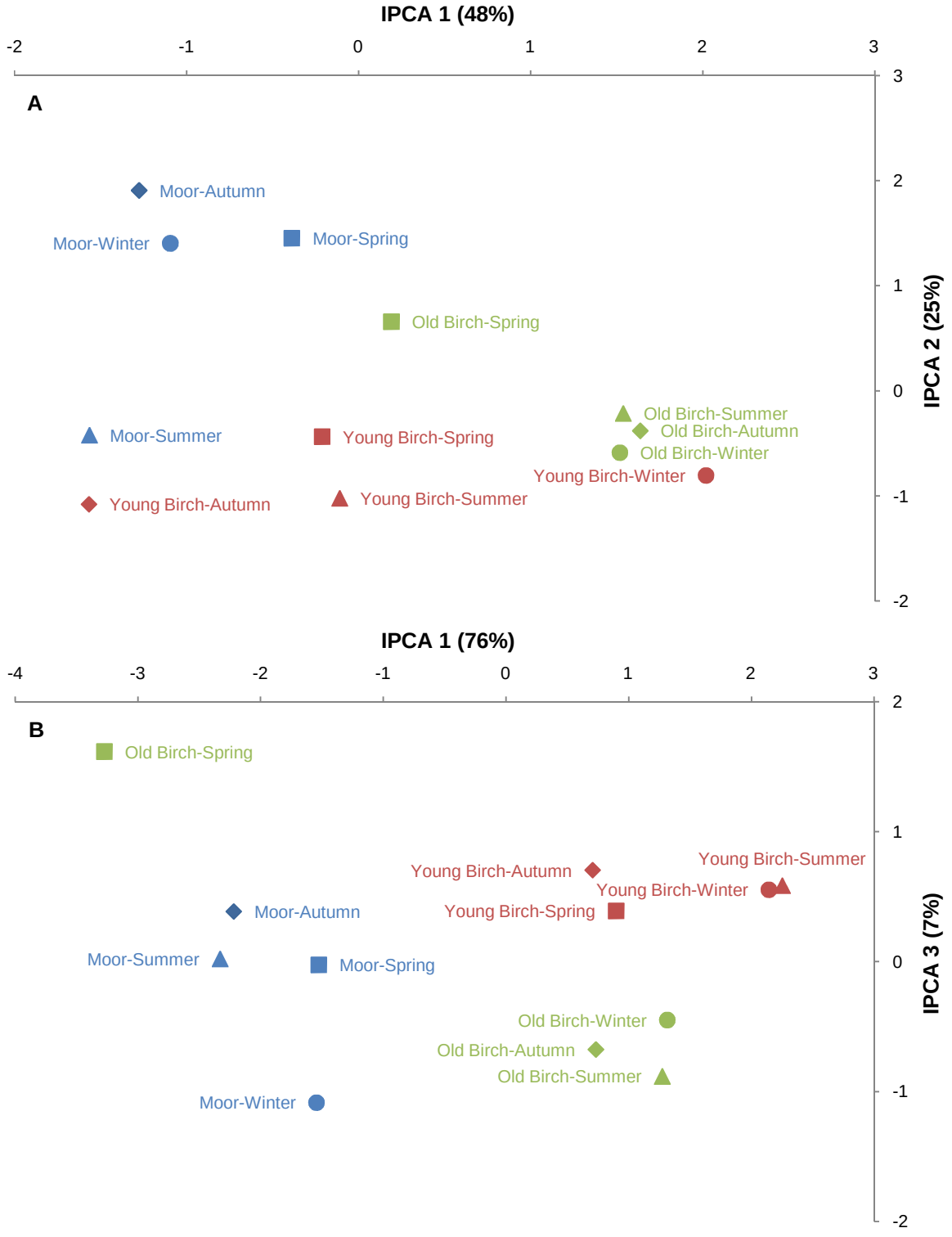

Figure 6.3: Methanotrophic community structure at Craggan (A) and Tulchan (B) after analysis of the T-RFLP profiles (digestion of *pmoA* with *Hha*I and *Msp*I) with the AMMI model.

The data points within each habitat represent the averages over replicates (n=4) of the IPC scores of each season, except for the spring season of the old birch forest at Tulchan for which only one sample was available.

4.1.2. Analysis of the 16S rRNA genes of type II and type I methanotrophs

The AMMI analysis, using habitats and seasons as environments (replicates were averaged), found a small difference in the community structure of type II and type I methanotrophs. The interaction effects were only ~7% and ~6% at Craggan for type II and type I, respectively. They were ~12% and ~8% at Tulchan (type II and type I, respectively). This means there was some interaction of the T-RFs with their environment (or treatment). This was confirmed by the MANOVAs on the four IPC scores of the AMMI analyses which showed an overall significant effect on type II and type I methanotrophs at both sites (IPCs 1 and 2, P=0.001) (**Table 6.5**). Some seasonal effects were also detected. These differences were observed on the graphical representation of the IPC scores of the AMMI models (**Figure 6.4**).

Like with the *pmoA* genes, afforestation and the age of the birch forest had a significant effect on the community structure (P<0.001), and resulted in the detection of a different methanotrophic community structure in each habitat (**Figure 6.4**). There was also an inconsistent seasonal effect between habitats and sites with type II microbial communities being similar in spring-summer under young birch at both sites; and type I methanotrophs being similar in spring-summer under heath at Craggan and under old birch at Tulchan (**Appendix Table 0.17** and **Appendix Table 0.18**).

Table 6.5: Effects of birch invasion and seasonal changes on the methanotrophic community at Craggan and Tulchan (16S rRNA of type II methanotrophs – digestion with *Mbo*I and *Msp*I; 16S rRNA of type I methanotrophs – digestion with *Hha*I and *Msp*I).

The data are *P* values corresponding to the first four IPC scores of the AMMI analyses. A more detailed version of this table, including multiple pairwise comparisons, can be found in **Appendix Table 0.17** and **Appendix Table 0.18**.

Type II		**IPC 1**	**IPC 2**	**IPC 3**	**IPC 4**	**MANOVA**
Craggan	% variation	56.0	25.3	7.8	4.5	
	Habitat	**<0.001**	**<0.001**	**0.004**	0.162	**<0.001**
	Habitat/Season	**<0.001**	0.066	0.051	**0.046**	**<0.001**
Tulchan	% variation	57.0	20.9	8.7	5.9	
	Habitat	**<0.001**	**0.002**	0.526	**0.039**	**<0.001**
	Habitat/Season	**0.001**	0.115	**0.032**	0.078	**<0.001**

Type I		**IPC 1**	**IPC 2**	**IPC 3**	**IPC 4**	**MANOVA**
Craggan	% variation	35.7	18.7	11.0	9.9	
	Habitat	**<0.001**	**<0.001**	0.427	**<0.001**	**<0.001**
	Habitat/Season	**0.010**	0.866	**<0.001**	0.430	**0.006**
Tulchan	% variation	44.6	22.0	9.3	7.7	
	Habitat	**<0.001**	**0.001**	**0.009**	**0.003**	**<0.001**
	Habitat/Season	**0.008**	0.057	0.202	0.304	**<0.001**

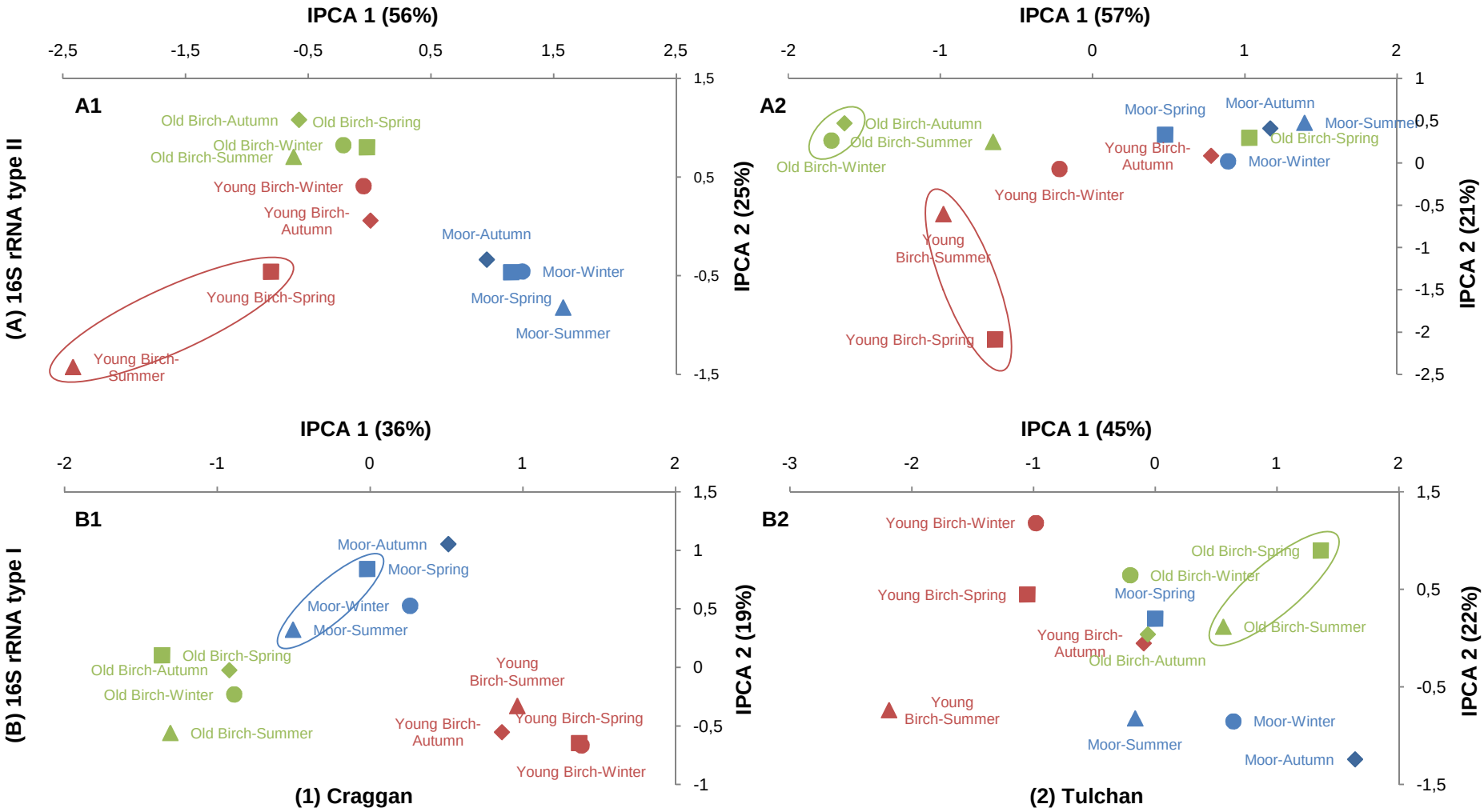

Figure 6.4: Type II (A) and type I (B) methanotrophic community structure at Craggan (1) and Tulchan (2) after analysis of the T-RFLP profiles (16S rRNA of type II methanotrophs – digestion with *Mbo*I and *Msp*I; 16S rRNA of type I methanotrophs – digestion with *Hha*I and *Msp*I) with the AMMI model.

The data points within each habitat represent the averages over replicates (n=4) of the IPC scores of each season. The circles show seasons that were statistically different within each habitat.

4.1.3. Diagnostic *pmoA* microarray

Type I methanotrophs were not detected at either site (data not shown). Also, neither nitrifiers nor any *Methylocapsa acidiphila* were found at either sites (**Figure 6.5**).

Similarly, no novel *pmoA* genes of type II methanotrophs were present. The probes detected the presence of the exact same type II methanotrophs at both sites (**Table 6.6**). Tree invasion and the age of the birch forest also influenced their relative abundance in a similar fashion: in the soils under moorland at Tulchan, the type II methanotrophic community consisted mainly of *Methylocystis*/*Methylosinus* spp. (probes Mcy413, Mcy459, Mcy522 and Msi232; P=0.001), peat-related type II methanotrophs (probe Peat264; P=0.040) and watershed 1 clade (probe Wsh1-566; P=0.014) organisms (**Table 6.6**). However, these species were not exclusively detected in the moorland soils at Craggan. Conversely, type II methanotrophs related to the RA14 cluster (probes RA14-299, RA14-594 and RA14-591) were never detected in the soils under the heathland at both sites or under the young birch forest at Craggan but they were present in the old birch forest soils at Craggan (P<0.001) (**Figure 6.5**). In contrast, the probes of the RA14 cluster were detected in the soils under both young and old birch forests at Tulchan (P<0.045) (**Table 6.6**) but the age of the birch forest had no significant influence on their abundance. PCA and subsequent MANOVA on the first five PCs indicated that birch invasion changed the methanotrophic community in the soils at Craggan (P=0.002) and Tulchan (P<0.001) (**Table 6.7**). However, it was only detected on the third PC at Craggan (P<0.001), which represented ~3% of the total variation, whereas the first PC (~90% of total variation) on the Tulchan data was sufficient to detect an effect of birch invasion (P=0.011).

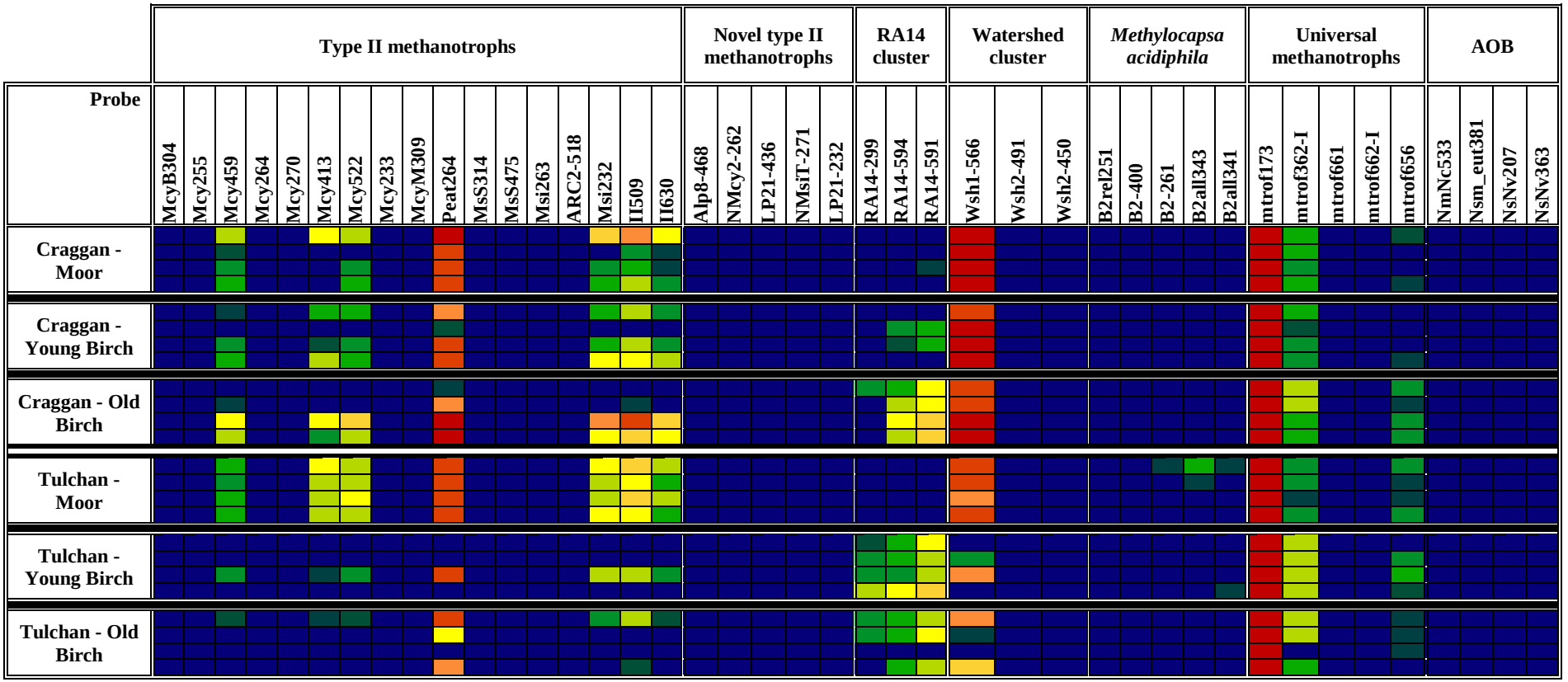

Figure 6.5: Type II methanotrophs and related organisms community analysis at Craggan and Tulchan using the *pmoA* microarray (n=4).

Within each habitat, each row represents a replicate. The results were first normalised to positive control probe mtrof173, then to the reference values determined individually for each probe (Bodrossy *et al.*, 2003). Colour coding is as such: red colour indicates maximum achievable signal for an individual probe, while blue colour indicates that no detectable PCR product hybridised to that probe. The colour gradient between blue and red reflects the proportion of hybridisation.

Table 6.6: Effects of birch invasion on the methanotrophic community at Craggan and Tulchan (*pmoA* microarray).

The data presented are some of the *pmoA* probes that showed higher levels of hybridisation, and their statistical difference (Greek letters [α, β]) between each habitat, according to multiple pairwise comparison ($P<0.05$).

Site	Habitat	Probe								
		Mcy522	**Mcy459**	**Mcy413**	**Msi232**	**Peat264**	**RA14-594**	**RA14-591**	**RA14-299**	**Wsh1-566**
Craggan	Moor	α	α	α	α	α	**α**	**α**	**α**	α
	Young birch	α	α	α	α	α	**α**	**α**	**αβ**	α
	Old birch	α	α	α	α	α	**β**	**β**	**β**	α
Tulchan	Moor	**α**	**α**	**α**	**α**	**α**	**α**	**α**	**α**	**α**
	Young birch	**β**	**β**	**β**	**β**	**β**	**β**	**β**	**β**	**β**
	Old birch	**β**	**β**	**β**	**β**	**αβ**	**αβ**	**αβ**	**αβ**	**β**

Table 6.7: Effects of birch invasion on the methanotrophic community at Craggan and Tulchan (PCA from the *pmoA* microarray).

The data are *P* values corresponding to the first five PC scores of the probe hybridisation intensities, and were obtained by MANOVA. Within each column, results followed by different Greek letters (α, β) are statistically different for each habitat, according to multiple pairwise comparison ($P<0.05$).

		PC 1	PC 2	PC 3	PC 4	PC 5	MANOVA
Site/Habitat	**% variation**	90.4	6.09	2.62	0.66	0.15	
	P	0.601	0.559	**<0.001**	0.125	0.758	**0.002**
Craggan	Moor	α	α	**α**	α	α	
	Young birch	α	α	**α**	α	α	
	Old birch	α	α	**β**	α	α	
Site/Habitat	**% variation**	89.71	5.27	3.65	1.04	0.21	
	P	**0.011**	0.501	0.482	0.064	0.762	**<0.001**
Tulchan	Moor	**α**	α	α	α	α	
	Young birch	**β**	α	α	α	α	
	Old birch	**β**	α	α	α	α	

4.2. Linking community structure with function

This was first investigated by simple linear regression analysis (**Figure 6.6**) between the *pmoA* IPCA scores of each habitat from **section 4.1.1** and the corresponding net CH_4 flux values from **section 3**. At both sites, birch invasion and change in net CH_4 flux were significantly related to a shift in the community structure ($P=0.027$ at Craggan; $P=0.015$ at Tulchan). However, the relationship was stronger at Tulchan ($R^2=0.5444$) when considering the first dimension, which accounted for 76% of the variation (**Figure 6.6B**). At Craggan, the correlation between CH_4 and community structure was significant only on the second dimension ($R^2=0.2426$), which accounted for only 25% of the variation (**Figure 6.6A**). The relationship was still significant ($P=0.012$) using the IPCA 1 (48%) but the R^2 was 0.1113 (**Appendix Figure 0.7**).

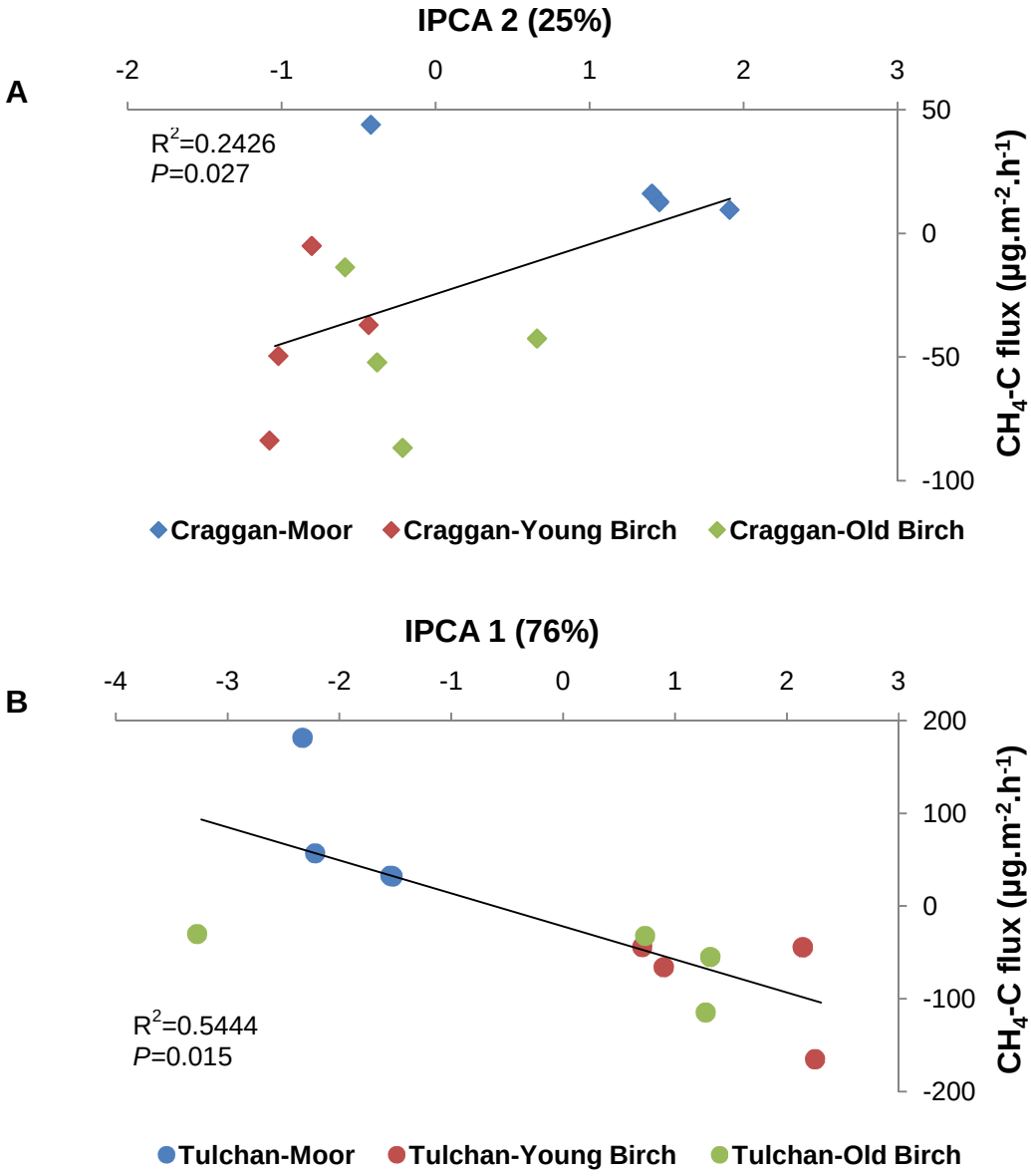

Figure 6.6: Relationship between net CH_4 flux and methanotrophic community structure at Craggan (A) and Tuchan (B).

The data points represent the IPCA scores displayed in **Figure 6.3** and the net CH_4 fluxes from **Figure 6.1**.

From the PLFA-SIP analysis, seasonal averages of the enriched PLFA content (% of ^{13}C-incorporation, **Figure 6.7**) were used for cluster analysis as described in Chapter 5. **Figure 6.8** shows that the active methanotrophs in the soils under all habitats were distant relatives (<85% similarity) of *Methylosinus sporium* and the *Beijerinckiaceae* family (containing *Methylocella* sp. and *Methylocapsa* sp.) due to a high incorporation of ^{13}C in PLFA 18:1ω7 (Figure 6.7). Heathland colonisation by birch impacted on the active methanotrophic

community in a similar fashion as observed with the *pmoA* microarray: at Craggan, the community structure was comparable in the soils under the moorland and young birch forest, while it was different in the soil under the old birch forest. In contrast, at Tulchan, the community structure in the moorland soil was different from the one in the young and old birch forest soils (**Figure 6.8**).

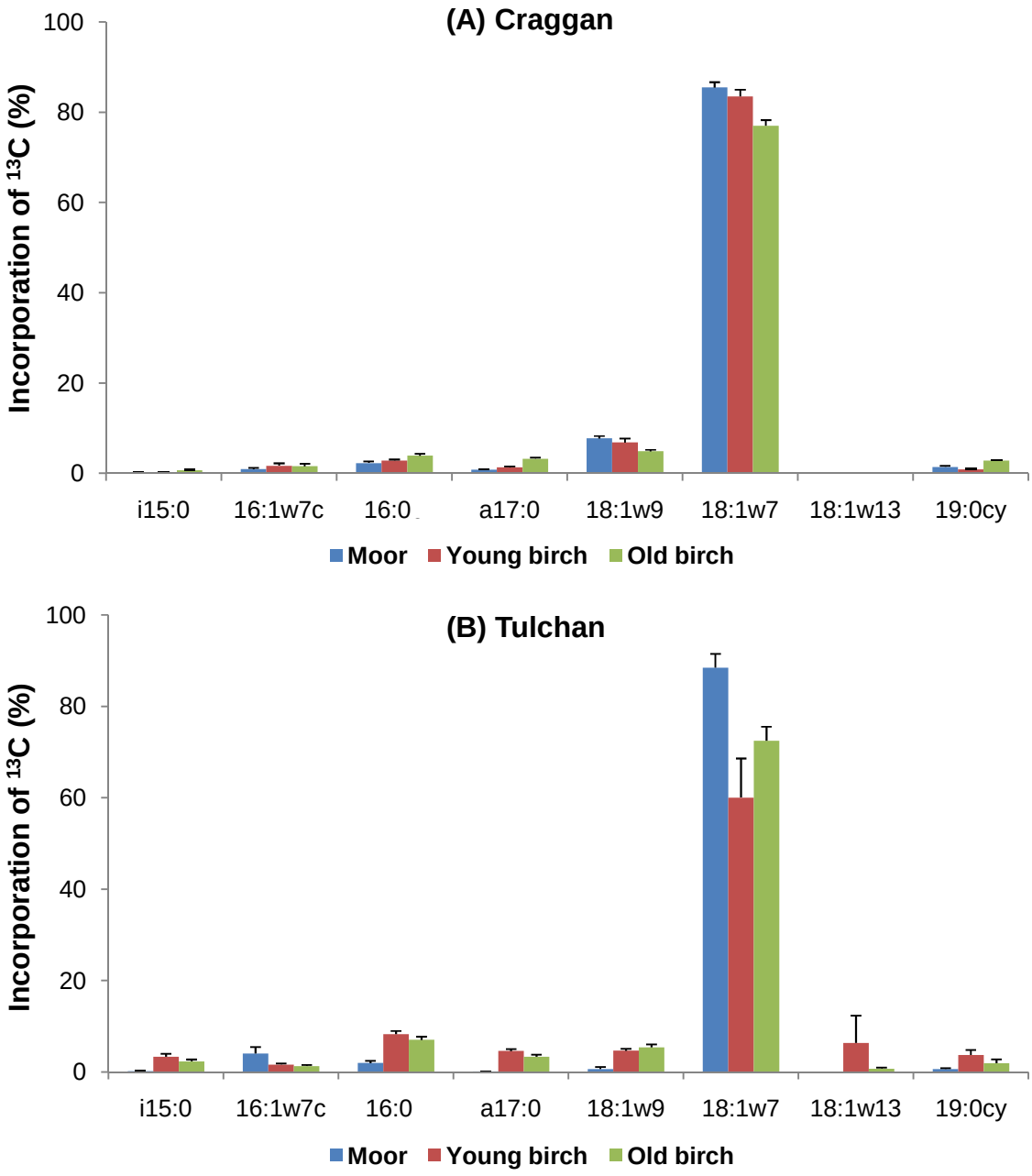

Figure 6.7: Percentage of incorporation of ^{13}C within the PLFAs after incubation with ~100 ppm of ^{13}C-CH_4 at Craggan (A) and Tulchan (B).

The data are seasonal average ± S.E.M. (n=8) of the enriched PLFA content.

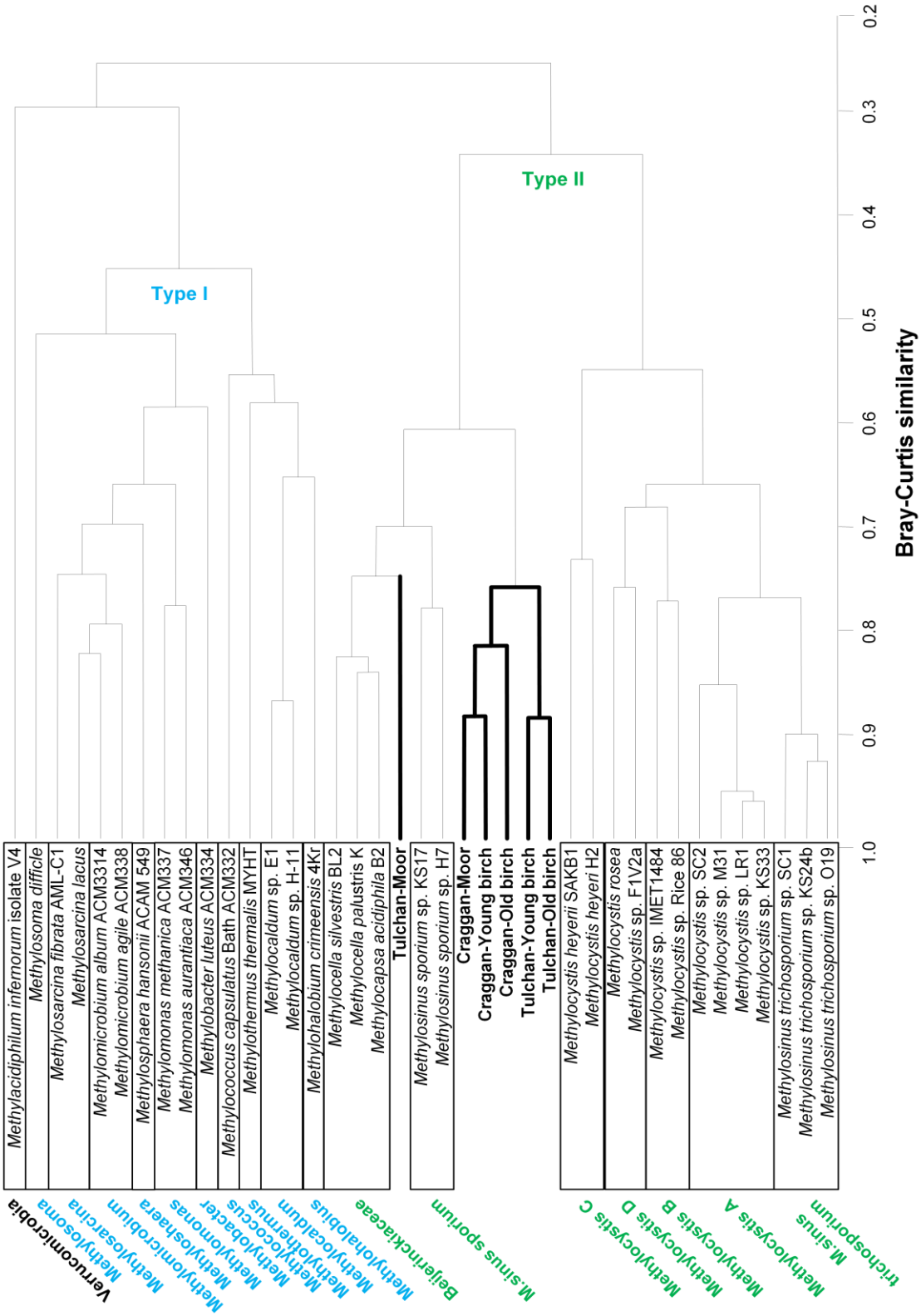

Figure 6.8: Cluster analysis of the PLFA profiles (based of % of ^{13}C-incorporation) of methanotrophs in the enriched soils (~100 ppm ^{13}C-CH_4) from Craggan and Tulchan (n=4).

The dendrogram was built using data from this study, combined with data from the literature (Bodelier *et al.*, 2009). A Bray-Curtis similarity matrix was used, from the square root-transformation of the PLFA data (see **Figure 6.7**), to perform a group average linking cluster analysis with GenStat® software.

5. Discussion

5.1. Effect of seasonal changes and birch invasion on abiotic properties

Contrary to the pine-afforested sites (Chapter 5), seasonal effects on soil chemical properties were more consistent. In fact, they were consistently not significant except in the birch forests at Craggan where total C and N and NH_4^+-N concentrations were increased in summer (Table 6.1 and Table 6.2), probably due to a higher activity of plants and N_2-fixing bacteria. In particular, total C increased greatly (~50%) between autumn (2008) and summer (2009). Such a large and fast difference was surprising and may be due to experimental variation. Like most of the other measurements, a seasonal replication would have been better, as well as replication of autumn sampling in 2009 in order to look for year-to-year consistency.

In contrast, colonisation by birch trees had important consequences on all the physico-chemical properties investigated and at both sites. Similar variations (*e.g.* increased pH and bulk density, decreased C:N ratio, moisture and porosity in the birch forests) were observed in other studies using the same sites (Keith *et al.*, 2006; Mitchell *et al.*, 2007; 2010; Nielsen *et al.*, 2008). The effect of the age of the forest was also congruent. Surprisingly, there was a 90% loss of C and N in the birch forests at Tulchan. A previous study at the same site detected a 50% decrease of these variables in the soil under birch woodland, when sampling at a depth of 5 cm (Dr U. Nielsen, private communication). I sampled soils to a depth of 10 cm where the mineral nature of the soil was obvious, in particular due to the presence of many stones. Considering this and the fact that the organic horizon in the birch forests at Tulchan was very shallow, one could assume an even lower C and N content in the 10 cm-deep profile compared to the 5-cm horizon. A similar but not as pronounced discrepancy in

total C and N concentration in the birch forests at Craggan was compared to a previous report by Mitchell *et al.* (2007), and could also be explained by a difference in the sampling depth. Thus, this would indicate that birch invasion of heathland induces large losses of C storage. This is confirmed by the work of Nielsen *et al.* (2010) who measured an important loss of C from 12 sites (heathland-birch woodland) around Scotland. The lower total C concentration was still observed in the old birch stands, which would suggest that soil C stocks under birch forests as old as 88 years never recover from soil disturbance.

It could be argued that birch invaded heathland because soil characteristics had started to change. However, Hester *et al.* (1991) thoroughly analysed the succession from heather moorland to birch woodland on the same Craggan and Tulchan sites. A natural chronosequence of birch invasion was available with ages of birch forests of *ca.* 17, 28, 36 and 63 years (at the time of the study). Vegetation (and soil properties) progressively changed with heather being replaced by bilberry as the birch canopy closes, and later, the establishment of grass as the woodland matures and the canopy opens out (Hester *et al.*, 1991). Therefore, it can be assumed that the changes observed (soil characteristics, as well as CH_4 fluxes and methanotrophic community structure – see below) were due to the establishment of birch woodland rather than the possibility that birch trees invaded heather due to more favourable soil properties.

5.2. Effect of afforestation on the net CH_4 fluxes

In line with the results of Chapter 5, birch invasion had a strong effect in inverting the net CH_4 fluxes so that birch forest soils became strong CH_4 sinks (Figure 6.1). This is in agreement with another study (Kruse & Iversen, 1995) investigating the invasion of a heathland with oak trees, which are hardwood trees like birch trees. The CH_4 oxidation rates observed were also in range with those in the oak woodland. Surprisingly, the improvement

in CH_4 sink by soils under birch forests was correlated to a lower soil aeration (increased bulk density, decreased porosity) and contrastingly to a lower soil compaction (decreased proportion of large-sized particles, which is usually associated to increased porosity) (Table 6.3). This lack of correlation between soil aeration and structure is unexpected since both help with gas diffusivity and therefore with net CH_4 flux, as discussed in Chapter 5. Finally, no improvement of CH_4 sinks was observed after 62 years as oxidation rates were similar at both sites and compared to the old birch forest at Craggan which was 88-years old. This indicates a better recovery time of disturbed soils compared to the 100-year estimate by Smith et al. (2000).

5.3. Effect of seasonal changes on the methanotrophic community structure

Little seasonal effect was observed, especially with the *pmoA*-based T-RFLP. Again, T-RFLP analysis of the 16S rRNA genes detected shifts in the methanotrophic community but a lack of consistency was apparent. As an example, the type II community structure was statistically different in summer and spring in the soil under young birch forest at Tulchan (Figure 6.4A2), which could be correlated to the significant increase in CH_4 oxidation rates observed in summer but not in spring (Figure 6.1). A similar shift was also identified at Craggan (Figure 6.4A1) though no seasonal effect was concomitantly observed on CH_4 sinks. The same could be applied to the type I community shift at Craggan under moorland in summer and the lack of significant difference in net CH_4 flux. Yet, this might indicate that changes in CH_4 oxidation rates during seasonal succession could be driven by a shift in the community of the methanotrophic bacteria.

5.4. Effect of afforestation on the methanotrophic community structure

As in Chapter 5, the different analytical techniques applied gave fairly consistent results. No type I methanotrophs were detected in the soils either by *pmoA*-based T-RFLP analysis or with the *pmoA* diagnostic microarray. Nevertheless, the T-RFLP analysis of 16S rRNA genes indicated the presence of type I methanotrophs and that afforestation change their structure (Figure 6.4B1 and B2) (see Chapter 5, section 5.4). Microbes related to type II methanotrophs – namely the *Methylocystaceae* family, RA14 group (USCα) and Watershed 1 cluster – were found to be dominant with both *pmoA*-based T-RFLP and microarray analyses (Figure 6.3 and Figure 6.5). They were the same species detected in Chapter 5 (see section 5.4).

Interestingly, the effect of birch invasion on the community structure was evident at Craggan and Tulchan with both AMMI and microarray analyses. However, the *pmoA* microarray was less efficient in detecting a community shift at Craggan. Firstly, a significant difference was only observed on the third dimension of the PCA, which represented 3% of the total variation (Table 6.7), whereas AMMI analysis of the *pmoA* gene detected a shift on the first two dimensions which captured a cumulated ~73% (Table 6.4). Secondly, the *pmoA* microarray did not detect a difference between the heathland and young birch forest while the AMMI analysis of the two genes (16S rRNA and *pmoA*) identified a dissimilar community in the soils under both birch stands. Finally, both *pmoA*-based techniques showed an increase in the abundance of RA14 cluster members in the birch forests but the *pmoA* microarray failed to detect a change in *Methylocystaceae* cells while *pmoA*-based T-RFLP identified a decrease in these methanotrophs in the birch stands (Figure 6.2 and Table 6.6). A similar trend in community shifts was observed at Tulchan except that the results of both techniques were congruent. PLFA-SIP data were matching the *pmoA* microarray, but both approaches have a lower resolution compared to T-RFLP. Nonetheless, all three techniques confirmed the

presence of active bacteria oxidising CH_4 at atmospheric levels. Overall, these findings on the effect of birch invasion were in agreement with the community shifts reported in Chapter 5.

5.5. Effect of community structure on net methane flux

As in Chapter 5, **Table 6.5** unequivocally identifies a strong relationship between land-use changes, change in CH_4 oxidation rates and shift in methanotrophic community structure. It was also evident that the age of the forest did not affect the CH_4 sinks and community structure since no transitional state was observed in the young birch forests. In contrast to the findings of Chapter5, this suggests that net CH_4 flux rates and methanotrophs recovered concomitantly from soil disturbance within the time-frame (55 years) of the study sites. Changes may also have been due to a modification in the methanogenic activity.

6. Conclusions

The present study confirmed and strengthened some of the findings from Chapter 4 and Chapter 5. The conversion of heathland to birch forests greatly improved the atmospheric CH_4 sinks and was associated with a shift in the soil methanotrophic community structure. The increase in CH_4 oxidation rates was fast in comparison to the 100-year estimate from Smith *et al.* (2000) and appeared to be stable 55 years after invasion of the moorland with birch started. As with afforestation with pine, a shift within the type II methanotrophic community was detected and consisted of the replacement of members of the *Methylocystaceae* family by bacteria of the USCα cluster. This seems to be uniquely associated to Scottish soils. The close association of change in net CH_4 flux with shift in the methanotrophic structure was unambiguously identified and was dependent on land-use change rather than being site-dependant. Changes in methanogenesis may have occurred in parallel but this was not investigated in this study.

However, a significant disturbance in soil C storage was identified which suggests than heather moorland colonisation with birch trees might not be recommended, despite the improvements in CH_4 oxidation rates induced by this land-use change.

Chapter 7 General discussion

1. Afforestation and reforestation enhance the atmospheric CH_4 sink in temperate forest soils

The study sites explored were situated in temperate regions of the Northern (Scotland) and Southern (New Zealand) Hemispheres. The land uses investigated were various and included non-forested (pasture, bog, heathland) and forested (pinewood, birchwood, shrubland and native forest) habitats over different types of soils (volcanic ash, peat, mineral). All sites showed a drastic improvement in the CH_4 consumption rates apparently induced by forestation, which is a phenomenon observed in many other studies (Dobbie & Smith, 2010; Dörr *et al.*, 2010; MacDonald *et al.*, 1996; Singh *et al.*, 2007; Singh *et al.*, 2009). Smith *et al.* (2000) estimated that 100 years should be needed for Northern European forest soils to revert to original CH_4 oxidation rates after soil disturbance. In contrast, New Zealand forests displayed higher rates of CH_4 consumption (Price *et al.*, 2003; Singh & Tate, 2007) and were shown to potentially recover twice as fast (<47 years – see Chapter 4). This may have been caused by the relatively lower anthropogenic impact and presence in New Zealand. The sites investigated in Scotland also showed reasonably fast recovery time of net CH_4 fluxes since they seemed to have reached stable CH_4 oxidation rates after 20 years in the pine-afforested sites (Bad à Cheo, Glensaugh – see Chapter 5) and 55 years in the birch-colonised sites (Craggan, Tulchan – see Chapter 6).

The net CH_4 fluxes from the seasonal measurements of each habitat in Scotland were upscaled to a yearly estimate (**Figure 7.1**; also see section 3 for calculation method). This

clearly showed how the non-forested habitats were net CH_4 emitters, while their conversion to forests turned them into net CH_4 sinks. These sink estimates are above the European average of 1.6 kg $CH_4.ha^{-1}.yr^{-1}$ calculated by Smith *et al.* (2000) but within range of UK forests estimates (Priemé *et al.*, 1997; Smith *et al.*, 2000). The results suggest that there was no difference in annual net CH_4 fluxes between the birch and pine forests, whereas other studies found that soils under hardwood trees were better sinks than soils under softwood trees (Borken *et al.*, 2003; Menyailo *et al.*, 2010; Menyailo & Hungate, 2003). The grassland site (Glensaugh) was a net emitter of CH_4 which does not agree with other studies showing that pastoral lands contribute to sinking CH_4 (Singh *et al.*, 2007; Singh *et al.*, 2009; Smith *et al.*, 2000). This is probably because the pasture site is treated yearly with fertilisers which are known to inhibit methanotrophy (Hütsch *et al.*, 1994; Mosier *et al.*, 1991). Maxfield *et al.* (2008) detected a 70% inhibition of high-affinity methanotrophs in an agricultural soil treated with inorganic fertiliser. It may explain the lack of atmospheric CH_4 sink in grassland soils.

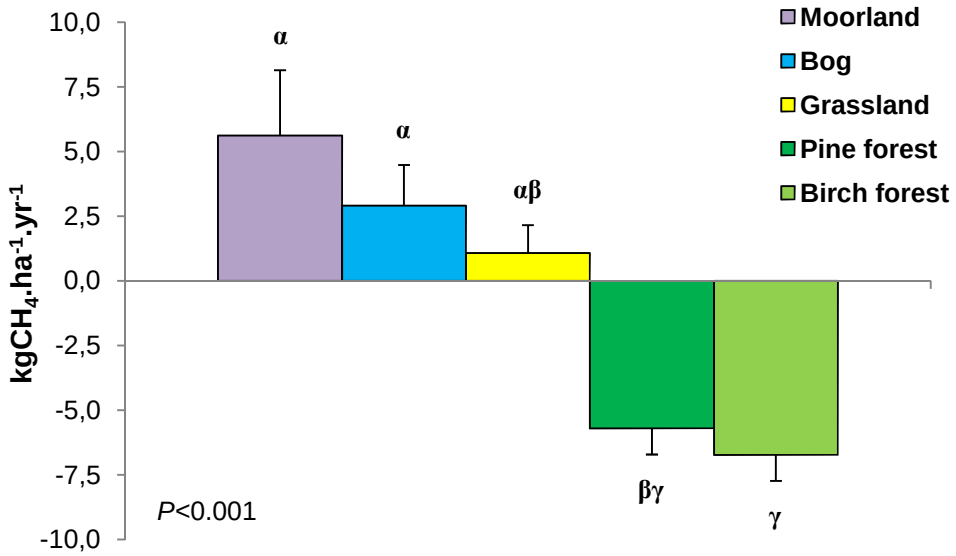

Figure 7.1: Methane fluxes from the non-forested and forested habitats.

Each histogram represents the net CH_4 flux average ± S.E.M. of the yearly estimate for each season (n=4), based on the upscaling of the net CH_4 flux measurements displayed in Chapter 5 (Figure 5.1) and Chapter 6 (Figure 6.1). Data from the four sampling sites (Craggan, Tulchan, Bad à Cheo and Glensaugh) which had similar land uses (heathland, bog, grassland, pine forest or birch forest) were combined during upscaling. Method used for upscaling was detailed in section 3. Land uses followed by different Greek letters (α, β, γ) are statistically different as per the multiple pairwise comparison test ($P<0.05$).

Effects on soil C stock and strategies for afforestation/reforestation

The presence of trees may have had an important impact on total C concentrations. As discussed previously, the birch invasion of heathland (Chapter 6) suggested potentially important and long-term C losses from soils, at least in the sites investigated in Scotland. This is in contradiction with the results of Paul *et al.* (2002) who found that in Australia deciduous hardwood tree soils accumulated C better than softwood trees did. Their results disagree with this study again since conversion of grassland and bog into pine forests preserved the soil C, or soil recovered from C losses within 20 years (Chapter 5). Other studies (Hargreaves *et al.*, 2003; Harrison *et al.*, 1995) reported that afforested peatland were beneficial in term of C sequestration. Yet, because the capacity of peatland for long-term storage of C is much higher than that which can be added by growing trees (Cannell *et al.*, 1993), it was suggested that 30 to 60-year tree rotations could maintain net C sinks in afforested peatlands (Hargreaves *et al.*, 2003; Jandl *et al.*, 2007; Paul *et al.*, 2002).

Regulation by climo-edaphic factors

Climate, in particular rainfall, may have had some effect at the shrubland site in New Zealand by limiting the improvement of the CH_4 sinks. This was due to reduced soil aeration from increased soil moisture. This is the main process that makes wetlands (bog and heathland) CH_4 emitters (and CO_2 sequesters). When peatlands are drained and planted with trees, the water table is lowered and the new oxic environment induces soil to stop emitting CH_4 but as a consequence, soil C is oxidised and released as CO_2. After a transitional growth phase, the trees start accumulating C through plant biomass and primary production (Dawson & Smith, 2007; Jandl *et al.*, 2007). Soil structure (pore size, water content, bulk density) is related to gas diffusivity (CH_4 flow and O_2 availability), hence these soil characteristics may strongly

influence CH_4 oxidation rates. This was not the case in most of the soils in Scotland where statistical significance was not always detected with some variables but trends were obvious. Soils with higher porosity and lower WFPS were consistently found to favour CH_4 sinks in forests compared to non-forested areas, as previously reported (Ball *et al.*, 1997; Singh *et al.*, 2009; Smith *et al.*, 2003; Tate *et al.*, 2007).

2. Land-use change triggers a shift in the soil methanotrophic community

Whenever afforestation/reforestation occurred, this induced a change in the structure of the methanotrophic community, except at Glensaugh. This was likely caused by modification of the soil properties due to tree planting. In particular, pH, porosity, WFPS and water content were affected by forest growth. However, only a trend or weak significance were observed for these variables. Whether it was in New Zealand or in Scotland, the change in rates of CH_4 oxidation were correlated to shifts in the structure of the methanotrophic community. The results from New Zealand identified the progressive effect of the age of the forest, while in Scotland the effect of different types of afforestation/reforestation on different type of habitat was demonstrated. A stable community structure was established in forest soils 10 years after planting in New Zealand which is close to what was observed in Scotland (20 years). To my knowledge, there are no other studies investigating the time a soil methanotrophic community takes to recover from soil disturbance and establish subsequent strong CH_4 oxidation rates (see section 1).

USCα as major atmospheric CH_4 oxidiser in forested areas

It seems that the general trend is that high-affinity type II methanotrophs distantly related to *Methylocapsa* sp. dominate many forest soils worldwide (see Discussion in Chapter 4). All the sites of this project had acidic soils, which constitute the preferred environment for type II methanotrophs involved in the oxidation of atmospheric CH_4 (Kolb, 2009). These are usually members of the so-called RA14 cluster, also known as USCα (Holmes *et al.*, 1999; Knief *et al.*, 2003). In this project, afforestation/reforestation always favoured USCα cells over type I methanotrophs (New Zealand) or over members of the *Methylocystaceae* family (Scotland). **Figure 7.2** shows for the first time the strong relationship between increase of net CH_4 uptake rates and dominance of USCα in forested areas compared to non-forested areas, except at Glensaugh (see Discussion in Chapter 5). It also shows an effect of the age of the forest at Craggan, or rather that the community was slower to adapt to land-use change at this site.

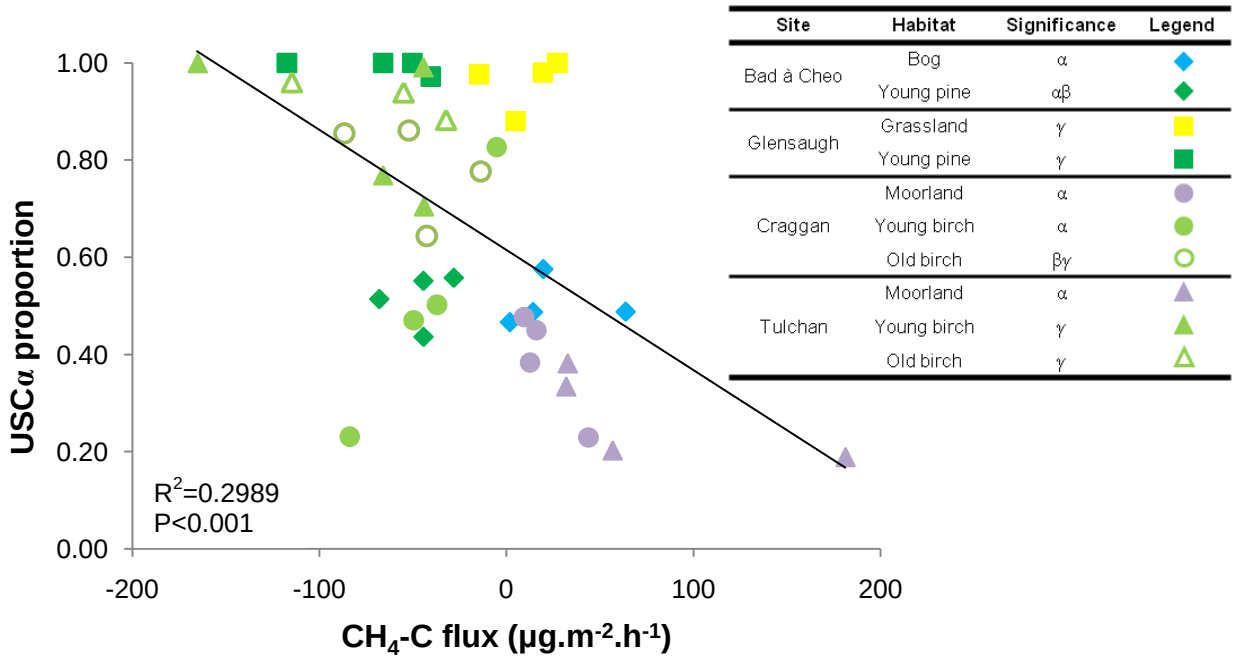

Figure 7.2: Relationship between the proportion of methanotrophs of the USCα cluster and changes in net CH_4 fluxes associated with land-use change in Scotland (n=4).

The proportion of USCα microorganisms was calculated as the ratio of the relative abundance of the T-RFs specific to *Methylocapsa* sp./USCα (T-RFs *Hha*-32, *Hha*-128 and *Msp*-25) to the sum of the T-RFs specific to USCα and the *Methylocystaceae* family (T-RFs *Hha*-81 and *Msp*-242). Refer to Appendix Figures 0.2, 0.3, 0.5 and 0.6 for T-RF reference values. The associated CH_4 oxidation rates correspond to the seasonal averages displayed in Figure 5.1 in Chapter 5 and Figure 6.1 in Chapter 6. For each habitat, n=4. Land uses followed by different Greek letters (α, β, γ) are statistically different according to the multiple pairwise comparison test ($P<0.05$).

Mechanisms of methanotrophic community shift during afforestation/reforestation

A recent study demonstrated that methanotrophic community composition was linked to CH_4 oxidation in a pine forest soils (Bengtson *et al.*, 2009). However, the authors based their community structure analysis on PLFA-SIP, whereas the use of T-RFLP analysis gave a higher degree of precision in this study. Furthermore, Bengston *et al.* (2009) did not look at the change of CH_4 oxidation due to a change in land-use. Figure 7.2 clearly identifies clusters in the proportion of USCα for each habitat investigated. In particular, the switch between net CH_4 emission and sink occurs when the relative abundance of USCα is about the same as *Methylocystaceae* (50/50). A similar threshold was observed in New Zealand except that USCα had to represent ~80% of the methanotrophs to observe significantly higher CH_4 consumption rates (see Chapter 4, Figure 4.3). As well as the proportion of USCα methanotrophs, other climo-edaphic factors had some influence on the net CH_4 fluxes due to afforestation/reforestation.

Finally, it appears that methanotrophs were adapted to different ecological niches. USCα cells were predominant in all forested sites in New Zealand and Scotland, irrespective of tree species. However, Kolb (2009) suggested that deciduous forests favoured the presence of *Methylocystis* spp. while coniferous tree species may promote their absence. This was not the case in this project. The non-forested habitats were more heterogeneous: type I methanotrophs were found in soils made of volcanic ash (New Zealand) but not in Scotland. In contrast, non-forested soils in Scotland also contained members of the *Methylocystaceae* family, except under grassland at Glensaugh.

3. Mitigation of the Scottish CH_4 budget through afforestation/ reforestation: a preliminary prediction by bottom-up approach

Steps of the upscaling process

The net CH_4 flux measurements from each site and from each habitat were used (see Chapter 5 and Chapter 6). The data from each seasonal sampling were upscaled to a yearly estimate and then averaged (Figure 7.1). Finally, the contribution of each of the five habitats under study (grassland, bog, heathland, pine and birch forests) to the Scottish national CH_4 budget were estimated based on the total surface area that each habitat covers in Scotland (**Figure 7.3**). The results are displayed in **Figure 7.4A** and discussed below.

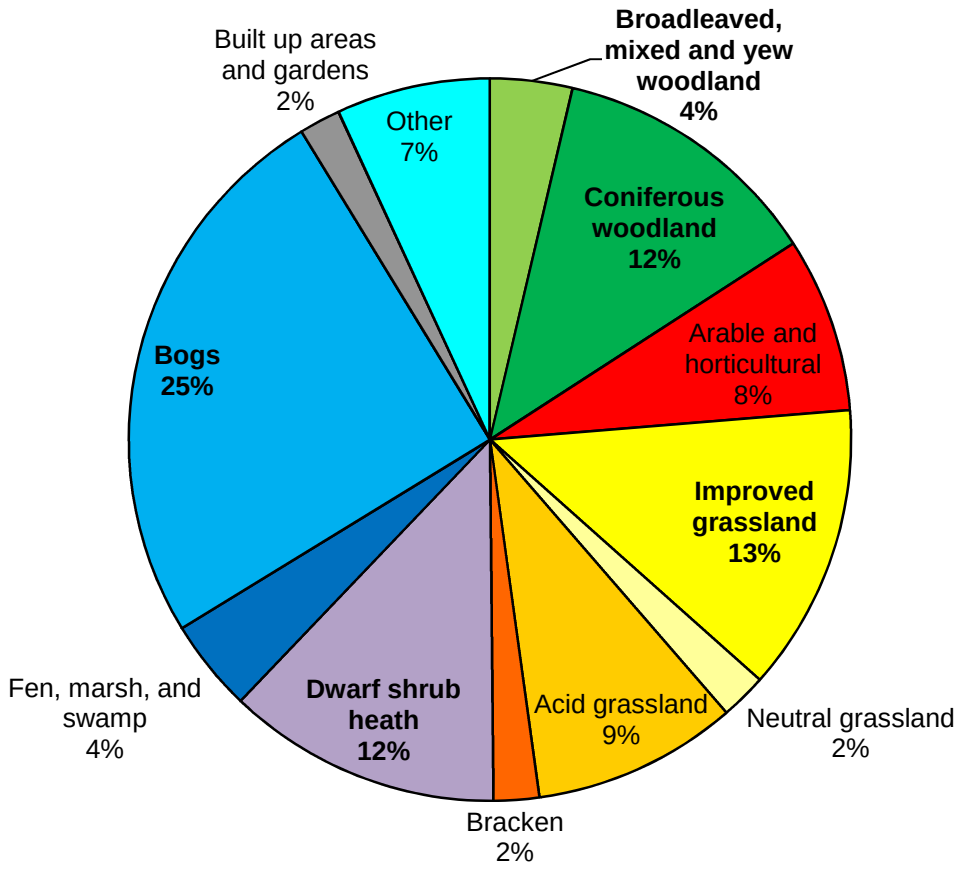

Figure 7.3: Proportions of the major habitats found in Scotland (81,550 km^2).
Adapted from McGowan *et al.* (2002).

Findings

Variations in the contribution of each habitat to the national CH_4 budget were compared based on the theoretical conversion to forest of 50% of each of the non-forested areas (**Figure 7.4**). Before simulation started, *i.e.* using the net CH_4 flux estimates from the habitats with their actual surface area, the comparison of net CH_4 fluxes from non-forested and afforested areas showed a balance between sources and sinks in favour of a positive emission of CH_4 (+4.9 kilotonnes) from non-forested areas (**Figure 7.4A**). Conversion of 50% of grassland into pine forests still resulted in a net CH_4 emissions (+1.0 kt) from non-forested areas (**Figure 7.4B**). Heathland conversion into birch woodland changed the balance into a net sink of CH_4 (-1.7 kt) in forested areas (**Figure 7.4C**). This effect was stronger (-3.8 kt) with the conversion of peatland bogs into pine forests (**Figure 7.4D**). These data show the positive impact that forestation could have on the mitigation CH_4 emissions. More specifically, this gives evidence that forestation and the subsequent improvement of CH_4 sinks in forest soils would have the potential to neutralise CH_4 emissions from other natural habitats at the national level. Bog afforestation with *Pinus radiata* trees was the most potent at offsetting CH_4 emissions in Scotland.

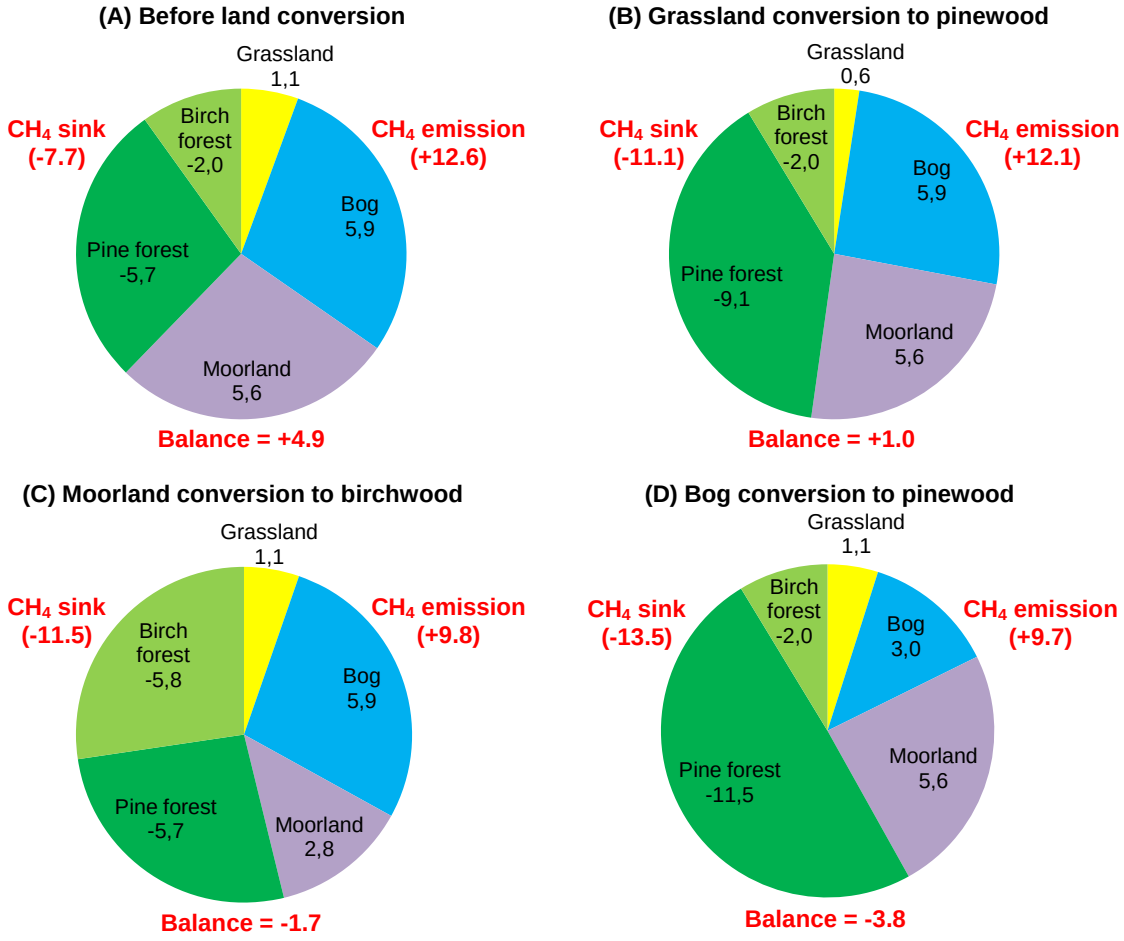

Figure 7.4: Contribution of different land-use changes to national CH_4 budget (300 kt) in Scotland before land conversion (A), after afforestation of grassland with pine trees (B), after conversion of heathland to birch forest (C) and after afforestation of bogs with pine trees (D).

Data indicate CH_4 emissions (positive values) and sinks (negative values) in kilotonne (kt) based on the upscaled net CH_4 fluxes (**Figure 7.1**) and on the area that each habitat represents in Scotland (**Figure 7.3**). The balance between CH_4 emissions and sinks in, respectively, the non-forested and forested areas is also indicated.

Limitations and perspectives

Firstly, the yearly estimates are based on one seasonal sampling during each of the four seasons. Although no seasonal effect on the net CH_4 fluxes was detected, except at Tulchan in summer, more regular sampling would add accuracy. Secondly, spatial variability of net CH_4 fluxes might be criticised since CH_4 emissions can vary considerably within a site, especially in wetlands (Minkkinen & Laine, 2006; Van den Pol-van Dasselaar *et al.*, 1999). This might be true for the bog or grassland sites since no other replicate site was used. Nevertheless, the sampling of soils under heathland at two different sites did not show a

significant difference in CH_4 emissions during most seasonal replications. A similar observation was made with site-to-site comparison of the net CH_4 fluxes from the (young and old) birch stands at Craggan and Tulchan and from the young pine forests at Bad à Cheo and Glensaugh. This site-to-site comparison was useful in giving more homogeneity to the yearly flux estimates (Figure 7.1) and to the contribution of each land use to the national CH_4 budget (Figure 7.4).

An identical bottom-up study was applied for estimating the positive potential on CH_4 sinks of afforestation/reforestation in New Zealand under provision of the Article 3.3 of the Kyoto Protocol (Scott *et al.*, 2001; Tate *et al.*, 2005). A more accurate approach was conducted by Glatzel & Bareth (2006), in which they accounted for the interaction between land use and soil type to estimate regional CH_4 emissions. However, because of the global over-estimation of the results, they acknowledged the need to link ecosystem approaches to process-based models, in which specific soil processes such as C and N cycles and their impact on net CH_4 fluxes are considered. The process-based model DNDC (DeNitrification and DeComposition) requires detailed information on site climate (daily precipitation and temperature), soil properties (texture, porosity, clay content, moisture) and land management (crop, fertilisation) (Li *et al.*, 1992a; 1992b; 2000). It was applied to estimate N_2O emissions from arable sites in the USA (Li *et al.*, 1996), China (Li *et al.*, 2001), Germany (Butterbach-Bahl *et al.*, 2001), Canada (Smith *et al.*, 2002) and the UK (Brown *et al.*, 2002). Recently, the DNDC model was adapted to New Zealand ("NZ-DNDC") for the modelling of N_20 emissions from grazed pastures (Saggar *et al.*, 2004) and was also successfully applied to the modelling of CH_4 consumption (Saggar *et al.*, 2007). However, these models do not account for the role of microorganisms in the soil processes responsible for CH_4 consumption, *i.e.* methanotrophy. Therefore, a new model including site/soil properties and information on the soil

methanotrophic community structure may significantly increase the precision of the estimates for national contributions to CH_4 budget.

Finally, it should be kept in mind that, in this study, the hypothetical change of 50% of one land use (*i.e.* peatland bog) into a (pine) forest is not feasible, at least on the short term. Also, the loss of peatland compared to the gain of forest should be considered since peatland are useful with respect to energy production, building and isolation, tourism, *etc.* but particularly ecological biodiversity whereas the main advantage of forestry would be wood trade. Furthermore, peatland conversion would be costly in terms of site preparation and in particular when looking at C fluxes. Although it was discussed in Chapter 5 that long forest rotation may preserve high C losses, the release of CO_2 after drainage of the bog, due in particular to the increase of the processes of soil organic matter decomposition and heterotrophic respiration, may have a bigger impact on the global GHG budget (Singh *et al.*, 2010; Smith, 2008). Therefore, the net CO_2 fluxes should have been investigated too in order to estimate the importance of the impact of such land-use change and thus to assess which GHG would be the most affected. Overall, it is essential to understand how GHG-emitting microbes influence the global GHG budget and how they could contribute to the mitigation of climate change. The importance of microorganisms to climate change through their contribution to carbon cycling and feedback responses to the main GHG (CO_2, CH_4 and N_20) was discussed in very interesting reviews from Bardgett *et al.* (2008) and Singh *et al.* (2010).

4. Conclusions

This project demonstrated the positive effect of afforestation/reforestation on atmospheric CH_4 sinks. In particular, through a preliminary upscaling approach, it helped to predict the national CH_4 production and consumption from the five main habitats in Scotland (cumulative surface area of 66%). The bottom-up procedure showed that the hypothetical conversion of 50% of the pastoral land to pine forest was not sufficient to reverse the natural net CH_4 emissions, whereas the colonisation of heathland and afforestation of bog were. However, birch invasion in Scotland proved to induce important (50-90%) and permanent losses in soil C stocks, therefore making it a poor candidate for CH_4 mitigation. In contrast, afforestation of bogs with pines seemed to be effective in creating strong CH_4 sinks while preserving C sequestration in soils within 20 years after forest growth started. Site preparation for afforestation and forest management should not be overlooked in order to optimise the conditions for atmospheric CH_4 oxidation and C sequestration. Afforestation/ reforestation in Scotland and shrubland regeneration after fire burning in New Zealand showed quicker recovery time (20-55 years) from soil disturbance than previously estimated.

The project also revealed a better understanding of the mechanisms underlying methanotrophy. Shifts in the methanotrophic community structure were clearly correlated to changes in CH_4 oxidation rates associated with various land-use changes. Specifically, the relative proportion of high-affinity (uncultivable) methanotrophs belonging to the USCα group – responsible for the oxidation of atmospheric levels of CH_4 – in a particular habitat was a strong predictor of whether a soil was a net CH_4 emitter or a net CH_4 sink. This was confirmed by the combined use of molecular methods (T-RFLP, diagnostic microarray and cloning/sequencing) and activity-specific techniques (PLFA-SIP). Finally, a niche-specific adaptation of the methanotrophs was suggested, which may be influenced by the sole presence of trees and/or the soil characteristics.

5. Future works

Impact of land-use change on the methanogenic community structure

Because the net CH_4 fluxes measured from the intact cores in the closed chamber were a combination of the methanotrophic and methanogenic activities, it is postulated that these were also influenced by changes in the structure of the methanogenic community due to land-use change. Therefore, a similar molecular approach should be applied to the study of methanogens. This would involved T-RFLP analysis of genes such as *mcrA* and 16S rRNA. Furthermore, for the global upscaling of this result, shifts in the methanotrophic community structure and their influence on the net CH_4 fluxes should be expanded to include investigation of:

- Effect of other land-use changes such as in arable, set-aside or deforested sites
- Effect of other forest types (oak, mixed)
- Effect of altitude and/or water table
- Effect of climate change (elevated CO_2, increased temperature, altered precipitation)

Modelling CH_4 emissions/sinks in Scotland in relation to methanotroph community structure

The DNDC and other models could be adapted to Scotland and the UK to improve the prediction of net CH_4 fluxes. This could be achieved by including in-depth information about the methanotrophic (and methanogenic) community structure, specifically the dominance of particular species in relation to the nature and structure of the soil of the different habitats.

References

Ali H., Scanlan J., Dumont M.G. & Murrell J.C. (2006). Duplication of the *mmoX* gene in *Methylosinus sporium*: cloning, sequencing and mutational analysis. *Microbiology*, **152**, 2931-2942.

Amaral J.A. & Knowles R. (1995). Growth of methanotrophs in methane and oxygen counter gradients. *FEMS Microbiology Letters*, **126**, 215-220.

Amaral J.A., Ren T. & Knowles R. (1998). Atmospheric methane consumption by forest soils and extracted bacteria at different pH values. *Applied Environmental Microbiology*, **64**, 2397-2402.

Anderson A., Pyatt D., Sayers J.M., Blackhall S.R. & Robinson H.D. (1992). Volume and mass budgets of blanket peat in the north of Scotland. *Suo (Helsinki)*, **43**, 195-198.

Baani M. & Liesack W. (2008). Two isozymes of particulate methane monooxygenase with different methane oxidation kinetics are found in *Methylocystis* sp. strain SC2. *Proceedings of the National Academy of Sciences U. S. A.*, **105**, 10203-10208.

Ball B.C., Smith K.A., Klemedtsson L., Brumme R., Sitaula B.K., Hansen S., Priemé A., MacDonald J. & Horgan G.W. (1997). The influence of soil gas transport properties on methane oxidation in a selection of northern European soils. *Journal of Geophysical Research-Atmospheres*, **102**, 23309-23317.

Ballantyne K.N., van Oorschot R.A. & Mitchell R.J. (2008). Reduce optimisation time and effort: Taguchi experimental design methods. *Forensic Science International: Genetics Supplement Series*, **1**, 7-8.

Ballantyne K.N., van Oorschot R.A.H. & Mitchell R.J. (2010). Increased amplification success from forensic samples with locked nucleic acids. *Forensic Science International: Genetics*, **In Press, Corrected Proof**.

Bardgett R.D., Freeman C. & Ostle N.J. (2008). Microbial contributions to climate change through carbon cycle feedbacks. *ISME J*, **2**, 805-814.

Baxter N.J., Hirt R.P., Bodrossy L., Kovacs K.L., Embley T.M., Prosser J.I. & Murrell J.C. (2002). The ribulose-1,5-bisphosphate carboxylase/oxygenase gene cluster of *Methylococcus capsulatus* (Bath). *Archives of Microbiology*, **177**, 279-289.

Beal E.J., House C.H. & Orphan V.J. (2009). Manganese- and iron-dependent marine methane oxidation. *Science*, **325**, 184-187.

Beerling D.J., Gardiner T., Leggett G., McLeod A. & Quick W.P. (2008). Missing methane emissions from leaves of terrestrial plants. *Global Change Biology*, **14**, 1821-1826.

Beets P.N. & Brownlie R.K. (1987). Puruki Experimental Catchment New Zealand Site Climate Forest Management and Research. *New Zealand Journal of Forestry Science,* **17**, 137-160.

Bender M. & Conrad R. (1992). Kinetics of CH_4 oxidation in oxic soils exposed to ambient air or high CH_4 mixing ratios. *FEMS Microbiology Letters,* **101**, 261-269.

Bender M. & Conrad R. (1995). Effect of CH_4 concentrations and soil conditions on the induction of CH_4 oxidation activity. *Soil Biology and Biochemistry,* **27**, 1517-1527.

Bengtson P., Basiliko N., Dumont M.G., Hills M., Murrell J.C., Roy R. & Grayston S.J. (2009). Links between methanotroph community composition and CH_4 oxidation in a pine forest soil. *FEMS Microbiology Ecology,* **70**, 356-366.

Blackwood C.B., Marsh T., Kim S.H. & Paul E.A. (2003). Terminal restriction fragment length polymorphism data analysis for quantitative comparison of microbial communities. *Applied Environmental Microbiology,* **69**, 926-932.

Blakemore L.C., Searle P.L. & Daly B.K. (1987). Methods for chemical analysis of soils. In: New Zealand Soil Bureau Scientific Report 80.

Bligh E.G. & Dyer W.J. (1959). A rapid method of total lipid extraction and purification. *Can. J. Biochem. Physiol,* **37**, 911-917.

Bodelier P.L.E., Gillisen M.J.B., Hordijk K., Damste J.S.S., Rijpstra W.I.C., Geenevasen J.A.J. & Dunfield P.F. (2009). A reanalysis of phospholipid fatty acids as ecological biomarkers for methanotrophic bacteria. *ISME Journal,* **3**, 606-617.

Bodelier P.L.E. & Laanbroek H.J. (2004). Nitrogen as a regulatory factor of methane oxidation in soils and sediments. *FEMS Microbiology Ecology,* **47**, 265-277.

Bodrossy L., Holmes E.M., Holmes A.J., Kovacs K.L. & Murrell J.C. (1997). Analysis of 16S rRNA and methane monooxygenase gene sequences reveals a novel group of thermotolerant and thermophilic methanotrophs, *Methylocaldum* gen. nov. *Archives of Microbiology,* **168**, 493-503.

Bodrossy L., Stralis-Pavese N., Murrell J.C., Radajewski S., Weilharter A. & Sessitsch A. (2003). Development and validation of a diagnostic microbial microarray for methanotrophs. *Environmental Microbiology,* **5**, 566-582.

Boeckx P., Van Cleemput O. & Meyer T. (1998). The influence of land use and pesticides on methane oxidation in some Belgian soils. *Biology and Fertility of Soils,* **27**, 293-298.

Boetius A., Ravenschlag K., Schubert C.J., Rickert D., Widdel F., Gieseke A., Amann R., Jorgensen B.B., Witte U. & Pfannkuche O. (2000). A marine microbial consortium apparently mediating anaerobic oxidation of methane. *Nature,* **407**, 623-626.

Bonacker L.G., Baudner S., Morschel E., Bocher R. & Thauer R.K. (1993). Properties of the two isoenzymes of methyl-coenzyme M reductase in *Methanobacterium thermoautotrophicum*. *European Journal of Biochemistry,* **217**, 587-595.

Bonacker L.G., Baudner S. & Thauer R.K. (1992). Differential expression of the two methyl-coenzyme M reductases in *Methanobacterium thermoautotrophicum* as determined immunochemically via isoenzyme-specific antisera. *European Journal of Biochemistry,* **206**, 87-92.

Boone D., Whitman W. & Rouvière P. (1993). Diversity and taxonomy of methanogens. In: *Methanogenesis*. Edited by: J.G. Ferry. Chapman and Hall Co, New York, pp. 35-80.

Borken W. & Beese F. (2006). Methane and nitrous oxide fluxes of soils in pure and mixed stands of European beech and Norway spruce. *European Journal of Soil Science,* **57**, 617-625.

Borken W., Xu Y.J. & Beese F. (2003). Conversion of hardwood forests to spruce and pine plantations strongly reduced soil methane sink in Germany. *Global Change Biology*, **9**, 956-966.

Born M., Dörr H. & Levin I. (1990). Methane consumption in aerated soils of the temperate zone. *Tellus B,* **42**, 2-8.

Boschker H.T.S. & Middelburg J.J. (2002). Stable isotopes and biomarkers in microbial ecology. *FEMS Microbiology Ecology,* **40**, 85-95.

Boschker H.T.S., Nold S.C., Wellsbury P., Bos D., de Graaf W., Pel R., Parkes R.J. & Cappenberg T.E. (1998). Direct linking of microbial populations to specific biogeochemical processes by ^{13}C-labelling of biomarkers. *Nature,* **392**, 801-805.

Bourne D.G., McDonald I.R. & Murrell J.C. (2001). Comparison of *pmoA* PCR primer sets as tools for investigating methanotroph diversity in three Danish soils. *Applied Environmental Microbiology,* **67**, 3802-3809.

Bousquet P., Ciais P., Miller J.B., Dlugokencky E.J., Hauglustaine D.A., Prigent C., van der Werf G.R., Peylin P., Brunke E.G., Carouge C., Langenfelds R.L., Lathiere J., Papa F., Ramonet M., Schmidt M., Steele L.P., Tyler S.C. & White J. (2006). Contribution of anthropogenic and natural sources to atmospheric methane variability. *Nature*, **443**, 439-443.

Bowman J.P., McCammon S.A. & Skerratt J.H. (1997). *Methylosphaera hansonii* gen. nov., sp. nov., a psychrophilic, group I methanotroph from Antarctic marine-salinity, meromictic lakes. *Microbiology,* **143 (Pt 4)**, 1451-1459.

Bowman J.P., Sly L.I., Nichols P.D. & Hayward A.C. (1993). Revised taxonomy of the methanotrophs: Description of *Methylobacter* gen. nov., emendation of *Methylococcus*, validation of *Methylosinus* and *Methylocystis* species, and a proposal that the family *Methylococcaceae* includes only the group I methanotrophs. *International Journal of Systematic and Evolutionary Microbiology,* **43**, 735-753.

Brown L., Syed B., Jarvis S.C., Sneath R.W., Phillips V.R., Goulding K.W.T. & Li C. (2002). Development and application of a mechanistic model to estimate emission of nitrous oxide from UK agriculture. *Atmospheric Environment,* **36**, 917-928.

Bruce K.D. (1997). Analysis of *mer* gene subclasses within bacterial communities in soils and sediments resolved by fluorescent-PCR-restriction fragment length polymorphism profiling. *Applied and Environmental Microbiology,* **63**, 4914-4919.

Bull I.D., Parekh N.R., Hall G.H., Ineson P. & Evershed R.P. (2000). Detection and classification of atmospheric methane oxidizing bacteria in soil. *Nature,* **405**, 175-178.

Butterbach-Bahl K., Papen H. & Rennenberg H. (1997). Impact of gas transport through rice cultivars on methane emission from rice paddy fields. *Plant, Cell & Environment,* **20**, 1175-1183.

Butterbach-Bahl K., Stange F., Papen H. & Li C. (2001). Regional inventory of nitric oxide and nitrous oxide emissions for forest soils of Southeast Germany using the biogeochemical model PnET-N-DNDC. *Journal Geophysical Research,* **106**, 34155-34165.

Caetano-Anollés G. (1998). DAF optimization using Taguchi methods and the effect of thermal cycling parameters on DNA amplification. *Biotechniques,* **25**, 472-480.

Cannell M.G.R., DEWAR R.C. & PYATT D.G. (1993). Conifer plantations on drained peatlands in Britain: a net gain or loss of carbon? *Forestry,* **66**, 353-369.

Castro M.S., Steudler P.A., Melillo J.M., Aber J.D. & Bowden R.D. (1995). Factors controlling atmospheric methane consumption by temperate forest soils. *Global Biogeochemical Cycles,* **9**, 1-10.

Chazelas B., Leger A. & Ollivier M. (2006). How to oxidize atmospheric CH_4? A challenge for the future. *Science of the Total Environment,* **354**, 292-294.

Chen Y., Crombie A., Rahman M.T., Dedysh S.N., Liesack W., Stott M.B., Alam M., Theisen A.R., Murrell J.C. & Dunfield P.F. (2010). Complete genome sequence of the aerobic facultative methanotroph *Methylocella silvestris* BL2. *Journal of Bacteriology,* **192**, 3840-3841.

Chen Y., Dumont M.G., Cebron A. & Murrell J.C. (2007). Identification of active methanotrophs in a landfill cover soil through detection of expression of 16S rRNA and functional genes. *Environmental Microbiology,* **9**, 2855-2869.

Chen Y., Dumont M.G., McNamara N.P., Chamberlain P.M., Bodrossy L., Stralis-Pavese N. & Murrell J.C. (2008). Diversity of the active methanotrophic community in acidic peatlands as assessed by mRNA and SIP-PLFA analyses. *Environmental Microbiology,* **10**, 446-459.

Choi D.W., Antholine W.E., Do Y.S., Semrau J.D., Kisting C.J., Kunz R.C., Campbell D., Rao V., Hartsel S.C. & Dispirito A.A. (2005). Effect of methanobactin on the activity and electron paramagnetic resonance spectra of the membrane-associated methane monooxygenase in *Methylococcus capsulatus* Bath. *Microbiology,* **151**, 3417-3426.

Choi D.W., Bandow N.L., McEllistrem M.T., Semrau J.D., Antholine W.E., Hartsel S.C., Gallagher W., Zea C.J., Pohl N.L., Zahn J.A. & Dispirito A.A. (2010). Spectral and thermodynamic properties of methanobactin from gamma-proteobacterial methane oxidizing bacteria: a case for copper competition on a molecular level. *Journal of Inorganic Biochemistry,* **104**, 1240-1247.

Chung T., Klumpp D.J. & LaPorte D.C. (1988). Glyoxylate bypass operon of *Escherichia coli*: cloning and determination of the functional map. *Journal of Bacteriology,* **170**, 386-392.

Cicerone R.J. & Oremland R.S. (1988). Biogeochemical aspects of atmospheric methane. *Global Biogeochemical Cycles,* **2**, 299-327.

Cobb B.D. & Clarkson J.M. (1994). A simple procedure for optimising the polymerase chain reaction (PCR) using modified Taguchi methods. *Nucleic Acids Research,* **22**, 3801-3805.

Colby J., Stirling D.I. & Dalton H. (1977). The soluble methane mono-oxygenase of *Methylococcus capsulatus* (Bath). Its ability to oxygenate n-alkanes, n-alkenes, ethers, and alicyclic, aromatic and heterocyclic compounds. *Biochemistry Journal,* **165**, 395-402.

Conrad R. (1996). Soil microorganisms as controllers of atmospheric trace gases (H_2, CO, CH_4, OCS, N_2O, and NO). *Microbiological Reviews,* **60**, 609-640.

Conrad R. (2009). The global methane cycle: recent advances in understanding the microbial processes involved. *Environmental Microbiology Reports,* **1**, 285-292.

Conrad R., Erkel C. & Liesack W. (2006). Rice Cluster I methanogens, an important group of *Archaea* producing greenhouse gas in soil. *Current Opinion in Biotechnology,* **17**, 262-267.

Conrad R. & Rothfuss F. (1991). Methane oxidation in the soil surface layer of a flooded rice field and the effect of ammonium. *Biology and Fertility of Soils,* **12**, 28-32.

Costello A.M. & Lidstrom M.E. (1999). Molecular characterization of functional and phylogenetic genes from natural populations of methanotrophs in lake sediments. *Applied Environmental Microbiology,* **65**, 5066-5074.

Cronin S.J., Neall V.E., Lecointre J.A., Hedley M.J. & Loganathan P. (2003). Environmental hazards of fluoride in volcanic ash: A case study from Ruapehu volcano, New Zealand. *Journal of Volcanology and Geothermal Research,* **121**, 271-291.

Crossman Z.M., Ineson P. & Evershed R.P. (2005). The use of C-13 labelling of bacterial lipids in the characterisation of ambient methane-oxidising bacteria in soils. *Organic Geochemistry,* **36**, 769-778.

Csáki R., Bodrossy L., Klem J., Murrell J.C. & Kovács K.L. (2003). Genes involved in the copper-dependent regulation of soluble methane monooxygenase of *Methylococcus capsulatus* (Bath): cloning, sequencing and mutational analysis. *Microbiology,* **149**, 1785-1795.

Culman S.W., Bukowski R., Gauch H.G., Cadillo-Quiroz H. & Buckley D.H. (2009). *T-REX*: Software for the processing and analysis of T-RFLP data. *BMC Bioinformatics,* **10**.

Culman S.W., Gauch H.G., Blackwood C.B. & Thies J.E. (2008). Analysis of T-RFLP data using analysis of variance and ordination methods: A comparative study. *Journal of Microbiological Methods,* **75**, 55-63.

Czepiel P.M., Crill P.M. & Harriss R.C. (1995). Environmental factors influencing the variability of methane oxidation in temperate zone soils. *Journal Geophysical Research,* **100**, 9359-9364.

Dawson J.J.C. & Smith P. (2007). Carbon losses from soil and its consequences for land-use management. *Science of the Total Environment,* **382**, 165-190.

Dedysh S.N., Belova S.E., Bodelier P.L., Smirnova K.V., Khmelenina V.N., Chidthaisong A., Trotsenko Y.A., Liesack W. & Dunfield P.F. (2007). *Methylocystis heyeri* sp. nov., a novel type II methanotrophic bacterium possessing 'signature' fatty acids of type I methanotrophs. *International Journal of Systematic and Evolutionary Microbiology,* **57**, 472-479.

Dedysh S.N., Berestovskaya Y.Y., Vasylieva L.V., Belova S.E., Khmelenina V.N., Suzina N.E., Trotsenko Y.A., Liesack W. & Zavarzin G.A. (2004). *Methylocella tundrae* sp. nov., a novel methanotrophic bacterium from acidic tundra peatlands. *International Journal of Systematic and Evolutionary Microbiology,* **54**, 151-156.

Dedysh S.N., Khmelenina V.N., Suzina N.E., Trotsenko Y.A., Semrau J.D., Liesack W. & Tiedje J.M. (2002). *Methylocapsa acidiphila* gen. nov., sp. nov., a novel methane-oxidizing and dinitrogen-fixing acidophilic bacterium from *Sphagnum* bog. *International Journal of Systematic and Evolutionary Microbiology,* **52**, 251-261.

Dedysh S.N., Knief C. & Dunfield P.F. (2005). *Methylocella* species are facultatively methanotrophic. *Journal of Bacteriology,* **187**, 4665-4670.

Dedysh S.N., Liesack W., Khmelenina V.N., Suzina N.E., Trotsenko Y.A., Semrau J.D., Bares A.M., Panikov N.S. & Tiedje J.M. (2000). *Methylocella palustris* gen. nov., sp. nov., a new methane-oxidizing acidophilic bacterium from peat bags, representing a novel subtype of serine-pathway methanotrophs. *International Journal of Systematic and Evolutionary Microbiology,* **50**, 955-969.

Deppenmeier U. (2002). The unique biochemistry of methanogenesis. *Progress in Nucleic Acid Research and Molecular Biology*, **71**, 223-283.

DiMarco A.A., Bobik T.A. & Wolfe R.S. (1990). Unusual coenzymes of methanogenesis. *Annual Review of Biochemistry,* **59**, 355-394.

DiSpirito A.A., Gulledge J., Shiemke A.K., Murrell J.C., Lidstrom M.E. & Krema C.L. (1991). Trichloroethylene oxidation by the membrane-associated methane monooxygenase in type I, type II and type X methanotrophs. *Biodegradation,* **2**, 151-164.

Dobbie K.E. & Smith K.A. (1996). Comparison of CH_4 oxidation rates in woodland, arable and set-aside soils. *Soil Biology and Biochemistry,* **28**, 1357-1365.

Dobbie K.E. & Smith K.A. (2010). Comparison of CH_4 oxidation rates in woodland, arable and set aside soils. *Soil Biology and Biochemistry,* **28**, 1357-1365.

Dörr N., Glaser B. & Kolb S. (2010). Methanotrophic communities in Brazilian ferralsols from naturally forested, afforested, and agricultural sites. *Applied Environmental Microbiology,* **76**, 1307-1310.

Dueck T.A., De Visser R., Poorter H., Persijn S., Gorissen A., De Visser W., Schapendonk A., Verhagen J., Snel J., Harren F.J.M., Ngai A.K.Y., Verstappen F., Bouwmeester H., Voesenek L.A.C.J. & van der Werf A. (2007). NO evidence for substantial aerobic methane emission by terrestrial plants: a ^{13}C-labelling approach. *New Phytologist*, **175**, 29-35.

Dumont M.G. & Murrell J.C. (2005). Stable isotope probing - linking microbial identity to function. *Nature Reviews Microbiology*, **3**, 499-504.

Dumont M.G., Pommerenke B., Casper P. & Conrad R. (2011). DNA-, rRNA- and mRNA-based stable isotope probing of aerobic methanotrophs in lake sediment. *Environmental Microbiology*.

Dumont M.G., Radajewski S.M., Miguez C.B., McDonald I.R. & Murrell J.C. (2006). Identification of a complete methane monooxygenase operon from soil by combining stable isotope probing and metagenomic analysis. *Environmental Microbiology*, **8**, 1240-1250.

Dunfield P.F., Belova S.E., Vorobev A.V., Cornish S.L. & Dedysh S.N. (2010). *Methylocapsa aurea* sp. nov., a facultative methanotroph possessing a particulate methane monooxygenase, and emended description of the genus *Methylocapsa*. *International Journal of Systematic and Evolutionary Microbiology*, **60**, 2659-2664.

Dunfield P.F., Khmelenina V.N., Suzina N.E., Trotsenko Y.A. & Dedysh S.N. (2003). *Methylocella silvestris* sp. nov., a novel methanotroph isolated from an acidic forest cambisol. *International Journal of Systematic and Evolutionary Microbiology*, **53**, 1231-1239.

Dunfield P.F., Tchawa Yimga M., Dedysh S.N., Berger U., Liesack W. & Heyer J. (2002). Isolation of a *Methylocystis* strain containing a novel *pmoA*-like gene. *FEMS Microbiology Ecology*, **41**, 17-26.

Dunfield P.F., Yuryev A., Senin P., Smirnova A.V., Stott M.B., Hou S., Ly B., Saw J.H., Zhou Z., Ren Y., Wang J., Mountain B.W., Crowe M.A., Weatherby T.M., Bodelier P.L., Liesack W., Feng L., Wang L. & Alam M. (2007). Methane oxidation by an extremely acidophilic bacterium of the phylum *Verrucomicrobia*. *Nature*, **450**, 879-882.

Erkel C., Kube M., Reinhardt R. & Liesack W. (2006). Genome of Rice Cluster I *archaea* -the key methane producers in the rice rhizosphere. *Science*, **313**, 370-372.

Ettwig K.F., Butler M.K., Le Paslier D., Pelletier E., Mangenot S., Kuypers M.M.M., Schreiber F., Dutilh B.E., Zedelius J., de Beer D., Gloerich J., Wessels H.J.C.T., van Alen T., Luesken F., Wu M.L., van de Pas-Schoonen K., Op den Camp H.J.M., Janssen-Megens E.M., Francoijs K.J., Stunnenberg H., Weissenbach J., Jetten M.S.M. & Strous M. (2010). Nitrite-driven anaerobic methane oxidation by oxygenic bacteria. *Nature*, **464**, 543-548.

Ferry J.G. (1997). Enzymology of the fermentation of acetate to methane by *Methanosarcina thermophila*. *Biofactors*, **6**, 25-35.

Ferry J.G. (1999). Enzymology of one-carbon metabolism in methanogenic pathways. *FEMS Microbiology Reviews*, **23**, 13-38.

Ferry J.G. (2010). The chemical biology of methanogenesis. *Planetary and Space Science,* **58**, 1775-1783.

Fitch M.W., Graham D.W., Arnold R.G., Agarwal S.K., Phelps P., Speitel G.E., Jr. & Georgiou G. (1993). Phenotypic characterization of copper-resistant mutants of *Methylosinus trichosporium* OB3b. *Applied Environmental Microbiology*, **59**, 2771-2776.

Fox B.G., Froland W.A., Dege J.E. & Lipscomb J.D. (1989). Methane monooxygenase from *Methylosinus trichosporium* Ob3B - Purification and properties of a 3-component system with high specific activity from A type II methanotroph. *Journal of Biological Chemistry,* **264**, 10023-10033.

Frostegård Å., Bååth E. & Tunlid A. (1993a). Shifts in the structure of soil microbial communities in limed forests as revealed by phospholipid fatty acid analysis. *Soil Biology and Biochemistry*, **25**, 723-730.

Frostegård Å., Tunlid A. & Bååth E. (1991). Microbial biomass measured as total lipid phosphate in soils of different organic content. *Journal of Microbiological Methods,* **14**, 151-163.

Frostegård Å., Tunlid A. & Bååth E. (1993b). Phospholipid fatty-acid composition, biomass, and activity of microbial communities from two soil types experimentally exposed to different heavy-metals. *Applied Environmental Microbiology,* **59**, 3605-3617.

Frostegård Å., Tunlid A. & Bååth E. (2010). Use and misuse of PLFA measurements in soils. *Soil Biology and Biochemistry,* **In Press, Corrected Proof**.

Fuse H., Ohta M., Takimura O., Murakami K., Inoue H., Yamaoka Y., Oclarit J.M. & Omori T. (1998). Oxidation of trichloroethylene and dimethyl sulfide by a marine *Methylomicrobium* strain containing soluble methane monooxygenase. *Bioscience, Biotechnology, and Biochemistry,* **62**, 1925-1931.

Gauch H.G. (1992). Statistical analysis of regional yield trials: AMMI analysis of factorial designs. In: Elsevier Science Publishers; Amsterdam; Netherlands.

Gauch H.G. (2007). MATMODEL Version 3.0: Open Source Software for AMMI and Related Analyses. *Crop and Soil Sciences, Cornell University, Ithaca, NY*.

Geymonat E., Ferrando L. & Tarlera S.E. (2010). *Methylogaea oryzae* gen. nov., sp. nov., a novel mesophilic methanotroph from a rice paddy field in Uruguay. *International Journal of Systematic and Evolutionary Microbiology*.

Gilbert B., McDonald I.R., Finch R., Stafford G.P., Nielsen A.K. & Murrell J.C. (2000). Molecular analysis of the *pmo* (particulate methane monooxygenase) operons from two type II methanotrophs. *Applied Environmental Microbiology*, **66**, 966-975.

Glatzel S. & Bareth G. (2006). Regional inventory approach to estimate methane emissions based on soil-land use classes. *Erdkunde,* **60**, 1-14.

Gorris L.G. & van der Drift C. (1994). Cofactor contents of methanogenic bacteria reviewed. *Biofactors,* **4**, 139-145.

Graham D.W., Chaudhary J.A., Hanson R.S. & Arnold R.G. (1993). Factors affecting competition between type I and type II methanotrophs in two-organism, continuous-flow reactors. *Microbial Ecology,* **25**, 1-17.

Green J. & Dalton H. (1985). Protein B of soluble methane monooxygenase from Methylococcus capsulatus (Bath). A novel regulatory protein of enzyme activity. *Journal of Biological Chemistry,* **260**, 15795-15801.

Green J., Prior S.D. & Dalton H. (1985). Copper ions as inhibitors of protein C of soluble methane monooxygenase of *Methylococcus capsulatus* (Bath). *European Journal of Biochemistry,* **153**, 137-144.

Großkopf R., Janssen P.H. & Liesack W. (1998). Diversity and structure of the methanogenic community in anoxic rice paddy soil microcosms as examined by cultivation and direct 16S rRNA gene sequence retrieval. *Applied and Environmental Microbiology,* **64**, 960-969.

Gunsalus R.P. & Wolfe R.S. (1980). Methyl coenzyme M reductase from *Methanobacterium thermoautotrophicum*. Resolution and properties of the components. *Journal of Biological Chemistry,* **255**, 1891-1895.

Gutierrez-Zamora M.L. & Manefield M. (2010). An appraisal of methods for linking environmental processes to specific microbial taxa. *Reviews in Environmental Science and Biotechnology,* **9**, 153-185.

Hakemian A.S. & Rosenzweig A.C. (2007). The biochemistry of methane oxidation. *Annual Review of Biochemistry,* **76**, 223-241.

Hanson R.S. & Hanson T.E. (1996). Methanotrophic bacteria. *Microbiological Reviews,* **60**, 439-471.

Hargreaves K.J., Milne R. & Cannell M.G.R. (2003). Carbon balance of afforested peatland in Scotland. *Forestry,* **76**, 299-317.

Harrison A.F., Howard P.J.A., Howard D.M., Howard D.C. & Hornung M. (1995). Carbon storage in forest soils. *Forestry,* **68**, 335-348.

Hedderich R. & Whitman W. (2006). Physiology and biochemistry of the methane-producing *Archaea*. In: *The Prokaryotes*. Edited by: M. Dworkin, S. Falkow, E. Rosenberg, K.H. Schleifer & E. Stackebrandt. Springer New York, pp. 1050-1079.

Hedley C.B., Saggar S. & Tate K.R. (2006). Procedure for fast simultaneous analysis of the greenhouse gases: Methane, carbon dioxide, and nitrous oxide in air samples. *Communications in Soil Science and Plant Analysis,* **37**, 1501-1510.

Henckel T., Jäckel U., Schnell S. & Conrad R. (2000a). Molecular analyses of novel methanotrophic communities in forest soil that oxidize atmospheric methane. *Applied Environmental Microbiology,* **66**, 1801-1808.

Henckel T., Roslev P. & Conrad R. (2000b). Effects of O_2 and CH_4 on presence and activity of the indigenous methanotrophic community in rice field soil. *Environmental Microbiology,* **2**, 666-679.

Hester A.J., Miles J. & Gimingham C.H. (1991). Succession from heather moorland to birch woodland. I. Experimental alteration of specific environmental conditions in the field. *Journal of Ecology,* **79**, 303-315.

Hewitt A.E. (1993). *New Zealand soil classification*. Landcare Research: Lincoln, New Zealand.

Heyer J., Berger U., Hardt M. & Dunfield P.F. (2005). *Methylohalobius crimeensis* gen. nov., sp. nov., a moderately halophilic, methanotrophic bacterium isolated from hypersaline lakes of Crimea. *International Journal of Systematic and Evolutionary Microbiology,* **55**, 1817-1826.

Hinrichs K.U., Hayes J.M., Sylva S.P., Brewer P.G. & DeLong E.F. (1999). Methane-consuming archaebacteria in marine sediments. *Nature,* **398**, 802-805.

Hirayama H., Suzuki Y., Abe M., Miyazaki M., Makita H., Inagaki F., Uematsu K. & Takai K. (2010). *Methylothermus subterraneus* sp. nov., a moderately thermophilic methanotrophic bacterium from a terrestrial subsurface hot aquifer in Japan. *International Journal of Systematic and Evolutionary Microbiology*.

Holmes A.J., Costello A.M., Lidstrom M.E. & Murrell J.C. (1995). Evidence that particulate methane monooxygenase and ammonia monooxygenase may be evolutionarily related. *FEMS Microbiology Letters,* **132**, 203-208.

Holmes A.J., Roslev P., McDonald I.R., Iversen N., Henriksen K. & Murrell J.C. (1999). Characterization of methanotrophic bacterial populations in soils showing atmospheric methane uptake. *Applied Environmental Microbiology,* **65**, 3312-3318.

Horz H.P., Rich V., Avrahami S. & Bohannan B.J. (2005). Methane-oxidizing bacteria in a California upland grassland soil: diversity and response to simulated global change. *Applied Environmental Microbiology,* **71**, 2642-2652.

Horz H.P., Yimga M.T. & Liesack W. (2001). Detection of methanotroph diversity on roots of submerged rice plants by molecular retrieval of *pmoA*, *mmoX*, *mxaF* and 16S rRNA and ribosomal DNA, including *pmoA*-based terminal restriction fragment length polymorphism profiling. *Applied Environmental Microbiology,* **67**, 4177-4185.

Hou S., Makarova K.S., Saw J.H., Senin P., Ly B.V., Zhou Z., Ren Y., Wang J., Galperin M.Y., Omelchenko M.V., Wolf Y.I., Yutin N., Koonin E.V., Stott M.B., Mountain B.W., Crowe M.A., Smirnova A.V., Dunfield P.F., Feng L., Wang L. & Alam M. (2008). Complete genome sequence of the extremely acidophilic methanotroph isolate V4, *Methylacidiphilum infernorum*, a representative of the bacterial phylum *Verrucomicrobia*. *Biology Direct,* **3**, 26.

Huang W.E., Ferguson A., Singer A.C., Lawson K., Thompson I.P., Kalin R.M., Larkin M.J., Bailey M.J. & Whiteley A.S. (2009). Resolving genetic functions within microbial populations: *in situ* analyses using rRNA and mRNA stable isotope probing coupled with single-cell raman-fluorescence *in situ* hybridization. *Applied Environmental Microbiology,* **75**, 234-241.

Hütsch B.W. (1996). Methane oxidation in soils of two long-term fertilization experiments in Germany. *Soil Biology and Biochemistry,* **28**, 773-782.

Hütsch B.W. (1998). Tillage and land use effects on methane oxidation rates and their vertical profiles in soil. *Biology and Fertility of Soils,* **27**, 284-292.

Hütsch B.W., Webster C.P. & Powlson D.S. (1994). Methane oxidation in soil as affected by land use, soil pH and N fertilization. *Soil Biology and Biochemistry,* **26**, 1613-1622.

Iguchi H., Yurimoto H. & Sakai Y. (2010a). *Methylovulum miyakonense* gen. nov., sp. nov., a novel type I methanotroph from a forest soil in Japan. *International Journal of Systematic and Evolutionary Microbiology.*

Iguchi H., Yurimoto H. & Sakai Y. (2010b). Soluble and particulate methane monooxygenase gene clusters of the type I methanotroph *Methylovulum miyakonense* HT12. *FEMS Microbiology Letters,* **312**, 71-76.

Iguchi H., Yurimoto H. & Sakai Y. (2011). *Methylovulum miyakonense* gen. nov., sp. nov., a type I methanotroph isolated from forest soil. *International Journal of Systematic and Evolutionary Microbiology,* **61**, 810-815.

IPCC (2001). Climate change 2001: The scientific basis. In: *Contribution of Working Group I to the third assessment report of the Intergovernmental Panel on Climate Change (IPCC).* Edited by: J.T. Houghton, Y. Ding, D.J. Griggs, M. Noguer, P.J. van der Linden, X. Dai, K. Maskell & C.A. Johnson. Cambridge University Press, Cambridge, United Kingdom and New York, NY, USA.

IPCC (2007). Climate change 2007: The physical science basis. In: *Contribution of Working Group I to the fourth assessment report of the Intergovernmental Panel on Climate Change (IPCC).* Edited by: S. Solomon, D. Qin, M. Manning, Z. Chen, M. Marquis, K.B. Averyt, M. Tignor & H.L. Miller. Cambridge University Press, Cambridge, United Kingdom and New York, NY, USA.

Islam T., Jensen S., Reigstad L.J., Larsen Ø. & Birkeland N.K. (2008). Methane oxidation at 55 degrees C and pH 2 by a thermoacidophilic bacterium belonging to the *Verrucomicrobia* phylum. *Proceedings of the National Academy of Sciences U. S. A.,* **105**, 300-304.

Jäckel U., Schnell S. & Conrad R. (2001). Effect of moisture, texture and aggregate size of paddy soil on production and consumption of CH_4. *Soil Biology and Biochemistry,* **33**, 965-971.

Jandl R., Lindner M., Vesterdal L., Bauwens B., Baritz R., Hagedorn F., Johnson D.W., Minkkinen K. & Byrne K.A. (2007). How strongly can forest management influence soil carbon sequestration? *Geoderma,* **137**, 253-268.

Jehmlich N., Schmidt F., Taubert M., Seifert J., Bastida F., von Bergen M., Richnow H.H. & Vogt C. (2010). Protein-based stable isotope probing. *Nature Protocols,* **5**, 1957-1966.

Jehmlich N., Schmidt F., von Bergen M., Richnow H.H. & Vogt C. (2008). Protein-based stable isotope probing (Protein-SIP) reveals active species within anoxic mixed cultures. *ISME Journal,* **2**, 1122-1133.

Jobbágy E.G. & Jackson R.B. (2003). Patterns and mechanisms of soil acidification in the conversion of grasslands to forests. *Biogeochemistry*, **64**, 205-229.

Johnson D.W. (1992). Effects of forest management on soil carbon storage. *Water, Air, & Soil Pollution*, **64**, 83-120.

Kaplan C.W. & Kitts C.L. (2003). Variation between observed and true terminal-restriction fragment length is dependent on true T-RF length and purine content. *Journal of Microbiological Methods*, **54**, 121-125.

Keith A.M., van der Wal R., Brooker R.W., Osler G.H.R., Chapman S.J. & Burslem D.F.R.P. (2006). Birch invasion of heather moorland increases nematode diversity and trophic complexity. *Soil Biology and Biochemistry*, **38**, 3421-3430.

Keller M., Mitre M.E. & Stallard R.F. (1990). Consumption of atmospheric methane in soils of central Panama: Effects of agricultural development. *Global Biogeochemical Cycles*, **4**, 21-27.

Keller M. & Reiners W.A. (1994). Soil atmosphere exchange of nitrous oxide, nitric oxide, and methane under secondary succession of pasture to forest in the Atlantic Lowlands of Costa Rica. *Global Biogeochemical Cycles*, **8**, 399-409.

Keppler F., Hamilton J.T.G., Brass M. & Röckmann T. (2006). Methane emissions from terrestrial plants under aerobic conditions. *Nature*, **439**, 187-191.

Khadem A.F., Pol A., Jetten M.S. & Op den Camp H.J. (2010). Nitrogen fixation by the verrucomicrobial methanotroph '*Methylacidiphilum fumariolicum*' SolV. *Microbiology*, **156**, 1052-1059.

Kim H.J., Galeva N., Larive C.K., Alterman M. & Graham D.W. (2005). Purification and physical-chemical properties of methanobactin: a chalkophore from *Methylosinus trichosporium* OB3b. *Biochemistry*, **44**, 5140-5148.

Kim H.J., Graham D.W., Dispirito A.A., Alterman M.A., Galeva N., Larive C.K., Asunskis D. & Sherwood P.M. (2004). Methanobactin, a copper-acquisition compound from methane-oxidizing bacteria. *Science*, **305**, 1612-1615.

Kitts C.L. (2001). Terminal-restriction fragment patterns: a tool for comparing microbial communities and assessing community dynamics. *Current Issues in Intestinal Microbiology*, **2**, 17-25.

Knapp C.W., Fowle D.A., Kulczycki E., Roberts J.A. & Graham D.W. (2007). Methane monooxygenase gene expression mediated by methanobactin in the presence of mineral copper sources. *Proceedings of the National Academy of Sciences U. S. A.*, **104**, 12040-12045.

Knief C. & Dunfield P.F. (2005). Response and adaptation of different methanotrophic bacteria to low methane mixing ratios. *Environmental Microbiology*, **7**, 1307-1317.

Knief C., Kolb S., Bodelier P.L., Lipski A. & Dunfield P.F. (2006). The active methanotrophic community in hydromorphic soils changes in response to changing methane concentration. *Environmental Microbiology*, **8**, 321-333.

Knief C., Lipski A. & Dunfield P.F. (2003). Diversity and activity of methanotrophic bacteria in different upland soils. *Applied Environmental Microbiology,* **69**, 6703-6714.

Knief C., Vanitchung S., Harvey N.W., Conrad R., Dunfield P.F. & Chidthaisong A. (2005). Diversity of methanotrophic bacteria in tropical upland soils under different land uses. *Applied Environmental Microbiology,* **71**, 3826-3831.

Koh S.C., Bowman J.P. & Sayler G.S. (1993). Soluble methane monooxygenase production and trichloroethylene degradation by a type I methanotroph, *Methylomonas methanica* 68-1. *Applied Environmental Microbiology,* **59**, 960-967.

Kolb S. (2009). The quest for atmospheric methane oxidizers in forest soils. *Environmental Microbiology Reports,* **1**, 336-346.

Korotkova N., Chistoserdova L., Kuksa V. & Lidstrom M.E. (2002). Glyoxylate regeneration pathway in the methylotroph *Methylobacterium extorquens* AM1. *Journal of Bacteriology,* **184**, 1750-1758.

Kravchenko I.K., Kizilova A.K., Bykova S.A., Men'ko E.V. & Gal'chenko V.F. (2010). Molecular analysis of high-affinity methane-oxidizing enrichment cultures isolated from a forest biocenosis and agrocenoses. *Microbiology,* **79**, 106-114.

Kruse C.W. & Iversen N. (1995). Effect of plant succession, ploughing, and fertilization on the microbiological oxidation of atmospheric methane in a heathland soil. *FEMS Microbiology Ecology,* **18**, 121-128.

Kumar S., Nei M., Dudley J. & Tamura K. (2008). MEGA: A biologist-centric software for evolutionary analysis of DNA and protein sequences. *Briefings in Bioinformatics,* **9**, 299-306.

Kvenvolden K.A. & Rogers B.W. (2005). Gaia's breath - global methane exhalations. *Marine and Petroleum Geology,* **22**, 579-590.

Lacis A., Hansen J., Lee P., Mitchell T. & Lebedeff S. (1981). Greenhouse effect of trace gases, 1970-1980. *Geophysical Research Letters,* **8**, 1035-1038.

Lawrence A.J. & Quayle J.R. (1970). Alternative carbon assimilation pathways in methane-utilizing bacteria. *Journal of General Microbiology,* **63**, 371-374.

Le Mer J. & Roger P. (2001). Production, oxidation, emission and consumption of methane by soils: A review. *European Journal of Soil Biology,* **37**, 25-50.

Lelieveld J. (2006). Climate change: a nasty surprise in the greenhouse. *Nature,* **443**, 405-406.

Lelieveld J., Crutzen P.J. & Dentener F.J. (1998). Changing concentration, lifetime and climate forcing of atmospheric methane. *Tellus B,* **50**, 128-150.

Lessard R., Rochette P., Topp E., Pattey E., Desjardins R.L. & Beaumont G. (1994). Methane and carbon dioxide fluxes from poorly drained adjacent cultivated and forest sites. *Canadian Journal of Soil Science,* **74**, 139-146.

Li C., Frolking S. & Frolking T.A. (1992a). A model of nitrous oxide evolution from soil driven by rainfall events: 1. Model structure and sensitivity. *Journal of Geophysical Research,* **97**, 9759-9776.

Li C., Frolking S. & Frolking T.A. (1992b). A model of nitrous oxide evolution from soil driven by rainfall events: 2. Model applications. *Journal of Geophysical Research,* **97**, 9777-9783.

Li C., Narayanan V. & Harriss R.C. (1996). Model estimates of nitrous oxide emissions from agricultural lands in the United States. *Global Biogeochemical Cycles,* **10**, 297-306.

Li C.S. (2000). Modeling trace gas emissions from agricultural ecosystems. *Nutrient Cycling in Agroecosystems,* **58**, 259-276.

Li C., Zhuang Y., Cao M., Crill P., Dai Z., Frolking S., Moore B., Salas W., Song W. & Wang X. (2001). Comparing a process-based agro-ecosystem model to the IPCC methodology for developing a national inventory of N_2O emissions from arable lands in China. *Nutrient Cycling in Agroecosystems,* **60**, 159-175.

Lieberman R.L. & Rosenzweig A.C. (2004). Biological methane oxidation: regulation, biochemistry, and active site structure of particulate methane monooxygenase. *Critical Reviews in Biochemistry and Molecular Biology,* **39**, 147-164.

Linn D.M. & Doran J.W. (1984). Effect of water-filled pore space on carbon dioxide and nitrous oxide production in tilled and nontilled soils. *Soil Science Society of America Journal,* **48**, 1267-1272.

Lipscomb J.D. (1994). Biochemistry of the soluble methane monooxygenase. *Annual Reviews in Microbiology,* **48**, 371-399.

Liu W.T., Marsh T.L., Cheng H. & Forney L.J. (1997). Characterization of microbial diversity by determining terminal-restriction fragment length polymorphisms of genes encoding 16S rRNA. *Applied Environmental Microbiology,* **63**, 4516-4522.

Liu Y. & Whitman W. (2008). Metabolic, phylogenetic, and ecological diversity of the methanogenic *Archaea*. *Annals of the New York Academy of Sciences,* **1125**, 171-189.

Lloyd J.S., Bhambra A., Murrell J.C. & Dalton H. (1997). Inactivation of the regulatory protein B of soluble methane monooxygenase from *Methylococcus capsulatus* (Bath) by proteolysis can be overcome by a Gly to Gin modification. *European Journal of Biochemistry,* **248**, 72-79.

Lueders T., Chin K.J., Conrad R. & Friedrich M. (2001). Molecular analyses of methyl-coenzyme M reductase alpha-subunit (*mcrA*) genes in rice field soil and enrichment cultures reveal the methanogenic phenotype of a novel archaeal lineage. *Environmental Microbiology,* **3**, 194-204.

Lueders T., Manefield M. & Friedrich M.W. (2004). Enhanced sensitivity of DNA- and rRNA-based stable isotope probing by fractionation and quantitative analysis of isopycnic centrifugation gradients. *Environmental Microbiology,* **6**, 73-78.

MacDonald J.A., Skiba U., Sheppard L.J., Ball B., Roberts J.D., Smith K.A. & Fowler D. (1997). The effect of nitrogen deposition and seasonal variability on methane oxidation and nitrous oxide emission rates in an upland spruce plantation and moorland. *Atmospheric Environment,* **31**, 3693-3706.

MacDonald J.A., Skiba U., Sheppard L.J., Hargreaves K.J., Smith K.A. & Fowler D. (1996). Soil environmental variables affecting the flux of methane from a range of forest, moorland and agricultural soils. *Biogeochemistry*, **34**, 113-132.

Manefield M., Whiteley A.S., Griffiths R.I. & Bailey M.J. (2002). RNA stable isotope probing, a novel means of linking microbial community function to phylogeny. *Applied Environmental Microbiology,* **68**, 5367-5373.

Maxfield P.J., Hornibrook E.R. & Evershed R.P. (2006). Estimating high-affinity methanotrophic bacterial biomass, growth, and turnover in soil by phospholipid fatty acid ^{13}C labeling. *Applied Environmental Microbiology,* **72**, 3901-3907.

Maxfield P.J., Hornibrook E.R.C. & Evershed R.P. (2008). Acute impact of agriculture on high-affinity methanotrophic bacterial populations. *Environmental Microbiology,* **10**, 1917-1924.

McDonald I.R., Bodrossy L., Chen Y. & Murrell J.C. (2008). Molecular ecology techniques for the study of aerobic methanotrophs. *Applied Environmental Microbiology*, **74**, 1305-1315.

McGowan G.M., Palmer S.C.F., French D.D., Barr C.J., Howard D.C., Smart S.M., Mackey E.C. & Shewry M.C. (2002). Trends in Broad Habitats: Scotland 1990-1998. In: Scottish Natural Heritage commissioned report F00NB03.

Megonigal J.P. & Guenther A.B. (2008). Methane emissions from upland forest soils and vegetation. *Tree Physiology,* **28**, 491-498.

Menyailo O.V., Abraham W.R. & Conrad R. (2010). Tree species affect atmospheric CH_4 oxidation without altering community composition of soil methanotrophs. *Soil Biology and Biochemistry*, **42**, 101-107.

Menyailo O.V. & Hungate B.A. (2003). Interactive effects of tree species and soil moisture on methane consumption. *Soil Biology and Biochemistry*, **35**, 625-628.

Merkx M. & Lippard S.J. (2002). Why OrfY? Characterization of MMOD, a long overlooked component of the soluble methane monooxygenase from *Methylococcus capsulatus* (Bath). *Journal of Biological Chemistry,* **277**, 5858-5865.

Miles J. (1981). *Effects of birch on moorlands*. Institute of Terrestrial Ecology, Banchory, UK.

Miles J. & Young W.F. (1980). The effects on heathland and moorland soils in scotland and northern england following colonization by birch (*Betula* spp.). *Bulletin D Ecologie*, **11**, 233-242.

Miller J.D., Anderson H.A., Ray D. & Anderson A.R. (1996). Impact of some initial forestry practices on the drainage waters from blanket peatlands. *Forestry,* **69**, 193-203.

Minkkinen K. & Laine J. (2006). Vegetation heterogeneity and ditches create spatial variability in methane fluxes from peatlands drained for forestry. *Plant and Soil,* **285**, 289-304.

Mitchell R.J., Campbell C.D., Chapman S.J., Osler G.H.R., Vanbergen A.J., Ross L.C., Cameron C.M. & Cole L. (2007). The cascading effects of birch on heather moorland: a test for the top-down control of an ecosystem engineer. *Journal of Ecology,* **95**, 540-554.

Mitchell R.J., Hester A., Campbell C.D., Chapman S.J., Cameron C.M., Hewison R. & Potts J. (2010). Is vegetation composition or soil chemistry the best predictor of the soil microbial community? *Plant and Soil,* **333**, 417-430.

Moeseneder M.M., Winter C., Arrieta J.M. & Herndl G.J. (2001). Terminal-restriction fragment length polymorphism (T-RFLP) screening of a marine archaeal clone library to determine the different phylotypes. *Journal of Microbiological Methods,* **44**, 159-172.

Mohanty S.R., Bodelier P.L.E., Floris V. & Conrad R. (2006). Differential effects of nitrogenous fertilizers on methane-consuming microbes in rice field and forest Soils. *Applied and Environmental Microbiology,* **72**, 1346-1354.

Mojeremane W., Rees R. & Mencuccini M. (2010). Effects of site preparation for afforestation on methane fluxes at Harwood Forest, NE England. *Biogeochemistry,* **97**, 89-107.

Morgan R.M., Pihl T.D., Nolling J. & Reeve J.N. (1997). Hydrogen regulation of growth, growth yields, and methane gene transcription in *Methanobacterium thermoautotrophicum* ΔH. *Journal of Bacteriology,* **179**, 889-898.

Mosier A., Schimel D., Valentine D., Bronson K. & Parton W. (1991). Methane and nitrous oxide fluxes in native, fertilized and cultivated grasslands. *Nature*, **350**, 330-332.

Murrell J.C. & Dalton H. (1983). Nitrogen fixation in obligate methanotrophs. *Journal of General Microbiology,* **129**, 3481-3486.

Murrell J.C., Gilbert B. & McDonald I.R. (2000a). Molecular biology and regulation of methane monooxygenase. *Archives of Microbiology,* **173**, 325-332.

Murrell J.C. & Jetten M.S.M. (2009). The microbial methane cycle. *Environmental Microbiology Reports*, **1**, 279-284.

Murrell J.C., McDonald I.R. & Gilbert B. (2000b). Regulation of expression of methane monooxygenases by copper ions. *Trends in Microbiology,* **8**, 221-225.

Murrell J.C. & Whiteley A.S. (2011). *Stable isotope probing and related technologies*. ASM Press.

Neue H.U., Wassmann R., Kludze H.K., Bujun W. & Lantin R.S. (1997). Factors and processes controlling methane emissions from rice fields. *Nutrient Cycling in Agroecosystems,* **49**, 111-117.

Neufeld J.D., Dumont M.G., Vohra J. & Murrell J.C. (2007a). Methodological considerations for the use of stable isotope probing in microbial ecology. *Microb. Ecol.*, **53**, 435-442.

Neufeld J.D., Vohra J., Dumont M.G., Lueders T., Manefield M., Friedrich M.W. & Murrell J.C. (2007b). DNA stable-isotope probing. *Nature Protocols*, **2**, 860-866.

Nielsen A.K., Gerdes K. & Murrell J.C. (1997). Copper-dependent reciprocal transcriptional regulation of methane monooxygenase genes in *Methylococcus capsulatus* and *Methylosinus trichosporium*. *Molecular Microbiology*, **25**, 399-409.

Nielsen U.N., Osler G.H.R., Campbell C.D., Burslem D.F.R.P. & van der Wal R. (2010). The influence of vegetation type, soil properties and precipitation on the composition of soil mite and microbial communities at the landscape scale. *Journal of Biogeography*, **37**, 1317-1328.

Nielsen U.N., Osler G.H.R., van der Wal R., Campbell C.D. & Burslem D.F.R.P. (2008). Soil pore volume and the abundance of soil mites in two contrasting habitats. *Soil Biology and Biochemistry*, **40**, 1538-1541.

Nisbet R.E.R., Fisher R., Nimmo R.H., Bendall D.S., Crill P.M., Gallego-Sala A.V., Hornibrook E.R.C., López-Juez E., Lowry D., Nisbet P.B.R., Shuckburgh E.F., Sriskantharajah S., Howe C.J. & Nisbet E.G. (2009). Emission of methane from plants. *Proceedings of the Royal Society B: Biological Sciences*, **276**, 1347-1354.

Noll M., Frenzel P. & Conrad R. (2008). Selective stimulation of type I methanotrophs in a rice paddy soil by urea fertilization revealed by RNA-based stable isotope probing. *FEMS Microbiology Ecology*, **65**, 125-132.

Oades J. (1988). The retention of organic matter in soils. *Biogeochemistry*, **5**, 35-70.

Ojima D.S., Valentine D.W., Mosier A.R., Parton W.J. & Schimel D.S. (1993). Effect of land-use change on methane oxidation in temperate forest and grassland soils. *Chemosphere*, **26**, 675-685.

Op den Camp H.J.M., Islam T., Stott M.B., Harhangi H.R., Hynes A., Schouten S., Jetten M.S.M., Birkeland N.K., Pol A. & Dunfield P.F. (2009). Environmental, genomic and taxonomic perspectives on methanotrophic *Verrucomicrobia*. *Environmental Microbiology Reports*, **1**, 293-306.

Osborn A.M., Moore E.R. & Timmis K.N. (2000). An evaluation of terminal-restriction fragment length polymorphism (T-RFLP) analysis for the study of microbial community structure and dynamics. *Environmental Microbiology*, **2**, 39-50.

Paterson E., Gebbing T., Abel C., Sim A. & Telfer G. (2007). Rhizodeposition shapes rhizosphere microbial community structure in organic soil. *New Phytologist*, **173**, 600-610.

Paul K.I., Polglase P.J., Nyakuengama J.G. & Khanna P.K. (2002). Change in soil carbon following afforestation. *Forest Ecology and Management*, **168**, 241-257.

Pennings J.L., Keltjens J.T. & Vogels G.D. (1998). Isolation and characterization of *Methanobacterium thermoautotrophicum* ΔH mutants unable to grow under hydrogen-deprived conditions. *Journal of Bacteriology*, **180**, 2676-2681.

Petersen J.M. & Dubilier N. (2009). Methanotrophic symbioses in marine invertebrates. *Environmental Microbiology Reports*, **1**, 319-335.

Phelps P.A., Agarwal S.K., Speitel G.E. & Georgiou G. (1992). *Methylosinus trichosporium* OB3b mutants having constitutive expression of soluble methane monooxygenase in the presence of high levels of copper. *Applied Environmental Microbiology*, **58**, 3701-3708.

Pihl T.D., Sharma S. & Reeve J.N. (1994). Growth phase-dependent transcription of the genes that encode the two methyl coenzyme M reductase isoenzymes and N5-methyltetrahydromethanopterin:coenzyme M methyltransferase in *Methanobacterium thermoautotrophicum* DeltaH. *Journal of Bacteriology*, **176**, 6384-6391.

Pol A., Heijmans K., Harhangi H.R., Tedesco D., Jetten M.S. & Op den Camp H.J. (2007). Methanotrophy below pH 1 by a new *Verrucomicrobia* species. *Nature*, **450**, 874-878.

Post W.M. & Kwon K.C. (2000). Soil carbon sequestration and land-use change: processes and potential. *Global Change Biology*, **6**, 317-327.

Price S.J., Sherlock R.R., Kelliher F.M., McSeveny T.M., Tate K.R. & Condron L.M. (2003). Pristine New Zealand forest soil is a strong methane sink. *Global Change Biology*, **10**, 16-26.

Priemé A., Christensen S., Dobbie K.E. & Smith K.A. (1997). Slow increase in rate of methane oxidation in soils with time following land use change from arable agriculture to woodland. *Soil Biology and Biochemistry*, **29**, 1269-1273.

Priemé A. & Ekelund F. (2001). Five pesticides decreased oxidation of atmospheric methane in a forest soil. *Soil Biology and Biochemistry*, **33**, 831-835.

Prior S.D. & Dalton H. (1985a). Acetylene as a suicide substrate and active site probe for methane monooxygenase from *Methylococcus capsulatus* (Bath). *FEMS Microbiology Letters*, **29**, 105-109.

Prior S.D. & Dalton H. (1985b). The effect of copper ions on membrane content and methane monooxygenase activity in methanol-grown cells of *Methylococcus capsulatus* (Bath). *Journal of General Microbiology*, **131**, 155-163.

Radajewski S., Ineson P., Parekh N.R. & Murrell J.C. (2000). Stable-isotope probing as a tool in microbial ecology. *Nature*, **403**, 646-649.

Raghoebarsing A.A., Pol A., van de Pas-Schoonen K., Smolders A.J.P., Ettwig K.F., Rijpstra W.I., Schouten S., Damste J.S.S., Op den Camp H.J.M., Jetten M.S.M. & Strous M. (2006). A microbial consortium couples anaerobic methane oxidation to denitrification. *Nature*, **440**, 918-921.

Raghoebarsing A.A., Smolders A.J.P., Schmid M.C., Rijpstra W.I., Wolters-Arts M., Derksen J., Jetten M.S.M., Schouten S., Sinninghe Damste J.S., Lamers L.P.M., Roelofs J.G.M., Op den Camp H.J.M. & Strous M. (2005). Methanotrophic symbionts provide carbon for photosynthesis in peat bogs. *Nature,* **436**, 1153-1156.

Rahalkar M., Bussmann I. & Schink B. (2007). *Methylosoma difficile* gen. nov., sp. nov., a novel methanotroph enriched by gradient cultivation from littoral sediment of Lake Constance. *International Journal of Systematic and Evolutionary Microbiology,* **57**, 1073-1080.

Rao R.S., Kumar C.G., Prakasham R.S. & Hobbs P.J. (2008). The Taguchi methodology as a statistical tool for biotechnological applications: A critical appraisal. *Biotechnology Journal*, **3**, 510-523.

Reay D.S., Nedwell D.B., McNamara N. & Ineson P. (2005). Effect of tree species on methane and ammonium oxidation capacity in forest soils. *Soil Biology and Biochemistry,* **37**, 719-730.

Reay D.S., Radajewski S., Murrell J.C., McNamara N. & Nedwell D.B. (2001). Effects of land-use on the activity and diversity of methane oxidizing bacteria in forest soils. *Soil Biology and Biochemistry,* **33**, 1613-1623.

Reay D.S., Smith P. & van Amstel A. (2010). *Methane and climate change*. Earthscan.

Reeburgh W.S. (2003). Global methane biogeochemistry. In: *Treatise on Geochemistry*. Edited by: D.H. Heinrich & K.T. Karl. Pergamon, Oxford, pp. 1-32.

Reeve J.N., Nolling J., Morgan R.M. & Smith D.R. (1997). Methanogenesis: genes, genomes, and who's on first? *Journal of Bacteriology*, **179**, 5975-5986.

Ricke P., Erkel C., Kube M., Reinhardt R. & Liesack W. (2004). Comparative analysis of the conventional and novel *pmo* (particulate methane monooxygenase) operons from *Methylocystis* strain SC2. *Applied Environmental Microbiology*, **70**, 3055-3063.

Ricke P., Kube M., Nakagawa S., Erkel C., Reinhardt R. & Liesack W. (2005). First genome data from uncultured upland soil cluster alpha methanotrophs provide further evidence for a close phylogenetic relationship to *Methylocapsa acidiphila* B2 and for high-affinity methanotrophy involving particulate methane monooxygenase. *Applied Environmental Microbiology*, **71**, 7472-7482.

Rogers G.M. (1994). North-Island Seral Tussock Grasslands .1. Origins and Land-Use History. *New Zealand Journal of Botany,* **32**, 271-286.

Ross D.J., Scott N.A., Lambie S.M., Trotter C.M., Rodda N.J. & Townsend J.A. (2009). Nitrogen and carbon cycling in a New Zealand pumice soil under a manuka (*Leptospermum scoparium*) and kanuka (*Kunzea ericoides*) shrubland. *Soil Research,* **47**, 725-736.

Ross D.J., Tate K.R., Scott N.A. & Feltham C.W. (1999). Land-use change: effects on soil carbon, nitrogen and phosphorus pools and fluxes in three adjacent ecosystems. *Soil Biology and Biochemistry*, **31**, 803-813.

Ruess L. & Chamberlain P.M. (2010). The fat that matters: Soil food web analysis using fatty acids and their carbon stable isotope signature. *Soil Biology and Biochemistry*, **42**, 1898-1910.

Saggar S., Andrew R.M., Tate K.R., Hedley C.B., Rodda N.J. & Townsend J.A. (2004). Modelling nitrous oxide emissions from dairy-grazed pastures. *Nutrient Cycling in Agroecosystems*, **68**, 243-255.

Saggar S., Hedley C.B., Giltrap D.L. & Lambie S.M. (2007). Measured and modelled estimates of nitrous oxide emission and methane consumption from a sheep-grazed pasture. *Agriculture Ecosystems & Environment*, **122**, 357-365.

Saggar S., Tate K., Giltrap D. & Singh J. (2008). Soil-atmosphere exchange of nitrous oxide and methane in New Zealand terrestrial ecosystems and their mitigation options: a review. *Plant and Soil*, **309**, 25-42.

Sakai S., Conrad R., Liesack W. & Imachi H. (2010). *Methanocella arvoryzae* sp. nov., a hydrogenotrophic methanogen isolated from rice field soil. *International Journal of Systematic and Evolutionary Microbiology*, **60**, 2918-2923.

Sakai S., Imachi H., Hanada S., Ohashi A., Harada H. & Kamagata Y. (2008). *Methanocella paludicola* gen. nov., sp. nov., a methane-producing archaeon, the first isolate of the lineage 'Rice Cluster I', and proposal of the new archaeal order *Methanocellales* ord. nov. *International Journal of Systematic and Evolutionary Microbiology*, **58**, 929-936.

Sakai S., Imachi H., Sekiguchi Y., Ohashi A., Harada H. & Kamagata Y. (2007). Isolation of key methanogens for global methane emission from rice paddy fields: a novel isolate affiliated with the clone cluster rice cluster I. *Applied Environmental Microbiology*, **73**, 4326-4331.

Sass R.L., Fisher F.M., Lewis S.T., Jund M.F. & Turner F.T. (1994). Methane emissions from rice fields: Effect of soil properties. *Global Biogeochemical Cycles*, **8**, 135-140.

Scanlan J., Dumont M.G. & Murrell J.C. (2009). Involvement of MmoR and MmoG in the transcriptional activation of soluble methane monooxygenase genes in *Methylosinus trichosporium* OB3b. *FEMS Microbiology Letters*, **301**, 181-187.

Schena M., Shalon D., Davis R.W. & Brown P.O. (1995). Quantitative monitoring of gene expression patterns with a complementary DNA microarray. *Science*, **270**, 467-470.

Schulze E.D., Luyssaert S., Ciais P., Freibauer A. & Janssens E.A. (2009). Importance of methane and nitrous oxide for Europe's terrestrial greenhouse-gas balance. *Nature Geoscience*, **2**, 842-850.

Schütte U.M., Abdo Z., Bent S.J., Shyu C., Williams C.J., Pierson J.D. & Forney L.J. (2008). Advances in the use of terminal-restriction fragment length polymorphism (T-RFLP) analysis of 16S rRNA genes to characterize microbial communities. *Applied Microbiology and Biotechnology*, **80**, 365-380.

Scott N.A., Tate K.R., Giltrap D.J., Newsome P.F., Davis M.R., Baisden W.T., Saggar S., Trotter C.M., Walcroft A.S., White J.D., Trustrum N.A. & Stephens P.R. (2001). Critical issues in quantifying land-use change effects on New Zealand's terrestrial carbon budget: Deforestation, afforestation, and reforestation. In: Sixth International Carbon Dioxide Conference, Sendai, Japan. Pp. 559-561, Extended abstract.

Scott N.A., White J.D., Townsend J.A., Whitehead D., Leathwick J.R., Hall G.M.J., Marden M., Rogers G.N.D., Watson A.J. & Whaley P.T. (2000). Carbon and nitrogen distribution and accumulation in a New Zealand scrubland ecosystem. *Canadian Journal of Forest Research-Revue Canadienne de Recherche Forestiere,* **30**, 1246-1255.

Seghers D., Siciliano S.D., Top E.M. & Verstraete W. (2005). Combined effect of fertilizer and herbicide applications on the abundance, community structure and performance of the soil methanotrophic community. *Soil Biology and Biochemistry,* **37**, 187-193.

Seghers D., Top E.M., Reheul D., Bulcke R., Boeckx P., Verstraete W. & Siciliano S.D. (2003a). Long-term effects of mineral versus organic fertilizers on activity and structure of the methanotrophic community in agricultural soils. *Environmental Microbiology,* **5**, 867-877.

Seghers D., Verthé K., Reheul D., Bulcke R., Siciliano S.D., Verstraete W. & Top E.M. (2003b). Effect of long-term herbicide applications on the bacterial community structure and function in an agricultural soil. *FEMS Microbiology Ecology,* **46**, 139-146.

Semrau J.D., Dispirito A.A. & Yoon S. (2010). Methanotrophs and copper. *FEMS Microbiology Reviews,* **34**, 496-531.

Semrau J.D., Zolandz D., Lidstrom M.E. & Chan S.I. (1995). The role of copper in the pMMO of *Methylococcus capsulatus* bath: a structural *vs*. catalytic function. *Journal of Inorganic Biochemistry,* **58**, 235-244.

Shigematsu T., Hanada S., Eguchi M., Kamagata Y., Kanagawa T. & Kurane R. (1999). Soluble methane monooxygenase gene clusters from trichloroethylene-degrading *Methylomonas* sp. strains and detection of methanotrophs during *in situ* bioremediation. *Applied Environmental Microbiology,* **65**, 5198-5206.

Shindell D.T., Faluvegi G., Koch D.M., Schmidt G.A., Unger N. & Bauer S.E. (2009). Improved attribution of climate forcing to emissions. *Science,* **326**, 716-718.

Singh B.K., Bardgett R.D., Smith P. & Reay D.S. (2010). Microorganisms and climate change: terrestrial feedbacks and mitigation options. *Nature Reviews Microbiology,* **8**, 779-790.

Singh B.K., Munro S., Reid E., Ord B., Potts J.M., Paterson E. & Millard P. (2006a). Investigating microbial community structure in soils by physiological, biochemical and molecular fingerprinting methods. *European Journal of Soil Science,* **57**, 72-82.

Singh B.K., Nazaries L., Munro S., Anderson I.C. & Campbell C.D. (2006b). Use of multiplex terminal-restriction fragment length polymorphism for rapid and simultaneous analysis of different components of the soil microbial community. *Applied Environmental Microbiology,* **72**, 7278-7285.

Singh B.K. & Tate K.R. (2007). Biochemical and molecular characterization of methanotrophs in soil from a pristine New Zealand beech forest. *FEMS Microbiology Letters,* **275**, 89-97.

Singh B.K., Tate K.R., Kolipaka G., Hedley C.B., Macdonald C.A., Millard P. & Murrell J.C. (2007). Effect of afforestation and reforestation of pastures on the activity and population dynamics of methanotrophic bacteria. *Applied Environmental Microbiology,* **73**, 5153-5161.

Singh B.K., Tate K.R., Ross D.J., Singh J., Dando J., Thomas N., Millard P. & Murrell J.C. (2009). Soil methane oxidation and methanotroph responses to afforestation of pastures with *Pinus radiata* stands. *Soil Biology and Biochemistry,* **41**, 2196-2205.

Singh B.K. & Thomas N. (2006). Multiplex-terminal restriction fragment length polymorphism. *Nature Protocols,* **1**, 2428-2433.

Sitaula B.K., Bakken L.R. & Abrahamsen G. (1995). CH_4 uptake by temperate forest soil: Effect of N input and soil acidification. *Soil Biology and Biochemistry,* **27**, 871-880.

Smith K.A., Ball T., Conen F., Dobbie K.E., Massheder J. & Rey A. (2003). Exchange of greenhouse gases between soil and atmosphere: interactions of soil physical factors and biological processes. *European Journal of Soil Science,* **54**, 779-791.

Smith K.A., Dobbie K.E., Ball B.C., Bakken L.R., Sitaula B.K., Hansen S., Brumme R., Borken W., Christensen S., Priemé A., Fowler D., MacDonald J.A., Skiba U., Klemedtsson L., Kasimir-Klemedtsson A., Degórska A. & Orlanski P. (2000). Oxidation of atmospheric methane in Northern European soils, comparison with other ecosystems, and uncertainties in the global terrestrial sink. *Global Change Biology,* **6**, 791-803.

Smith P. (2008). Land use change and soil organic carbon dynamics. *Nutrient Cycling in Agroecosystems,* **81**, 169-178.

Smith W.N., Desjardins R.L., Grant B., Li C., Lemke R., Corre M.D. & Pennock D. (2002). Testing the DNDC model using N_2O emissions at two experimental sites in Canada. *Canadian Journal of Soil Science,* **82**, 365-374.

Sneddon S., Brophy N., Li Y., MacCarthy J., Martinez C., Murrells T., Passant N., Thomas J., Thistlethwaite G., Tsagatakis I., Walker H., Thomson A. & Cardenas L. (2010). Greenhouse Gas Inventories for England, Scotland, Wales and Northern Ireland: 1990 - 2008. In: Department of Energy and Climate Change, The Scottish Government, The Welsh Assembly Government, The Northern Ireland Department of Environment.

Stafford G.P., Scanlan J., McDonald I.R. & Murrell J.C. (2003). *rpoN*, *mmoR* and *mmoG*, genes involved in regulating the expression of soluble methane monooxygenase in *Methylosinus trichosporium* OB3b. *Microbiology,* **149**, 1771-1784.

Stainthorpe A.C., Lees V., Salmond G.P., Dalton H. & Murrell J.C. (1990). The methane monooxygenase gene cluster of *Methylococcus capsulatus* (Bath). *Gene,* **91**, 27-34.

Stams A.J.M. (1994). Metabolic interactions between anaerobic bacteria in methanogenic environments. *Antonie van Leeuwenhoek,* **66**, 271-294.

Stams A.J.M. & Plugge C.M. (2009). Electron transfer in syntrophic communities of anaerobic bacteria and archaea. *Nature Reviews Microbiology,* **7**, 568-577.

Stanley S.H. & Dalton H. (1982). Role of ribulose-1,5-bisphosphate carboxylase/oxygenase in *Methylococcus capsulatus* (Bath). *Journal of General Microbiology,* **128**, 2927-2935.

Stanley S.H., Prior S.D., Leak D.J. & Dalton H. (1983). Copper stress underlies the fundamental change in intracellular location of methane mono-oxygenase in methane-oxidizing organisms - Studies in batch and continuous cultures. *Biotechnology Letters,* **5**, 487-492.

Steigerwald V.J., Stroup D., Hennigan A.N., Palmer J.R., Pihl T.D., Daniels C.J. & Reeve J.N. (1993). Methyl coenzyme-M reductase II genes and their close linkage to the methyl viologen-reducing hydrogenase-polyferredoxin operon in the genomes of *Methanobacterium thermoautotrophicum* and *Methanothermus fervidus.* In: *Industrial Microorganisms: Basic and Applied Molecular Genetics*. Edited by: R.H. Baltz, G.D. Hegeman & P.L. Skatrud. Washington, DC: American Society for Microbiology Press, pp. 109-115.

Stirling D.I. & Dalton H. (1979). Properties of the methane mono-oxygenase from extracts of *Methylosinus trichosporium* OB3b and evidence for its similarity to the enzyme from *Methylococcus capsulatus* (Bath). *European Journal of Biochemistry,* **96**, 205-212.

Stoecker K., Bendinger B., Schoning B., Nielsen P.H., Nielsen J.L., Baranyi C., Toenshoff E.R., Daims H. & Wagner M. (2006). Cohn's *Crenothrix* is a filamentous methane oxidizer with an unusual methane monooxygenase. *Proceedings of the National Academy of Sciences U. S. A.,* **103**, 2363-2367.

Stolyar S., Costello A.M., Peeples T.L. & Lidstrom M.E. (1999). Role of multiple gene copies in particulate methane monooxygenase activity in the methane-oxidizing bacterium *Methylococcus capsulatus* Bath. *Microbiology,* **145 (Pt 5)**, 1235-1244.

Stolyar S., Franke M. & Lidstrom M.E. (2001). Expression of individual copies of *Methylococcus capsulatus* bath particulate methane monooxygenase genes. *Journal of Bacteriology,* **183**, 1810-1812.

Stralis-Pavese N., Abell G.C.J., Sessitsch A. & Bodrossy L. (2011). Analysis of methanotroph community composition using a pmoA-based microbial diagnostic microarray. *Nature Protocols,* **6**, 609-624.

Stralis-Pavese N., Sessitsch A., Weilharter A., Reichenauer T., Riesing J., Csontos J., Murrell J.C. & Bodrossy L. (2004). Optimization of diagnostic microarray for application in analysing landfill methanotroph communities under different plant covers. *Environmental Microbiology,* **6**, 347-363.

Striegl R.G., McConnaughey T.A., Thorstenson D.C., Weeks E.P. & Woodward J.C. (1992). Consumption of atmospheric methane by desert soils. *Nature,* **357**, 145-147.

Sundh I., Borjesson G. & Tunlid A. (2000). Methane oxidation and phospholipid fatty acid composition in a podzolic soil profile. *Soil Biology and Biochemistry,* **32**, 1025-1028.

Szubert J., Reiff C., Thorburn A. & Singh B.K. (2007). REMA: A computer-based mapping tool for analysis of restriction sites in multiple DNA sequences. *Journal of Microbiological Methods,* **69**, 411-413.

Taguchi G. (1986). *Introduction to Quality Engineering*. Asian Productivity Organisation, Tokyo.

Tate K.R., Hedley C.B., Dando J. & Saggar S. (2005). Does afforestation of pastures increase soil methane oxidation? In: Lancare Reseach Report LC0405/100 prepared for the Ministry of Agriculture and Forestry, New Zealand.

Tate K.R., Ross D.J., Saggar S., Hedley C.B., Dando J., Singh B.K. & Lambie S.M. (2007). Methane uptake in soils from *Pinus radiata* plantations, a reverting shrubland and adjacent pastures: Effects of land-use change, and soil texture, water and mineral nitrogen. *Soil Biology and Biochemistry,* **39**, 1437-1449.

Tate K.R., Ross D.J., Scott N.A., Rodda N.J., Townsend J.A. & Arnold G.C. (2006). Post-harvest patterns of carbon dioxide production, methane uptake and nitrous oxide production in a *Pinus radiata* D. Don plantation. *Forest Ecology and Management,* **228**, 40-50.

Tchawa Yimga M., Dunfield P.F., Ricke P., Heyer J. & Liesack W. (2003). Wide distribution of a novel *pmoA*-like gene copy among type II methanotrophs, and its expression in *Methylocystis* strain SC2. *Applied Environmental Microbiology,* **69**, 5593-5602.

Thauer R.K. (1998). Biochemistry of methanogenesis: a tribute to Marjory Stephenson. *Microbiology,* **144**, 2377-2406.

Thauer R.K. & Shima S. (2008). Methane as fuel for anaerobic microorganisms. *Annals of the New York Academy of Sciences,* **1125**, 158-170.

Theisen A.R. & Murrell J.C. (2005). Facultative methanotrophs revisited. *Journal of Bacteriology,* **187**, 4303-4305.

Thies J.E. (2007). Soil microbial community analysis using terminal restriction fragment length polymorphisms. *Soil Science Society of America Journal,* **71**, 579-591.

Tiedje J.M., Asuming-Brempong S., Nüsslein K., Marsh T.L. & Flynn S.J. (1999). Opening the black box of soil microbial diversity. *Applied Soil Ecology,* **13**, 109-122.

Topp E. (1993). Effects of selected agrochemicals on methane oxidation by an organic agricultural soil. *Canadian Journal of Soil Science,* **73**, 287-291.

Topp E. & Pattey E. (1997). Soils as sources and sinks for atmospheric methane. *Canadian Journal of Soil Science,* **77**, 167-178.

Torsvik V. & Ovreas L. (2002). Microbial diversity and function in soil: from genes to ecosystems. *Current Opinion in Microbiology,* **5**, 240-245.

Trotsenko Y.A. & Khmelenina V.N. (2002). Biology of extremophilic and extremotolerant methanotrophs. *Archives of Microbiology,* **177**, 123-131.

Trotsenko Y.A. & Murrell J.C. (2008). Metabolic aspects of aerobic obligate methanotrophy. *Advances in Applied Microbiology,* **63**, 183-229.

Trotter C., Tate K., Scott N., Townsend J., Wilde H., Lambie S., Marden M. & Pinkney T. (2005). Afforestation/reforestation of New Zealand marginal pasture lands by indigenous shrublands: the potential for Kyoto forest sinks. *Annals of Forest Science,* **62**, 865-871.

Tsubota J., Eshinimaev B.T., Khmelenina V.N. & Trotsenko Y.A. (2005). *Methylothermus thermalis* gen. nov., sp. nov., a novel moderately thermophilic obligate methanotroph from a hot spring in Japan. *International Journal of Systematic and Evolutionary Microbiology,* **55**, 1877-1884.

UNFCCC (1998). The Kyoto Protocol to the United Nations Framework Convention on Climate Change. In: UNEP/INC/98/2, Information Unit for Conventions, United Nations Environment Programme, Tokyo
http://unfccc.int/resource/docs/convkp/keng.pdf.

Van den Pol-van Dasselaar A., van Beusichem M.L. & Oenema O. (1999). Determinants of spatial variability of methane emissions from wet grasslands on peat soil. *Biogeochemistry,* **44**, 221-237.

van Winden J.F., Kip N., Talbot H.M., Reichart G.J., McNamara N.P., Bentien A., Jetten M.S.M., Op den Camp H.J.M. & Sinninghe Damste J.S. (2010). Symbiotic methane-oxidizing bacteria in peat moss: microbial diversity and environmental relevance. In: EGU General Assembly, Geophysical Research Abstracts.

Vigliotta G., Nutricati E., Carata E., Tredici S.M., De Stefano M., Pontieri P., Massardo D.R., Prati M.V., De Bellis L. & Alifano P. (2007). *Clonothrix fusca* Roze 1896, a filamentous, sheathed, methanotrophic gamma-proteobacterium. *Applied Environmental Microbiology,* **73**, 3556-3565.

Vorobev A.V., Baani M., Doronina N.V., Brady A.L., Liesack W., Dunfield P.F. & Dedysh S.N. (2010). *Methyloferula stellata* gen. nov., sp. nov., an acidophilic, obligately methanotrophic bacterium possessing only a soluble methane monooxygenase. *International Journal of Systematic and Evolutionary Microbiology*.

Ward N., Larsen Ø., Sakwa J., Bruseth L., Khouri H., Durkin A.S., Dimitrov G., Jiang L., Scanlan D., Kang K.H., Lewis M., Nelson K.E., Methe B., Wu M., Heidelberg J.F., Paulsen I.T., Fouts D., Ravel J., Tettelin H., Ren Q., Read T., DeBoy R.T., Seshadri R., Salzberg S.L., Jensen H.B., Birkeland N.K., Nelson W.C., Dodson R.J., Grindhaug S.H., Holt I., Eidhammer I., Jonasen I., Vanaken S., Utterback T., Feldblyum T.V., Fraser C.M., Lillehaug J.R. & Eisen J.A. (2004). Genomic insights into methanotrophy: the complete genome sequence of *Methylococcus capsulatus* (Bath). *PLoS Biology,* **2**, e303.

Whalen S.C. & Reeburgh W.S. (1990). A methane flux transect along the trans-Alaska pipeline haul road. *Tellus B,* **42**, 237-249.

Whalen S.C. & Reeburgh W.S. (1992). Interannual variations in tundra methane emission: A 4-year time series at fixed sites. *Global Biogeochemical Cycles,* **6**, 139-159.

Whalen S.C., Reeburgh W.S. & Sandbeck K.A. (1990). Rapid methane oxidation in a landfill cover soil. *Applied and Environmental Microbiology,* **56**, 3405-3411.

Whitehead D., Walcroft A.S., Scott N.A., Townsend J.A., Trotter C.M. & Rogers G.N.D. (2004). Characteristics of photosynthesis and stomatal conductance in the shrubland species manuka (*Leptospermum scoparium*) and kanuka (*Kunzea ericoides*) for the estimation of annual canopy carbon uptake. *Tree Physiology,* **24**, 795-804.

Whiteley A.S., Thomson B., Lueders T. & Manefield M. (2007). RNA stable-isotope probing. *Nature Protocols*, **2**, 838-844.

Whitman W., Bone D. & Keswani J. (2001). Taxonomy of methanogenic *Archaea*. In: *Bergey's manual of systematic bacteriology*. Edited by: D. Boone, R.W. Castenholz & G.M. Garrity. Springer New York, pp. 211-294.

Whittenbury R., Phillips K.C. & Wilkinson J.F. (1970). Enrichment, isolation and some properties of methane-utilizing bacteria. *Journal of General Microbiology,* **61**, 205-218.

Willison T.W., Webster C.P., Goulding K.W.T. & Powlson D.S. (1995). Methane oxidation in temperate soils: Effects of land use and the chemical form of nitrogen fertilizer. *Chemosphere,* **30**, 539-546.

Wood A.P., Aurikko J.P. & Kelly D.P. (2004). A challenge for 21st century molecular biology and biochemistry: what are the causes of obligate autotrophy and methanotrophy? *FEMS Microbiology Reviews,* **28**, 335-352.

Wu L., Thompson D.K., Li G., Hurt R.A., Tiedje J.M. & Zhou J. (2001). Development and evaluation of functional gene arrays for detection of selected genes in the environment. *Applied Environmental Microbiology,* **67**, 5780-5790.

Wu M.L., Ettwig K.F., Jetten M.S., Strous M., Keltjens J.T. & van Niftrik L. (2011). A new intra-aerobic metabolism in the nitrite-dependent anaerobic methane-oxidizing bacterium *Candidatus* 'Methylomirabilis oxyfera'. *Biochemical Society Transactions,* **39**, 243-248.

Yoon S., Kraemer S.M., Dispirito A.A. & Semrau J.D. (2010). An assay for screening microbial cultures for chalkophore production. *Environmental Microbiology Reports*, **2**, 295-303.

Zahn J.A. & Dispirito A.A. (1996). Membrane-associated methane monooxygenase from *Methylococcus capsulatus* (Bath). *Journal of Bacteriology,* **178**, 1018-1029.

Zerva A. & Mencuccini M. (2005). Short-term effects of clearfelling on soil CO_2, CH_4, and N_2O fluxes in a Sitka spruce plantation. *Soil Biology and Biochemistry,* **37**, 2025-2036.

Appendices

List of appendix tables

List of Appendix Figures

Appendix Table 0.1: Selection of oligonucleotide probes used in the microarray for the detection of *pmoA* genes.

Melting temperatures were calculated by the nearest neighbour method (Stralis-Pavese *et al.*, 2004). *M.bacter = Methylobacter, M.monas = Methylomonas, M.microbium = Methylomicrobium, M.sarcina = Methylosarcina, M.coccus = Methylococcus, M.thermus = Methylothermus, M.caldum = Methylocaldum*. Probes are organised according to the class of methanotrophs they hybridise with, as follows: type Ia methanotrophs, type Ib methanotrophs, type II methanotrophs, novel *pmoA* of type II methanotrophs, RA14 cluster, watershed cluster, *Methylococcus capsulatus*, universal methanotrophs, ammonia-oxidising bacteria. Representatives of Crenothrix, Clonothrix and Methylacidiphylum are not included. Adapted from Stralis-Pavese *et al.* (2011)

Methanotroph class	Name [a]	Intended specificity	Sequence (5' to 3') [b]	Length (bp)	GC%	T_m
Type Ia methanotrophs	MbA557	*Methylobacter*	CAATGGCATGATGTTCACTCTGGCT	25	48.0	61.5
	MbA486	*Methylobacter*	AGCATGACATTGACAGCGGTTGTT	24	45.8	61.6
	Mb460	*Methylobacter*	GACAGTTACAGCGGTAATCGGTGG	24	54.2	60.9
	Mb_LW12-211	*Methylobacter*	CGTCTTTGGGTTACTGTTGTGCC	23	52.2	60.0
	Mb_SL#3-300	*Methylobacter*	GGCGCTGTTGTTTGTGTATTGGGT	24	50.0	62.2
	Jpn284	clone Jpn 07061	ACCGTATCGCATGGGGTG	18	61.1	58.0
	BB51-302	*Methylobacter*	CGGTTGTTTGTGTCTTAGGTCTG	23	47.8	57.2
	Mb267	*Methylobacter*	GCATGCTTGTGGTTCCGTTAC	21	52.4	58.1
	Mb292	*Methylobacter*	CCGTTACCGTCTGCCTTTCG	20	60.0	59.1
	Mb282	*Methylobacter*	TTACCGTCTGCCTTTCGGC	19	57.9	58.6
	Mb_URC278	*Methylobacter*	GTTCCGTTACAGACTGCCTTTCGG	24	54.2	61.3
	511-436	*Methylobacter*	GTTTTGATGCTGTCTGGCAG	20	50.0	55.5
	511-436L	*Methylobacter* 511 group	GUUUUGAUGCUGUCUGGCAGCA	22	50.0	60.0
	LP10-424	*Methylobacter* LP 10 group	GTACTTGATTGTATCTTGATGCTGTCAG	28	39.3	55.7
	LF1a-456	*Methylobacter* LF 1a group	CATGGTATTGACTGCTGTTATCGGTG	26	46.2	57.7

Mb_C11-403	*Methylobacter*	CAAACTTCATGCCTGGTGCTATCGT	25	48.0	61.4
Mb380	*M.bacter* broad group A universal	CAGTAAATTTCTGCTTCCCTTCAAATCT	28	35.7	55.8
Mb271	*Methylobacter*	TTGTGGTGGCGTTACCGT	18	55.6	58.0
S14m2-270	Marine type Ia cluster, S14m#2	CTTATGGTACCGTTACAGATTGCCTTA	27	40,7	56.4
S14m2-406	Marine type Ia cluster, S14m#2	TTAATTCCTGGTGCAATTGCACTTGAC	27	40.7	58.3
PS80-291	clone PS-80	ACCAATAGGCGCAACACTTAGT	22	45.5	58.3
MS1-440	Marine type Ia cluster, Marine sediment #1	TGATGTTGTCTGGTAGCTTCACATTAAC	28	39.3	57.1
Mm_pel467	*Methylomicrobium pelagicum*	ACTGCGGTAATCGATGGTTTGGC	23	52.2	61.6
Kuro18-205	Marine type Ia cluster, Kuro18	AGACGTTTGTGGGTGACAGTTGC	23	52.2	60.0
DS1-401	Deep sea cluster #1	GCGCGGTAGTTTGTGTTATGGCT	23	52.2	61.7
Mm531	*Methylomonas*	CTCCATTGCACGTGCCTGTAGA	22	54.5	60.7
Mm_M430	*Methylomonas*	TGGACGTGATTTTGATGTTGGGCAA	25	44.0	61.6
Mm_RS311	*M.monas methanica*, RS clade(10-286)	CTGTTGTTGCTCTGATGCTGGG	22	54.5	58.6
Mm_ES294	*Methylomonas*	CCAATCGGTGCAACAATTTCTGTAGT	26	42.3	59.8
Mm_ES543	*Methylomonas*	GTGCCAGTTGAGTATAACGGCATGA	25	48.0	60.9
Mm_ES546	*Methylomonas*	CCAGTTGAGTATAACGGCATGATGAT	26	42.3	58.7
Mm_MV421	*Methylomonas*	CTATCGTGCTGGATACAATCCTGATGT	27	44.4	60.0
Mm451	*Methylomonas*	CTGATGTTGGGTAACAGCATGACT	24	45.8	58.8
Mm275	*Methylomonas*	GTGGTGGAGATACCGTTTGCC	21	57.1	59.2
Alp7-441	Alpine soil *Methylomonas*, Alp#7 (10-282)	GATGTTAGGTAACAGCATGACACTGAC	27	44.4	57.4
peat_1_3-287	*Methylomonas*-related peat clones	AACTGCCTTTAGGCGCTACC	20	55.0	58.6

	Est514	*Methylomicrobium*-related clones	AATTGGCCTATGGTTGCGCC	20	55.0	59.9
	Mmb259	*Methylomicrobium album* + Landfill *M.microbia*	CTGTTCAAGCAGTTGTGTGGTATCG	25	48.0	59.8
	Mmb303	*Methylomicrobium album*	CAATGCTGGCTGTTCTGGGC	20	60.0	60.3
	Mmb304	*M.microbium album* + Landfill *M.microbia* and related	ATGCTGGCTGTTCTGGGCTTG	21	57.1	60.6
	LW14-639	*Methylomicrobium* LW14 group	AAAAGGUACUUGGAGAACCUUCGGU	25	44.0	60.0
	Mmb_RS2-443	*Methylomicrobium, Mmb_RS2*	TGCTGGGCAACAGCATGCAGT	21	57.1	62.8
	Mmb562	*M.microbium album* and *Methylosarcina*	ATGGTAATGACCCTGGCTGACTTG	24	50.0	60.6
	Mm229	Deep-branching *M.monas* group	CCAATCGTTGGAATCACTTTCCCAGC	26	50.0	60.2
	MsQ290	*M.sarcina quisquilliarum*-related	TGCCATTCGGCGCTGTAATTTCAGTA	26	46,2	60.8
	MsQ295	*M.sarcina quisquilliarum*	CGGCGCGGTTCTTTCTGTACTG	22	59.1	60.6
	LP20-644	*Methylomicrobium*-related clones	GTACACTGCGTACTTTCGGTAA	22	45.5	56.0
	LP20-607	LP20 group (Type Ia, deep branching-*M.microbium*)	ACTGGTATGCCTGAATACATCCGTA	25	44.0	57.4
	Ia193	Type Ia (*M.bacter – M.monas – M.microbium)*	GACTGGAAAGATAGACGTCTATGGG	25	48.0	57.8
	Ia575	Type Ia (*M.bacter – M.monas – M.microbium-M.sarcina)*	TGGCTGACTTGCAAGGTTACCAC	23	52.2	61.3
Type Ib methanotrophs	501-375	*Methylococcus*-related marine and freshwater sediment clones	CTTCCCGGTGAACTTCGTGTTCC	23	56.5	61.3
	501-286	*Methylococcus*-related marine and freshwater sediment clones	GTCAGCCGTGGGGCGCCA	18	77.8	66.7
	USC3-305	Upland soil cluster #3	CACGGTCTGCGTTCTGGC	18	66.7	59.5
	Mc396	*Methylococcus*	CCCTGCCTCGCTGGTGCC	18	77.8	64.4
	MclT272	*Methylocaldum tepidum*	GGCTTGGGAGCGGTTCCG	18	72.2	61.9
	MclG281	*Methylocaldum gracile*	AAAGTTCCGCAACCCCTGGG	20	60.0	61.5

MclS402	*Methylocaldum szegediense*	GCGCTGTTGGTTCCGGGT	18	66.7	61.8
MclS394	*Methylocaldum szegediense* and related	TTCCCGGCGCTGTTGGTTCC	20	65.0	63.3
MclS400	*Methylocaldum szegediense* and related	CGGCGCTGTTGGTTCCGGGT	20	70.0	65.7
MclE302	*Methylocaldum* E10	CGCAACCATGGCCGTTCTG	19	63.2	60.3
Mcl404	*M.caldum tepidum – M.caldum gracile – M.caldum szegediense* and related	TTTTGGTTCCGGGTGCGATTT	21	47.6	58.0
Mcl408	*Methylocaldum*	GGTTCCGGGTGCGATTTTG	19	57.9	57.8
JHTY1-267	JH-TY#1	TTGGTTGTGGGAAAACTTCCGT	22	45.5	57.4
JRC4-432	Japanese rice cluster #4	GACGTTGTCCTGGCTCTGAG	20	60.0	58.3
OSC220	Finnish organic soil clones and related	TCACCGTCGTACCTATCGTACTGG	24	54.2	60.8
OSC300	Finnish organic soil clones and related	GGCGCCACCGTATGTGTACTG	21	61.9	61.4
JRC3-535	Japanese Rice Cluster #3	CGTTCCACGTTCCGGTTGAG	20	60.0	59.3
LK580	fw-1 group + Lake Konstanz sediment cluster	CCGACATCATTGGCTACAACTATGT	25	44.0	58.7
RSM1-419	RSM#1	CCATTCTGCTCGACGTGGTTCT	22	54.5	59.4
JHTY2-562	JH-TY#2	ATGCTGTTGTCGATCGCCGACTTGC	25	56.0	63.6
JHTY2-578	JH-TY#2	CCGACTTGCAAGGCTACAACTATGTC	26	50.0	59.5
JRC2-447	Japanese Rice Cluster #2	CTGAGCACCAGCTACCTGTTCA	22	54.5	60.2
LW21-374	LW21 group	CTACTTCCCGATCACCATGTGCT	23	52.2	60.2
LW21-391	LW21 group	TGTGCTTCCCCTCGCAGATC	20	60.0	60.5
M90-574	*M.coccus – M.caldum* related marine and freshwater sediment clones	ATCGCCGACCTGCTGGGTTA	20	60.0	62.2
M90-253	*M.coccus – M.caldum* related marine and freshwater sediment clones	GCTGCTGTACAGGCGTTCCTG	21	61.9	61.7

	Mth413	*Methylothermus*	CACATGGCGATCTTTTTAGACGTTG	25	44.0	58.3
	Mha-500	*Methylohalobius – M.thermus* and related	TGATGTACCCGGGCAACTGGC	21	61.9	62.3
	DS3-446	Deep sea cluster #3	AGCTGTCTGGCAGTTTCCTGTTCA	24	50.0	62.5
	PmoC640	PmoC	AAGGGAACGCTTCGTACGTTTGG	23	52.2	59.8
	PmoC308	PmoC	CCTGTGTGCTGGCGATTCTGCT	22	62.3	59.1
	Ib453	Type I b (*M.thermus – M.coccus – M.caldum* and related)	GGCAGCTACCTGTTCACCGC	20	65.0	61.7
	Ib559	Type I b (*M.thermus – M.coccus – M.caldum* and related)	GGCATGCTGATGTCGATTGCCG	22	59.1	62.5
Type II methanotrophs	McyB304	*M.cystis B (parvus/echinoides/*strain M)	CGTTTTCGCGGCTCTGGGC	19	68.4	62.7
	Mcy255	*M.cystis B (parvus/echinoides/*strain M)	GGCGTCGCAGGCTTTCTGG	19	68.4	62.3
	Mcy459	*Methylocystis*	GTGATCACGGCGATTGTTGGTTC	23	52.2	60.2
	Mcy264	*Methylocystis*	CAGGCGTTCTGGTGGGTGAA	20	60.0	61.0
	Mcy270	*Methylocystis*	TTCTGGTGGGTGAACTTCCGTCT	23	52.2	61.8
	Mcy413	*Methylocystis*	TTCCGGCGATCTGGCTTGACG	21	61.9	63.2
	Mcy522	*Methlocystis* A + peat clones	GGCGATTGCGGCGTTCCA	18	66.7	62.3
	Mcy233	*Methylocystis*	ATTCTCGGCGTGACCTTCTGC	21	57.1	60.9
	McyM309	*M.cystis* strain M and related	GGTTCTGGGCCTGATGATCGG	21	61.9	61.0
	Peat264	peat clones	GGCGTTTTTCTGGGTCAACTTCC	23	52.2	60.3
	MsS314	*Methylosinus sporium*	GGTTCTGGGTCTGCTCATCGG	21	61.9	60.8
	MsS475	*Methylosinus sporium*	TGGTCGGCGCCCTGGGCT	18	77.8	68.3
	Msi263	*Methylosinus sporium* + 1 *M.sinus trichosporium subclaster*	GGCGTTCCTGTGGGAGAACTTC	22	59.1	61.2

	Msi423	*Methylosinus*	CTGTGGCTGGACATCATCCTGC	22	59.1	61.4
	MsT214	*Methylosinus trichosporium* OB3b and related	TGGCCGACCGTGGTTCCG	18	72.2	63.5
	MsT343	*Methylosinus trichosporium* OB3b and related	TCAACCGCTACTGCAACTTCTGG	23	52.2	60.9
	MM_MsT343	*Methylosinus trichosporium* OB3b and related – MM control probe!	TCAACCGCTACTTCAACTTCTGG	23	47.8	58.5
	Msi520	*Methylosinus trichosporium*	GCGATCGCGGCTCTGCA	17	70.6	61.6
	Msi269	*Methylosinus trichosporium*	TCTTCTGGGAGAACTTCAAGCTGC	24	50.0	60.6
	Msi294	*Methylosinus*	GTTCGGCGCGACCTTCGC	18	72.2	62.5
	ARC2-518	Deep branching type II clade ARC2 – *Methylosinus trichosporium* 15-084 group	GGCCGGCGATTGGTCAGTATCA	22	59.1	61.7
	Msi232	*M.sinus* + most *M.cystis* – considered as additional type II probe	ATCCTGGGCGTGACCTTCGC	20	65.0	63.3
	II509	Type II	CGAACAACTGGCCGGCGAT	19	63.2	61.7
	II630	Type II	CATGGTCGAGCGCGGCAC	18	72.2	62.4
Novel *pmoA* of type II methanotrophs	Alp8-468	Type II novel *pmoA*, Alpine cluster Alp#8	CGCGCTCCTTGGCTCGTTGG	20	70.0	64.0
	xb6-539	Novel *pmoA* copy of type II and related environmental clones	AGGCCGCCGAGGTCGAC	17	76.5	63.0
	LP21-190	Novel *pmoA* copy of type II and related environmental clones	ATCGACTTCAAGGATCGCCG	20	55.0	58.2
	LP21-260	Novel *pmoA* copy of type II and related environmental clones	CGCAGTCCTTCTTCTGGACG	20	60.0	58.6
	NMcy1-247	Novel *pmoA* copy of *M.cystis* #1	TCGACATCGTGCTGATGATCTCGG	24	54.2	62.1
	NMsi1-469	Novel *pmoA* copy of *M.sinus*	GCGCTGGTCGGCTCCATGG	19	73.7	64.3

	NMcy2-262	Novel *pmoA* copy of *M.cystis* #2	CAGTCCTTCTTCTGGCAGAAGTTCC	25	52.0	60.9
	LP21-436	*Mcy* + *Msi* novel *pmoA* #1 groups	GTGCTGATGATGTCGGGCAGCTGGC	25	64.0	66.1
	NMsiT-271	Novel *pmoA* copy of *M.sinus trichpsporium*	AGCGCTTCCGTCTGCCGAT	19	63.2	62.9
	LP21-232	Novel *pmoA* copy of type II and related environmental clones	ATCGTCGCCATGTGCTTCGC	20	60.0	61.9
RA14 cluster	RA14-299	RA14 related clones	GCGCGACGTTCCTTTGTGTC	20	60.0	59.5
	RA14-594	RA14 related clones	CCACAACGTTCGTACCTCGA	20	55.0	57.9
	RA14-591	RA14 related clones	GGCTTCCACAACGTTCGTACCT	22	54.5	60.9
Watershed cluster	Wsh1-566	Watershed + flooded upland cluster 1	GCTCATGAGCTTGGCCGACATC	22	59.1	61.8
	Wsh2-491	Watershed + flooded upland cluster 2	TCATTTGGCCAACCTCTCTCATTCC	25	48.0	60.9
	Wsh2-450	Watershed + flooded upland cluster 2	CAAGAGCTGGATCATCACGATG	22	50.0	56.8
Methylocapsa acidiphila	B2rel251	*Methylocapsa*-related clones	CCGCCGCGGCCCAGTATTA	19	68.4	63.4
	B2-400	*Methylocapsa*	ACCTCTTTGGTCCCGGCTGC	20	65.0	63.4
	B2-261	*Methylocapsa*	TCAGGCCTATTTCTGGGAAAGCT	23	47.8	58.3
	B2all343	*Methylocapsa* and related clones	AACCGCTACACCAATTTCTGGGG	23	52.2	61.2
	B2all341	*Methylocapsa* and related clones	TCAACCGCTACACCAATTTCTGGG	24	50.0	61.1
Universal methanotrophs	mtrof173	Universal	GGbGACTGGGACTTCTGG	18	66.7	57.4
	mtrof362-I	Methanotrophs	TGGGGCTGGACCTACTTCC	19	63.2	59.5
	mtrof661	Methanotrophs	GGTAARGACGTTGCKCCGG	19	63.2	60.4
	mtrof662-I	Methanotrophs	GGTAAGGACGTTGCGCCGG	19	68.4	61.9
	mtrof656	Methanotrophs	ACCTTCGGTAAGGACGT	17	52.9	53.2

Ammonia-oxidising bacteria	NmNc533	*Nitrosomonas – Nitrosococcus*	CAACCCATTTGCCAATCGTTGTAG	24	45.8	58.6
	Nsm_eut381	*Nitrosomonas eutropha*	CCACTCAATTTTGTAACCCCAGGTAT	26	42.3	59.0
	PS5-226	*Nitrosomonas – Nitrosococcus*-related clones	ACCCCGATTGTTGGGATGATGTA	23	47.8	59.9
	Pl6-306	*Nitrosomonas – Nitrosococcus*-related clones	GGCACTCTGTATCGTATGCCTGTTAG	26	50.0	60.5
	NsNv207	*Nitrosospira – Nitrosovibrio*	TCAATGGTGGCCGGTGG	17	64.7	58.5
	NsNv363	*Nitrosospira – Nitrosovibrio*	TACTGGTGGTCGCACTACCC	20	60.0	59.6
	SV308	*Svalbard* clade	TGAGCATCTCTGGGCTTGTCGT	22	54.5	60.7
	SVrel583	*Svalbard clade* and related	TACATGGGATTCACATTTGTGAGGAC	26	42.3	57.0
	Nit_rel471	AOB-related clones/probably methanotrophs	CGTTCGCGATGATGTTTGGTCC	22	54.5	60.1
	Sed585	Ssedi#1	GGGCATTCGCGATGATGTTTTATCCGA	27	48.1	61.2
	Sed422	Ssedi#1 and related	TGATCCTAGACTGCACCCTGTTG	23	52.2	58.5
	Nit_rel223	AOB-related clones/probably methanotrophs	GTCACACCGATCGTAGAGGT	20	55.0	56.9
	Nit_rel417	Arctic soil related #1, subgroup	CGCGTTGATCTTTGATTGCACCCTGTT	27	48.1	61.8
	Nit_rel419	Arctic soil related #1, subgroup	CGTTGATCCTTGATTGCACCCTGTT	25	48.0	59.8
	Nit_rel526	JRC#1+CCd#1 groups	GCCATCAACCATTGGTTGCGGA	22	54.5	60.8
	Nit_rel652	Arctic soil MOB	CGTACATTCGGTGGTCACACTG	22	54.5	57.9

[a] Numbers at the end of the probe names refer to their relative position on the *Methylococcus capsulatus* (Bath) *pmoA* gene.

[b] sequences are of the sense strand.

Appendix Table 0.2: Taguchi orthogonal array selector.

The subscript number next to the letter L corresponds to the number of experiments required. For example, a L_9 (3^4) array is capable to examine 4 factors at 3 levels each by performing 9 experiments instead of 81 (3^4).

		Number of factors						
		3	**4**	**5**	**6**	**7**	**8**	**9**
Number of levels	**2**	L_4	L_8	L_8	L_8	L_8	L_{12}	L_{12}
	3	L_9	L_9	L_{18}	L_{18}	L_{18}	L_{18}	L_{27}
	5	L_{25}	L_{25}	L_{25}	L_{25}	L_{50}	L_{50}	L_{50}

Appendix Table 0.3: Summary of the characteristics of the three primer sets used for the detection of aerobic methanotrophs.

	Primer set for *pmoA* genes		
Primer conditions	**pmoA189F/ pmoA682R**	**pmoA189F/ pmoA661R**	**pmoA189F/ pmoA650R**
Primer sequence	GGNGACTGGGACTTCTGG/ GAASGCNGAGAAGAASGC	GGNGACTGGGACTTCTGG/ CCGGMGCAACGTCYTTACC	GGNGACTGGGACTTCTGG/ ACGTCCTTACCGAAGGT
Primer length (bp) [a]	18 18	18 19	18 17
GC content (%) [a]	63.9 58.4	63.9 53.2	63.9 52.9
Melting temp. (ºC) [a,b]	61.2/**62.5**/64.5 60.3/**61.6**/63.6	61.2/**62.5**/64.5 63.0/**65.1**/67.7 ºC	61.2/**62.5**/64.5 **60.1**
Mean Tm (ºC) [c]	62	64	61
Fragment size (bp)	542	513	500
Reference	Holmes *et al.* (1995)	Costello & Lidstrom (1999)	Bourne *et al.* (2001)

[a] Characteristics calculated using the OligoAnalyzer tool from the Integrated DNA technologies website at www.idtdna.com.
[b] Values are respectively minimum/mean/maximum T_m.
[c] Calculated as the average of the mean T_m of each primer.

Appendix Table 0.4: Taguchi orthogonal array L_{18} for the optimisation of six components of the PCR master mix, each at three concentrations (A, B and C).

	Factor					
Experiment	**BSA** *	**$MgCl_2$**	**dNTPs**	**Enzyme**	**Primer**	**DNA template**
1	A	A	A	A	A	A
2	A	A	B	B	B	B
3	A	A	C	C	C	C
4	A	B	A	A	B	B
5	A	B	B	B	C	C
6	A	B	C	C	A	A
7	A	C	A	B	A	C
8	A	C	B	C	B	A
9	A	C	C	A	C	B
10	B	A	A	C	C	B
11	B	A	B	A	A	C
12	B	A	C	B	B	A
13	B	B	A	B	C	A
14	B	B	B	C	A	B
15	B	B	C	A	B	C
16	B	C	A	C	B	C
17	B	C	B	B	C	A
18	B	C	C	A	A	B

* Only two concentrations of BSA were tested. The letters A, B and C can also be replaced by the numerical values found in Table 3.6.

Appendix Table 0.5: Cycling parameters of the original basic PCR and optimised TD PCR for amplification of the *pmoA* genes.

Cycle step	Original basic PCR	Optimised TD PCR
Initial denaturation time (s)	300	420
Initial denaturation temperature (°C)	95	95
TD denaturation time (s)	60	60
TD denaturation temperature (°C)	94	94
TD annealing time (s)	60	90
TD (starting) annealing temperature (°C)	60	65
TD extension time (s)	60	60
TD extension temperature (°C)	72	72
Temperature decrement (°C/cycle)	-	0.8
TD number of cycles	30	15
Post-TD denaturation time (s)	-	60
Post-TD denaturation temperature (°C)	-	94
Post-TD annealing time (s)	-	90
Final TD annealing temperature (°C) or Post-TD annealing temperature (°C)	-	53 *
Post-TD extension time (s)	-	60
Post-TD extension temperature (°C)	-	72
Post-TD number of cycles	-	20
Final extension time (s)	600	600
Final extension temperature (°C)	72	72

* The post-TD annealing temperature for the TD programme was calculated based on a TD (starting) annealing temperature of 65°C and a temperature decrement of 0.8°C/cycle for 15 cycles.

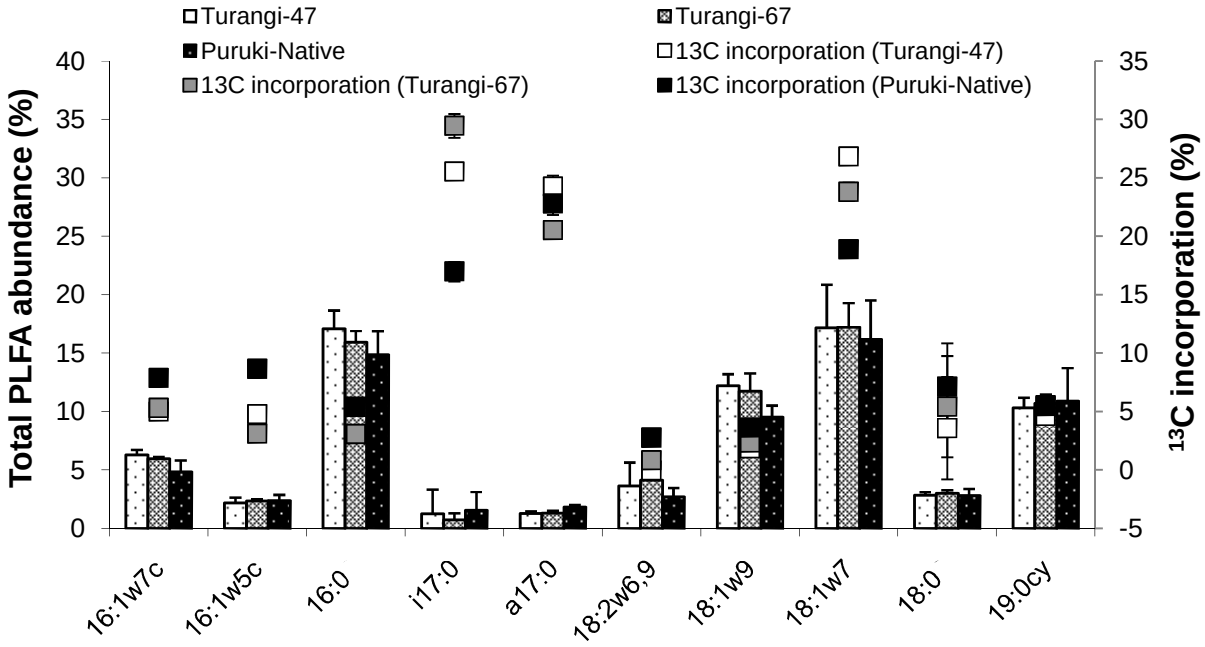

Appendix Figure 0.1: Relative incorporation of ^{13}C (incubation with ~50 ppm of ^{13}C-CH_4) within the PLFAs extracted from soils under the shrublands (Turangi) and native forest (Puruki).

The bars represent the PLFA abundance. Error bars are S.E.M.

Appendix Table 0.6: 16S rRNA clones of type II methanotrophs from the soils under shrublands (Turangi) and native forest (Puruki).

Clones were matched against the GenBank database.

Site	Clone	AC	Gene	Match	Total	(%)
Turangi	c1Tur	GU731305.1	Bacterium enrichment culture clone heteroC61_4W 16S ribosomal RNA gene, partial sequence	514	519	99
	c2Tur	DQ823224.1	Uncultured bacterium clone ORCA-17N121 16S ribosomal RNA gene, partial sequence	518	522	99
	c3Tur	EU459446.1	Uncultured bacterium clone CAP_aah97c04 16S ribosomal RNA gene, partial sequence	476	520	91
	c4Tur	GU205291.1	Uncultured alpha proteobacterium clone RSC_CP2A02 16S ribosomal RNA gene, partial sequence	513	518	99
	c5Tur	DQ977627.1	Uncultured bacterium clone HC_0-5#5 16S ribosomal RNA gene, partial sequence	518	519	99
	c6Tur	DQ823224.1	Uncultured bacterium clone ORCA-17N121 16S ribosomal RNA gene, partial sequence	520	522	99
	c7Tur	GQ918782.1	Uncultured soil bacterium clone 19_45KE10 16S ribosomal RNA gene, partial sequence	517	521	99
	c8Tur	AM992777.1	Uncultured bacterium partial 16S rRNA gene, clone QL4-6	511	518	98
	c9Tur	EF018692.1	Uncultured *Hyphomicrobiaceae* bacterium clone Amb_16S_985 16S ribosomal RNA gene, partial seq.	517	523	98
	c10Tur	EU449617.1	Uncultured *Sphingomonadaceae* bacterium clone Plot4-2H12 16S ribosomal RNA gene, partial sequence	515	519	99
	c11Tur	**NR_025596.1**	***Methylocella tundrae* strain T4 16S ribosomal RNA, partial sequence**	**518**	**522**	**99**
	c12Tur	EF212393.1	Uncultured bacterium clone RCL_RII_28 16S ribosomal RNA gene, partial sequence	508	521	97
	c13Tur	GU731305.1	Bacterium enrichment culture clone heteroC61_4W 16S ribosomal RNA gene, partial sequence	519	521	99
	c14Tur	EF019191.1	Uncultured *Hyphomicrobiaceae* bacterium clone Amb_16S_1862 16S ribosomal RNA gene, partial seq.	515	520	99
	c15Tur	DQ823224.1	Uncultured bacterium clone ORCA-17N121 16S ribosomal RNA gene, partial sequence	521	522	99
Puruki	c1Pur	AM162434.1	Uncultured bacterium partial 16S rRNA gene, clone B112	505	520	97
	c2Pur	AM085995.1	Phyllobacterium sp. STM1417 partial 16S rRNA gene	515	518	99
	c3Pur	FJ024546.1	Uncultured bacterium clone U000130368 16S ribosomal RNA gene, partial sequence	480	491	97
	c4Pur	**CP001280.1**	***Methylocella silvestris* BL2, complete genome**	**517**	**522**	**99**
	c5Pur	EF019169.1	Uncultured *Methylocystaceae* bacterium clone Amb_16S_1821 16S ribosomal RNA gene, partial seq.	512	522	98
	c6Pur	GU731305.1	Bacterium enrichment culture clone heteroC61_4W 16S ribosomal RNA gene, partial sequence	519	521	99
	c8Pur	AY913613.1	Uncultured forest soil bacterium clone DUNssu474 16S ribosomal RNA gene, partial sequence	511	516	99
	c9Pur	EU445211.1	Uncultured bacterium clone R26 16S ribosomal RNA gene, partial sequence	507	519	97
	c10Pur	FM253573.1	Uncultured alpha proteobacterium 16S rRNA gene, clone A10-1	510	523	97
	c11Pur	AM180661.1	Uncultured bacterium partial 16S rRNA gene, isolate 4pt	512	521	98
	c12Pur	EF212388.1	Uncultured bacterium clone RCL_RII_10 16S ribosomal RNA gene, partial sequence	517	521	99
	c14Pur	GU393529.1	Uncultured bacterium clone NPR-T7-26 16S ribosomal RNA gene, partial sequence	511	514	99
	c15Pur	EU445211.1	Uncultured bacterium clone R26 16S ribosomal RNA gene, partial sequence	505	517	97
	c16Pur	GQ402766.1	Uncultured bacterium clone PW362 16S ribosomal RNA gene, partial sequence	512	521	98

Appendix Table 0.7: Relative abundance of the most abundant T-RFs after digestion of *pmoA* with *Hha*I (Bad à Cheo, n=4).

The data are means ± S.E.M. of each season for each habitat. Within each column, statistical differences between seasons within each habitat are indicated by different Roman letters (a, b), while Greek letters (α, β) indicate statistical differences between habitats, according to multiple pairwise comparison ($P<0.05$).

Habitat	Season	Terminal restriction fragment relative abundance (%)									
		T-RF 32		T-RF 37		T-RF 81		T-RF 129		T-RF 266	
Bog	Autumn	17±6	**a α**	2.7± 2.37	**a α**	30±6	**a α**	30±3	**a α**	4.5± 1.63	**a α**
	Spring	17±3		4.0± 1.21		33±5		25±2		9.2± 1.34	**ab**
	Summer	19±2		4.3± 2.04		26±6		28±7		17±10	**b**
	Winter	17±3		1.9± 1.20		34±7		33±6		0.35± 0.35	**a**
Young Pine	Autumn	12±4	**a α**	0	**a β**	31±8	**a α**	34±6	**a α**	0	**a β**
	Spring	15±7		0		48±12		29±7		1.9± 1.17	
	Summer	23±8		0		38±5		36±3		0	
	Winter	34±7		0		35±5		19±5		7.5± 3.56	

Appendix Table 0.8: Relative abundance of the most abundant T-RFs after digestion of *pmoA* with *Msp*I (Bad à Cheo, n=4).

The data are means ± S.E.M. of each season for each habitat. Within each column, statistical differences between seasons within each habitat are indicated by different Roman letters (a, b), while Greek letters (α, β) indicate statistical differences between habitats, according to multiple pairwise comparison ($P<0.05$).

Habitat	Season	Terminal restriction fragment relative abundance (%)									
		T-RF 196		T-RF 242		T-RF 293		T-RF 444		T-RF 499	
Bog	Autumn	2.9± 1.46	**a α**	19±5	**ab α**	3.2± 1.09	**ab α**	3.6± 1.36	**a α**	64±9	**a α**
	Spring	2.6± 0.60		11±2		8.4± 1.20		2.0± 0.43		70±5	
	Summer	4.9± 2.62		9±2	**a α**	12±7	**b α**	2.5± 0.60		61±8	
	Winter	0		23±3	**b α**	0	**a α**	4.0± 0.95		62±7	
Young Pine	Autumn	0	**a β**	11±2	**a β**	0	**a β**	1.5± 0.53	**a β**	85±3	**a β**
	Spring	0		10±1		1.7± 1.04		2.5± 1.08		84±2	
	Summer	0		8.4± 2.50		0		0		90±2	
	Winter	1.6± 0.97		8.2± 1.14		6.0± 2.75		0.90± 0.51		81±5	

Appendix Table 0.9: Relative abundance of the most abundant T-RFs after digestion of *pmoA* with *Hha*I (Glensaugh, n=4).

The data are means ± S.E.M. of each season for each habitat. Within each column, statistical differences between seasons within each habitat are indicated by different Roman letters (a, b), while Greek letters (α, β) indicate statistical differences between habitats, according to multiple pairwise comparison ($P<0.05$).

Habitat	Season	Terminal restriction fragment relative abundance (%)													
		T-RF 32		T-RF 81		T-RF 128		T-RF 134		T-RF 179		T-RF 200		T-RF 252	
Grassland	Autumn	58±21	**a α**	12±12	**a α**	15±8	**a α**	0	**a α**	0	**a**	0	**a**	0	**a α**
	Spring	51±6		1.8± 1.75		8.7± 3.26		0		7.6± 2.75	**b**	7.4± 2.62	**b**	0	
	Summer	74±21		0		3.4± 3.40		0		0	**a**	0	**a**	0	
	Winter	62±10		2.2± 2.16		8.7± 3.82		0		7.4± 2.95	**b**	8.0± 3.12	**b**	0	
Young Pine	Autumn	75±8	**a α**	2.7± 2.73	**a α**	9.4± 1.33	**a α**	5.2± 3.47	**a β**	0	**a β**	0	**a β**	5.8± 3.86	**a β**
	Spring	65±25		0		8.2± 4.08		1.2± 1.20		0		0		1.8± 1.81	
	Summer	69±4		0		10±2		8.6± 1.53		0		0		12±2	
	Winter	74±8		0		16±4		4.6± 4.64		0		0		5.4± 5.36	

Appendix Table 0.10: Relative abundance of the most abundant T-RFs after digestion of *pmoA* with *Msp*I (Glensaugh, n=4).

The data are means ± S.E.M. of each season for each habitat. Within each column, statistical differences between seasons within each habitat are indicated by different Roman letters (a, b), while Greek letters (α, β) indicate statistical differences between habitats, according to multiple pairwise comparison ($P<0.05$).

Habitat	Season	Terminal restriction fragment relative abundance (%)									
		T-RF 25		T-RF 76		T-RF 229		T-RF 403		T-RF 499	
Grassland	Autumn	18±10	**ab**	0		0		0		69±9	
	Spring	12±1	**b**	0		1.6± 1.62		0		82±3	
			α		**a α**		**a α**		**a α**		**a α**
	Summer	8.2± 4.80	**b**	0		0		0		92±5	
	Winter	36±8	**a**	4.6± 2.66		0		0		56±11	
Young Pine	Autumn	9.7± 1.36		1.9± 0.71		5.3± 3.93		5.0± 3.57		78±2	
	Spring	3.5± 2.00		1.4± 0.79		0.4± 0.43		0.9± 0.90		94±4	
			a β		**a α**		**a α**		**a β**		**a α**
	Summer	8.6± 1.16		3.4± 0.10		1.4± 1.35		8.6± 1.47		78±1	
	Winter	11±2		0.9± 0.94		6.7± 3.31		9.8± 6.63		69±8	

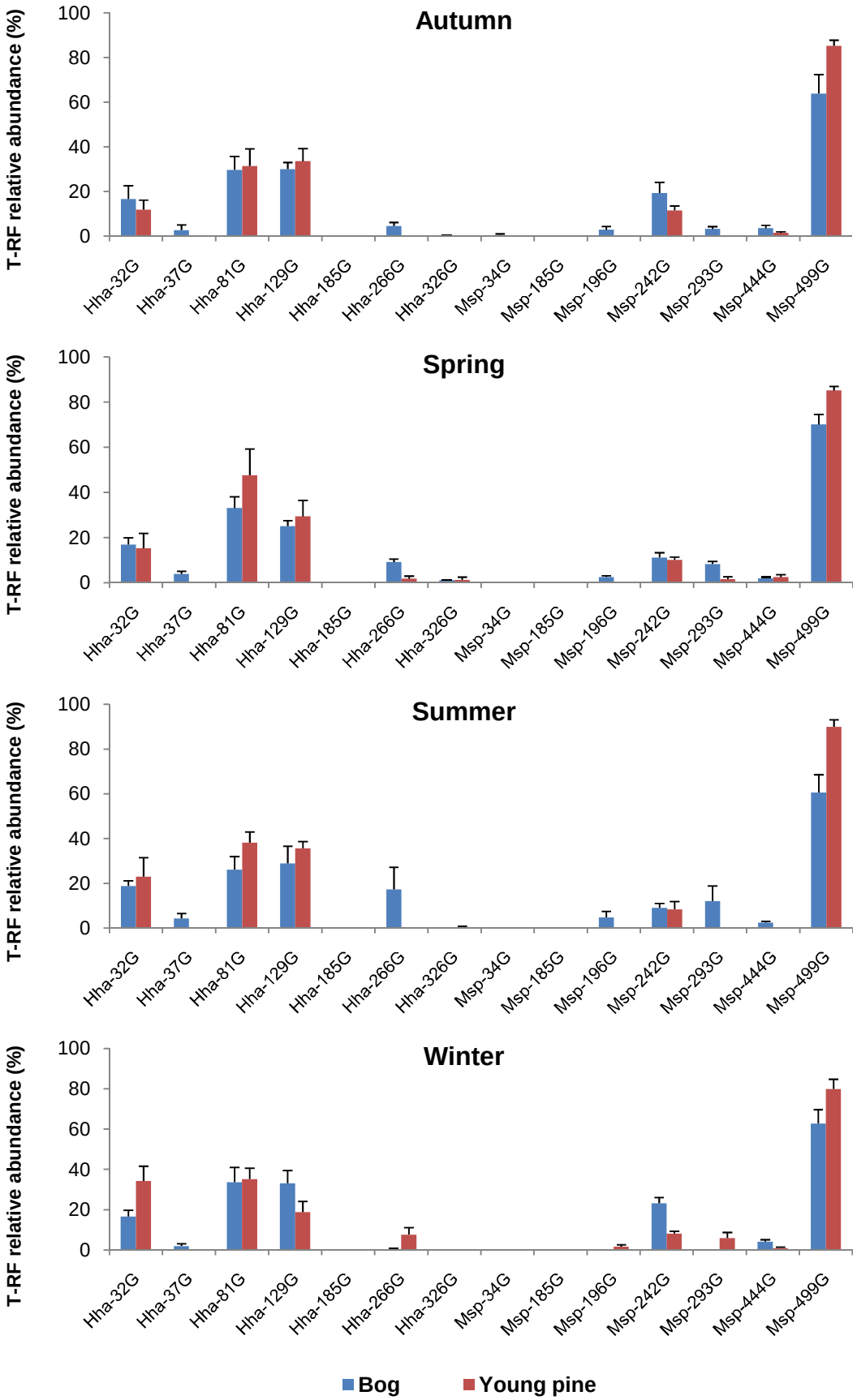

Appendix Figure 0.2: T-RFLP profiles of the methanotrophs (*pmoA*) for each season at Bad à Cheo.

The total relative abundance of the T-RFs (n=4) generated by *Hha*I or *Msp*I is accounted for separately. The letter G (green) represents the colour of the dye.

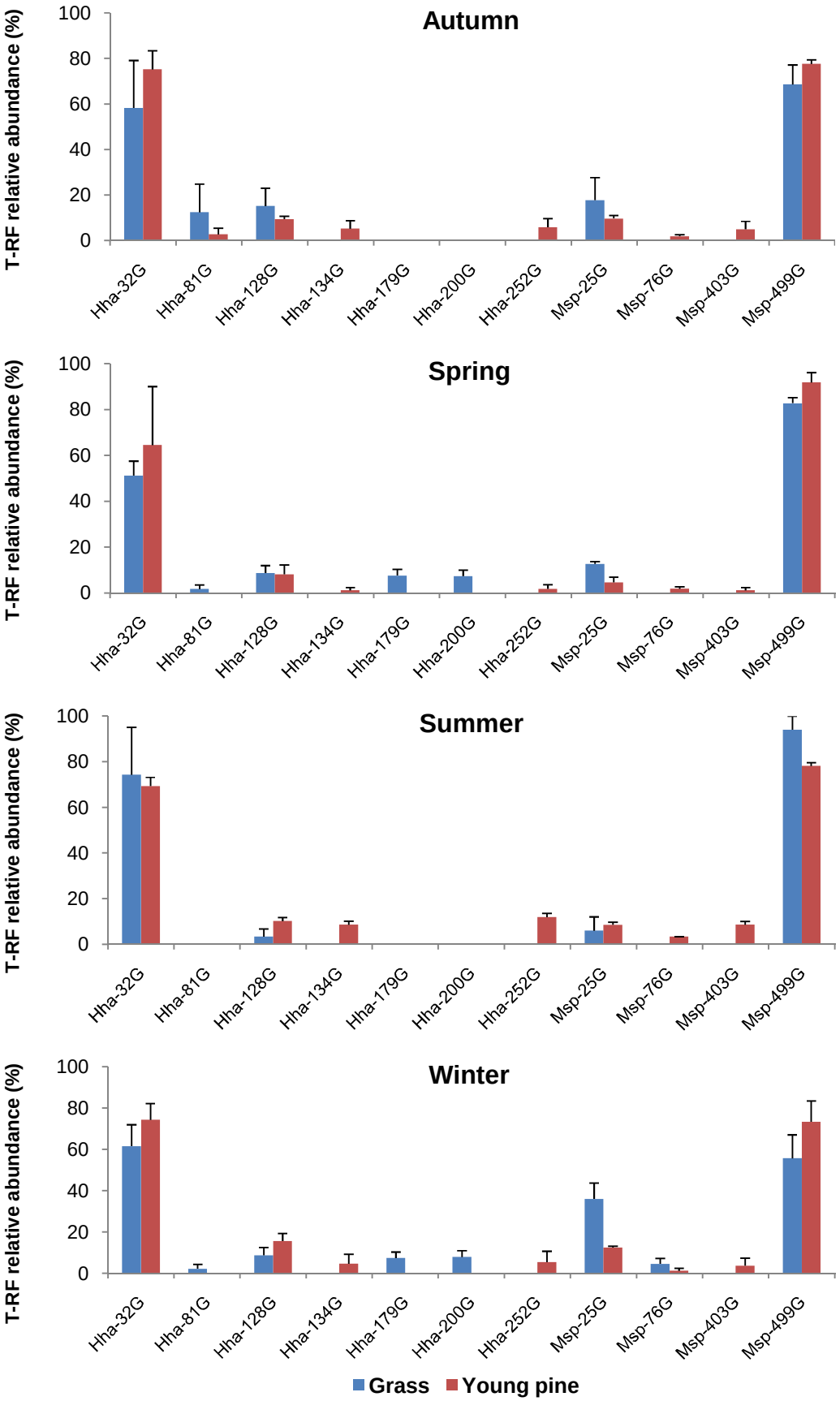

Appendix Figure 0.3: T-RFLP profiles of the methanotrophs (*pmoA*) for each season in Glensaugh.

The total relative abundance of the T-RFs (n=4) generated by *Hha*I or *Msp*I is accounted for separately. The letter G (green) represents the colour of the dye.

Appendix Table 0.11: Effects of afforestation and seasonal changes on the methanotrophic community at Bad à Cheo and Glensaugh (digestion of 16S rRNA of type II methanotrophs with *Mbo*I and *Msp*I).

The data are *P* values corresponding to the first four IPC scores of the AMMI analyses, and were obtained by nested ANOVA and MANOVA. Within each column, statistical differences between seasons within each habitat are indicated by different Roman letters (a, b), while Greek letters (α, β, γ) indicate statistical differences between habitats, according to multiple pairwise comparison ($P<0.05$).

		IPC 1	**IPC 2**	**IPC 3**	**IPC 4**	**MANOVA**
Bad à Cheo	% variation	73.2	19.4	5.0	1.0	
	Habitat	**<0.001**	**<0.001**	0.067	0.751	**<0.001**
	Habitat/Season	0.682	**0.002**	**0.034**	0.273	**0.014**
Bog	Autumn		**a**			
	Spring	**a α**	**b α**	**a α**	**a α**	
	Summer		**b**			
	Winter		**a**			
Young Pine	Autumn		**a**	**a**		
	Spring	**a α**	**b β**	**a α**	**a α**	
	Summer		**b**	**b**		
	Winter		**a**	**a**		
Old Pine	Autumn			**a**		
	Spring	**a β**	**a γ**	**b α**	**a α**	
	Summer			**b**		
	Winter			**a**		
		IPC 1	**IPC 2**	**IPC 3**	**IPC 4**	**MANOVA**
Glensaugh	% variation	55.1	22.8	13.4	4.2	
	Habitat	**<0.001**	0.168	0.374	0.568	**<0.001**
	Habitat/Season	**<0.001**	**<0.001**	**0.031**	**0.009**	**<0.001**
Grassland	Autumn	**a**	**a**		**a**	
	Spring	**b α**	**b α**	**a α**	**a α**	
	Summer	**b**	**b**		**b**	
	Winter	**b**	**b**		**a**	
Young Pine	Autumn	**a**	**a**	**a**		
	Spring	**b β**	**b α**	**ab α**	**a α**	
	Summer	**a**	**b**	**b**		
	Winter	**a**	**a**	**a**		

Appendix Table 0.12: Effects of afforestation and seasonal changes on the methanotrophic community at Bad à Cheo and Glensaugh (digestion of 16S rRNA of type I methanotrophs with *Hha*I and *Msp*I).

The data are *P* values corresponding to the first four IPC scores of the AMMI analyses, and were obtained by nested ANOVA and MANOVA. Within each column, statistical differences between seasons within each habitat are indicated by different Roman letters (a, b, c), while Greek letters (α, β, γ) indicate statistical differences between habitats, according to multiple pairwise comparison ($P<0.05$).

		IPC 1	**IPC 2**	**IPC 3**	**IPC 4**	**MANOVA**
Bad à Cheo	% variation	71.0	9.1	5.8	4.4	
	Habitat	**<0.001**	**<0.001**	**0.004**	0.720	**<0.001**
	Habitat/Season	0.063	**0.006**	**0.012**	**0.007**	**<0.001**
Bog	Autumn	**a α**	**ab α**	**a α**	**a α**	
	Spring		**a**	**a**		
	Summer		**ab**	**a**		
	Winter		**b**	**b**		
Young Pine	Autumn	**a α**	**a β**	**a β**	**a α**	
	Spring		**a**			
	Summer		**b**			
	Winter		**a**			
Old Pine	Autumn	**a β**	**ab γ**	**a α**	**a α**	
	Spring		**ab**		**b**	
	Summer		**a**		**b**	
	Winter		**b**		**a**	
		IPC 1	**IPC 2**	**IPC 3**	**IPC 4**	**MANOVA**
Glensaugh	% variation	41.2	17.6	15.2	8.1	
	Habitat	**<0.001**	**0.035**	**0.013**	0.249	**<0.001**
	Habitat/Season	0.860	0.550	0.321	**0.002**	0.063
Grassland	Autumn	**a α**	**a α**	**a α**	**a**	
	Spring				**a**	
	Summer				**b**	**α**
	Winter				**a**	
Young Pine	Autumn	**a β**	**a β**	**a β**	**a**	
	Spring				**b**	
	Summer				**c**	**α**
	Winter				**b**	

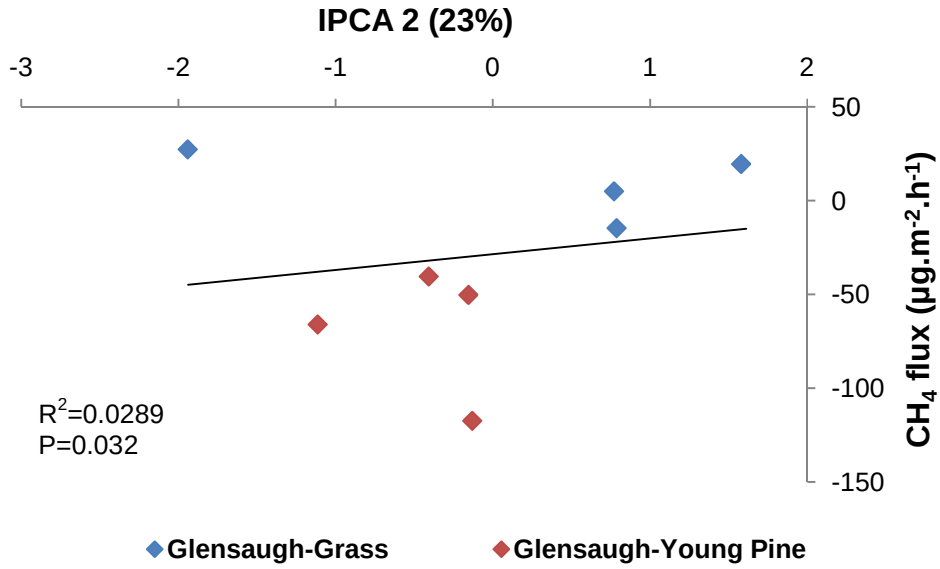

Appendix Figure 0.4: Relationship between net CH_4 flux and methanotrophic community structure at Glensaugh.

The data points represent the IPCA 2 scores displayed in **Figure 5.3** and the net CH_4 fluxes from **Figure 5.1**.

Appendix Table 0.13: Relative abundance of the most abundant T-RFs after digestion of *pmoA* with *Hha*I (Craggan, n=4).

The data are means ± S.E.M. of each season for each habitat. Within each column, statistical differences between seasons within each habitat are indicated by different Roman letters (a, b, c), while Greek letters (α, β) indicate statistical differences between habitats, according to multiple pairwise comparison ($P<0.05$).

Habitat	Season	Terminal restriction fragment relative abundance (%)																	
		T-RF 32			T-RF 50			T-RF 73			T-RF 81			T-RF 128			T-RF 191		
Moor	Autumn	14±3			8.9± 1.35			4.4± 2.81			25±3			19±4			18±4	**a**	
	Spring	29±0	**a**	**α**	23±23	**a**	**α**	0	**a**	**α**	35± 35	**a**	**αβ**	0	**a**	**α**	0	**b**	
	Summer	19±2			10±6			3.9± 3.9			59±7			3.7± 2.16			1.6± 1.61	**b**	**α**
	Winter	15±2			13±7			8.4± 4.02			25±8			14±4			11±5	**c**	
Young Birch	Autumn	19±7			7.0± 3.25			0			67±2			4.6± 2.67			2.0± 2.04		
	Spring	42±8	**a**	**β**	12±4	**a**	**αβ**	0	**a**	**β**	43±8	**a**	**α**	3.0± 2.95	**a**	**β**	0	**a**	**β**
	Summer	46±22			5.5± 3.25			0			49±19			0			0		
	Winter	81±15			0			0			16±16			2.7± 2.71			0		
Old Birch	Autumn	64±19			1.64± 1.64			0			13±8			4.2± 4.20			0		
	Spring	37±18	**a**	**β**	1.35± 1.35	**a**	**β**	0	**a**	**β**	25±16	**a**	**β**	8.4± 8.40	**a**	**αβ**	0	**a**	**β**
	Summer	65±5			0			0			12±10			13±6			0		
	Winter	68±22			0			0			17±11			6.4± 3.71			0		

Appendix Table 0.14: Relative abundance of the most abundant T-RFs after digestion of *pmoA* with *Msp*I (Craggan, n=4).

The data are means ± S.E.M. of each season for each habitat. Within each column, statistical differences between seasons within each habitat are indicated by different Roman letters (a, b), while Greek letters (α, β) indicate statistical differences between habitats, according to multiple pairwise comparison ($P<0.05$).

Habitat	Season	Terminal restriction fragment relative abundance (%)									
		T-RF 25		T-RF 242		T-RF 314		T-RF 451		T-RF 499	
Moor	Autumn	2.1± 2.11	**a α**	13±2	**a α**	18±4	**a α**	17±3	**a α**	30±6	**a α**
	Spring	0		11±11		0	**b**	33±33		39±39	
	Summer	0		18±3		1.3± 1.33	**b**	18±10		60±7	
	Winter	1.8± 1.83		12±4		8.1± 3.36	**b**	23±8		39±10	
Young Birch	Autumn	0	**a α**	13±1	**a α**	2.2± 2.21	**a β**	12±3	**a αβ**	72±3	**a β**
	Spring	3.7± 2.11		4.4± 2.55		0		19±4		73±4	
	Summer	6.0± 3.71		9.3± 5.78		0		7.8± 4.51		77±7	
	Winter	8.5± 4.65		2.9± 2.85		0		2.3± 2.26		87±3	
Old Birch	Autumn	23±5	**a β**	2.1± 2.06	**a α**	0	**a β**	2.1± 2.13	**a β**	72±6	**a β**
	Spring	26±6		14±10		0		1.7± 1.65		52±10	
	Summer	17±3		4.0± 4.02		0		2.3± 1.14		75±7	
	Winter	11±6		8.0± 6.26		0		4.2± 3.55		77±8	

Appendix Table 0.15: Relative abundance of the most abundant T-RFs after digestion of *pmoA* with *Hha*I (Tulchan, n=4).

The data are means ± S.E.M. of each season for each habitat. Within each column, statistical differences between seasons within each habitat are indicated by different Roman letters (a, b), while Greek letters (α, β) indicate statistical differences between habitats, according to multiple pairwise comparison ($P<0.05$).

Habitat	Season	Terminal restriction fragment relative abundance (%)											
		T-RF 32		T-RF 81		T-RF 129		T-RF 190		T-RF 247		T-RF 359	
Moor	Autumn	10±5	**a α**	58±8	**a α**	13±2	**a α**	4.5± 4.51	**a α**	0.51± 0.51	**a αβ**	0	**a α**
	Spring	21±12		53±18		9.8± 3.40		2.1± 1.74		2.3± 2.04		1.9± 1.91	
	Summer	6.5± 1.79		73±6		14±6		0.58± 0.58		0.34± 0.34		0	
	Winter	14±2		38±6		18±3		13±6		1.2± 1.23		0	
Young Birch	Autumn	70±21	**a β**	27±19	**a β**	2.8± 1.62	**a β**	0	**a β**	0	**a α**	0	**a α**
	Spring	70±20		22±15		4.5± 3.03		0		0		0	
	Summer	98±1		0		1.9± 1.00		0		0		0	
	Winter	95±3		0.94± 0.94		1.4± 1.39		0		0		0	
Old Birch	Autumn	58±13	**a β**	7.7± 7.65	**a β**	12±6	**a β**	0	**a β**	3.4± 1.73	**a β**	4.8± 3.10	**a β**
	Spring †	0		90	**b β**	0		0		0		0	
	Summer	68±19		3.1± 3.07	**a**	12±6		0		4.2± 2.12		7.5± 4.49	
	Winter	73±11		5.3± 4.32	**a**	10±5		0		3.2± 2.29		5.1± 4.09	

† Only one sample was available.

Appendix Table 0.16: Relative abundance of the most abundant T-RFs after digestion of *pmoA* with *Msp*I (Tulchan, n=4).

The data are means ± S.E.M. of each season for each habitat. Within each column, statistical differences between seasons within each habitat are indicated by different Roman letters (a, b), while Greek letters (α, β, γ) indicate statistical differences between habitats, according to multiple pairwise comparison ($P<0.05$).

Habitat	Season	Terminal restriction fragment relative abundance (%)																	
		T-RF 25			T-RF 242			T-RF 314			T-RF 444			T-RF 451			T-RF 499		
Moor	Autumn	0			33±7			2.1± 2.12	**a**		4.8± 1.91			0	**a**		43±11		
	Spring	3.1± 3.12	**a**	**α**	15±6	**a**	**α**	1.7± 1.35	**a**	**α**	3.7± 1.28	**a**	**α**	8.1± 3.03	**b**	**α**	63±7	**a**	**α**
	Summer	0			17±2			0.8± 0.81	**a**		3.4± 0.54			1.8± 1.11	**ab**		74±2		
	Winter	2.2± 2.15			19±1			8.4± 2.54	**b**		3.3± 0.33			0.70± 0.70	**ab**		47±12		
Young Birch	Autumn	8.7± 3.02			7.3± 5.83			0			0.9± 0.89			1.0± 1.02			81±4		
	Spring	7.0± 2.38	**a**	**β**	2.9± 1.98	**a**	**β**	0.4± 0.37	**a**	**β**	1.1± 1.10	**a**	**β**	2.1± 2.14	**a**	**α**	85±3	**a**	**β**
	Summer	8.5± 0.74			0			0			0			0			89±1		
	Winter	12±2			0			0			0			2.2± 1.24			86±2		
Old Birch	Autumn	18±7			4.0± 4.01	**a**		0			0	**a**		2.0± 1.24			59±12		
	Spring †	0	**a**	**γ**	39	**b**	**β**	0	**a**	**β**	11	**b**	**β**	0	**a**	**α**	50	**a**	**α**
	Summer	18±13			1.0± 1.01	**a**		0			0	**a**		0			75±16		
	Winter	26±4			1.7± 1.71	**a**		0			0	**a**		0			67±7		

† Only one sample was available.

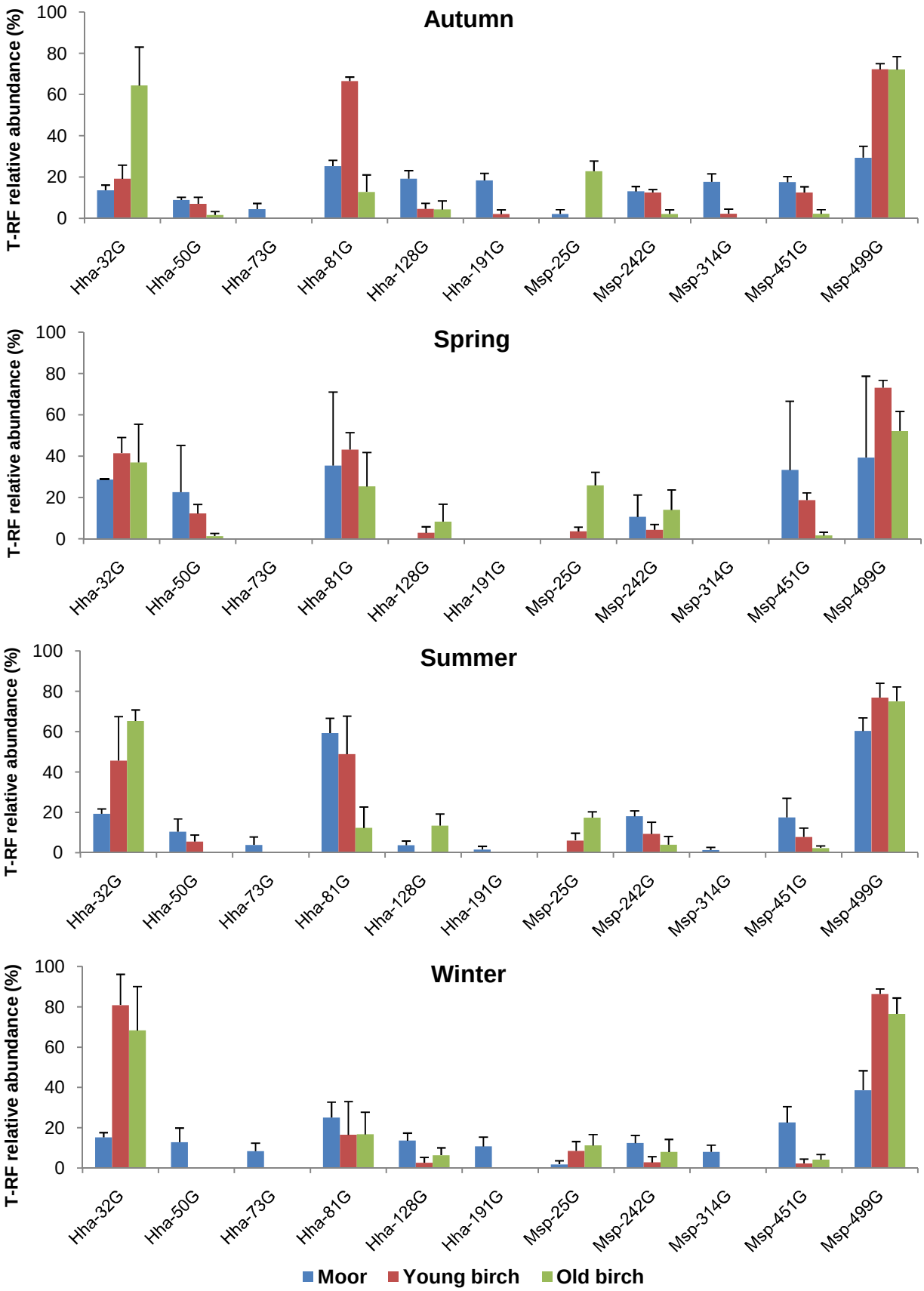

Appendix Figure 0.5: T-RFLP profiles of the methanotrophs (*pmoA*) for each season at Craggan.

The total relative abundance of the T-RFs (n=4) generated by *Hha*I or *Msp*I is accounted for separately. The letter G (green) represents the colour of the dye.

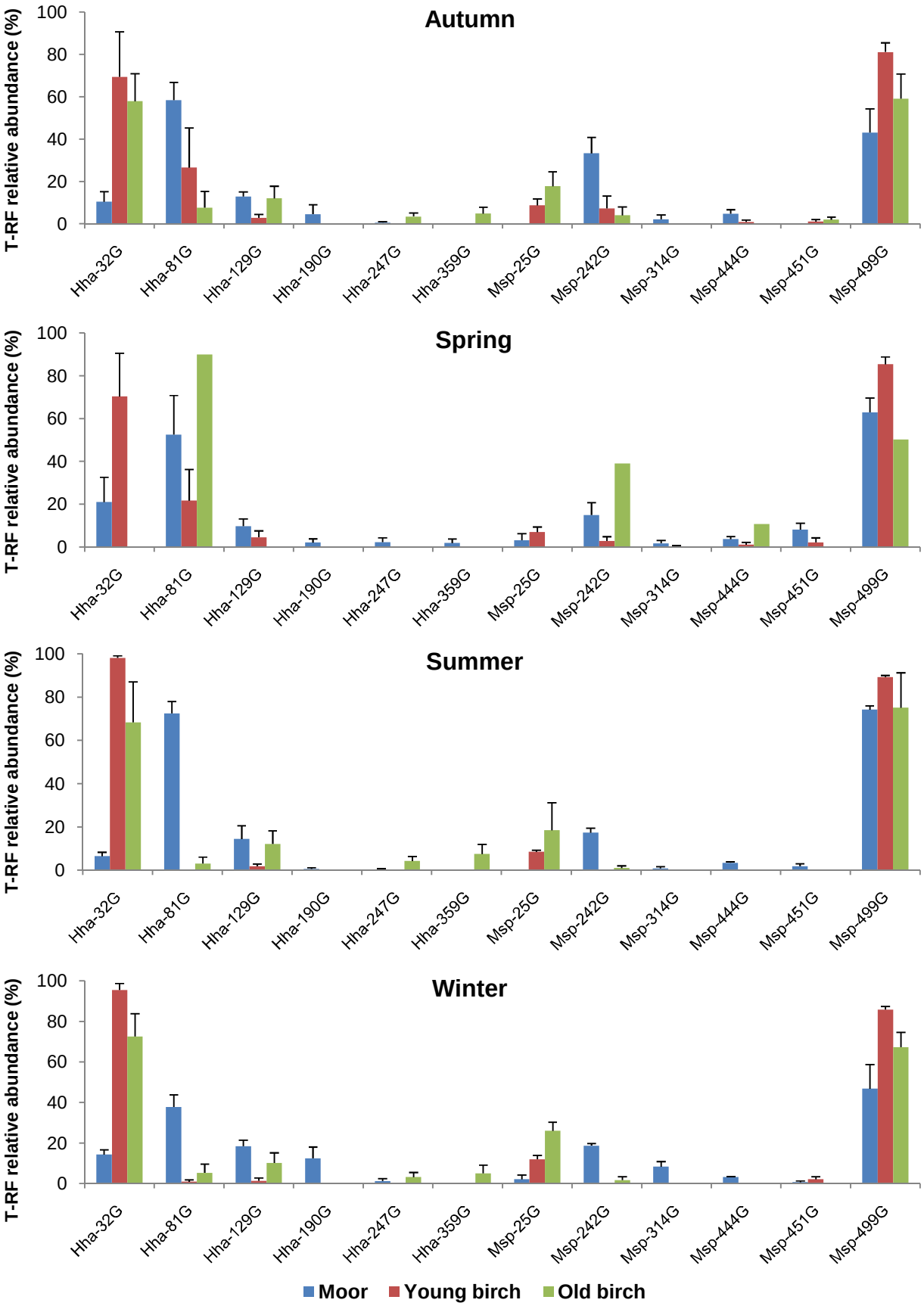

Appendix Figure 0.6: T-RFLP profiles of the methanotrophs (*pmoA*) for each season in Tulchan.

The total relative abundance of the T-RFs (n=4) generated by *Hha*I or *Msp*I is accounted for separately. The letter G (green) represents the colour of the dye.

Appendix Table 0.17: Effects of birch invasion and seasonal changes on the methanotrophic community at Craggan and Tulchan (16S rRNA of type II methanotrophs – *Mbo*I and *Msp*I).

The data are *P* values corresponding to the first four IPC scores of the AMMI analyses, and were obtained by nested ANOVA and MANOVA. Within each column, statistical differences between seasons within each habitat are indicated by different Roman letters (a, b, c), while Greek letters (α, β) indicate statistical differences between habitats, according to multiple pairwise comparison ($P<0.05$).

		IPC 1	IPC 2	IPC 3	IPC 4	MANOVA
Craggan	% variation	56.0	25.3	7.8	4.5	
	Habitat	**<0.001**	**<0.001**	**0.004**	0.162	**<0.001**
	Habitat/Season	**<0.001**	0.066	0.051	**0.046**	**<0.001**
Moor	Autumn Spring Summer Winter	**a α**	**a α**	**a α**	**a α**	
Young Birch	Autumn	**a**				
	Spring	**b**	**β**	**a α**	**a β**	**a α**
	Summer	**c**				
	Winter	**a**				
Old Birch	Autumn				**a**	
	Spring	**a β**	**a β**	**a αβ**	**b**	**α**
	Summer				**b**	
	Winter				**a**	
		IPC 1	**IPC 2**	**IPC 3**	**IPC 4**	**MANOVA**
Tulchan	% variation	57.0	20.9	8.7	5.9	
	Habitat	**<0.001**	**0.002**	0.526	**0.039**	**<0.001**
	Habitat/Season	**0.001**	0.115	**0.032**	0.078	**<0.001**
Moor	Autumn Spring Summer Winter	**a α**	**a α**	**a α**	**a α**	
Young Birch	Autumn	**a**		**ab**		
	Spring	**ab**	**β**	**a β**	**ab**	**α**	**a β**
	Summer	**b**			**a**	
	Winter	**ab**			**b**	
Old Birch	Autumn	**a**				
	Spring	**b**	**β**	**a α**	**a α**	**a α**
	Summer	**ab**				
	Winter	**a**				

Appendix Table 0.18: Effects of birch invasion and seasonal changes on the methanotrophic community at Craggan and Tulchan (16S rRNA of type I methanotrophs – *Hha*I and *Msp*I).

The data are *P* values corresponding to the first four IPC scores of the AMMI analyses, and were obtained by nested ANOVA and MANOVA. Within each column, statistical differences between seasons within each habitat are indicated by different Roman letters (a, b), while Greek letters (α, β, γ) indicate statistical differences between habitats, according to multiple pairwise comparison ($P<0.05$).

		IPC 1	IPC 2	IPC 3	IPC 4	MANOVA
Craggan	% variation	35.7	18.7	11.0	9.9	
	Habitat	**<0.001**	**<0.001**	0.427	**<0.001**	**<0.001**
	Habitat/Season	**0.010**	0.866	**<0.001**	0.430	**0.006**
Moor	Autumn	**a**		**a**		
	Spring	**ab**	**α**	**b**	**α**	**a α**
	Summer	**b**	**a α**	**ab**	**a α**	
	Winter	**ab**		**ab**		
Young Birch	Autumn					
	Spring					
	Summer	**a β**	**a β**	**a α**	**a β**	
	Winter					
Old Birch	Autumn			**ab**		
	Spring			**a**		
	Summer	**a γ**	**a β**	**ab**	**α**	**a β**
	Winter			**b**		
		IPC 1	**IPC 2**	**IPC 3**	**IPC 4**	**MANOVA**
Tulchan	% variation	44.6	22.0	9.3	7.7	
	Habitat	**<0.001**	**0.001**	**0.009**	**0.003**	**<0.001**
	Habitat/Season	**0.008**	0.057	0.202	0.304	**<0.001**
Moor	Autumn					
	Spring					
	Summer	**a α**	**a α**	**a α**	**a α**	
	Winter					
Young Birch	Autumn					
	Spring					
	Summer	**a β**	**a β**	**a β**	**a β**	
	Winter					
Old Birch	Autumn	**a**				
	Spring	**b**	**α**			
	Summer	**b**	**a β**	**a β**	**a α**	
	Winter	**a**				

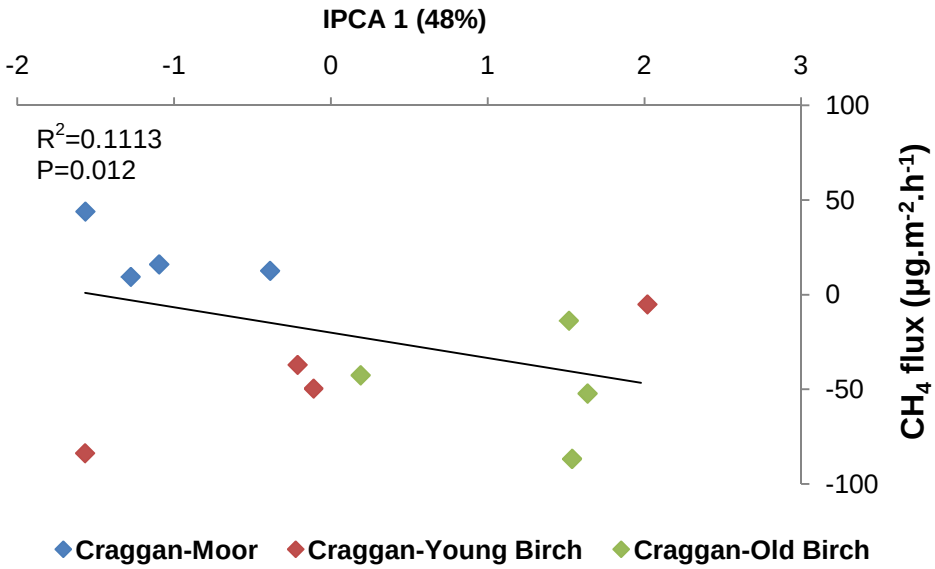

Appendix Figure 0.7: Relationship between net CH_4 flux and methanotrophic community structure at Craggan.

The data points represent the IPCA 1 scores displayed in **Figure 6.3** and the net CH_4 fluxes from **Figure 6.1**.